Load Testing of Prestressed Concrete Girder Bridges in Texas

by

Patrick Joseph Wagener, Jr., B.S.C.E.

Thesis

Presented to the Faculty of the Graduate School

of The University of Texas at Austin

in Partial Fulfillment

of the Requirements

for the Degree of

Master of Science in Engineering

The University of Texas at Austin

May 2002

Load Testing of Prestressed Concrete Girder Bridges in Texas

APPROVED BY

SUPERVISING COMMITTEE:

____

____

Dedication

This work is dedicated first to my family, who have shown me nothing but continued support and love throughout all of my academic endeavors. To Elisabeth, who kept a smile on my face through the toughest of times and has shown me the true meaning of friendship. To my professors and teachers, for their undying efforts to cultivate sharp minds.

Acknowledgements

I would like to thank Dr. Sharon L. Wood and Dr. Michael E. Kreger for their guidance, patience, and hard work throughout the completion of this project and this thesis.

I would like to sincerely thank the Texas Department of Transportation for their continued support, both financial and otherwise, that made the work on this project possible. I would like to thank Mr. Keith Ramsey for his assistance and his extraordinary efforts in coordinating the logistical aspects of the bridge load tests.

I would like to thank my family and friends who supported me and always convinced me of the value of my work. I would like to thank Scott for always keeping me one inch away from insanity, and I would like to thank Greg for showing me places and things to do for fun that I would have never dreamed of on my own.

Finally, I would like to thank Michael Hagenberger for many things. First, for being a good friend who always seemed to have the right piece of advice for any dilemma. Second, for sharing his experience, wisdom, and insight into the matters of the real world. And most of all, for making the past two years seem like anything but work.

Abstract

Load Testing of Prestressed Concrete Girder Bridges in Texas

by

Patrick Joseph Wagener, Jr., M.S.E.

The University of Texas at Austin

SUPERVISORS: Michael E. Kreger
Sharon L. Wood

There are numerous prestressed concrete girder bridges in Texas that fail to meet load rating criteria set forth by the American Association of State Highway and Transportation Officials (AASHTO). As such, they must be fully inspected and evaluated by personnel from the Texas Department of Transportation each year, rather than every two years, which is the standard inspection interval for public bridges. It is important to be certain that the true strength and performance of bridges that fail load rating criteria are not being underestimated by prescriptive load rating methods. Therefore, load testing of five bridges that fail load rating criteria as well as two bridges that pass was conducted in order to gain a more complete understanding of the actual condition and behavior of a sample of aging prestressed concrete girder bridges in Texas. The goals of load testing included a more accurate assessment of moment capacity, a better understanding and characterization of live load distribution, and ultimately, an assessment of the value of spending additional time and money on load testing.

Table of Contents

List of Tables

List of Figures

Chapter 1 – Introduction

Currently, a number of prestressed concrete girder bridges in Texas do not meet load rating criteria set forth by the American Association of State Highway and Transportation Officials, or AASHTO. The load rating criteria are strength and serviceability limits used in computation of permissible bridge loads. These limits are derived using a standard design vehicle specified by AASHTO. The total weight of this design vehicle has increased in recent years. As a result, older prestressed concrete girder bridges in Texas that were originally designed based on lighter design vehicles may not meet the current strength and serviceability requirements prescribed by AASHTO.

1.1 CONSEQUENCES OF AN AGING INFRASTRUCTURE

The consequences of a bridge not satisfying the AASHTO load rating criteria are costly. First, a structural evaluation must be performed in order to determine the maximum safe loads permitted on the bridge, and these loads must then be posted and updated regularly. Second, a bridge that does not satisfy the load rating criteria must be inspected by the Texas Department of Transportation, or TxDOT, on a yearly basis rather than once every two years, thus increasing inspection costs. Finally, the most costly, worst-case scenario involves a bridge that fails the AASHTO load rating criteria and is deemed inadequate following further evaluation. Such a bridge must be removed from service, be rehabilitated, or be replaced.

There are numerous businesses and individuals that depend on the infrastructure in Texas to conduct their day-to-day activities. A vital component of the infrastructure is the state's bridge system. This system must be maintained at an operational level, otherwise there can be severe economic impacts. A prime example is the collapse of three spans of the Queen Isabella Causeway in South Padre, Texas, in September 2001, which severely crippled the tourism-based economy of South Padre Island for several months. While this is an extreme example, it is representative of the economic impact that bridge closings and restrictions can have on the communities in the state of Texas. Because the consequences of a substandard infrastructure can be severe, it is the goal of TxDOT to accurately assess the bridge system in the state of Texas.

1.2 DIAGNOSTIC LOAD TESTING

In order to better assess aging bridges in Texas, diagnostic load testing may be completed for potentially inadequate bridges. The goal of this type of testing is to gain a better understanding of the actual live load response of bridges in service. Some of the live load response parameters include live load moment, lateral live load distribution, degree of composite action, maximum tensile strains, and contribution of curbs, rails, and parapets. Gathering these quantities through diagnostic load testing ultimately leads to a better assessment of the condition of bridges than is offered by prescriptive equations and empirical methods.

Diagnostic load testing is relatively simple. A loading vehicle of known weight is driven across a bridge, and response characteristics are measured. The response characteristics that can be measured directly include concrete strains, girder displacements, and girder end rotations. Once these data are obtained, other quantities can be inferred using structural mechanics. For instance, live load moments, neutral axis depths, and lateral live load distribution factors can all be calculated simply from strain data.

While the concept of diagnostic load testing is simple, its implementation is much more involved. Careful attention must be paid to how load tests are conducted so that the end product is useful data that can be processed to characterize the live load response.

1.3 SCOPE AND OBJECTIVES OF THIS STUDY

The purpose of this research project, designated TxDOT Project 1895, was to gather data during diagnostic load testing of five bridges that currently fail the

AASHTO load rating criteria. The data measured in the field were then analyzed using known bridge properties. Special attention was paid during analysis to determine if differences in diaphragm configurations affected lateral live load distribution. The load rating for each bridge was calculated using the current AASHTO method and knowledge gained from the load tests. Subsequently, an assessment was made regarding the value of extra work involved in diagnostic load testing based on the results.

In addition to field testing of the five older prestressed concrete bridges, a new analysis of previously measured data from two other bridges was conducted to attempt to explain some of the peculiarities that arose in the analysis of that data. The data come from TxDOT Project 2986, which was completed in the spring of 1998. Following analysis of that data, the original researchers concluded that the two bridges behaved in an unexpected manner based on their construction. With the observations made and new trends established during the analysis of the five bridges studied in Project 1895, a revised analysis was made to ascertain the applicability of the analysis methods used on the five bridges from Project 1895 to the analysis of the two bridges in Project 2986.

The five bridges studied in Project 1895 are referred to as the Chandler Creek bridge, the Lake LBJ bridge, the Lampasas River bridge, the Willis Creek bridge, and the Wimberley bridge. The two bridges studied in Project 2986 are referred to as the Slaughter Creek bridge and the Nolanville bridge. With the exception of the Nolanville bridge, all bridges were within a ninety-minute drive from the Ferguson Structural Engineering Laboratory facilities. In addition, the bridges were chosen based on ease of accessibility and a relatively low amount of traffic.

During the load tests at all bridges, strain measurements were made at various locations on the prestressed concrete girders. From those strains, live load moments and neutral axis depths were inferred based on two sets of bridge properties. Then, the lateral live load distribution factors for each girder were calculated using the live load moments obtained in the previous step. Finally, the AASHTO load ratings were calculated using both design section properties and a set of adjusted section properties based on material test data. These two ratings were then compared to evaluate the results of the diagnostic load tests.

Chapter 2 – Description of the Prestressed Concrete Girder Bridges

This chapter presents the various material and section properties of all seven bridges considered in this study. These properties are used throughout the analyses found in Chapters Five, Six, and Seven. The first section deals with the general bridge descriptions, including geographic location and traffic volumes. The second section presents the cross-section properties of each of bridge. The third section covers the dimensions and properties of the bridge girders, including the assumed properties of the composite sections. The fourth section of this chapter deals with the properties of the materials in all the bridges. Finally, the fifth section details the diaphragm dimensions and locations for each bridge.

2.1 GENERAL BRIDGE DESCRIPTIONS

As mentioned in Chapter 1, each of the five bridges in Project 1895 were chosen because they fail the load rating criteria and they provided easy access. The two bridges in Project 2986 were chosen because of their close proximity and the availability of test vehicles. Table 2.1 shows the location of each bridge, the year construction was completed, and the daily traffic volumes including the percentage of truck traffic, as recorded between 1999 and 2000 by the Texas

Department of Transportation (TxDOT) in their Bridge Inventory and Inspection Files (Texas Department of Transportation 2002).

Table 2.1 General Bridge Information

Bridge Name	Year Completed	Location	Daily Traffic Volume	%Truck Traffic
Chandler Creek	1965	IH 35 @ Chandler Creek	7,951	25%
Lake LBJ	1964	FM 1431 @ Lake LBJ	8,300	5%
Lampasas River	1970	FM 2657 @ Lampasas River	2,100	12%
Willis Creek	1961	FM 972 @ Willis Creek	800	16%
Wimberley	1959	RM 12 @ Blanco River	10,200	5%
Slaughter Creek	1991	IH 35 @ Slaughter Creek	9,000	17%
Nolanville	1977	Highway 190 in Nolanville	14,040	7%

As shown in Table 2.1, the bridges studied in Project 1895 were constructed between 1959 and 1970, the Nolanville bridge was constructed in 1977, and the Slaughter Creek bridge was constructed in 1991. This wide range of completion dates provides an opportunity to see the evolution of design philosophies and practices used by TxDOT bridge engineers and their effects on live load response and performance.

Table 2.2 lists the span lengths, roadway widths, girder spacing, number of girders in each span, and skew angle for all seven bridges considered in this study. The overall span lengths range from forty feet to over one hundred feet, which is a representative sample of typical prestressed concrete girder bridges in Texas.

Table 2.2 Overall Bridge Dimensions

Bridge Name	Overall Span Length	Roadway Width	Number of Girders per Span	Girder Spacing	Skew Angle
Chandler Creek – 40’ Span	40’	30’-4”	4	8’-0”	30^{o}
Chandler Creek – 60’ Span	60’	30’-4”	4	8’-0”	30^{o}
Lake LBJ	65’	29’-6”	4	8’-0”	0^{o}
Lampasas River	75’	28’-2”	4	7’-4”	0^{o}
Willis Creek	65’	25’-8”	4	6’-8”	0^{o}
Wimberley	40’	31’-2”	5	6’-11”	22^{o}
Slaughter Creek	100’	38’-0”	5	8’-0”	15^{o}
Nolanville	102’	43’-8”	5	9’-6”	0^{o}

The following figures show the plan views of all seven bridges considered in this study, along with a photograph of each bridge. The dashed lines in the drawings indicate the placement of the bridge girders beneath the bridge deck. The Wimberley Bridge is both skewed and curved in plan, which is the reason for its irregular shape compared to the other six bridges.

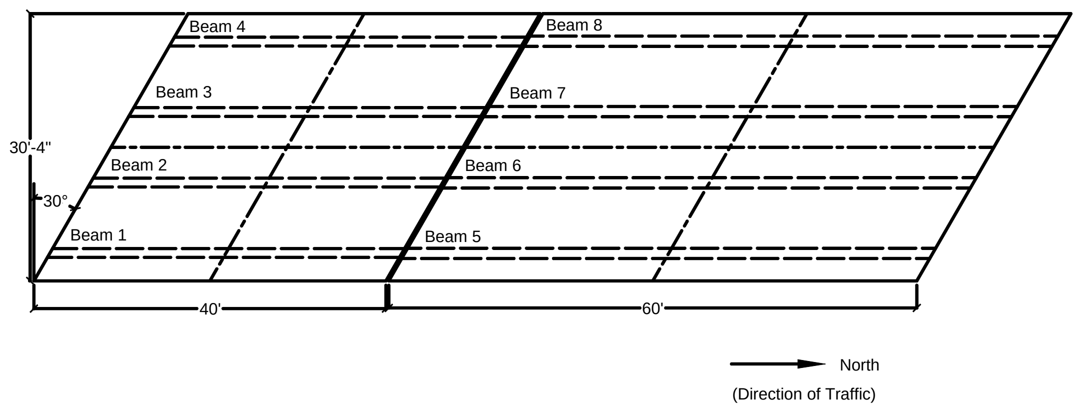

Figure 2.1 Chandler Creek Bridge Layout

Figure 2.2 Chandler Creek Bridge

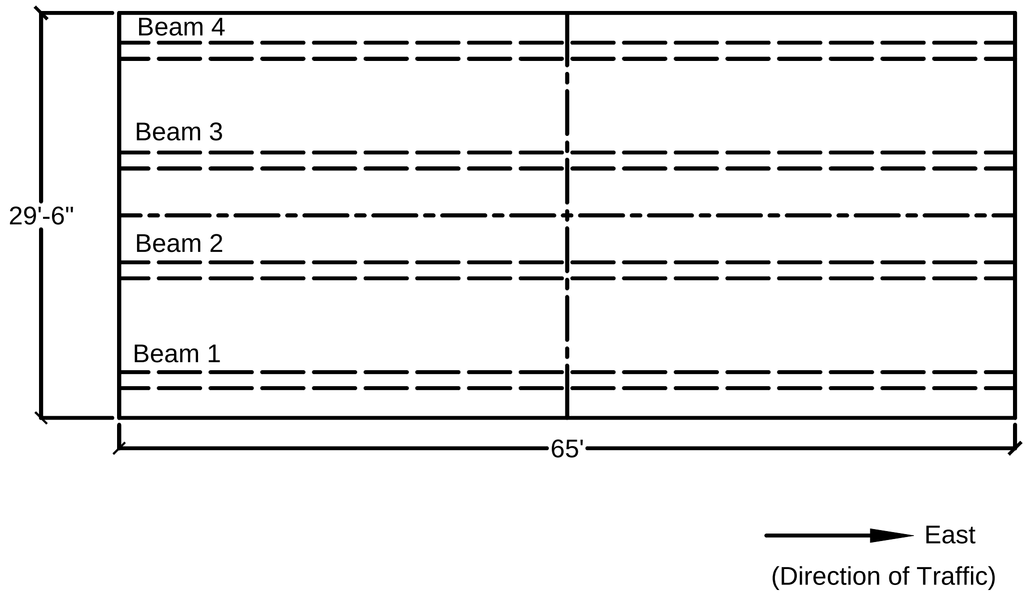

Figure 2.3 Lake LBJ Bridge Layout

Figure 2.4 Lake LBJ Bridge

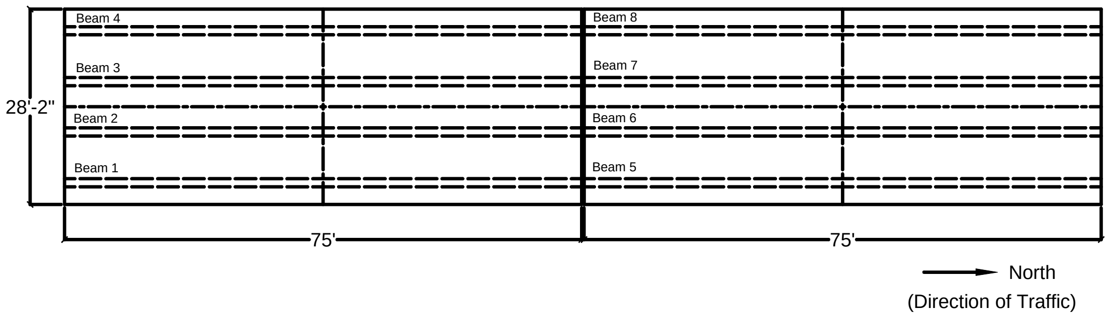

Figure 2.5 Lampasas River Bridge Layout

Figure 2.6 Lampasas River Bridge

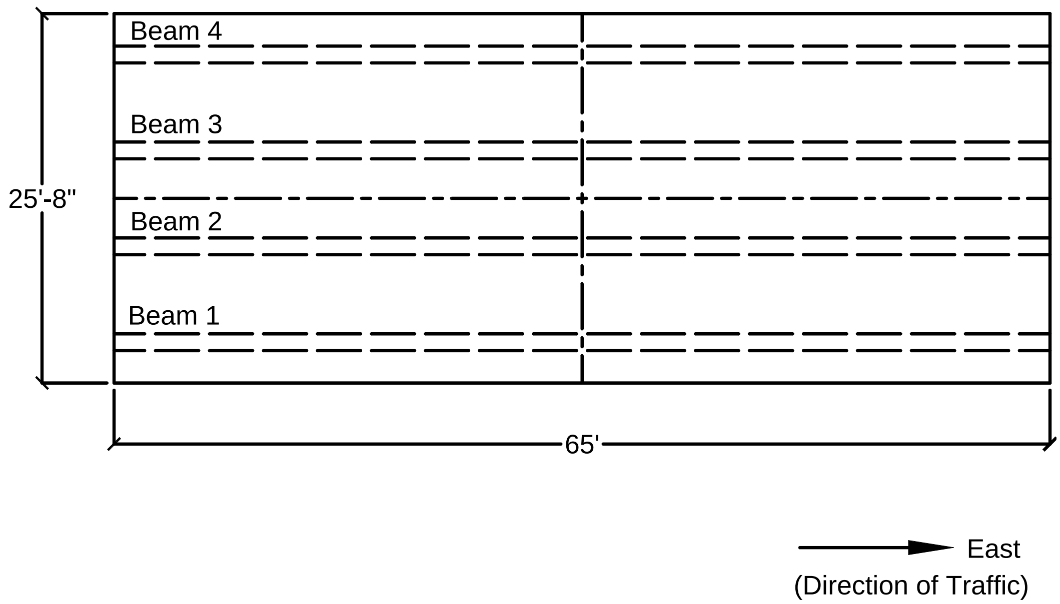

Figure 2.7 Willis Creek Bridge Layout

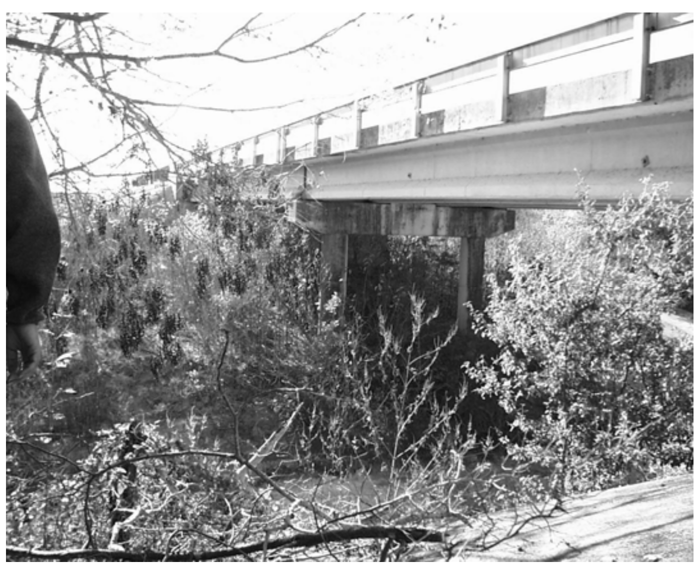

Figure 2.8 Willis Creek Bridge

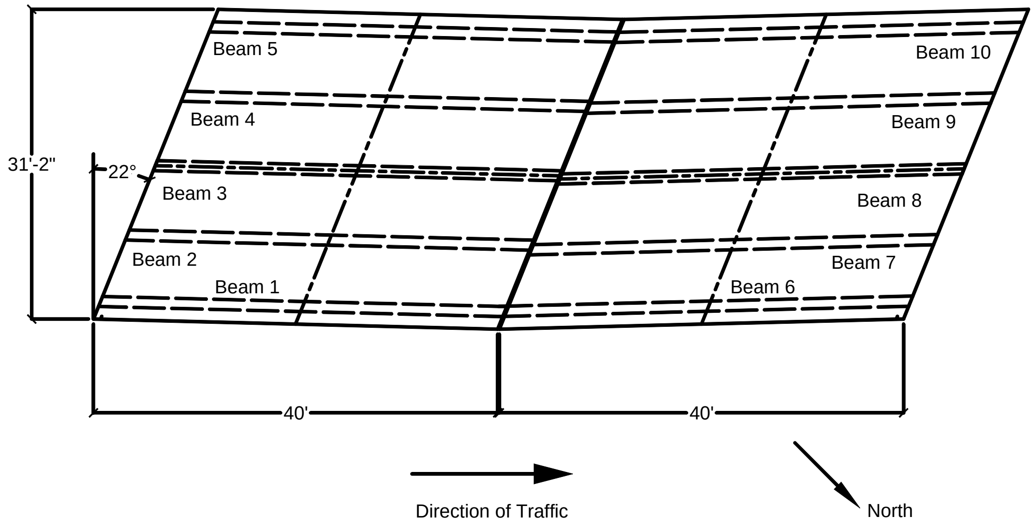

Figure 2.9 Wimberley Bridge Layout

Figure 2.10 Wimberley Bridge

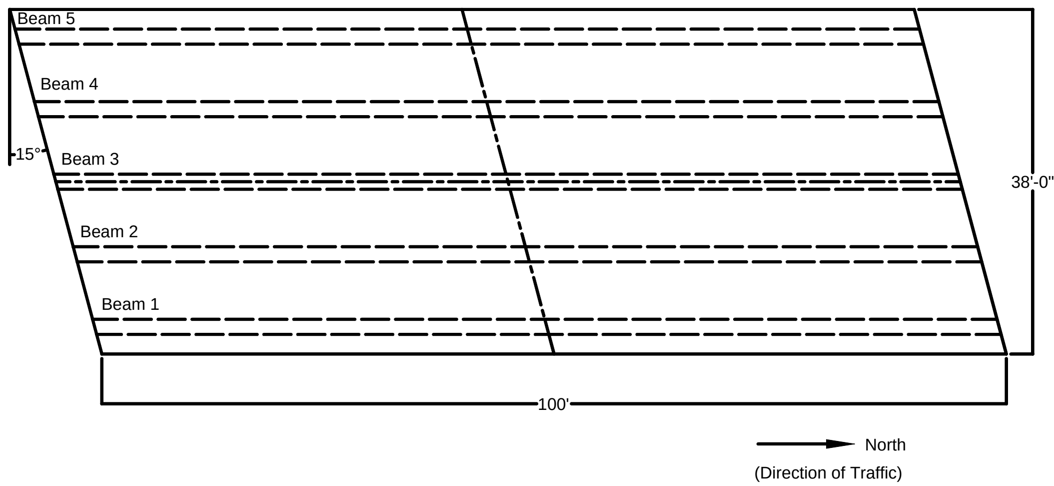

Figure 2.11 Slaughter Creek Bridge Layout

Figure 2.12 Slaughter Creek Bridge (Matsis 1999)

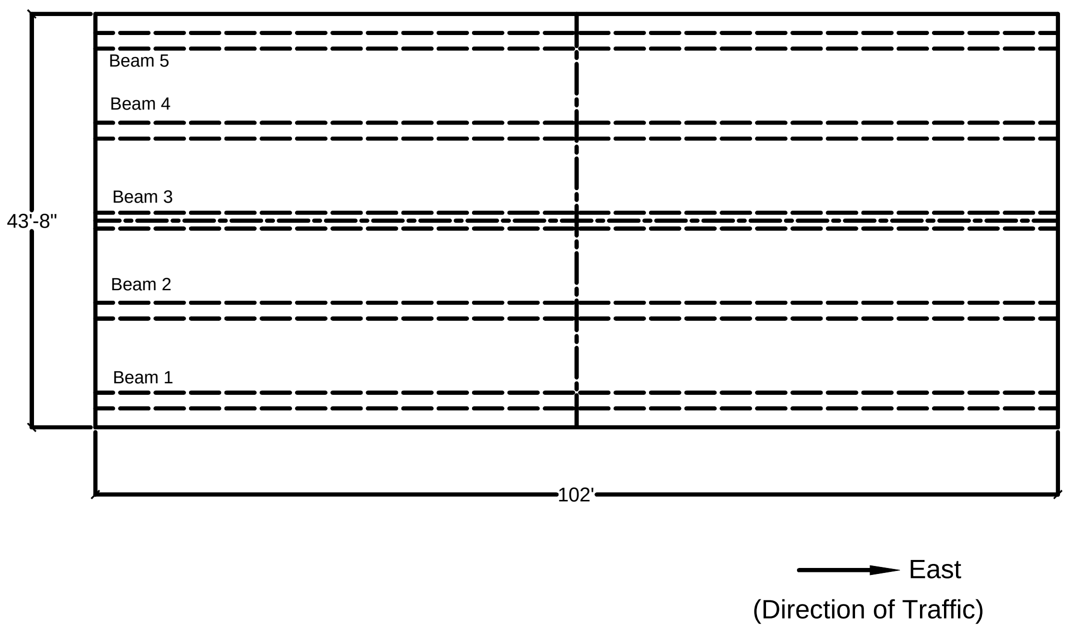

Figure 2.13 Nolanville Bridge Layout

Figure 2.14 Nolanville Bridge (Matsis 1999)

2.2 BRIDGE CROSS-SECTION PROPERTIES

For each of the seven prestressed concrete girder bridges considered in this study, the cross-section dimensions were taken from the contract drawings and then were verified in the field. For the five bridges tested in Project 1895, all girders were either Type B or Type C girders, with a girder height of thirty-four inches and forty inches, respectively. For the two bridges tested in Project 2986, all girders were Type IV girders, with a girder height of fifty-four inches.

Table 2.3 shows the relevant cross-section properties for each of the bridges, taken from the contract drawings. With the exception of the Nolanville bridge, all dimensions shown come from the midspan cross section because only midspan data are reported here. Three-quarter span data are reported for the Nolanville bridge. For some of the bridges, a thin concrete "strip" was cast between the girder and the slab, and its thickness is indicated in the "Strip Thickness" column. For the Lake LBJ bridge and the Lampasas River bridge, there was no indication of a concrete strip in the contract drawings; however, field observation revealed its presence.

Table 2.3 General Cross-Section Properties

Bridge Name	Girder Type	Girder Height (in)	Slab Thickness (in)	Concrete Curb	Strip Thickness (in)
Chandler Creek – 40’ Span	B	34	7.25	No	N/A
Chandler Creek – 60’ Span	C	40	7.25	No	N/A
Lake LBJ	C	40	7.25	Yes	1
Lampasas River	C	40	6.50	No	2
Willis Creek	C	40	6.00	Yes	N/A
Wimberley	B	34	6.25	Yes	N/A
Slaughter Creek	IV	54	7.25	Yes	0.5
Nolanville	IV	54	8.25/9.25*	No	0.5

*The contract drawings for the Nolanville bridge specify an 8.25” slab thickness at the edge and a 9.25” slab thickness at the centerline.

The following figures show the bridge cross sections with dimensions as specified on the contract drawings. With the exception of the Slaughter Creek bridge, each of the bridges has aluminum rails, but they are not shown in the following figures because it was assumed that they do not contribute to the bending stiffness of the exterior composite sections.

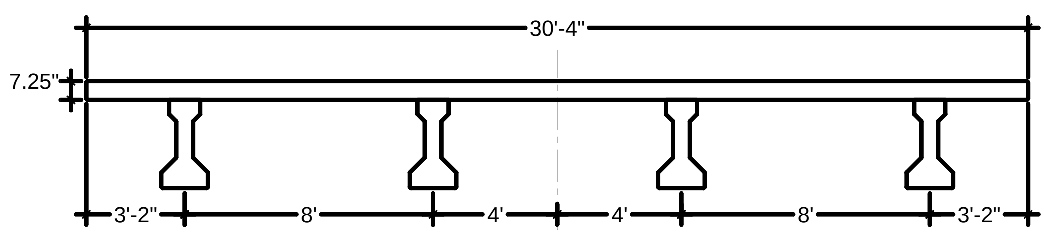

Figure 2.15 Chandler Creek Bridge Cross Section – 40’ Span

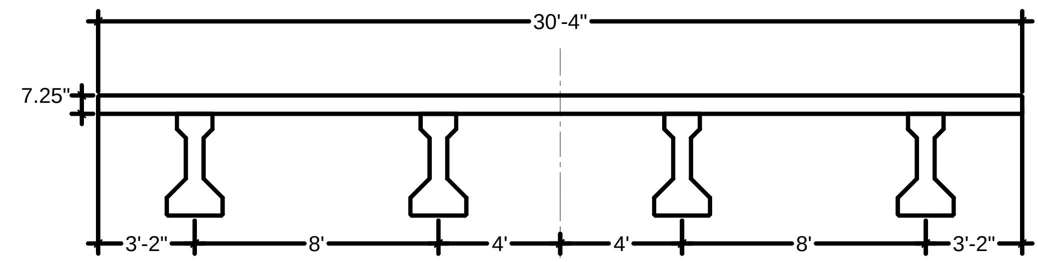

Figure 2.16 Chandler Creek Bridge Cross Section – 60' Span

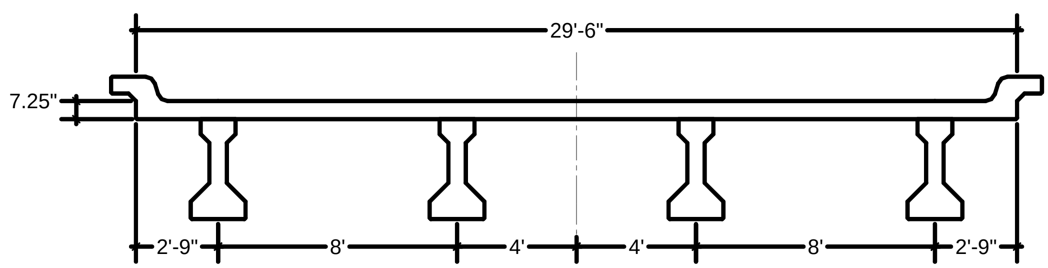

Figure 2.17 Lake LBJ Bridge Cross Section

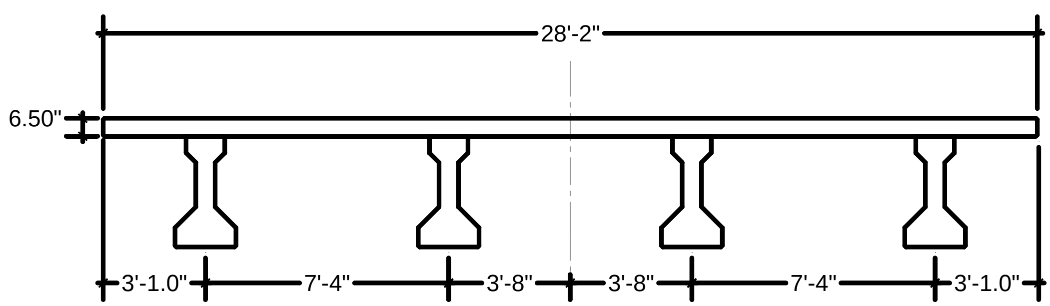

Figure 2.18 Lampasas River Bridge Cross Section

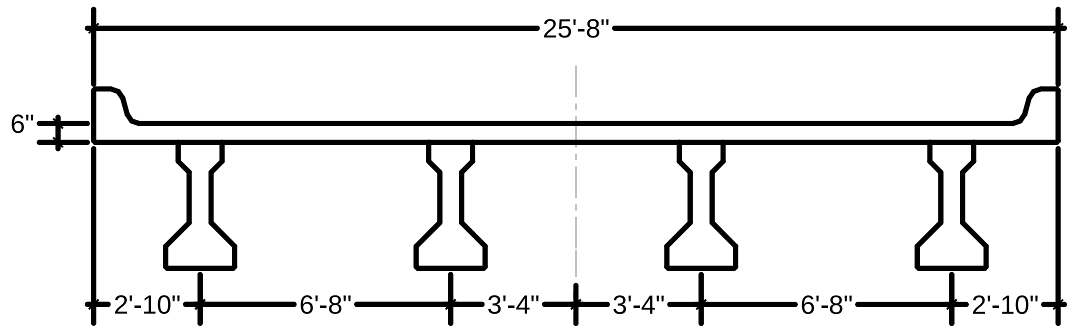

Figure 2.19 Willis Creek Bridge Cross Section

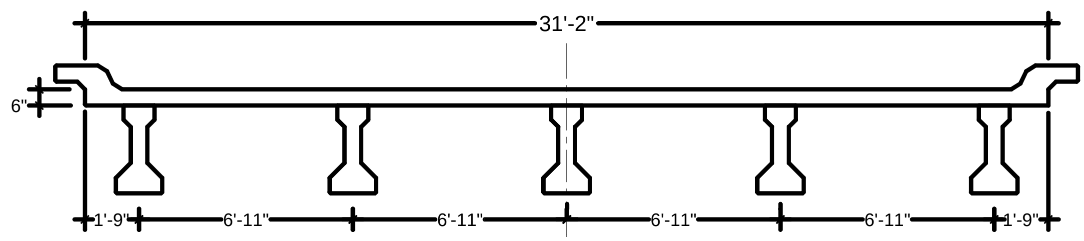

Figure 2.20 Wimberley Bridge Cross Section

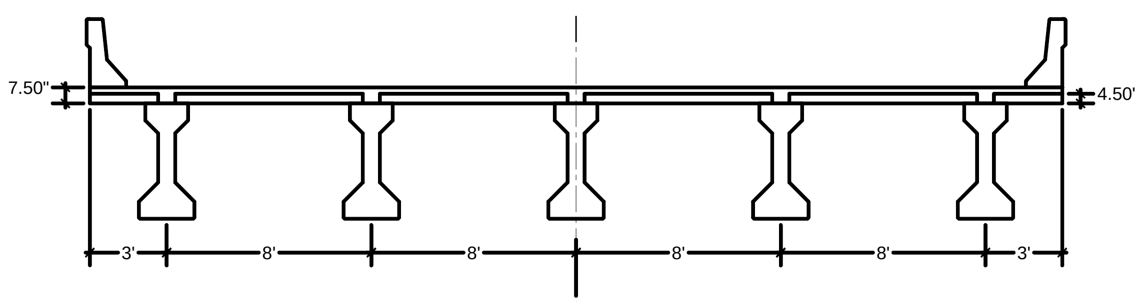

Figure 2.21 Slaughter Creek Bridge Cross Section

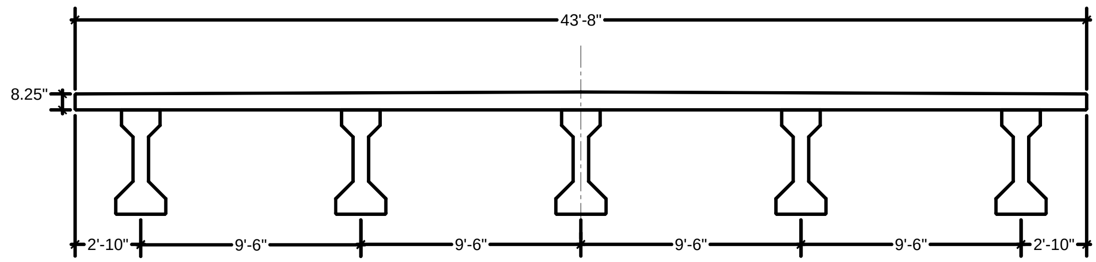

Figure 2.22 Nolanville Bridge Cross Section

As mentioned previously, the concrete curbs and parapets were assumed to contribute to the overall bending stiffness of the exterior composite sections. Therefore, the curb dimensions were measured in the field and then curb properties were calculated during the analysis. The following figures show the curb details for the Lake LBJ bridge, Willis Creek bridge, and Wimberley bridge. The parapet details for the Slaughter Creek bridge are shown in Figure 2.26.

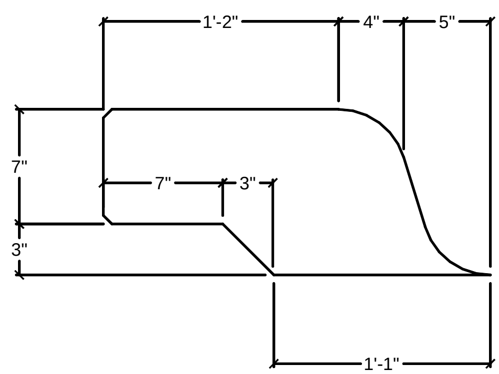

Figure 2.23 Curb Detail for the Lake LBJ Bridge

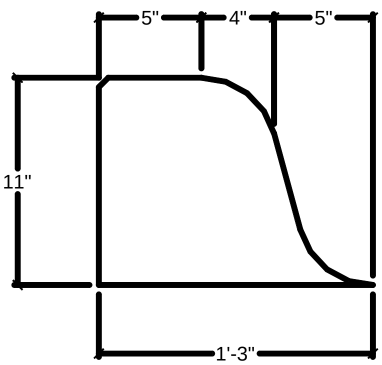

Figure 2.24 Curb Detail for the Willis Creek Bridge

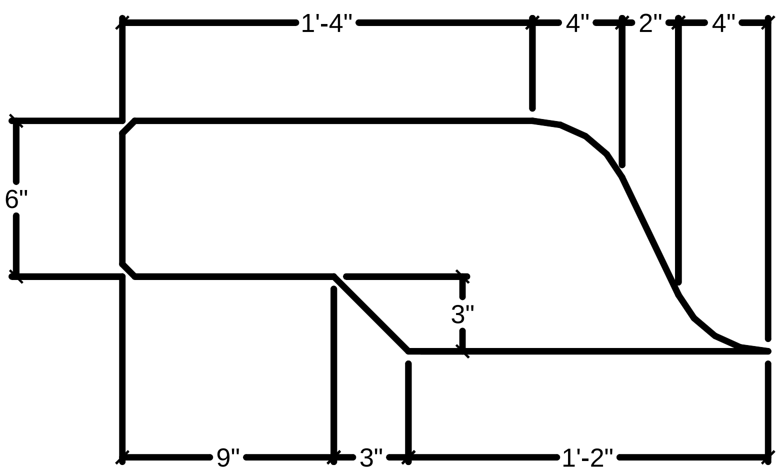

Figure 2.25 Curb Detail for the Wimberley Bridge

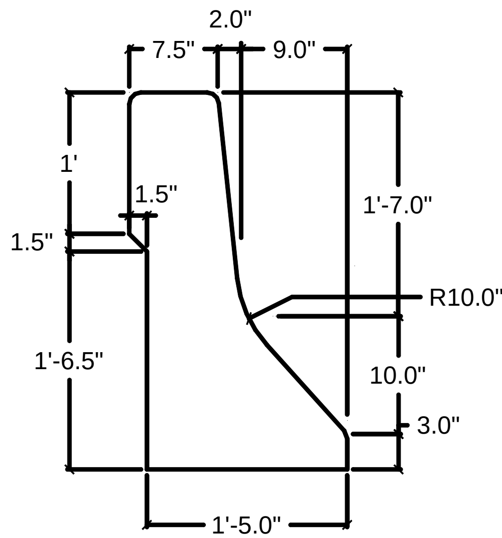

Figure 2.26 AASHTO Type T502 Concrete Parapet Detail for the Slaughter Creek Bridge

2.3 GIRDER AND COMPOSITE SECTION PROPERTIES

The dimensions and various properties of the bridge girders and the assumed composite sections are presented in this section. The girder and slab dimensions were taken from the contract drawings, and the arrangement of prestressing strands was taken from the contract drawings except for the Willis Creek and Slaughter Creek bridges, for which the as-built drawings were available.

The following figures show the girder cross sections for each of the seven bridges considered in this study. In addition to the girder dimensions, the prestressing strand arrangement is shown based on contract drawings or as-built drawings. The prestressing strands are arranged in a grid with a nominal two-inch center-to-center spacing.

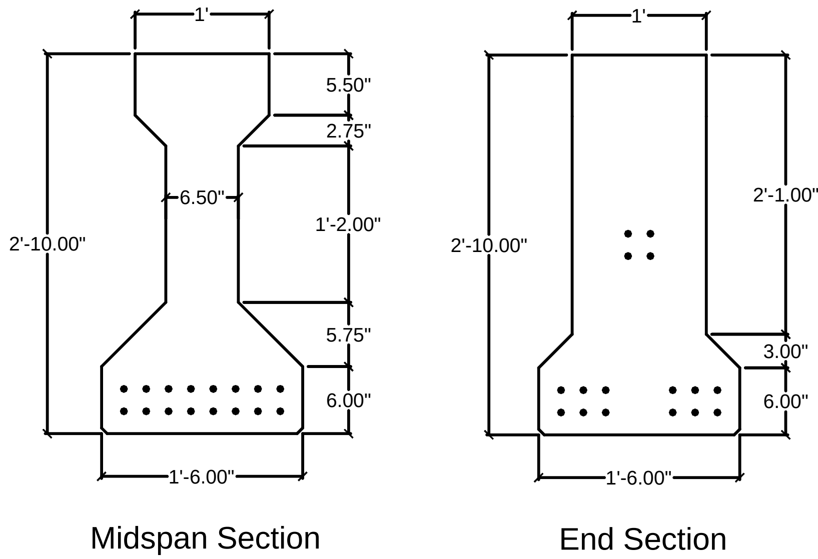

Figure 2.27 Type B Girders – Chandler Creek Bridge – 40' Span

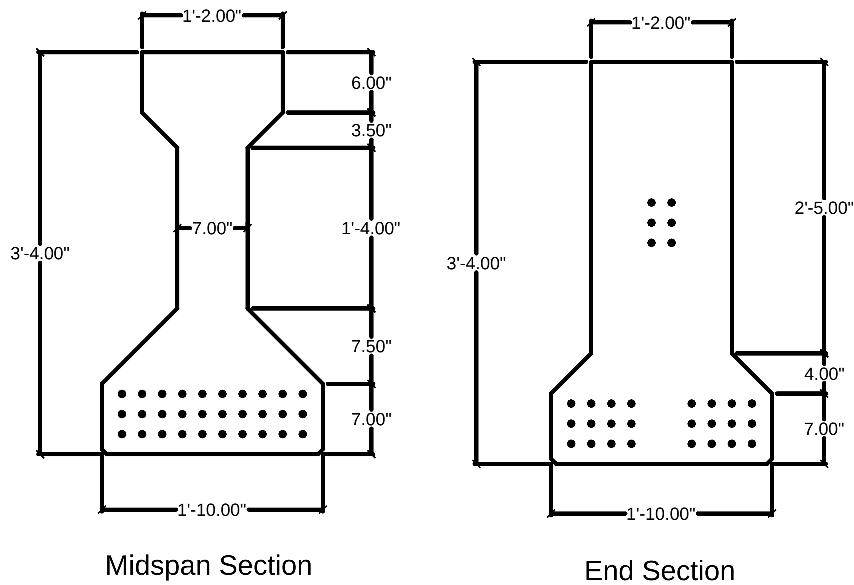

Figure 2.28 Type C Girders – Chandler Creek Bridge – 60' Span

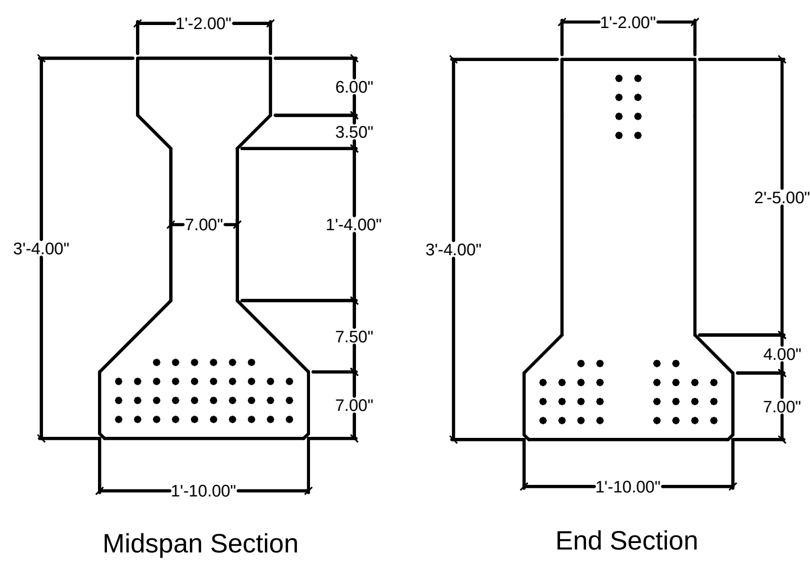

Figure 2.29 Type C Girders – Lake LBJ Bridge

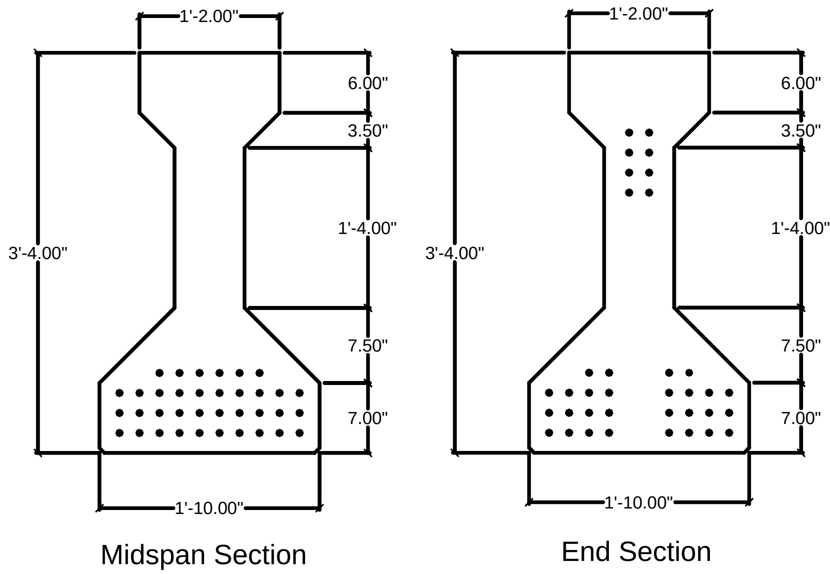

Figure 2.30 Type C Girders – Lampasas River Bridge

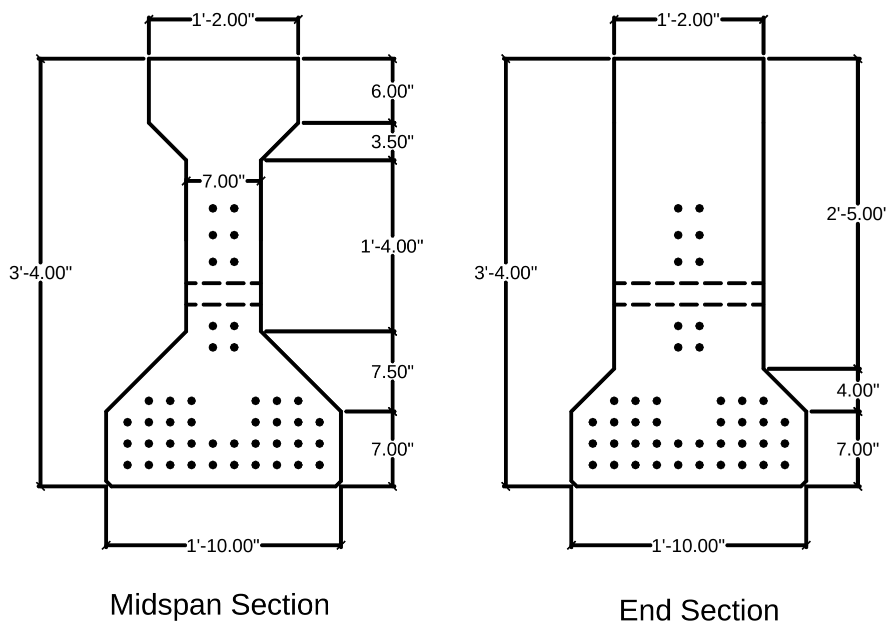

Figure 2.31 Type C Girders – Willis Creek Bridge

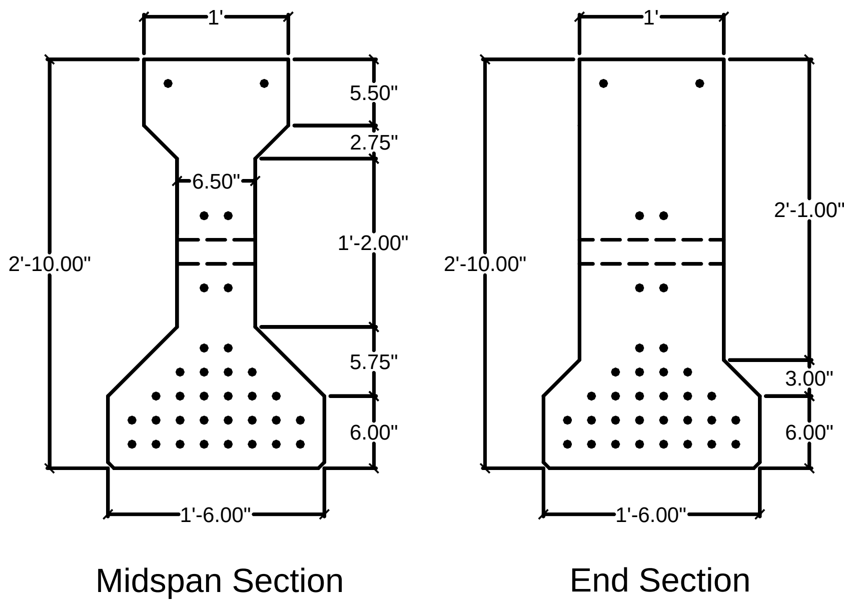

Figure 2.32 Type B Girders – Wimberley Bridge

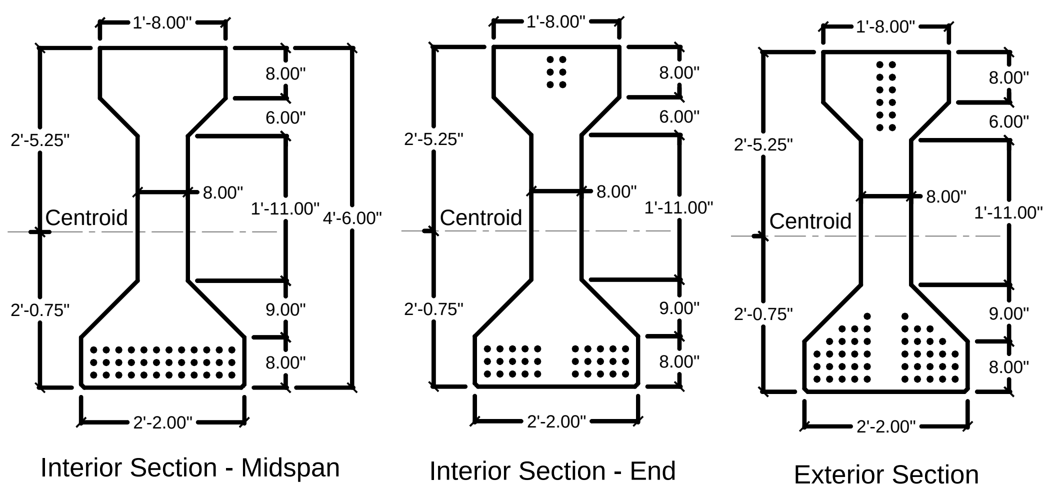

Figure 2.33 Type IV Girders – Slaughter Creek Bridge

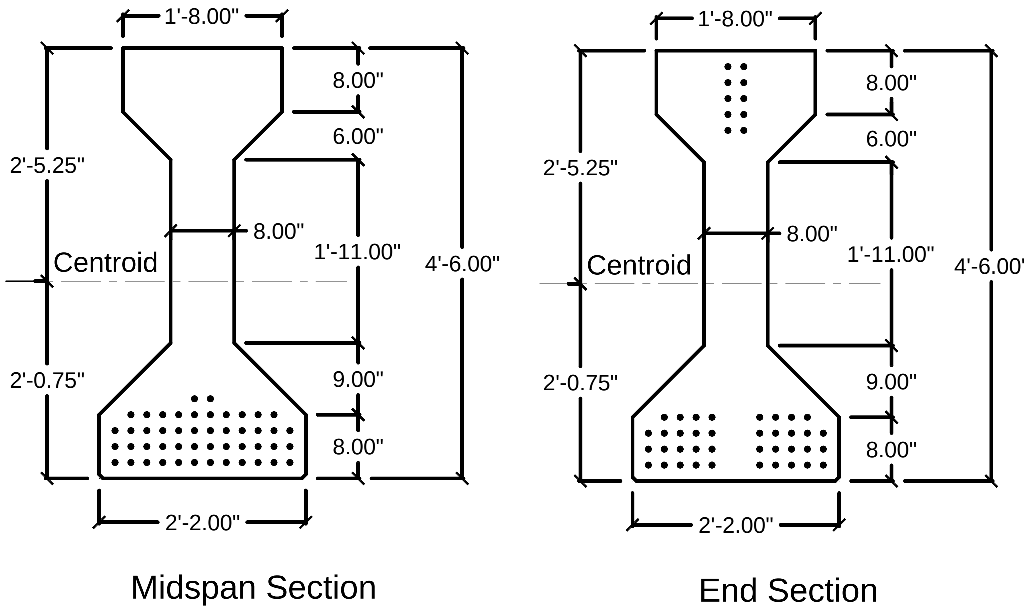

Figure 2.34 Type IV Girders – Nolanville Bridge

Tables 2.4 and 2.5 show the relevant properties for the prestressing strands used in the seven bridges in this study. These properties and dimensions are used throughout the analyses that are summarized in Chapters Five, Six, and Seven. Table 2.4 shows the general strand properties, and Table 2.5 lists strand eccentricities at midspan and at the ends of the prestressed girders. Table 2.6 shows the individual girder properties calculated based on uncracked sections.

Table 2.4 Prestressing Strand Properties

Bridge Name	f_{pu} (ksi)	f_{pi} (ksi)	Type	D_{strand} (in)	A_{strand} (in)	N_{strand} Interior	N_{strand} Exterior	A_{total} (in^2) Interior	A_{total} (in^2) Exterior
Chandler Creek 40’ Span	250	175	Stress-relieved	7/16	0.108	16	16	1.73	1.73
Chandler Creek 60’ Span	250	175	Stress-relieved	7/16	0.108	30	30	3.24	3.24
Lake LBJ	250	175	Stress-relieved	7/16	0.108	36	36	3.89	3.89
Lampasas River	250	175	Stress-relieved	7/16	0.108	36	36	3.89	3.89
Willis Creek	250	175	Stress-relieved	3/8	0.080	44	44	3.52	3.52
Wimberley	250	175	Stress-relieved	3/8	0.080	34	34	2.72	2.72
Slaughter Creek	270	202.5	Low-relaxation	1/2	0.153	36	58	5.51	8.87
Nolanville	270	202.5	Low-relaxation	1/2	0.153	48	48	7.34	7.34

Table 2.5 Strand Eccentricities

Bridge Name	Interior Girders		Exterior Girders		Number of Depressed Strands
	e_{end} (in)	e_{mid} (in)	e_{end} (in)	e_{mid} (in)	
Chandler Creek – 40’ Span	8.40	11.90	8.40	11.90	4
Chandler Creek – 60’ Span	9.07	13.07	9.07	13.07	6
Lake LBJ	5.74	12.40	5.74	12.40	8
Lampasas River	7.09	12.42	7.09	12.42	8
Willis Creek	8.02	8.02	8.02	8.02	0
Wimberley	8.14	8.14	8.14	8.14	0
Slaughter Creek	13.08	20.75	10.41	10.41	6/12
Nolanville	10.92	19.67	10.92	19.67	10

Table 2.6 Girder Properties

Bridge Name	A_{girder} (in^2)	I_{girder} (in^4)	$y_{b-girder}$ (in)	$y_{t-girder}$ (in)
Chandler Creek – 40’ Span	360	43300	14.9	19.1
Chandler Creek – 60’ Span	496	82800	17.1	22.9
Lake LBJ	496	82800	17.1	22.9
Lampasas River	496	82800	17.1	22.9
Willis Creek	496	82800	17.1	22.9
Wimberley	360	43300	14.9	19.1
Slaughter Creek	789	261000	24.7	29.3
Nolanville	789	261000	24.7	29.3

The next step in quantifying the composite section properties for each bridge is to consider the slab contribution. The effective width of the slab for each composite section was calculated according to the current AASHTO LRFD Bridge Design Specifications (American Association of State Highway and Transportation Officials 2000a). Table 2.7 shows the effective slab widths for the interior and exterior composite sections of each bridge, as well as the curb properties that were used for exterior section calculations. The values for "y_{curb}" are defined as the distance from the top of the slab to the centroid of the curb section.

Table 2.7 Slab Dimensions and Properties

Bridge Name	$b_{effective}$ (in) Interior	$b_{effective}$ (in) Exterior	A_{curb} (in^2)	y_{curb} (in)	I_{curb} (in^4)
Chandler Creek – 40' Span	93.0	84.5	N/A	N/A	N/A
Chandler Creek – 60' Span	94.0	85.0	N/A	N/A	N/A
Lake LBJ	94.0	80.0	158	6.3	1500
Lampasas River	85.0	80.0	N/A	N/A	N/A
Willis Creek	79.0	73.5	99	5.3	1000
Wimberley	81.0	61.5	137	5.3	700
Slaughter Creek	96.0	68.0	330	15.3	29800
Nolanville	107.0	70.0	N/A	N/A	N/A

Given the effective slab widths and curb properties, the section properties for the interior and exterior composite sections for each bridge were calculated. In this study, the composite section properties were calculated using three different sets of concrete strengths. The first set of strengths comes from the specified design concrete strengths shown on the contract drawings. The second set of strengths comes from material test data supplied by the girder manufacturers during casting, and is called the lower-bound strengths. The final set of strengths, called the upper-bound strengths, was obtained by taking the lower-bound concrete strengths and extrapolating to the present using equations first published in the 1991 CEB-FIP Model Code, created by the Comite Euro-International Du Beton. In this study, the lower-bound values are used as the adjusted values in all analyses. A more detailed discussion of concrete strengths is presented in the next section.

Table 2.8 through Table 2.10 show the calculated composite section properties for each of the seven bridges. Table 2.8 shows the composite section properties calculated from specified design dimensions and material strengths. Table 2.9 shows the composite section properties calculated using the

Table 2.8 Design Composite Section Properties

Bridge Name	**Interior Section**				**Exterior Section**			
	A_{comp} (in^2)	I_{comp} (in^4)	$y_{b\text{-}comp}$ (in)	$y_{t\text{-}comp}$ (in)	A_{comp} (in^2)	I_{comp} (in^4)	$y_{b\text{-}comp}$ (in)	$y_{t\text{-}comp}$ (in)
Chandler Creek – 40’ Span	880	164000	28.0	13.3	840	159000	27.5	13.8
Chandler Creek – 60’ Span	1020	282000	30.2	17.1	970	272000	29.5	17.8
Lake LBJ	1040	286000	30.2	17.0	1100	334000	31.7	15.5
Lampasas River	920	257000	28.4	18.1	890	251000	28.0	18.5
Willis Creek	865	235000	27.6	18.4	940	270000	29.1	16.9
Wimberley	890	145000	26.0	14.3	930	173000	27.3	13.0
Slaughter Creek	1470	714000	39.4	22.6	1480	912000	42.1	19.9
Nolanville	1510	743000	40.3	22.7	1360	687000	38.4	24.6

lower-bound concrete strengths. Table 2.10 shows the composite section properties calculated using the upper-bound concrete strengths.

Table 2.9 Adjusted Composite Section Properties – Lower Bound

Bridge Name	Interior Section				Exterior Section			
	A_{comp} (in^2)	I_{comp} (in^4)	$y_{b\text{-}comp}$ (in)	$y_{t\text{-}comp}$ (in)	A_{comp} (in^2)	I_{comp} (in^4)	$y_{b\text{-}comp}$ (in)	$y_{t\text{-}comp}$ (in)
Chandler Creek – 40' Span	960	169000	28.9	12.4	910	165000	28.3	12.9
Chandler Creek – 60' Span	1060	284000	30.8	16.5	1010	275000	30.1	17.1
Lake LBJ	1090	291000	31.0	16.3	1130	344000	32.7	14.6
Lampasas River	970	237000	29.3	17.2	940	258000	28.9	17.6
Willis Creek	890	239000	28.2	17.8	950	276000	29.7	16.3
Wimberley	920	147000	26.6	13.7	930	176000	27.9	12.3
Slaughter Creek	1490	713000	40.0	22.0	1550	960000	43.5	18.5
Nolanville	1680	799000	42.5	20.5	1500	745000	40.5	22.5

Table 2.10 Adjusted Composite Section Properties – Upper Bound

Bridge Name	Interior Section				Exterior Section			
	A_{comp} (in^2)	I_{comp} (in^4)	$y_{b\text{-}comp}$ (in)	$y_{t\text{-}comp}$ (in)	A_{comp} (in^2)	I_{comp} (in^4)	$y_{b\text{-}comp}$ (in)	$y_{t\text{-}comp}$ (in)
Chandler Creek – 40' Span	900	163000	28.3	13.0	850	158000	27.8	13.5
Chandler Creek – 60' Span	1010	274000	30.3	17.0	960	265000	29.6	17.7
Lake LBJ	1030	280000	30.4	16.9	1070	327000	31.9	15.4
Lampasas River	900	246000	28.3	18.1	870	241000	27.9	18.6
Willis Creek	870	234000	27.9	18.1	920	268000	29.3	16.7
Wimberley	90	144000	26.4	13.9	910	171000	27.6	12.7
Slaughter Creek	1470	700000	39.7	22.3	1570	932000	43.3	18.7
Nolanville	1550	748000	40.9	22.1	1400	693000	38.9	24.1

2.4 CONCRETE STRENGTHS

Perhaps one of the most important parameters in a research project of this nature is the strength of concrete in the various bridge components. Due to the complex nature of concrete, the task of quantifying its strength can be difficult. Destructive material testing, such as coring, can be extremely helpful in estimating in-situ concrete strengths; however, none of the bridges were available for coring during field testing. Therefore, an empirical approach was used to estimate the actual concrete strengths. In this study, three different approaches were taken to obtain the concrete strengths used in the analyses.

The first approach was to simply use the specified minimum concrete strengths for design, which were found on the contract drawings. However, given that concrete is constantly gaining strength over time, and that a concrete supplier will rarely deliver concrete to a project that only reaches the specified design strength, this approach is the most conservative, but also the most certain.

The second approach for estimating actual concrete strengths was to gather and interpret any available material test data. The prestressed concrete plants that produced the girders in these bridges were required to report concrete strengths at various times to ensure quality, and these test data were obtained from the Texas Department of Transportation. Once the data were gathered and analyzed, the average concrete strengths were obtained. For this approach, the present concrete strengths were assumed to be approximately equal to the average strengths, taken between seven and twenty-one days. While this approach is still conservative, due to the fact that the concrete has gained strength since casting, it is a much better indication of actual concrete strengths when compared to the design values. The concrete strengths obtained in this manner are designated the "lower-bound" values.

The final approach, and most abstract, involved taking the average strengths from the second approach and extrapolating to the present using predictive equations that first appeared in the 1991 CEB-FIP Model Code (Comite Euro-International Du Beton 1991). While the equations were tailored to the conditions of the bridges in this study, the resulting concrete strengths seemed to be very high relative to the design strengths and at times appeared unrealistic based on the available concrete technology during the era in which some of the older bridges were constructed. As a result, these values are designated as the "upper-bound" values, and only the lower-bound values were used in the analyses.

Tables 2.11 through 2.13 show the concrete strengths obtained using the three approaches described above. Table 2.11 shows the design concrete strengths, Table 2.12 shows the lower-bound concrete strengths, and Table 2.13 shows the upper-bound concrete strengths. For concrete material test data and a detailed description of the third approach, refer to Appendix A.

Table 2.11 Design Concrete Strengths

Bridge Name	Girder		Deck		Parapet/Curb
	$f'_{c\text{-interior}}$ (psi)	$f'_{c\text{-exterior}}$ (psi)	$f'_{c\text{-slab}}$ (psi)	$f'_{c\text{-panel}}$ (psi)	f'_{c} (psi)
Chandler Creek – 40' Span	5000	5000	3000	N/A	N/A
Chandler Creek – 60' Span	5000	5000	3000	N/A	N/A
Lake LBJ	5000	5000	3000	N/A	3000
Lampasas River	5100	5100	3000	N/A	N/A
Willis Creek	5000	5000	3000	N/A	3000
Wimberley	5000	5000	3000	N/A	3000
Slaughter Creek	5000	7700	3600	5000	3600
Nolanville	6200	6200	3600	N/A	N/A

Table 2.12 Assumed Concrete Strengths – Lower Bound

Bridge Name	Girder		Deck		Parapet/Curb
	$f'_{c\text{-interior}}$ (psi)	$f'_{c\text{-exterior}}$ (psi)	$f'_{c\text{-slab}}$ (psi)	$f'_{c\text{-panel}}$ (psi)	f'_{c} (psi)
Chandler Creek – 40' Span	7500	7500	6000	N/A	N/A
Chandler Creek – 60' Span	8700	8700	6000	N/A	N/A
Lake LBJ	8000	8000	6000	N/A	6000
Lampasas River	8200	8200	6000	N/A	N/A
Willis Creek	8600	8600	6000	N/A	6000
Wimberley	8500	8500	6000	N/A	6000
Slaughter Creek	8300	12000	7200	8300	7200
Nolanville	9000	9000	7200	N/A	N/A

Table 2.13 Assumed Concrete Strengths – Upper Bound

Bridge Name	Girder		Deck		Parapet/Curb
	$f'_{c\text{-interior}}$ (psi)	$f'_{c\text{-exterior}}$ (psi)	$f'_{c\text{-slab}}$ (psi)	$f'_{c\text{-panel}}$ (psi)	f'_{c} (psi)
Chandler Creek – 40' Span	10400	10400	6700	N/A	N/A
Chandler Creek – 60' Span	11600	11600	6700	N/A	N/A
Lake LBJ	10800	10800	6700	N/A	6700
Lampasas River	12700	12700	6700	N/A	N/A
Willis Creek	10600	10600	6700	N/A	6700
Wimberley	10300	10300	6700	N/A	6700
Slaughter Creek	9900	15000	7200	9900	7200
Nolanville	10900	10900	7200	N/A	N/A

2.5 DIAPHRAGM DETAILS

For prestressed concrete girder bridges, as well as any other type of highway bridge, the issue of how diaphragm configuration and placement affect live load distribution arises. As mentioned in Chapter 1, one of the objectives of this study was to determine if different diaphragm configurations yield significantly different live load distribution patterns. As such, one aspect of the field survey of each bridge was to measure the diaphragm dimensions and record their locations.

Figures 2.36 through 2.51 show the diaphragm dimensions and their locations with respect to the bridge layout. All diaphragms are made of concrete, and in general, they appear in the field as they were shown on contract drawings. Figure 2.35 shows the dimensions that are used to describe both the end diaphragms and the intermediate diaphragms. The dimensions measured in the field are shown in Table 2.14.

Table 2.14 Diaphragm Dimensions

Bridge Name	$h_{diaphragm}$ (in)	h_{clear} (in)	$h_{diagonal}$ (in)	$t_{diaphragm}$ (in) End	$t_{diaphragm}$ (in) Intermediate
Chandler Creek – 40’ Span	14.75	10.25	N/A	8.5	8.25
Chandler Creek – 60’ Span	20.75	11.5	N/A	8.25	8.25
Lake LBJ	21	12	N/A	8.5	8
Lampasas River	22.5	14.5	N/A	8.5	8.5
Willis Creek	25.75	12	5	8	8.5
Wimberley	15.5	11	5	8.5	8.5
Slaughter Creek	52	N/A	N/A	49	N/A
Nolanville	32	14	N/A	8	8

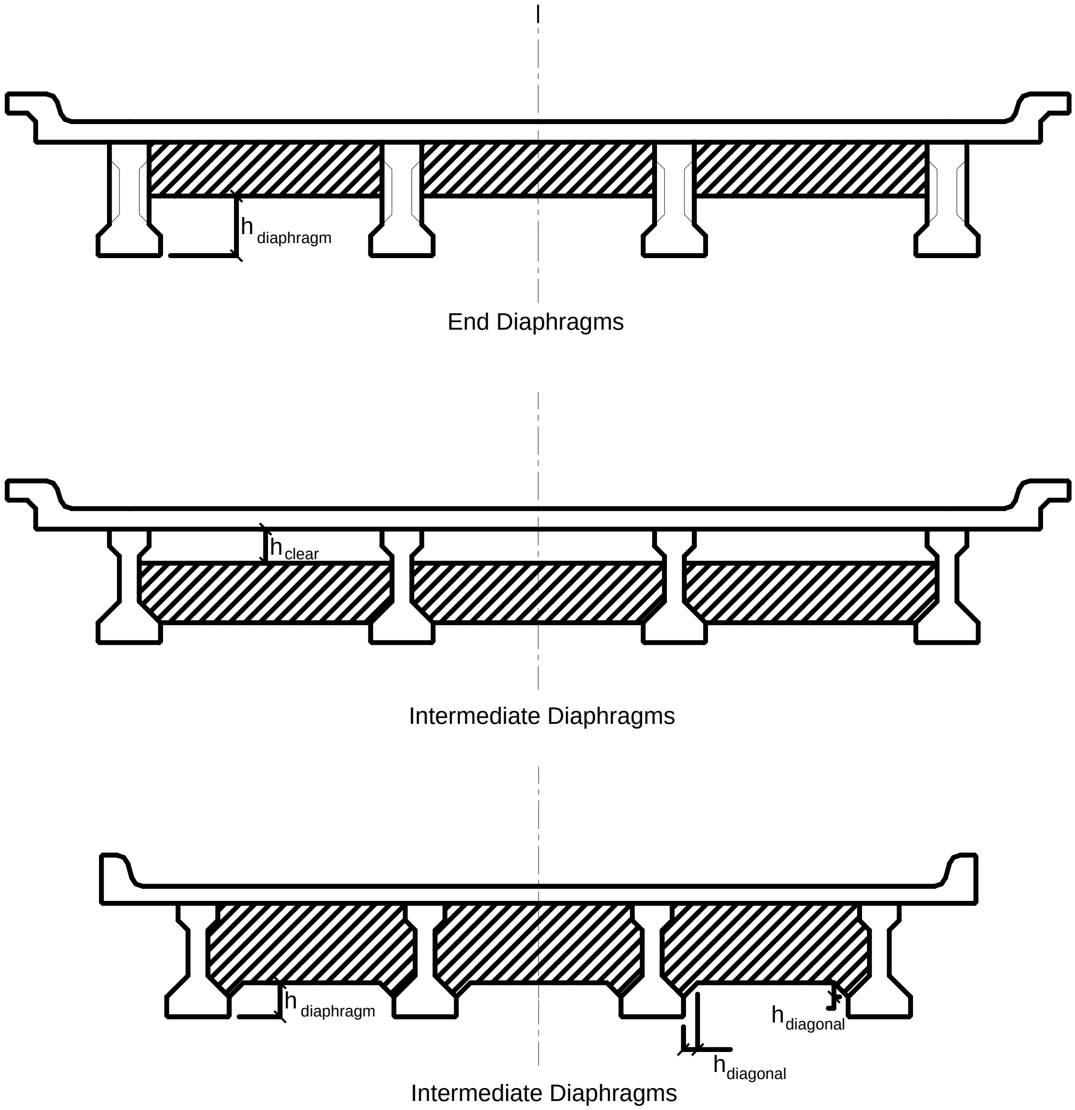

Figure 2.35 Diaphragm Measurements

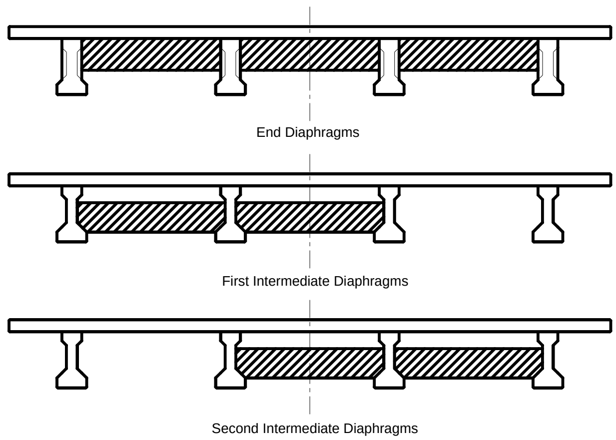

Figure 2.36 Diaphragm Configuration – Chandler Creek Bridge – 40' Span

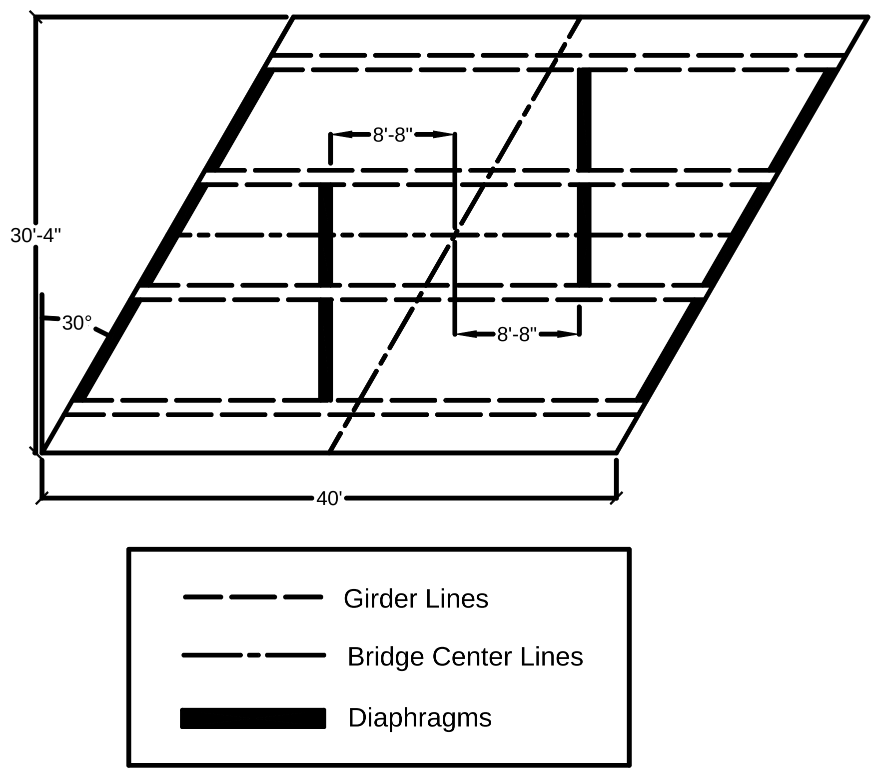

Figure 2.37 Diaphragm Layout – Chandler Creek Bridge – 40' Span

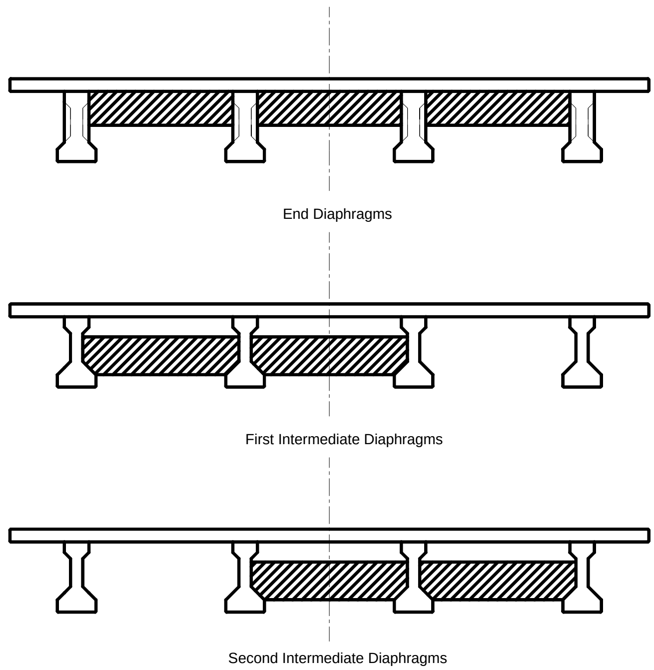

Figure 2.38 Diaphragm Configuration – Chandler Creek Bridge – 60' Span

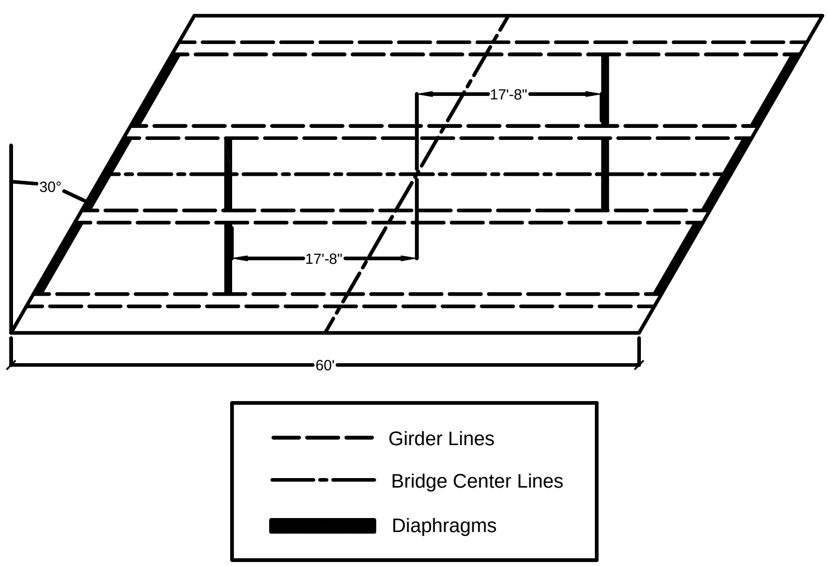

Figure 2.39 Diaphragm Layout – Chandler Creek Bridge- 60' Span

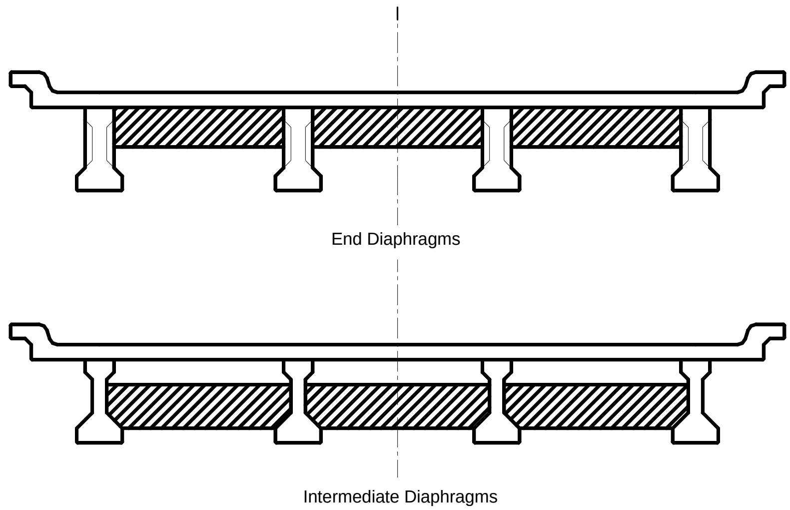

Figure 2.40 Diaphragm Configuration – Lake LBJ Bridge

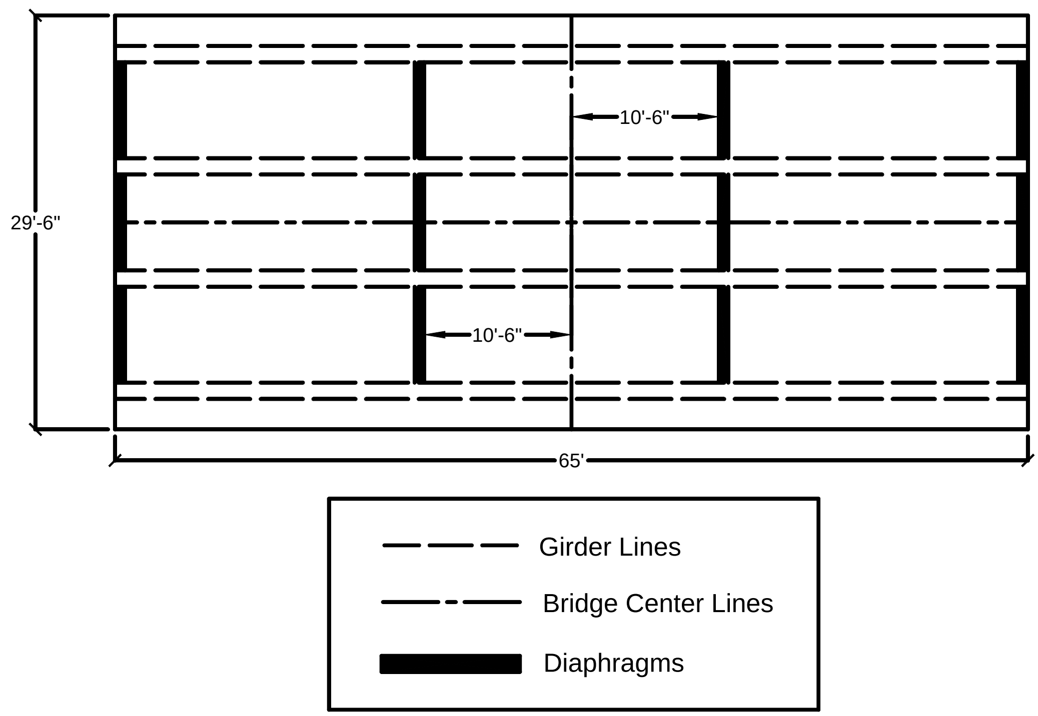

Figure 2.41 Diaphragm Layout – Lake LBJ Bridge

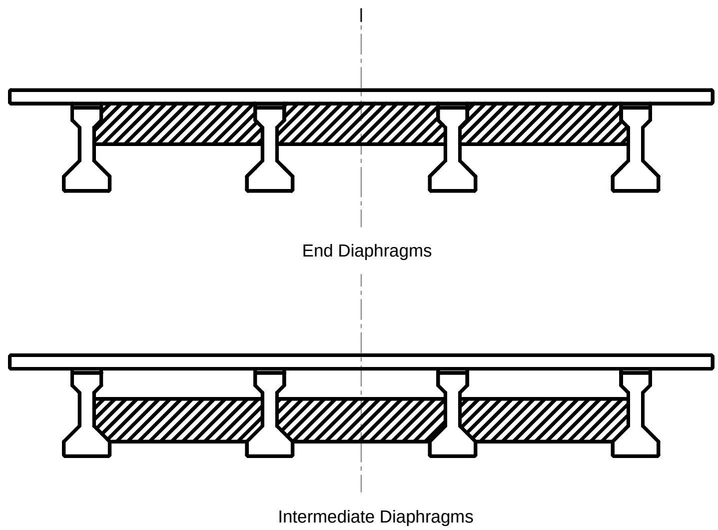

Figure 2.42 Diaphragm Configuration – Lampasas River Bridge

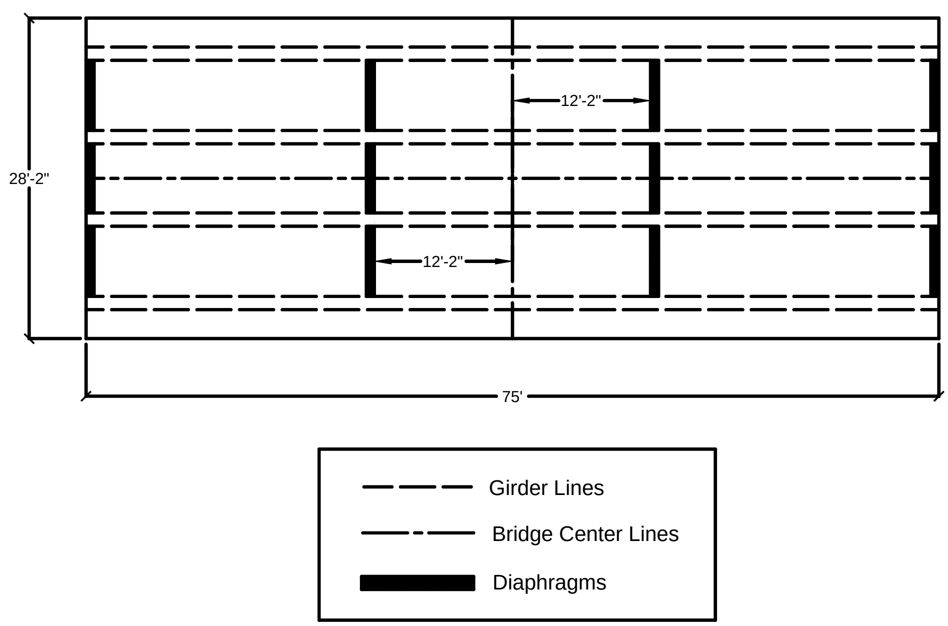

Figure 2.43 Diaphragm Layout – Lampasas River Bridge

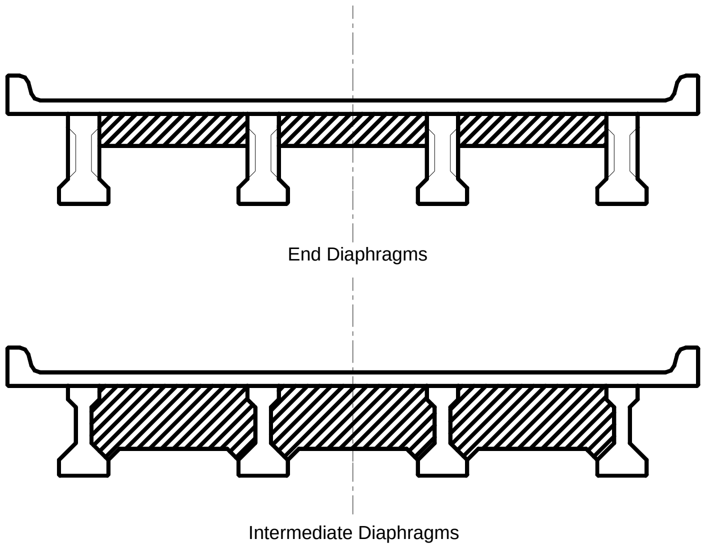

Figure 2.44 Diaphragm Configuration – Willis Creek Bridge

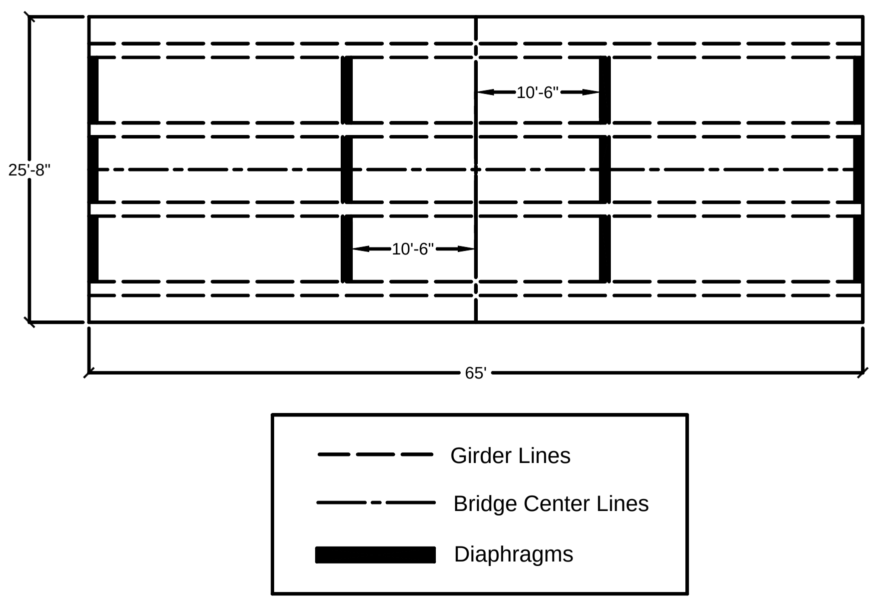

Figure 2.45 Diaphragm Layout – Willis Creek Bridge

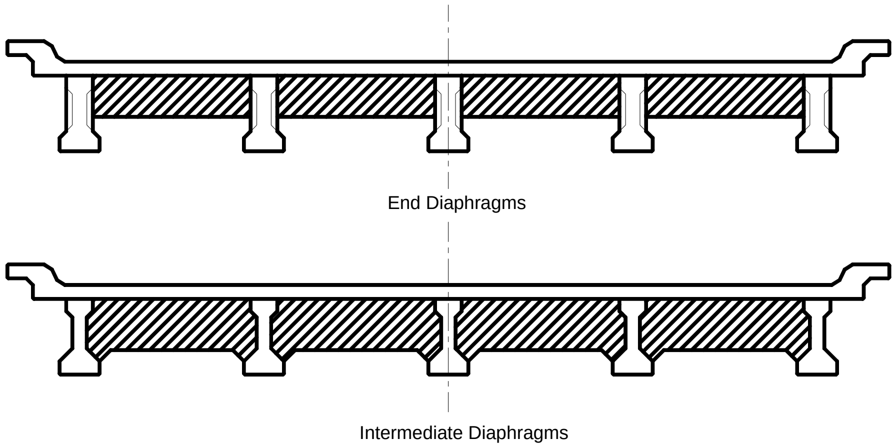

Figure 2.46 Diaphragm Configuration – Wimberley Bridge

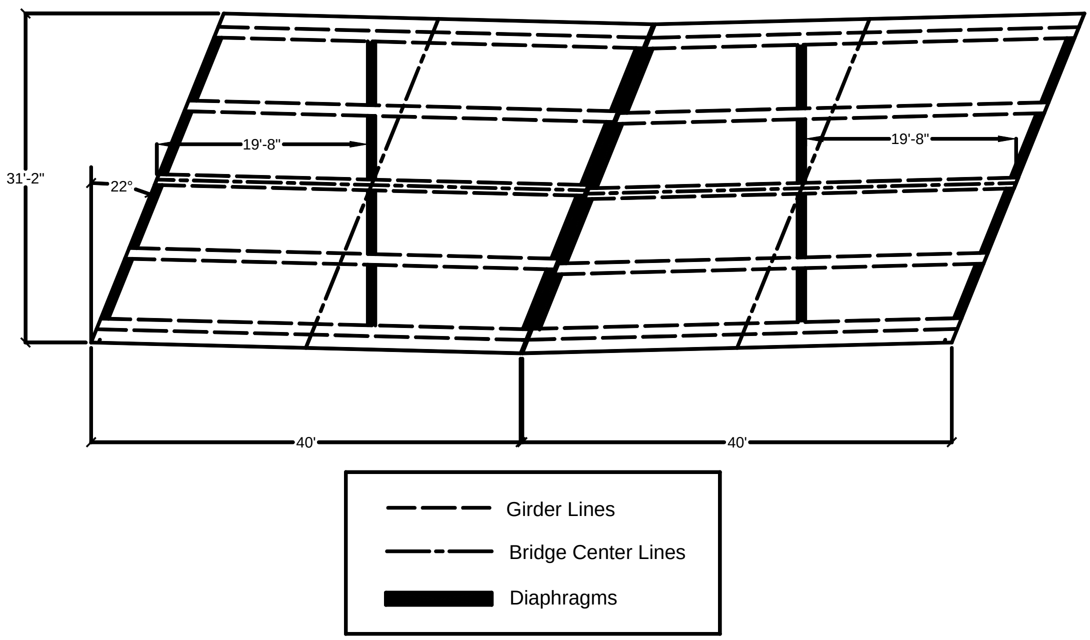

Figure 2.47 Diaphragm Layout – Wimberley Bridge

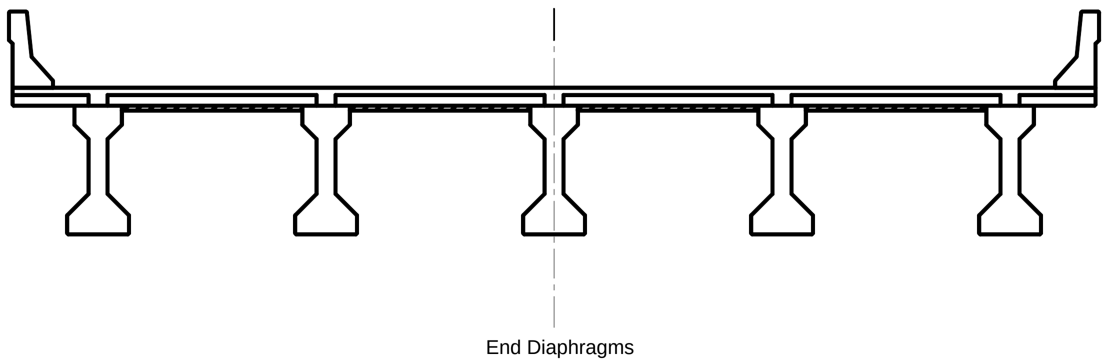

Figure 2.48 Diaphragm Configuration – Slaughter Creek Bridge

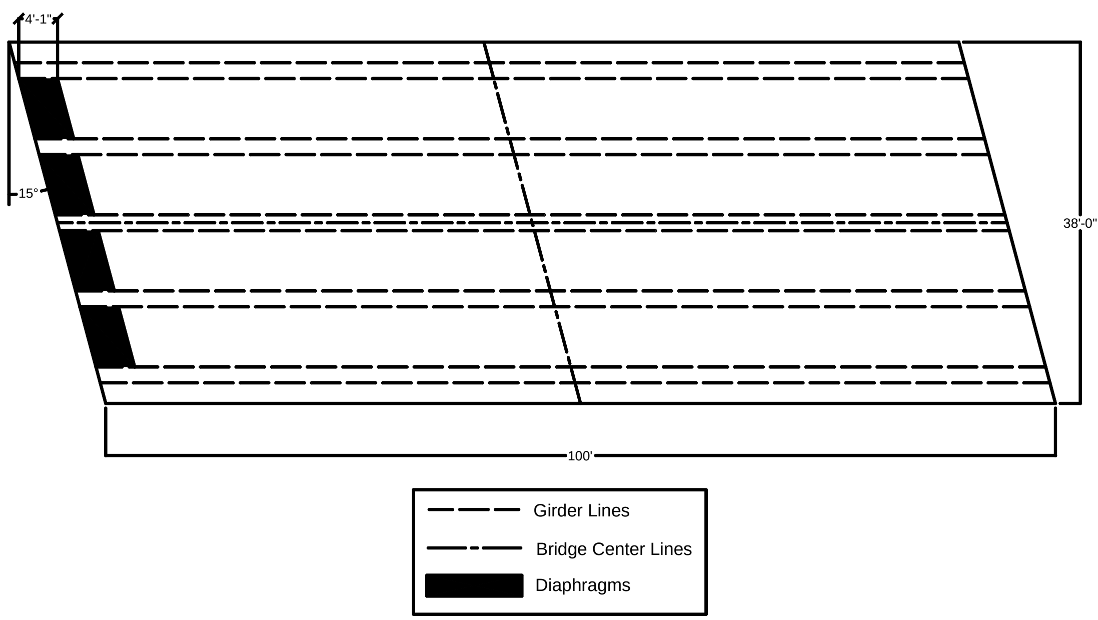

Figure 2.49 Diaphragm Layout – Slaughter Creek Bridge

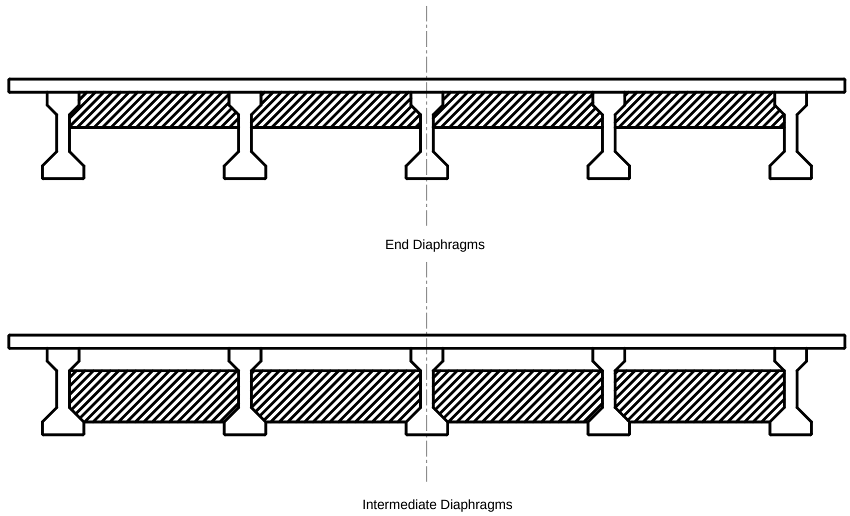

Figure 2.50 Diaphragm Configuration – Nolanville Bridge

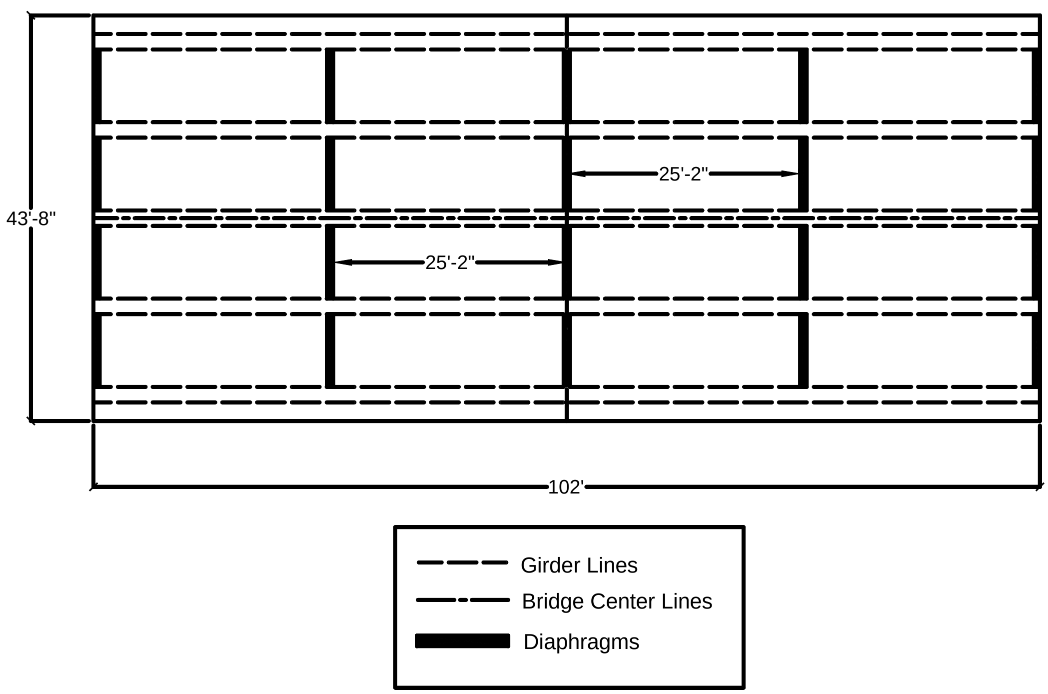

Figure 2.51 Diaphragm Layout – Nolanville Bridge

Chapter 3 – Description of Test Procedure

This chapter describes the load testing procedures used in Project 1895 and Project 2986. The first section contains information about the data acquisition system that was used in the testing of all seven bridges. The second section describes the strain gages used during load testing, including their placement on the prestressed concrete girders. Finally, the third section deals with the loading vehicles used to test each bridge, including the vehicle dimensions, axle weights, and test configurations.

3.1 DATA ACQUISITION SYSTEM

The data acquisition system used in Project 1895 is the same system used in Project 2986. The system is composed of a laptop computer to save the recorded data, a data acquisition unit made by Campbell-Scientific and designated the CR9000, a 12-volt DC source, a "clicker" to record truck positions, primary cables, junction boxes, secondary cables, completion boxes, and finally, the strain gages. Figure 3.1 is a simple diagram of how all these components are arranged, and Figure 3.2 shows a photograph of some of the system components. Figure 3.3 shows an example of the arrangement of the various components in the data acquisition system.

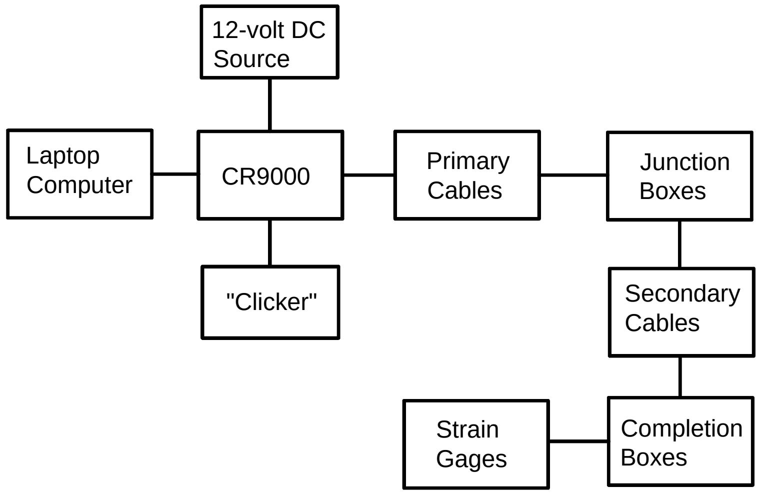

Figure 3.1 Components of the Data Acquisition System

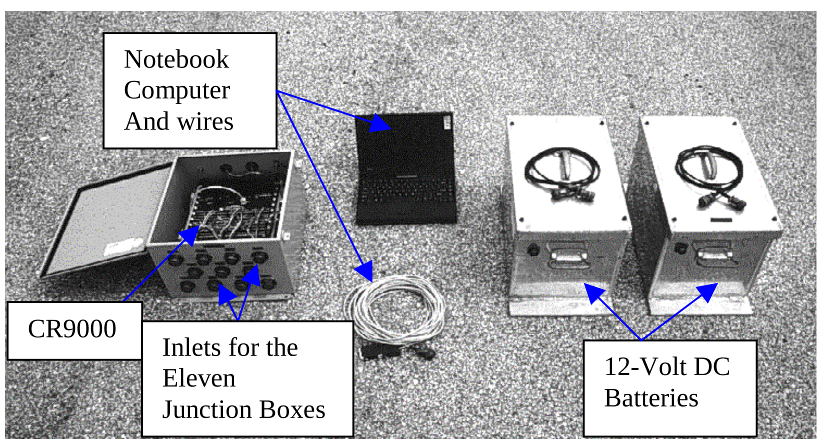

Figure 3.2 Data Acquisition System Hardware (Matsis 1999)

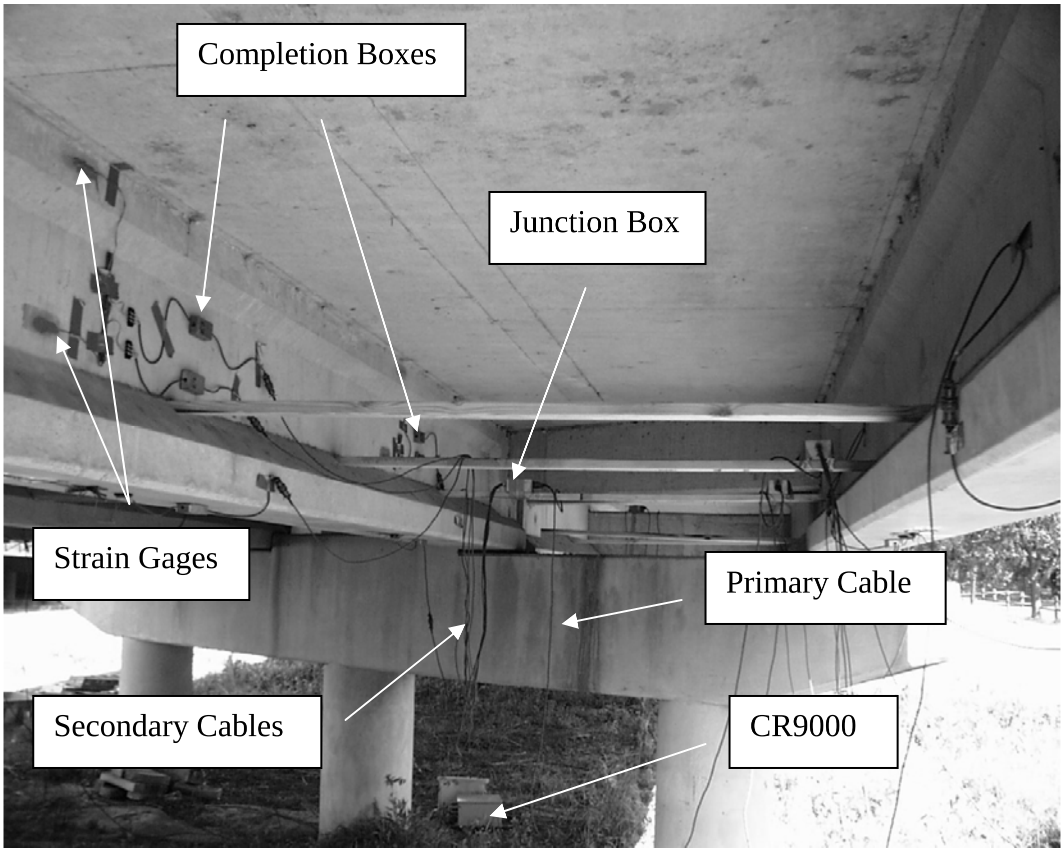

Figure 3.3 Arrangement of CR 9000, Primary Cables, Junction Boxes, Secondary Cables, Completion Boxes, and Strain Gages

Before each load test, all strain gages were set to zero. Then, as the loading vehicles passed over each bridge, their location was recorded by using the "clicker," which manually drops all readings of excitation voltage to zero, "marking" the truck location in the output file. While the load tests were being conducted, the CR9000 sampled the strain gage output voltages at a constant rate of ten Hertz.

The entire data acquisition system was grounded during each test to ensure electrical stability. Both the primary and secondary cables were shielded from electromagnetic interference (EMI), and the junction boxes and completion boxes were designed to minimize fluctuations in output voltage, or "noise." The CR9000 allowed fifty-five channels of input. During Project 1895, the entire data acquisition system was thoroughly inspected to ensure that none of the cables were damaged, all connections within the junction boxes and completion boxes were sound, and the CR9000 data acquisition unit was functioning properly. In addition, the software used to record data from the CR9000 unit was updated to the most current version available from Campbell-Scientific.

3.2 STRAIN GAGES

In both Project 1895 and Project 2986, concrete strains were measured using 120-ohm electrical resistance strain gages. The gage length for all gages is two inches. The actual strain gage was slightly longer to permit proper installation. The gages used in Project 2986 were not temperature-compensating when purchased from the manufacturer, but they were modified with a third wire by the researchers in order to make them so (Matsis 1999). The gages used in Project 1895 were manufactured with three wires, and thus were temperature-compensating without any further modification.

To install the gages, the gage locations were carefully measured and marked on each prestressed concrete girder. Then, the girders were agitated with a wire brush and cleaned with rubbing alcohol. A thin coat of five-minute epoxy was then applied in a two-inch by six-inch rectangle around the intended gage location. Once the epoxy layer was allowed to cure for twenty-four hours, it was sanded to the minimum possible thickness using an electric sander. Once the epoxy surface was cleaned with rubbing alcohol, the gages were installed over the epoxy rectangles according to the manufacturer's instructions. Careful consideration was given to ensure that the gages were installed precisely over their intended location, parallel to the longitudinal axis of the girders.

For the bridges in Project 1895, strain gages were placed at the quarter span, midspan, and three-quarter span to evaluate the consistency of measured data. Only the midspan data are reported here. Figure 3.4 shows the approximate locations of the "bottom," "web," and "top" gages on a prestressed concrete girder. Figures 3.5 and 3.6 show an example of the placement of web and top gages, and a bottom gage, respectively. Because the curb conditions varied for each bridge, the "curb" gages were placed in the most convenient position allowable. Locations of the "curb" gages, as well as detailed gage locations for each bridge, are presented in Appendix B.

For the bridges in Project 2986, strain gages were placed at various positions along the span length according to diaphragm locations. There are no curbs on the Nolanville bridge, and the Slaughter Creek bridge has a thirty-two inch tall concrete parapet on which strain gages were placed. Figure 3.7 shows the approximate locations of the "bottom," "middle," and "top" gages on the prestressed concrete girders in Project 2986.

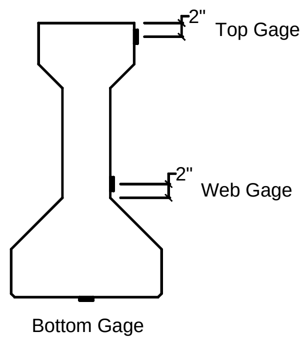

Figure 3.4 Approximate Gage Locations for Project 1895

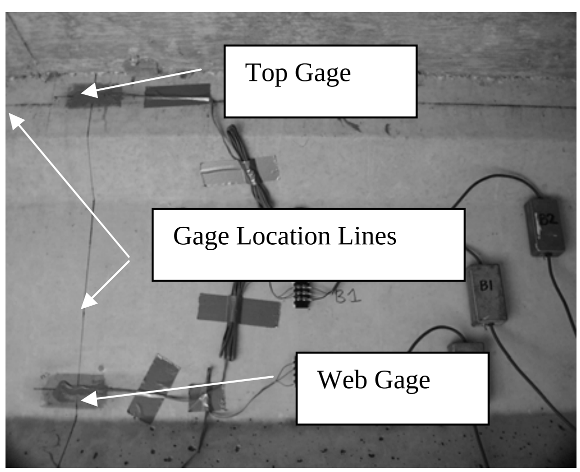

Figure 3.5 Example Placement of Web and Top Strain Gages

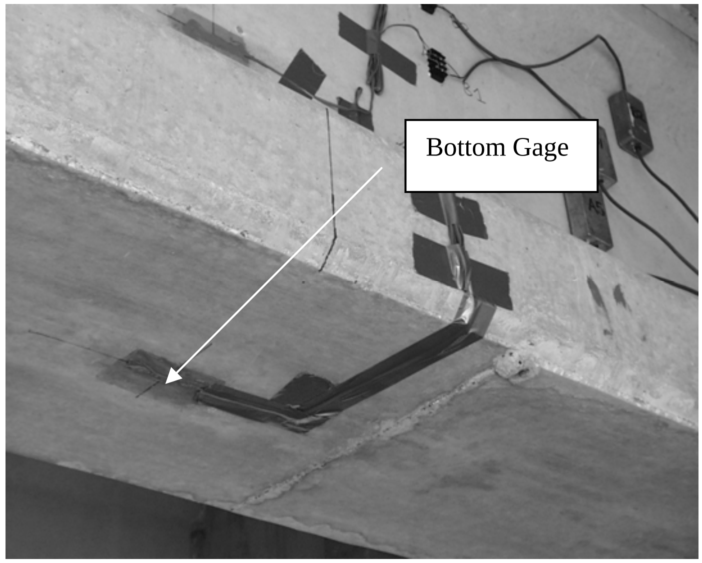

Figure 3.6 Example Placement of Bottom Strain Gage

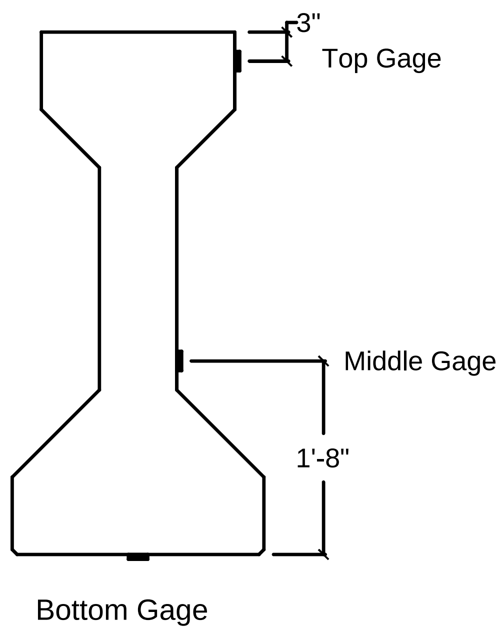

Figure 3.7 Approximate Gage Locations for Project 2986

3.3 TEST VEHICLES

3.3.1 Description of Test Vehicles

For the load tests in this study, two types of test vehicles were used for live loading. The first type of test vehicle, used on all bridges, was a ten cubic-yard dump truck, loaded with fill, that was provided by the Texas Department of Transportation. At the Nolanville bridge, the U.S. Army provided a Heavy Equipment Transportation System (HETS).

Figure 3.8 shows an example of a dump truck used in the load tests. Figures 3.9 through 3.11 show diagrams of the wheel and axle layout for the various dump trucks used. Figure 3.9 shows the layout for all the dump trucks used in Project 1895. Figure 3.10 shows the layout of one of the dump trucks used at the Slaughter Creek bridge, designated D1. Figure 3.11 shows the layout of the rest of the dump trucks used at both the Slaughter Creek bridge and the Nolanville bridge, designated D2 and D3, and D4, respectively.

Figure 3.8 Ten Cubic-Yard Dump Truck Used for Load Testing

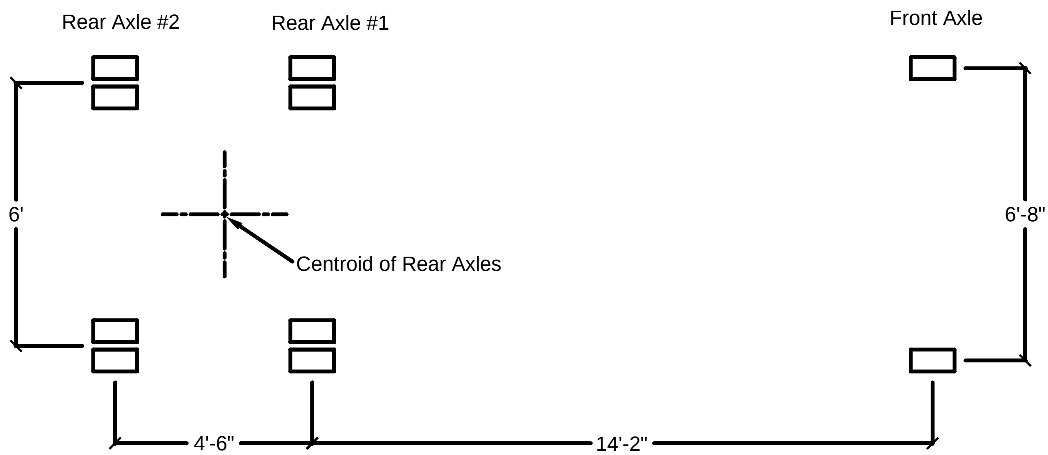

Figure 3.9 Wheel and Axle Locations for Dump Trucks Used in Project 1895

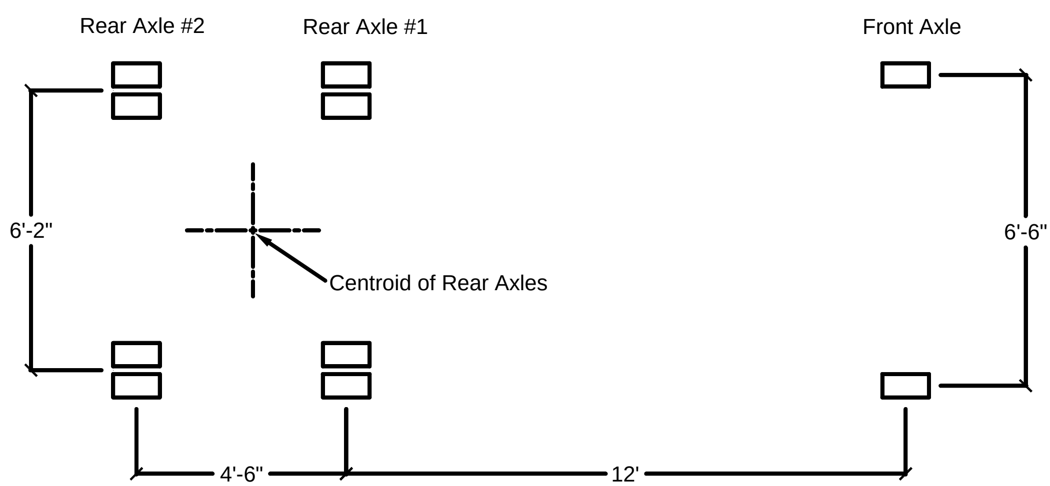

Figure 3.10 Wheel and Axle Locations for Dump Truck D1 Used at the Slaughter Creek Bridge

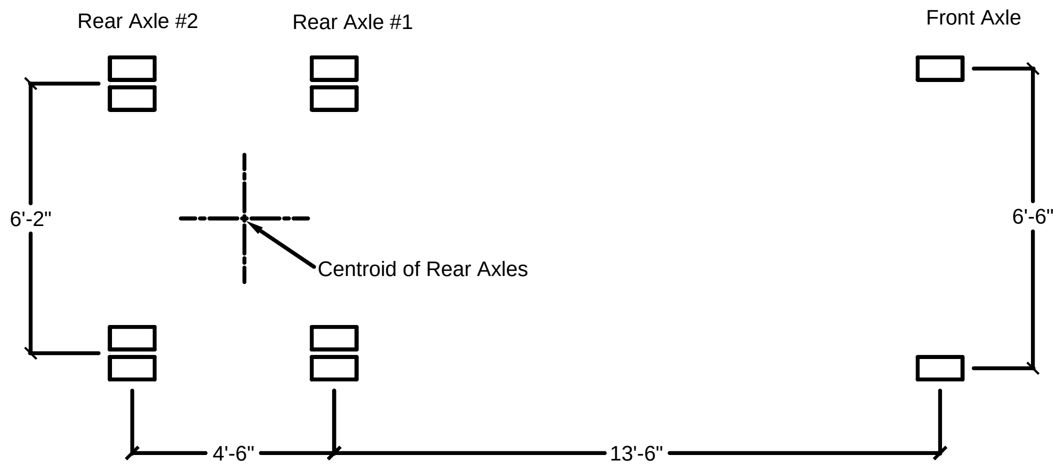

Figure 3.11 Wheel and Axle Locations Dump Trucks D2, D3, and D4 Used at the Slaughter Creek Bridge and Nolanville Bridge

Before arriving at the bridge sites, the dump trucks were loaded to capacity with fill, then the axle weights were measured at a weigh station. During load tests at the Chandler Creek bridge and the Willis Creek bridge, axle weights were also measured in the field using a portable wheel scale provided by the Travis County Sheriff's Department, which measured to the nearest fifty pounds. Those weights were used in analyses of those two bridges. Table 3.1 lists the axle weights for all dump trucks used in both Project 1895 and Project 2986.

Table 3.1 Dump Truck Axle Weights

Bridge Name	Truck Number	Front Axle (kips)	First Rear Axle (kips)	Second Rear Axle (kips)	Total Weight (kips)
Chandler Creek	1	10.7	15.5	14.3	40.5
	2	11.1	15.0	14.0	40.1
Lake LBJ	1	12.7	18.0	18.0	48.7
	2	10.8	17.6	17.6	46.0
Lampasas River	1	10.9	17.2	17.2	45.3
	2	10.7	16.7	16.7	44.1
Willis Creek	1	12.6	18.6	17.9	49.1
	2	10.6	18.2	17.8	46.6
Wimberley	1	13.3	18.6	18.6	50.5
	2	9.9	18.0	18.0	45.9
Slaughter Creek	D1	11.8	14.3	14.3	40.4
	D2	11.6	15.4	15.4	42.4
	D3	10.2	14.8	14.8	39.8
Nolanville	D4	10.1	18.2	18.2	46.5

At the Nolanville bridge, the U.S. Army provided a Heavy Equipment Transportation System (HETS) for loading. Figure 3.12 shows a photograph of the HETS with an army tank positioned on the trailer. Figure 3.13 shows a diagram of the axle layout and dimensions of the HETS test vehicle, and Table 3.2 lists the axle weights. The total vehicle weight was 215.2 kips.

Figure 3.12 Heavy Equipment Transportation System (HETS), Provided by the U.S. Army (Matsis 1999)

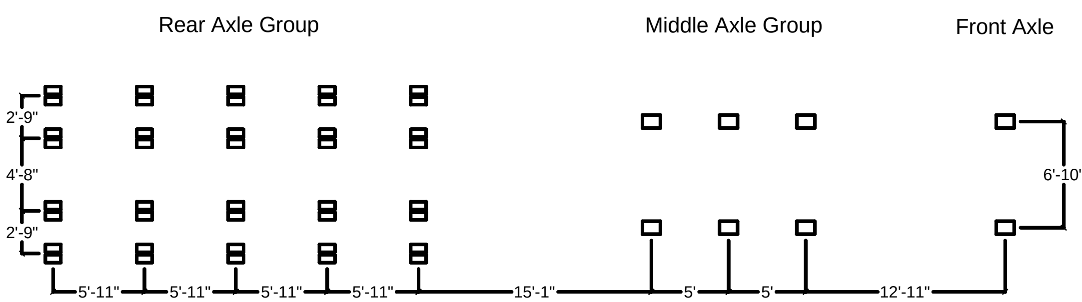

Figure 3.13 Dimensions of the HETS Used at the Nolanville Bridge

Table 3.2 HETS Axle Weights

Axle Designation	Axle Weight (kips)
Front Axle	21.9
Middle Axle #1	19.7
Middle Axle #2	19.2
Middle Axle #3	18.6
Rear Axle #1	23.9
Rear Axle #2	28.9
Rear Axle #3	27.9
Rear Axle #4	28.1
Rear Axle #5	27.0

3.3.2 Test Vehicle Loading Configurations

In order to analyze various levels of bridge response, several configurations of the test vehicles were used. In Project 1895, the loading configurations were designated “back-to-back,” “side-by-side,” and “single-truck.” Figures 3.14 through 3.19 show simple diagrams and photographs of the loading configurations used in Project 1895. The dashed lines indicate the reference lines that were used in aligning the trucks on the bridge spans. In Project 2986, the loading configurations were designated “single-truck,” “combination,” and “HETS.” The single-truck configuration was the same as the single-truck configuration used in Project 1895, and the combination configuration was the same as the side-by-side configuration used in Project 1895.

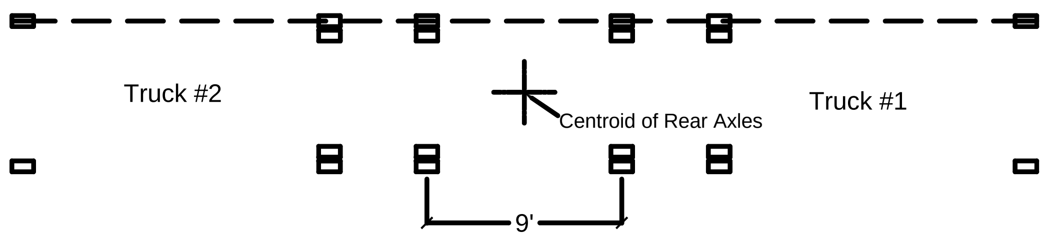

Figure 3.14 Diagram of the Back-to-Back Loading Configuration

Figure 3.15 Photograph of the Back-to-Back Loading Configuration

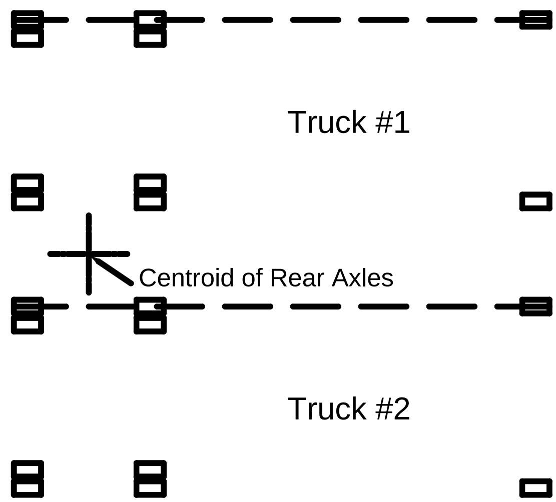

Figure 3.16 Diagram of the Side-by-Side and Combination Loading Configuration

Figure 3.17 Photograph of the Side-by-Side and Combination Loading Configuration

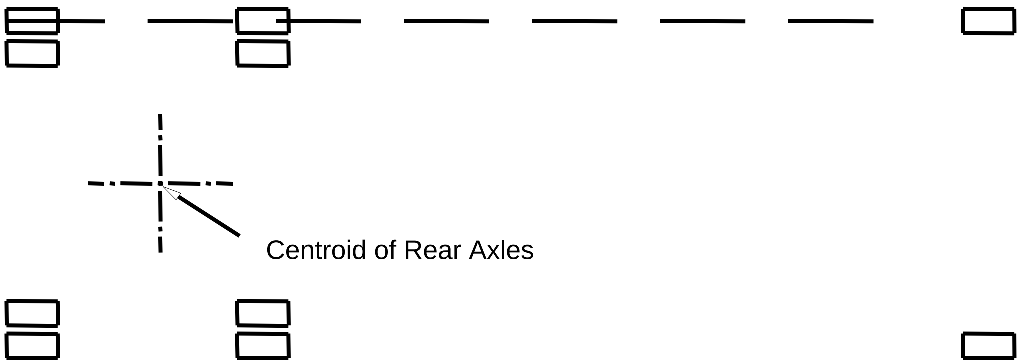

Figure 3.18 Diagram of the Single-Truck Loading Configuration

Figure 3.19 Photograph of the Single-Truck Loading Configuration

3.3.3 Loading Paths

At each bridge, the loading vehicles were driven across the spans along various paths in order to obtain a comprehensive view of the live load distribution. The loading paths were chosen so that the wheels on the loading vehicles were centered between adjacent girders or centered over interior girders. Figures 3.20 through 3.26 show the loading paths for each of the seven bridges.

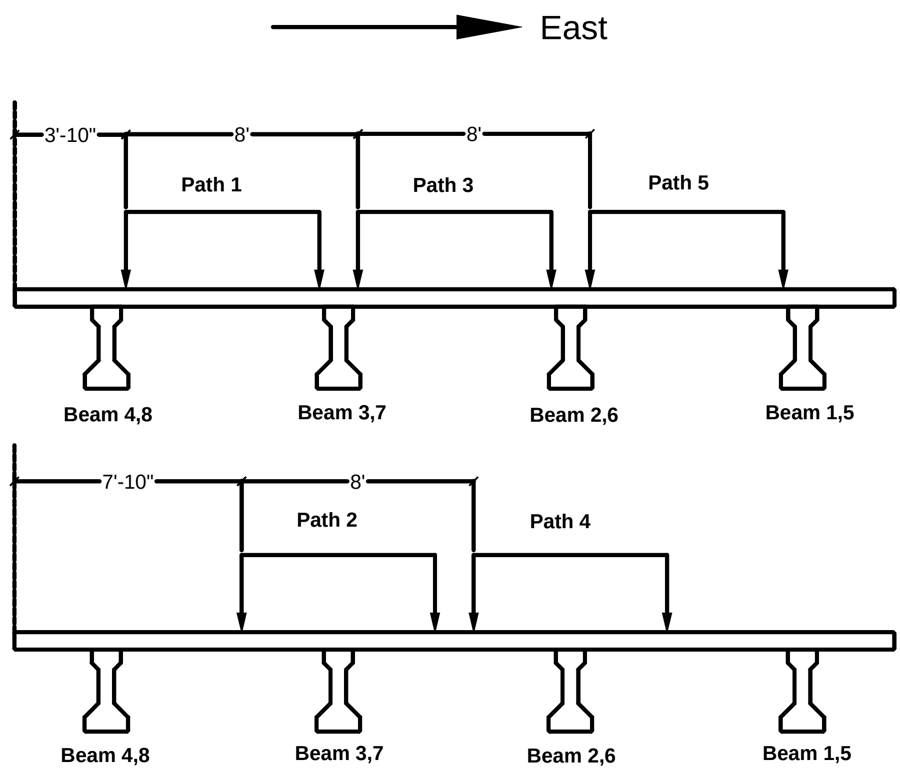

Figure 3.20 Loading Paths at the Chandler Creek Bridge

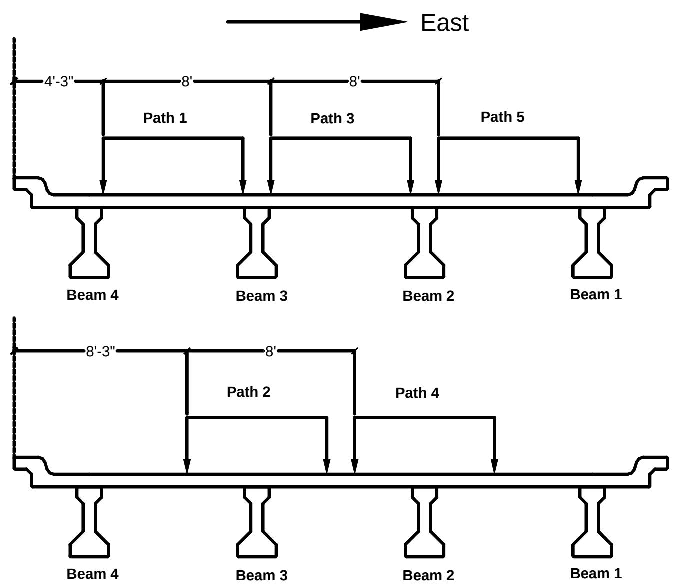

Figure 3.21 Loading Paths at the Lake LBJ Bridge

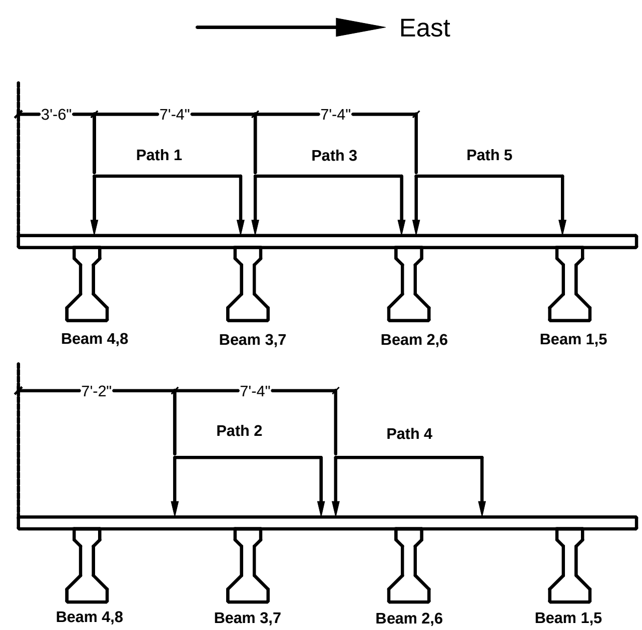

Figure 3.22 Loading Paths at the Lampasas River Bridge

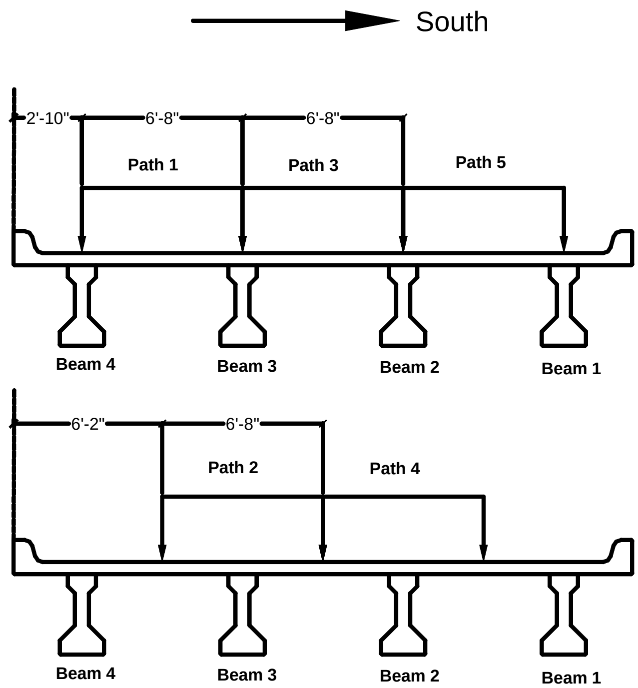

Figure 3.23 Loading Paths at the Willis Creek Bridge

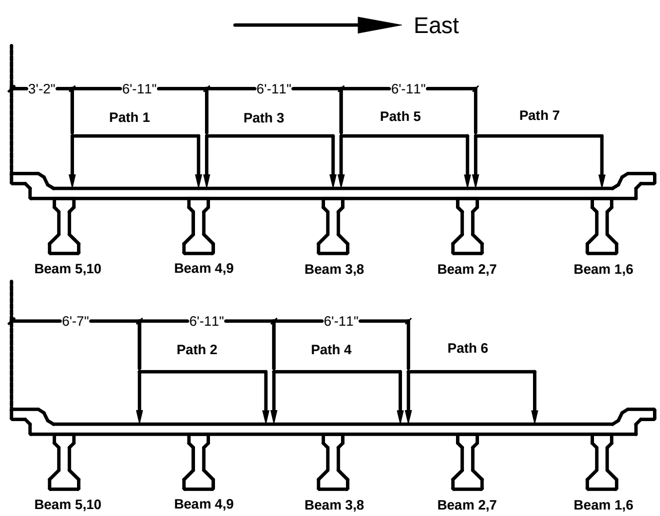

Figure 3.24 Loading Paths at the Wimberley Bridge

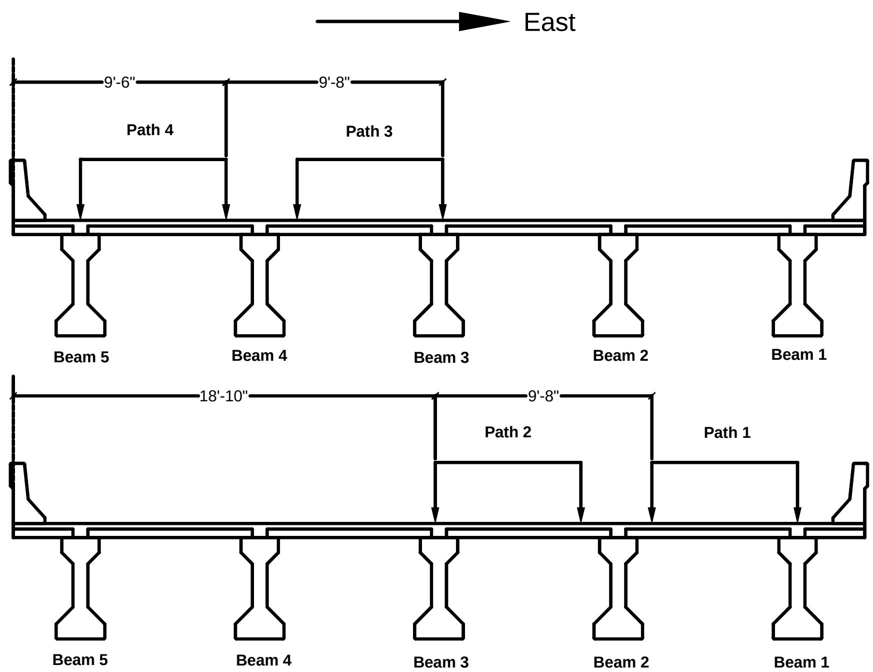

Figure 3.25 Loading Paths at the Slaughter Creek Bridge

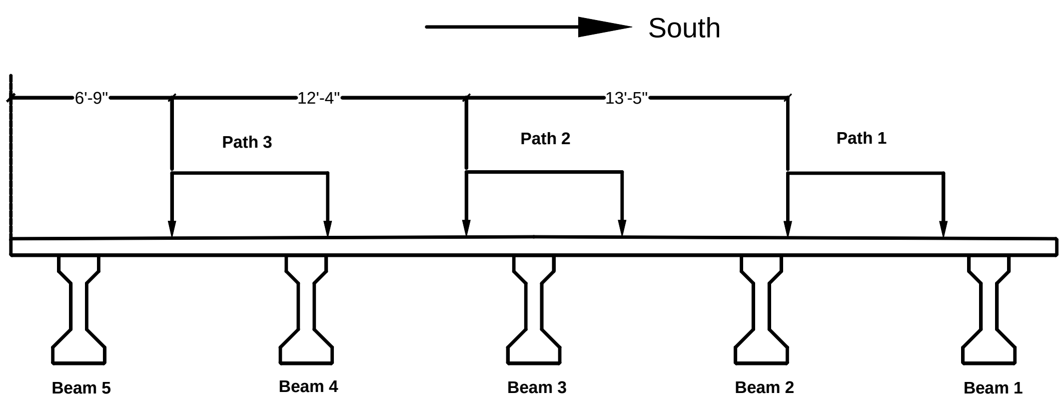

Figure 3.26 Loading Paths at the Nolanville Bridge

3.3.4 Test Runs

At each bridge, every load test was given a number, designated the "run number." The number of total runs over a bridge ranged between ten and twenty-two, depending on the amount of traffic. In general, two runs were completed for each loading path in order to establish repeatability and also for redundancy in case unusable data were collected. Tables 3.3 through 3.9 show the list of test runs for each bridge.

Table 3.3 Test Runs at the Chandler Creek Bridge

Run Number	Loading Configuration	Truck 1 Path Number	Truck 2 Path Number
1	Side-by-Side	1	4
2	Side-by-Side	1	4
3	Side-by-Side	1	5
4	Side-by-Side	1	5
5	Side-by-Side	2	5
6	Side-by-Side	2	5
7	Back-to-Back	1	1
8	Back-to-Back	1	1
9	Back-to-Back	3	3
10	Back-to-Back	3	3
11	Back-to-Back	5	5
12	Back-to-Back	5	5
13	Single-Truck	1	1
14	Single-Truck	3	3
15	Single-Truck	5	5

Table 3.4 Test Runs at the Lake LBJ Bridge

Run Number	Loading Configuration	Truck 1 Path Number	Truck 2 Path Number
1	Back-to-Back	1	1
2	Back-to-Back	1	1
3	Back-to-Back	2	2
4	Back-to-Back	2	2
5	Back-to-Back	3	3
6	Back-to-Back	3	3
7	Back-to-Back	4	4
8	Side-by-Side	1	5
9	Side-by-Side	1	5
10	Single-Truck	1	1
11	Single-Truck	3	3
12	Single-Truck	5	5
13	Side-by-Side	1	5
14	Side-by-Side	1	5
15	Side-by-Side	1	5

Table 3.5 Test Runs at the Lampasas River Bridge

Run Number	Loading Configuration	Truck 1 Path Number	Truck 2 Path Number
1	Back-to-Back	1	1
2	Back-to-Back	1	1
3	Back-to-Back	1	1
4	Back-to-Back	2	2
5	Back-to-Back	2	2
6	Back-to-Back	3	3
7	Back-to-Back	3	3
8	Side-by-Side	1	5
9	Side-by-Side	1	5
10	Single-Truck	1	1
11	Single-Truck	3	3
12	Single-Truck	5	5
13	Side-by-Side	1	5
14	Side-by-Side	1	5
15	Back-to-Back	1	1
16	Back-to-Back	1	1

Table 3.6 Test Runs at the Willis Creek Bridge

Run Number	Loading Configuration	Truck 1 Path Number	Truck 2 Path Number
1	Side-by-Side	1	5
2	Side-by-Side	1	5
3	Back-to-Back	1	1
4	Back-to-Back	1	1
5	Back-to-Back	1	1
6	Back-to-Back	1	1
7	Back-to-Back	2	2
8	Back-to-Back	2	2
9	Back-to-Back	3	3
10	Back-to-Back	3	3
11	Back-to-Back	4	4
12	Back-to-Back	4	4
13	Back-to-Back	5	5
14	Back-to-Back	5	5
15	Single-Truck	1	1
16	Single-Truck	2	2
17	Single-Truck	3	3
18	Single-Truck	4	4
19	Single-Truck	5	5
20	Side-by-Side	1	5

Table 3.7 Test Runs at the Wimberley Bridge

Run Number	Loading Configuration	Truck 1 Path Number	Truck 2 Path Number
1	Back-to-Back	1	1
2	Back-to-Back	1	1
3	Back-to-Back	4	4
4	Back-to-Back	4	4
5	Back-to-Back	7	7
6	Back-to-Back	7	7
7	Side-by-Side	2	6
8	Side-by-Side	2	6
9	Single-Truck	1	1
10	Single-Truck	2	2
11	Single-Truck	3	3
12	Single-Truck	4	4
13	Single-Truck	5	5
14	Single-Truck	6	6
15	Single-Truck	7	7
16	Side-by-Side	1	7
17	Side-by-Side	1	7

Table 3.8 Test Runs at the Slaughter Creek Bridge

Run Number	Loading Configuration	Truck 1 Path Number	Truck 2 Path Number
1	Single-Truck	4	N/A
2	Single-Truck	4	N/A
3	Single-Truck	3	N/A
4	Single-Truck	3	N/A
5	Single-Truck	2	N/A
6	Single-Truck	2	N/A
7	Single-Truck	1	N/A
8	Single-Truck	1	N/A
9	Combination	1	4
10	Combination	1	4
11	Combination	3	4
12	Combination	3	4
13	Combination	1	2
14	Combination	1	2
15	Single-Truck	4	N/A
16	Single-Truck	4	N/A
17	Single-Truck	3	N/A
18	Single-Truck	3	N/A
19	Single-Truck	2	N/A
20	Single-Truck	2	N/A
21	Single-Truck	1	N/A
22	Single-Truck	1	N/A

Table 3.9 Test Runs at the Nolanville Bridge

Run Number	Loading Configuration	Truck 1 Path Number	Truck 2 Path Number
1	HETS	1	N/A
2	HETS	3	N/A
3	HETS	2	N/A
4	HETS	2	N/A
5	HETS	2	N/A
6	Single-Truck	3	N/A
7	Single-Truck	3	N/A
8	Single-Truck	2	N/A
9	Single-Truck	2	N/A
10	Single-Truck	1	N/A
11	Single-Truck	1	N/A

Chapter 4 – Measured Strains

This chapter contains an overview of the measured strain responses during the various load tests. The first section explains the process for calculating concrete strains from the output voltages measured and recorded by the CR9000 data acquisition system. The second section shows sample strain histories from each bridge, including maximum recorded strains for each girder of each bridge. The third and final section contains a general discussion of noteworthy trends in the measured data.

4.1 CALCULATING CONCRETE STRAINS

During the load tests, the CR9000 data acquisition system measured and recorded voltages that were output from strain gages attached to the bridge girders. From the measured output voltages, microstrains were calculated using Equation 4.1. In this equation, E_{out} is the output voltage from the concrete

$$\mu\varepsilon = \frac{4\left(E_{out}\right)}{(GF)\left(E_{in}\right)} \cdot 10^6 \qquad (4.1)$$

strain gages (millivolts), GF is the strain gage factor, which is 2.09 for concrete strain gages, and E_{in} is the input, or excitation voltage, supplied by the CR9000 unit, and is equal to approximately 5000 mV. During testing, the CR9000 unit gathered the output voltages at a sampling rate of 10 Hz, and then averaged those gathered data using a five-point average before outputting the data to a file. Each piece of output data in the output file is identified as a record, and assigned a record number.

4.2 MEASURED STRAINS

4.2.1 Strain Gage Notation

For convenience, each strain gage was assigned a name based on the beam number and gage location. Figure 4.1 shows a sample gage name and an explanation of the notation used in Project 1895. The beam number was between one and ten, depending on the bridge and the number of instrumented spans. The span location denoted the location of the strain gage in relation to the span

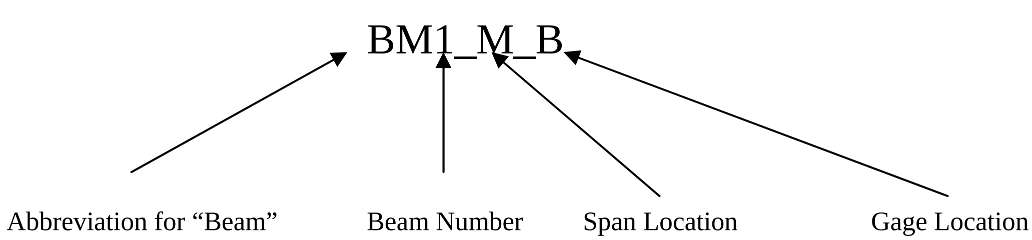

Figure 4.1 Strain Gage Notation Used in Project 1895

length; “Q” for quarter span gages, “M” for midspan gages, and “3Q” for three-quarter span gages. The gage location denotes where the strain gage was placed on the beam; “B” for bottom gages, “W” for gages placed on the web, “T” for gages placed on the top flange, and “C” for gages placed on the concrete curbs.

Figure 4.2 shows a sample gage name and explanation of the notation used in Project 2986. The beam number was between one and five for both the Slaughter Creek and Nolanville bridges. The gage location specified the placement of the strain gages on the beam; “B” for bottom gages, “M” for gages attached to the girder web, and “T” for gages attached to the top flange. Finally, the span location indicates the location of the strain gage in the span, measured from the abutment end. For the Slaughter Creek bridge, the span locations were 50 feet, 66 feet, or 83 feet; for the Nolanville bridge, the span locations were 51 feet or 76.5 feet.

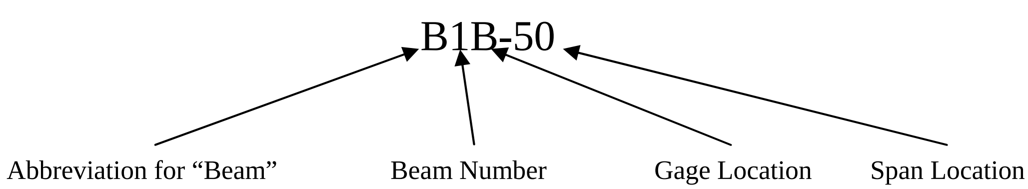

Figure 4.2 Strain Gage Notation Used in Project 2986

For strain gages placed on the concrete parapets at the Slaughter Creek bridge, an alternate form of notation was used, as shown in Figure 4.3. The parapet number identifies the parapet; Parapet 1 is adjacent to Beam 1, and Parapet 2 is adjacent to Beam 5. As before, the span location indicates the location of the strain gage on the span, measured from the abutment end.

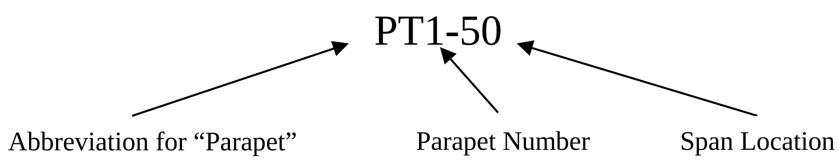

Figure 4.3 Notation Used for Parapet Gages – Project 2986

4.2.2 Sample Strain Histories

This section contains sample strain histories from midspan of each of the seven bridges considered in this study. Before completing any data analysis, careful examination of the strain histories revealed general trends in measured data and in the live load response of the bridges. Figures 4.4 through 4.11 show strain histories from each of the bridges in Project 1895. Figures 4.12 through 4.14 show strain histories from the two bridges in Project 2986, including parapet strains measured at the Slaughter Creek bridge.

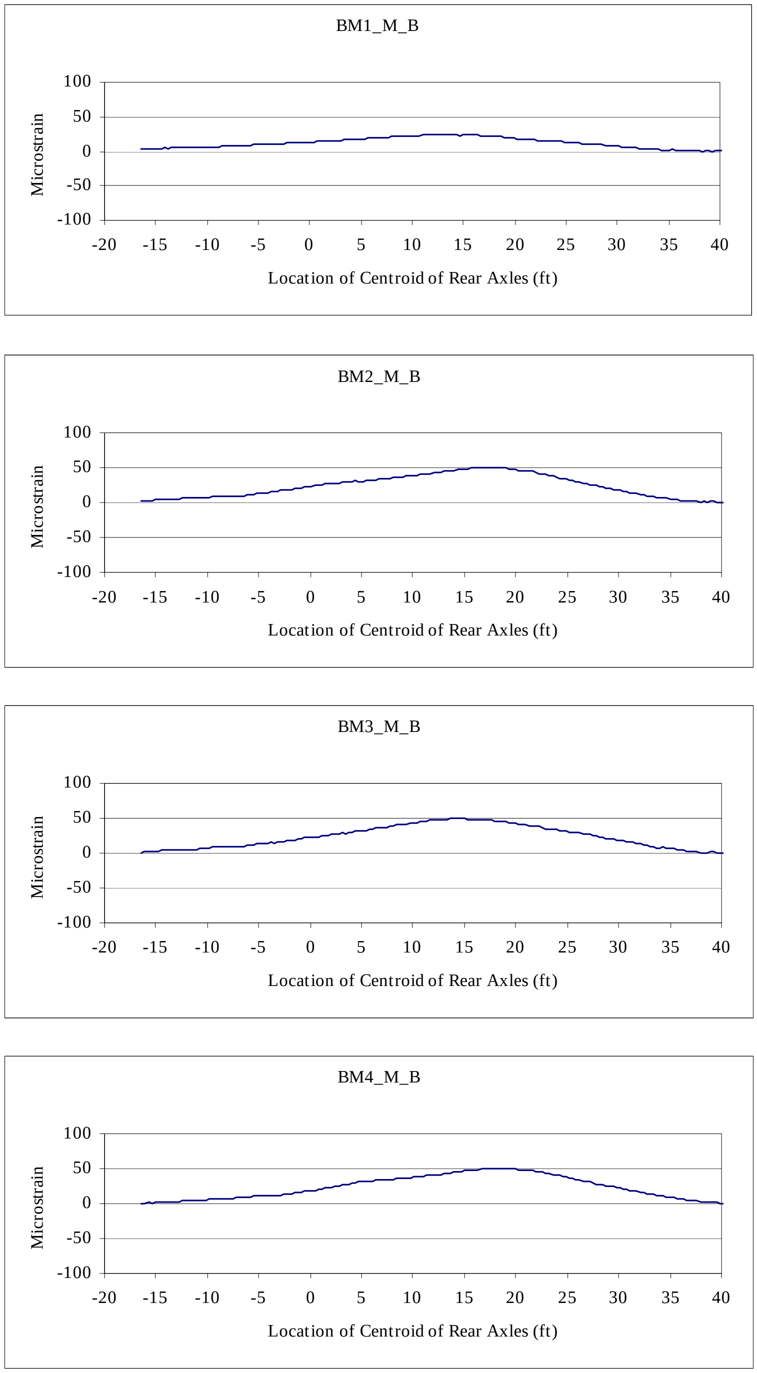

Figure 4.4 Sample Strain History – Chandler Creek Bridge – 40' Span – Run 1 – Side-by-Side Configuration

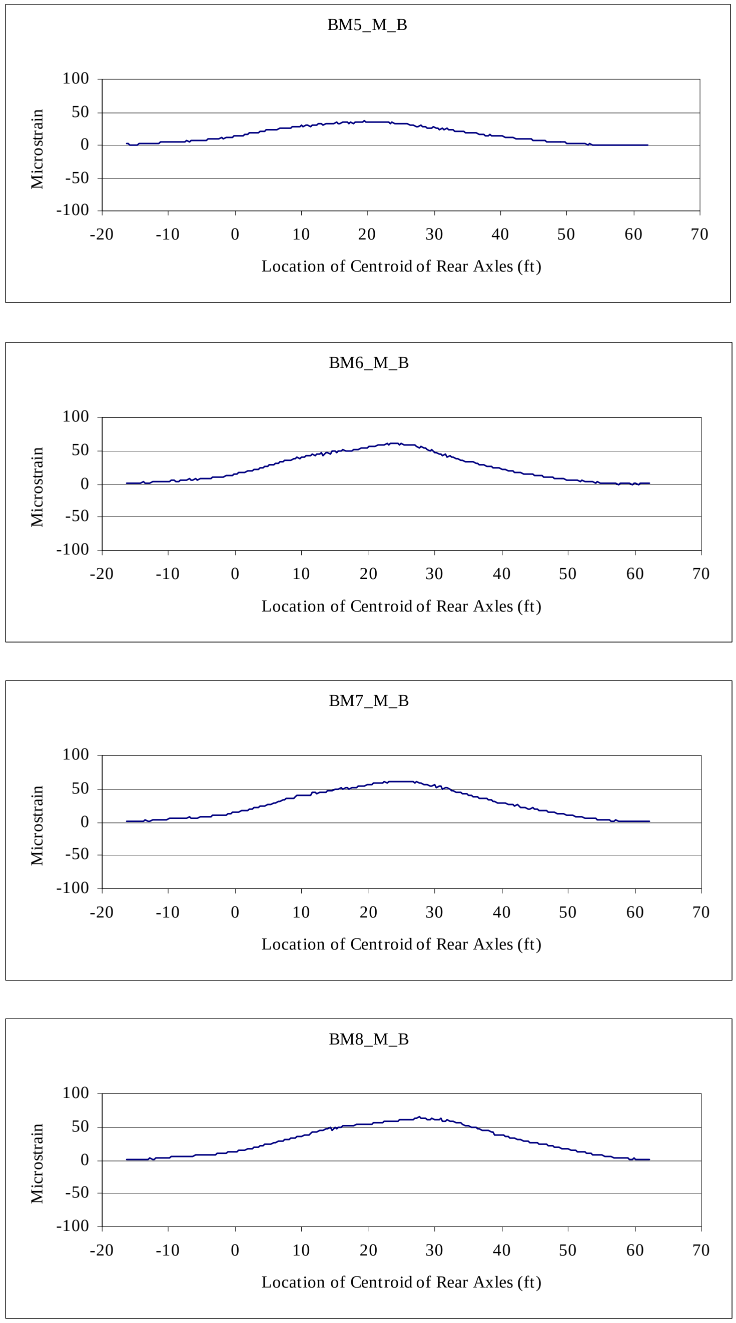

Figure 4.5 Sample Strain History – Chandler Creek Bridge – 60' Span – Run 1 – Side-by-Side Configuration

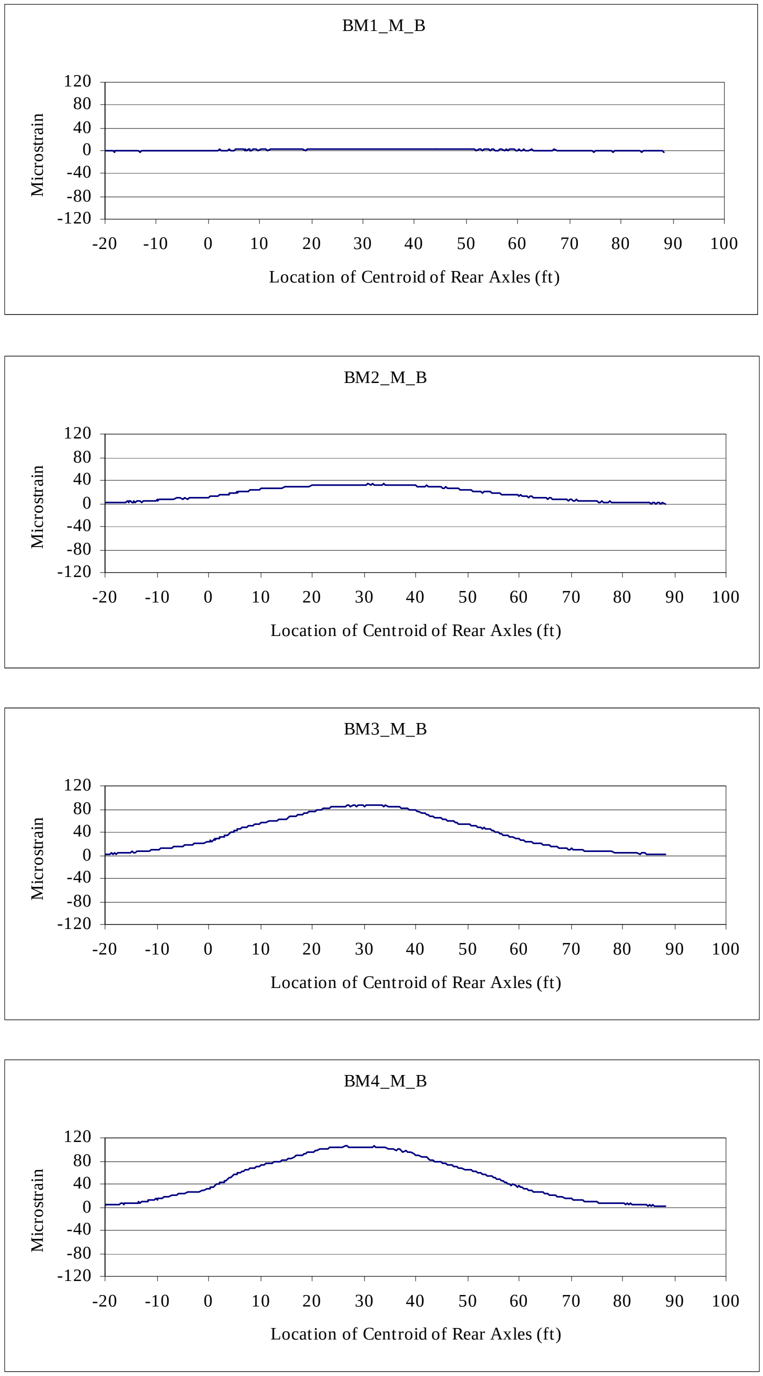

Figure 4.6 Sample Strain History – Lake LBJ Bridge – Run 1 – Back-to-Back Configuration

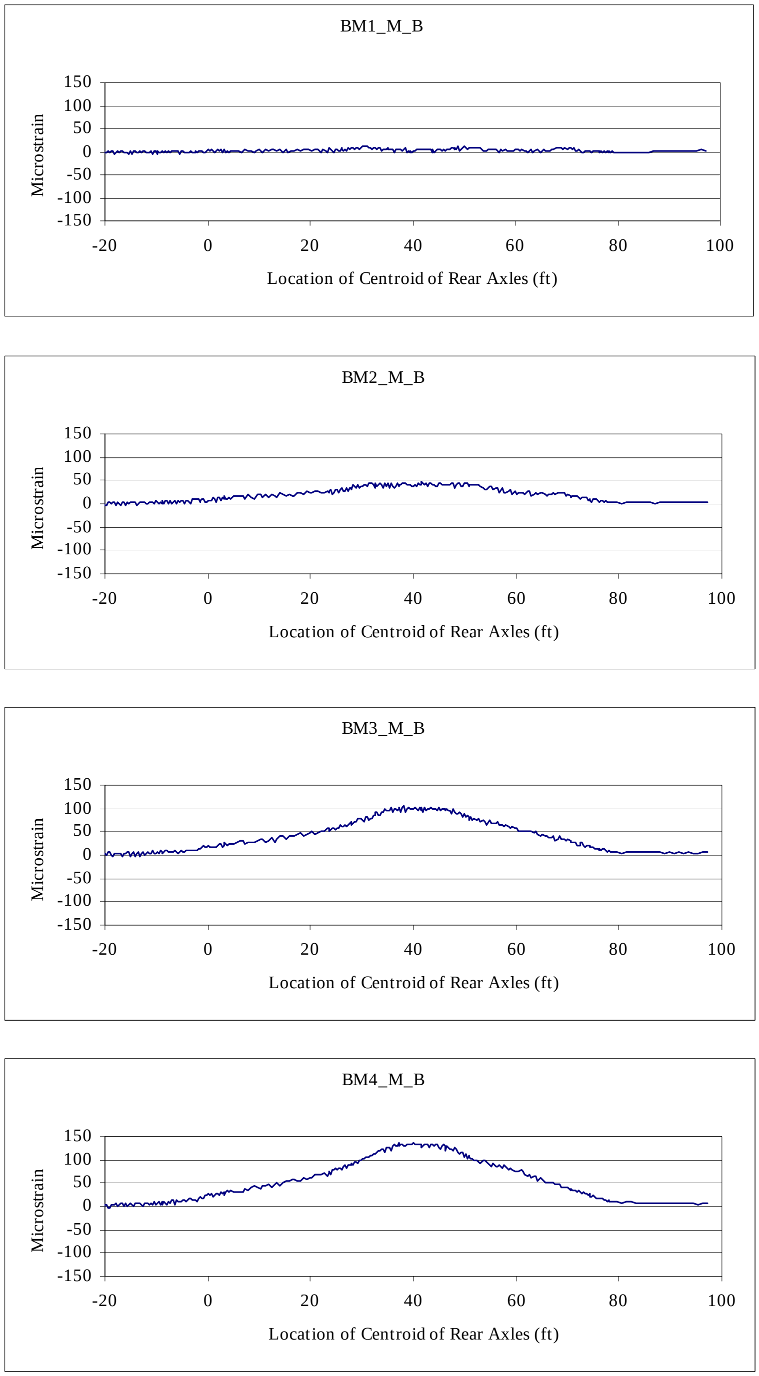

Figure 4.7 Sample Strain History – Lampasas River Bridge – Span 1 – Run 1 – Back-to-Back Configuration

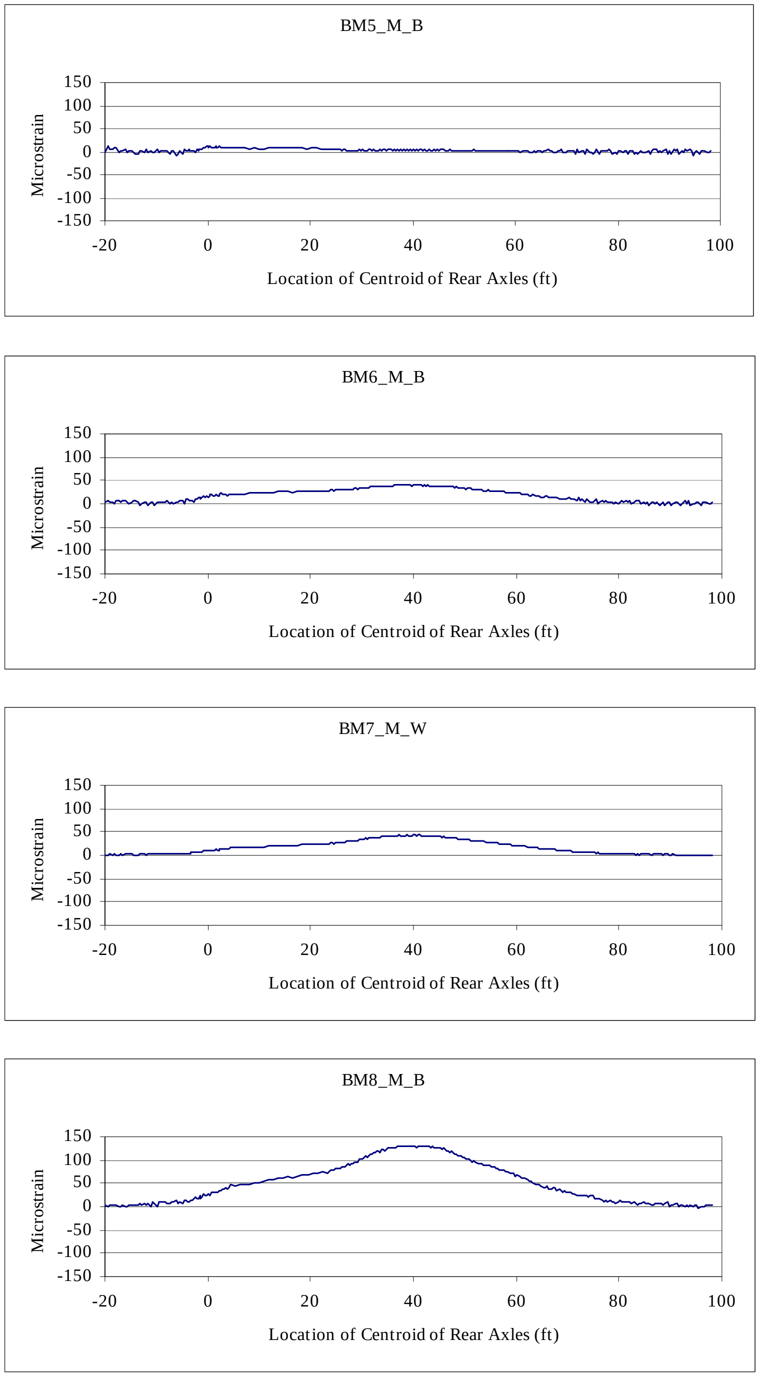

Figure 4.8 Sample Strain History – Lampasas River Bridge – Span 2 – Run 1 – Back-to-Back Configuration

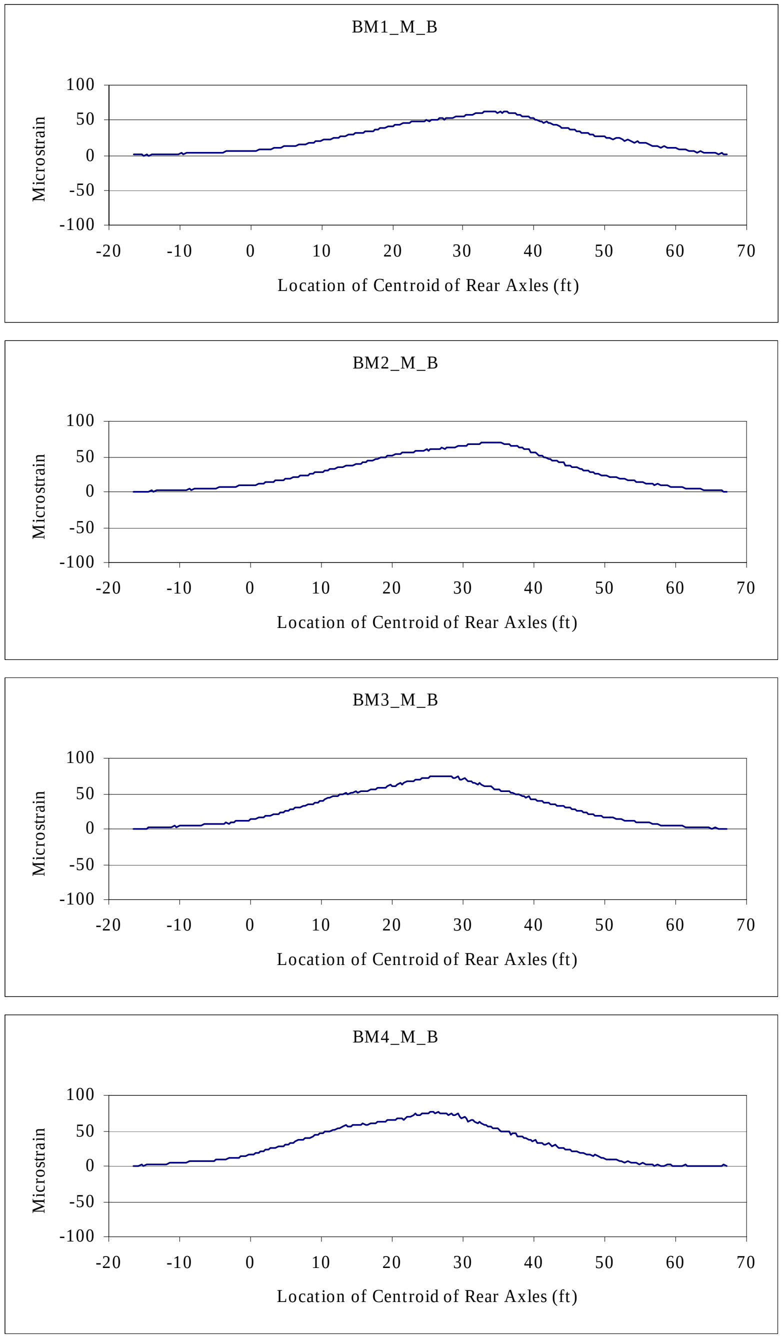

Figure 4.9 Sample Strain History – Willis Creek Bridge – Run 1 – Side-by-Side Configuration

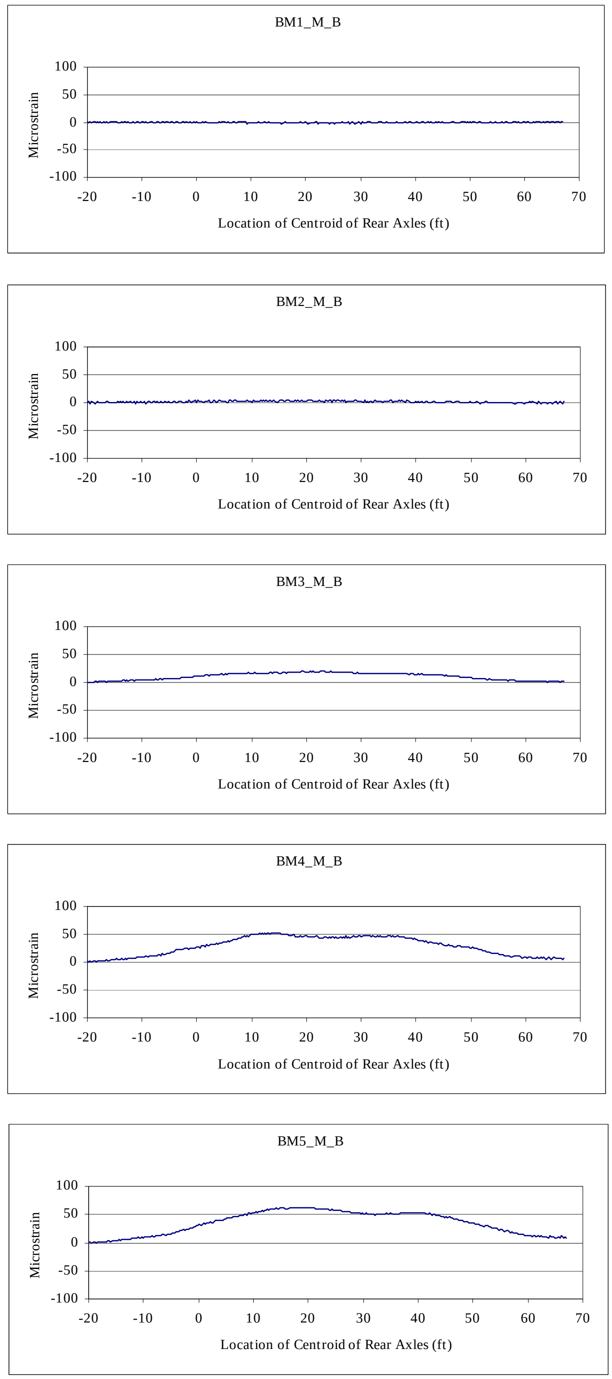

Figure 4.10 Sample Strain History – Wimberley Bridge – Span 1 – Run 1 – Back-to-Back Configuration

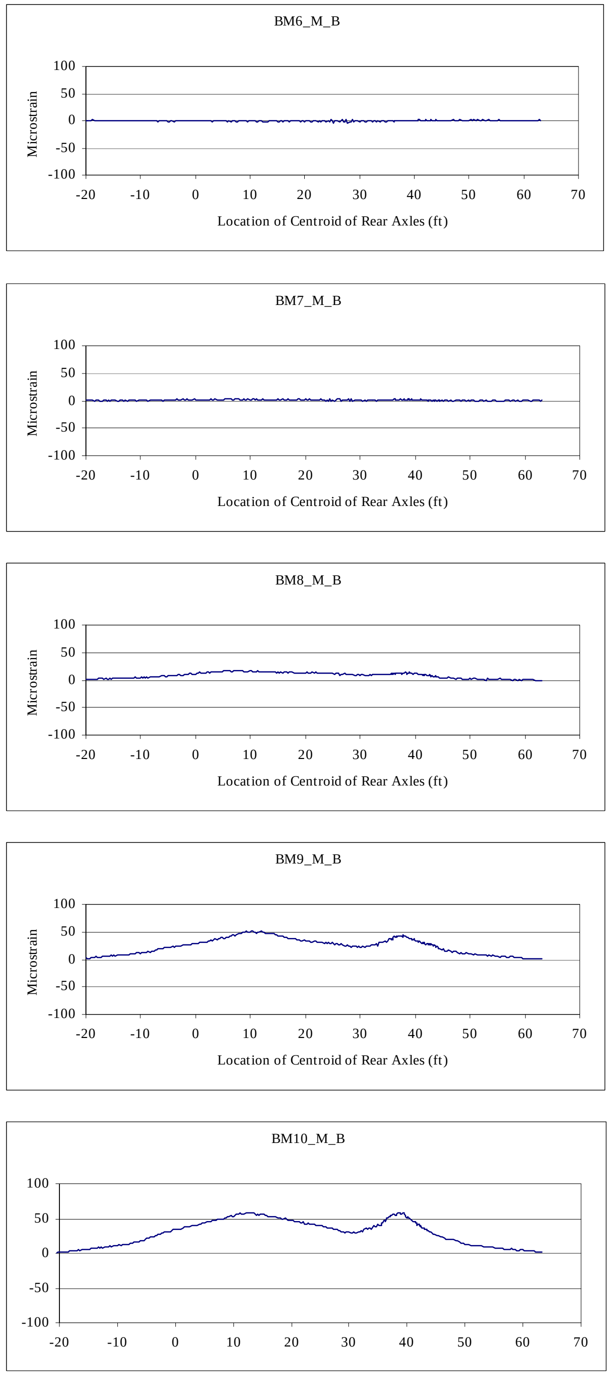

Figure 4.11 Sample Strain History – Wimberley Bridge – Span 2 – Run 1 – Back-to-Back Configuration

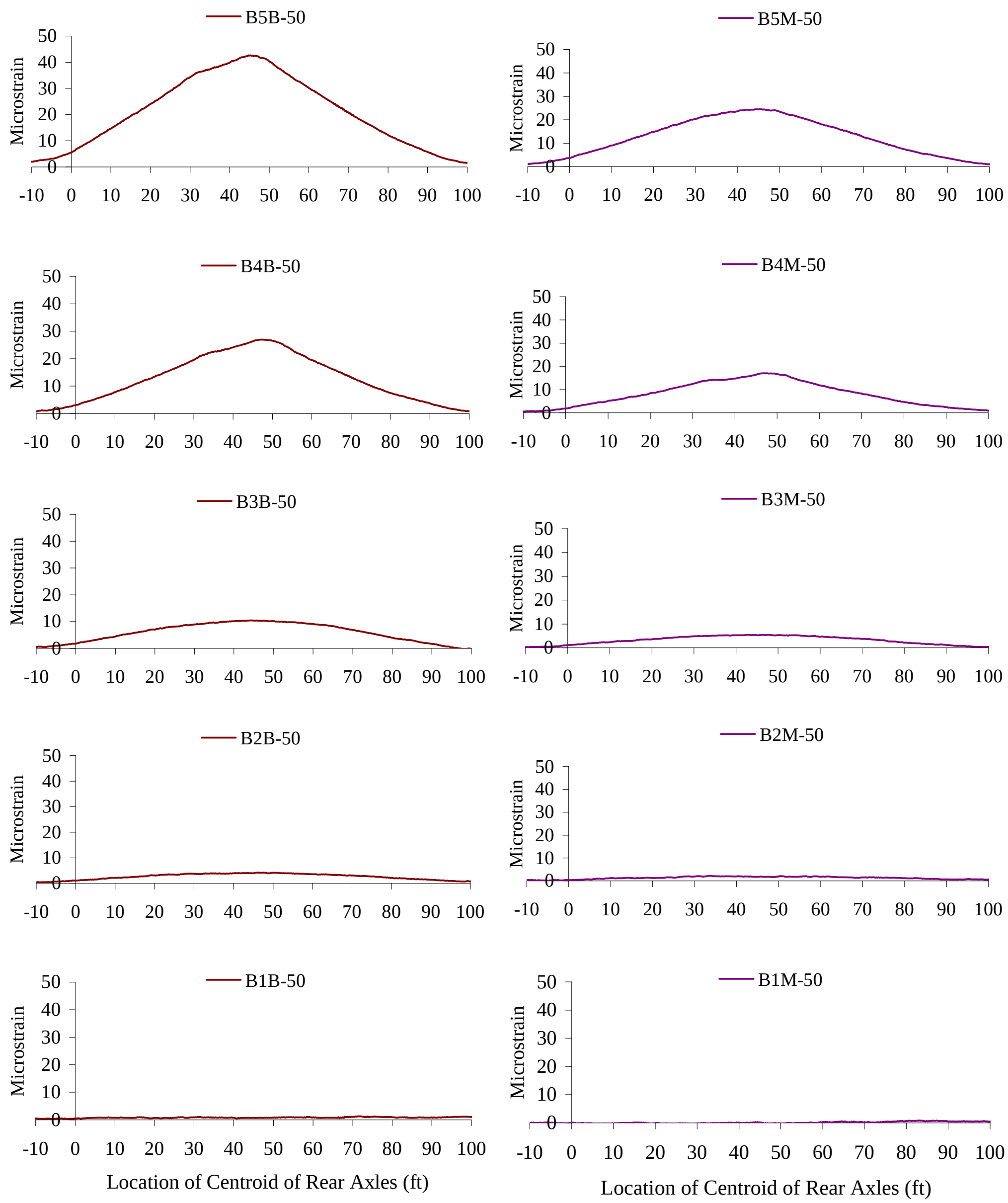

Figure 4.12 Sample Strain History – Slaughter Creek Bridge – Run 16 – Single-Truck Configuration (Matsis 1999)

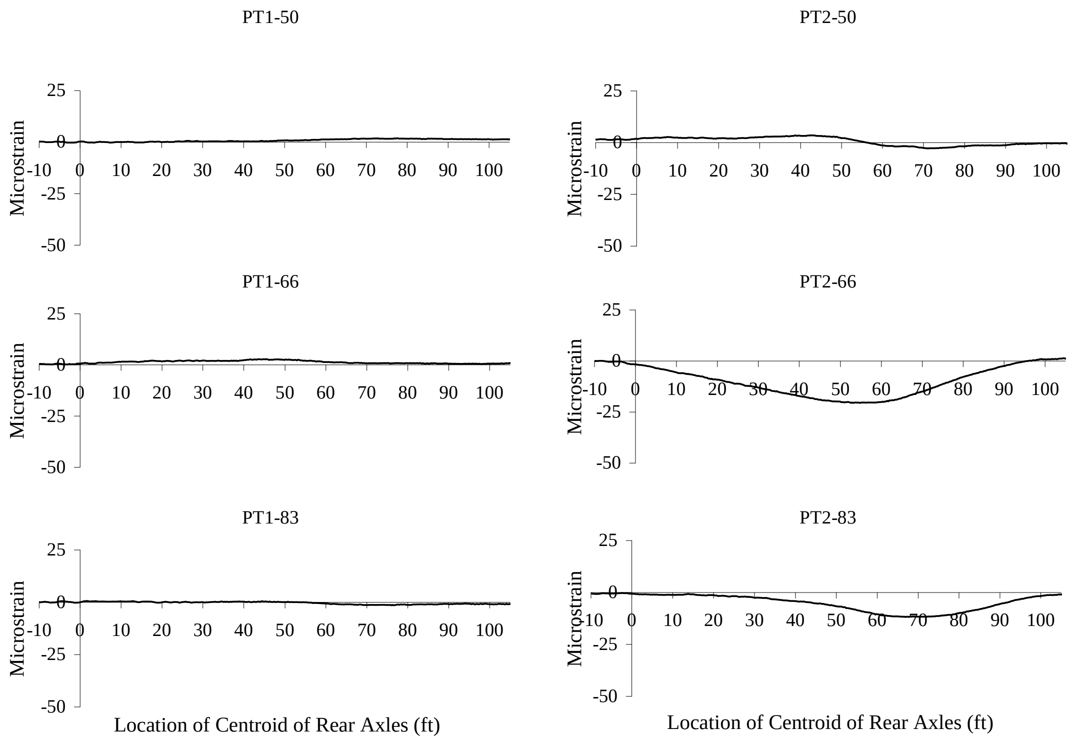

Figure 4.13 Sample Strain History – Slaughter Creek Bridge Parapets – Run 16 – Single-Truck Configuration (Matsis 1999)

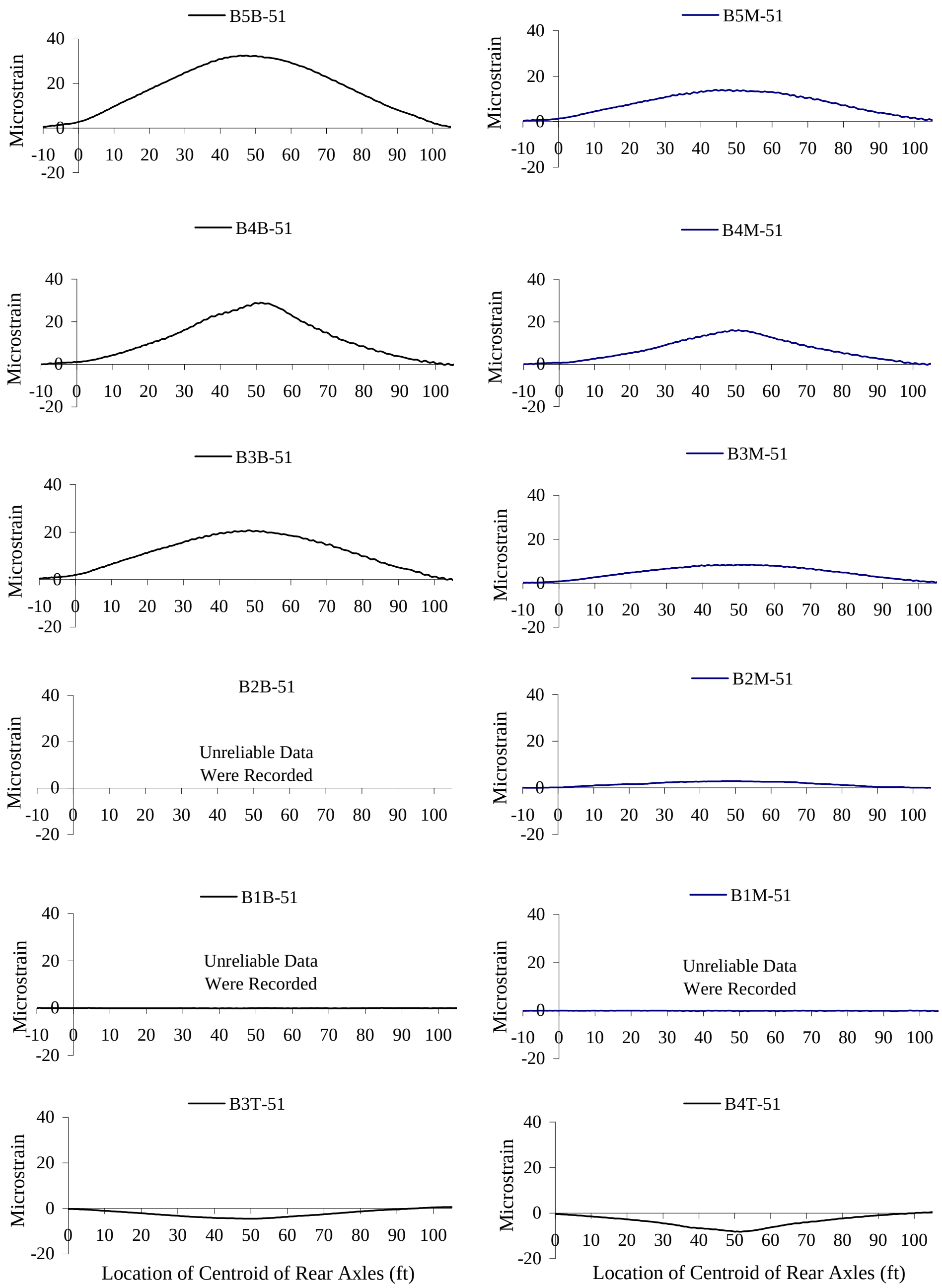

Figure 4.14 Sample Strain History – Nolanville Bridge – Run 28 – Single-Truck Configuration (Matsis 1999)

4.2.3 Maximum Measured Strains

This section includes the maximum measured strains at each bridge. Tables 4.1 through 4.4 show the maximum measured concrete strains at midspan during load testing of all seven bridges in this study. All values are in units of microstrain. Positive values indicate tensile strain while negative values indicate compressive strain. There are no data for Beam 1 and Beam 2 on the Nolanville bridge because the measured data were unusable.

Table 4.1 Maximum Measured Concrete Tensile Strains From Midspan Bottom Gages

Bridge Name	Beam 1	Beam 2	Beam 3	Beam 4	Beam 5
Chandler Creek – 40’ Span	66	52	51	61	N/A
Chandler Creek – 60’ Span	86	68	63	84	N/A
Lake LBJ	71	88	104	105	N/A
Lampasas River – Span 1	89	92	108	139	N/A
Lampasas River – Span 2	83	84	97	131	N/A
Willis Creek	101	87	91	117	N/A
Wimberley – Span 1	76	68	65	61	73
Wimberley – Span 2	76	63	69	66	78
Slaughter Creek	52	52	46	53	54
Nolanville	-	-	99	79	102

Table 4.2 Maximum Measured Concrete Tensile Strains From Midspan Web Gages

Bridge Name	Beam 1	Beam 2	Beam 3	Beam 4	Beam 5
Chandler Creek – 40' Span	28	26	26	28	N/A
Chandler Creek – 60' Span	39	32	30	37	N/A
Lake LBJ	32	46	56	48	N/A
Lampasas River – Span 1	41	53	50	68	N/A
Lampasas River – Span 2	39	42	47	69	N/A
Willis Creek	51	41	40	50	N/A
Wimberley – Span 1	40	30	30	27	37
Wimberley – Span 2	40	Out of Range	33	29	36
Slaughter Creek	29	28	22	31	29
Nolanville	-	51	51	51	53

Table 4.3 Maximum Measured Concrete Compressive Strains From Midspan Top Gages

Bridge Name	Beam 1	Beam 2	Beam 3	Beam 4	Beam 5
Chandler Creek – 40' Span	-9	-9	-7	-6	N/A
Chandler Creek – 60' Span	-19	-16	-13	-15	N/A
Lake LBJ	-8	-10	-12	-10	N/A
Lampasas River – Span 1	-18	-18	-25	-30	N/A
Lampasas River – Span 2	-17	-19	-21	-25	N/A
Willis Creek	-26	-32	-31	-29	N/A
Wimberley – Span 1	N/A	-11	-5	-11	N/A
Wimberley – Span 2	N/A	-14	-16	-15	N/A
Slaughter Creek	N/A	N/A	N/A	N/A	N/A
Nolanville	N/A	N/A	-17	-24	N/A

Table 4.4 Maximum Measured Concrete Compressive Strains From Midspan Curb Gages

Bridge Name	Beam 1	Beam 2	Beam 3	Beam 4	Beam 5
Chandler Creek – 40’ Span	-33	N/A	N/A	-31	N/A
Chandler Creek – 60’ Span	-43	N/A	N/A	-13	N/A
Lake LBJ	-38	N/A	N/A	-68	N/A
Lampasas River – Span 1	-53	N/A	N/A	-60	N/A
Lampasas River – Span 2	-44	N/A	N/A	-70	N/A
Willis Creek	-84	N/A	N/A	-90	N/A
Wimberley – Span 1	-52	N/A	N/A	N/A	-47
Wimberley – Span 2	-54	N/A	N/A	N/A	-53
Slaughter Creek	-4	N/A	N/A	N/A	-3
Nolanville	N/A	N/A	N/A	N/A	N/A

4.3 GENERAL TRENDS IN MEASURED STRAINS

4.3.1 Noise

Because the data acquisition system used in the bridge load tests was an electrical system, the issue of fluctuations in output voltages, commonly called noise, had to be addressed. If the noise in the output data was excessively high, then the data became unusable. This was the case for Beam 1 and Beam 2 of the Nolanville bridge, as previously mentioned. In Project 1895, the Willis Creek bridge was the first bridge that was tested. Upon reviewing the data, it was deemed too noisy to be of any value, and the bridge had to be tested again. Figure 4.15 shows a sample strain plot from the first series of load tests at the Willis Creek bridge.

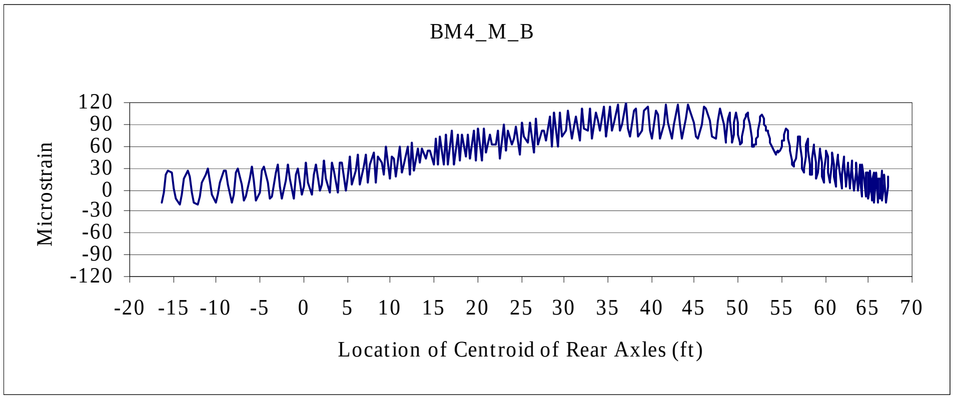

Figure 4.15 Sample Strain Plot From First Series of Load Tests at the Willis Creek Bridge

As shown in Figure 4.15, the noise in the data is approximately equal to 30+ microstrain. If the noise was not present, then the maximum response would be approximately ninety microstrain. Therefore, the noise is approximately one-third of the maximum response, which makes this data unreliable and not usable. To overcome this problem, all components of the data acquisition system were checked visually and overhauled as necessary to tighten loose connections and repair damaged wires. As a result, the noise level dropped dramatically, as illustrated by representative strain data in the previous section.

In Project 2986, the problem of noise level was dealt with during analysis by using a moving average. For the first eight runs, the data were averaged using up to 30 points because sampling was done at a frequency of 100 Hz. For subsequent runs, a five-point moving average was used because data were sampled at only 10 Hz. Figure 4.16 shows an example of the reduction in noise by using a moving average.

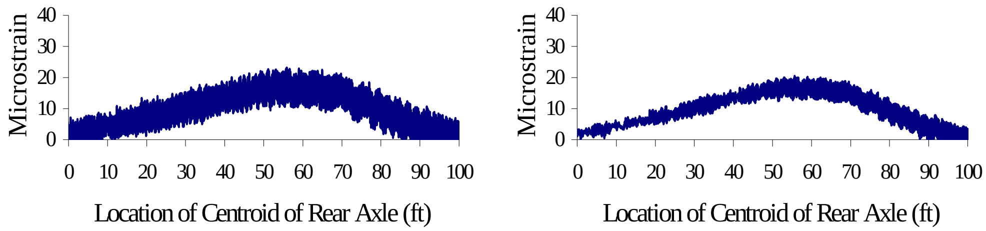

Figure 4.16 Noise Reduction Through Use of a Moving Average (Matsis 1999)

4.3.2 Drift

In Project 1895, during field testing, there appeared to be no problem with short-term drift in the data. Because the strain gages were temperature-compensating and the actual truck runs lasted only a matter of seconds, there was no significant level of drift. In addition, all strain gage readings were set to zero at the beginning of each truck run.

In Project 2986, a significant problem with drift did arise during data analysis. To overcome this problem, strain data were adjusted by subtracting the initial strain reading from all strain values in a test run. Figure 4.17 shows an example of strain data from Project 2986.

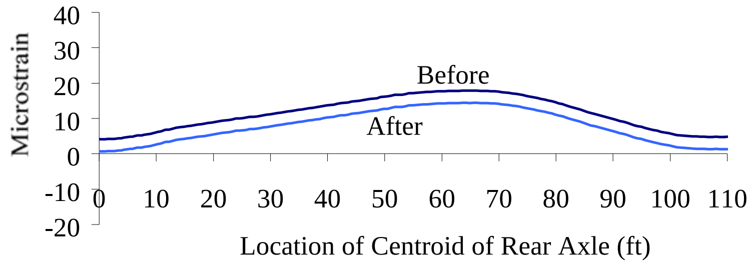

Figure 4.17 Example of Adjustment for Drift – Project 2986 (Matsis 1999)

4.3.3 Uplift

For some of the bridges in Project 1895, an interesting trend was observed during runs involving the back-to-back loading configuration. Curb gages on the opposite side of the bridge relative to the trucks measured small amounts of positive strain. This behavior occurred because the load from the test vehicles was so high and so concentrated on one side of the bridge that the other side of the bridge deflected slightly upward, resulting in a slight "uplift." Table 4.5 shows the maximum positive strains measured in the curb gages during runs involving the back-to-back loading configuration.

Table 4.5 Maximum Positive Strains in the Midspan Curb Gages During Runs Involving the Back-to-Back Loading Configuration – Project 1895

Bridge Name	Beam 1	Beam 4/5
Chandler Creek – 40' Span	7	5
Chandler Creek – 60' Span	4	4
Lake LBJ	18	0
Lampasas River – Span 1	15	3
Lampasas River – Span 2	10	6
Willis Creek	5	5
Wimberley – Span 1	3	3
Wimberley – Span 2	5	4

Chapter 5 – Analysis And Evaluation of Measured Data

This chapter addresses the analysis and evaluation of data measured during field testing. The first section details the neutral axis depths inferred from measured strain values, in addition to the comparison of those values with neutral axis depths calculated using both design and adjusted section properties. The calculation of total moments from simple statics, which are used to verify the inferred moments, is presented in the second section. The third section deals with live load moments inferred from measured strain values, using both design and adjusted section properties. This chapter ends with a discussion of the disparities between calculated values for live load moment and neutral axis depths and values inferred from strain measurements taken during field testing.

5.1 NEUTRAL AXIS DEPTHS

5.1.1 Neutral Axis Depths Inferred from Measured Strains

The calculation of neutral axis depths from measured strains relies on the assumption of a linear strain profile over the full depth of the composite section. Assuming that the response to live load is in the linear elastic range of the moment-curvature response, this assumption is reasonable (Hurst 1998). The field tests for this study were conducted so there were at least two strain gages at each location on every girder to facilitate calculation of neutral axis depths.

A simplified representation of this calculation is shown in Figure 5.1. As shown in the figure, the neutral axis is measured from the top, and a straight line is assumed between any pair of strain readings. The neutral axis can be calculated

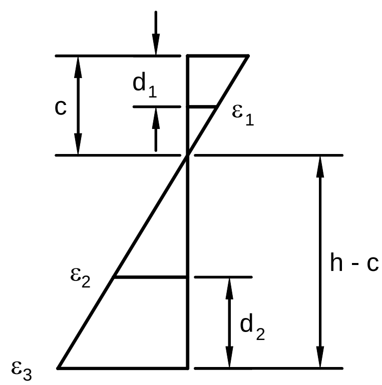

$$c = \frac{\varepsilon_1 \cdot h + \varepsilon_3 \cdot d_1}{\varepsilon_1 + \varepsilon_3}$$

$$c = \frac{(\varepsilon_2 - \varepsilon_3)h + \varepsilon_3 \cdot d_2}{\varepsilon_2 - \varepsilon_3}$$

$$c = \frac{\varepsilon_1 \cdot (h - d_2) + \varepsilon_2 \cdot d_1}{\varepsilon_1 + \varepsilon_2}$$

Figure 5.1 Calculation of Neutral Axis Depths

using three different pairs of strain values. The ability to calculate the neutral axis location using several pairs of strain readings for a given test run yields more data and a better chance to accurately estimate the neutral axis value. This calculation was carried out for each record number in a data file, yielding one inferred neutral axis depth for every pair of strain gages at a girder section. Neutral axis depths were then plotted versus truck location in order to identify general trends in the live load response. Figure 5.2 shows a sample plot of neutral axis depths inferred from measured strains on the second span during Run 1 at the Chandler Creek Bridge.

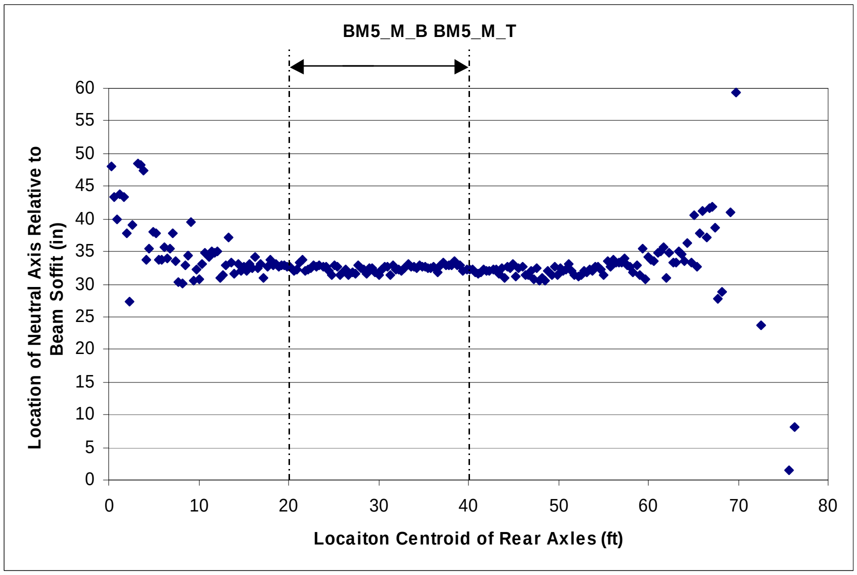

Figure 5.2 Sample Neutral Axis Plot

Figure 5.2 shows that near the ends of the span, the data tend to scatter. When the average neutral axis depths were calculated, only a certain interval of the records was considered to avoid averaging the portions of data that exhibit excessive scatter. For example, in Figure 5.2, the average neutral axis was calculated using the data points between twenty feet and forty feet, as indicated by the two vertical lines. Neutral axis depths displayed in Figure 5.2 are based on strains measured using the bottom and top gages on Beam 5, as indicated by the notation at the top of the chart.

Once the average neutral axis depths were calculated from measured data, the values were used to calculate adjusted moments of inertia for all the composite sections. Tables 5.1 and 5.2 show the inferred values for neutral axis depths for all seven bridges. For the Nolanville bridge, all values computed

Table 5.1 Inferred Neutral Axis Depths – Project 1895

Beam Description	Span Number	Inferred Neutral Axis Depth (inches)
Chandler Creek		
Beam 1-4	1	12.9
Beam 5-8	2	15.9
Lake LBJ		
Beam 1,4	1	12.8
Beam 2,3	1	14.0
Lampasas River		
Beam 1-4	1	15.2
Beam 5-8	2	15.2
Willis Creek		
Beam 1-4	1	16.5
Wimberley		
Beam 1,5	1	21.1
Beam 2-4	1	14.0
Beam 6,10	2	21.1
Beam 7-9	2	14.0

Table 5.2 Inferred Neutral Axis Depths – Project 2986

Beam Description	Interior / Exterior	Inferred Neutral Axis Depth (inches)
Slaughter Creek		
Beam 1	Exterior	30.0
Beam 2	Interior	17.6
Beam 3	Interior	22.7
Beam 4	Interior	21.0
Beam 5	Exterior	22.8
Nolanville		
Beam 1	Exterior	21.8
Beam 2	Interior	19.3
Beam 3	Interior	19.5
Beam 4	Interior	21.6
Beam 5	Exterior	20.8

in this study were based on three-quarter span data, because several gages at midspan recorded unusable data.

The values in Table 5.1 were determined by first taking an average of all the neutral axis values for each beam at each location. Then, the standard deviation and coefficient of variation of the neutral axis depths were calculated. For the purposes of this analysis, any pair of strain gages that yielded an average neutral axis value with a coefficient of variation greater than 0.10 was not considered. Next, the neutral axis values were averaged to yield a single value for each beam in each span. If there was no significant difference in the neutral axis depths for all beams in a span, then a single value was chosen to represent the entire bridge cross-section. Conversely, if there was an appreciable difference in the neutral axis depths, then a different value was assigned to the interior and exterior composite sections.

5.1.2 Comparison of Inferred Neutral Axis Depths With Design Values

The values for neutral axis depths calculated using the design section properties are presented in Chapter 2. In this section, those values are compared with the inferred values for neutral axis depths to evaluate the recorded data and the behavior of the bridges. Significant differences between inferred values and design values may indicate conditions in the field that were not considered in design calculations. For instance, cracking of the slab and/or girders due to occasional overloads can shift the neutral axis closer to the top. In addition, if the actual material properties in the field are different from those assumed in design calculations, then the neutral axis locations may be different.

Table 5.3 shows inferred and calculated values for neutral axis depths for all seven bridges. The relative difference between the inferred and calculated values is given by a percent difference, which is the calculated value minus the inferred value, divided by the inferred value. With the exception of the two bridges from Project 2986 and the Lake LBJ and Lampasas River bridge, the difference is roughly ten percent or less. For the Slaughter Creek and Nolanville bridges, the difference is generally between five and twenty percent, which could be the result of several factors. First, there were fewer gages placed on each beam, which in turn leads to fewer gage pairs from which to calculate neutral axes. In addition, the raw data tend to exhibit more scatter, which naturally leads to a wider range of values inferred from that data.

Table 5.3 Comparison of Calculated and Inferred Neutral Axis Depths Using Design Section Properties

Beam Description	Calculated Neutral Axis Depth (inches)	Inferred Neutral Axis Depth (inches)	% Difference
Chandler Creek			
Beam 1,4	13.8	12.9	7.0%
Beam 2,3	13.3	12.9	3.1%
Beam 5,8	17.8	15.9	11.9%
Beam 6,7	17.1	15.9	7.5%
Lake LBJ			
Beam 1,4	15.5	12.8	21.1%
Beam 2,3	17.0	14.0	21.4%
Lampasas River			
Beam 1,4,5,8	18.5	15.2	21.7%
Beam 2,3,6,7	18.5	15.2	21.7%
Willis Creek			
Beam 1,4	16.9	16.5	2.4%
Beam 2,3	18.4	16.5	11.5%
Wimberley			
Beam 1,5,6,10	13.0	12.1	7.4%
Beam 2-4, 7-9	14.3	14.0	2.1%
Slaughter Creek			
Beam 1	19.9	30.0	-33.7%
Beam 2	22.6	17.6	28.4%
Beam 3	22.6	22.7	-0.4%
Beam 4	22.6	21.0	7.6%
Beam 5	19.9	22.8	-12.7%
Nolanville			
Beam 1	24.6	21.8	12.8%
Beam 2	22.7	19.3	17.6%
Beam 3	22.7	19.5	16.4%
Beam 4	22.7	21.6	5.1%
Beam 5	24.6	20.8	18.3%

There is a noticeable trend in the difference in neutral axis values for the first five bridges. As shown in Table 5.3, the inferred neutral axis depths are less than the calculated neutral axis depths (i.e. the neutral axis is actually higher in the section than the calculated value). This difference may be due to the two factors mentioned at the beginning of this section. First, because each of the five bridges in Project 1895 was constructed between 1960 and 1970, there is a high probability that some cracking has occurred due to occasional overloads. In addition, as the material test data in Appendix A show, the in-situ concrete strengths are much higher than the design values.

5.1.3 Effect of Neutral Axis Location on Calculated Live Load Moments

It is important to be accurate when estimating the actual neutral axis depth, because live load moments inferred from measured strains depend upon this value. As shown in Equation 5.1, the neutral axis depth is used directly to calculate live load moments. Because the value appears in the denominator, the calculated moment varies inversely with neutral axis depth. In the equation, M is the live load moment (kip-in), E is the modulus of elasticity of the girders (ksi), I is the composite moment of inertia (in^4), ϕ is the curvature, ε_{gage} is the strain value for a given strain gage, and d_{gage} is the distance to the strain gage (in).

$$M = EI\phi = \frac{EI\varepsilon_{gage}}{d_{gage}} \tag{5.1}$$

The neutral axis depth also gives general information about the live load behavior of these bridges. For instance, if neutral axis depths inferred from measured strains are shallower than predicted, significant cracking of the prestressed concrete girders may have occurred, resulting in reduced bending stiffness, or moment of inertia. Figure 5.3 shows a schematic representation of this scenario.

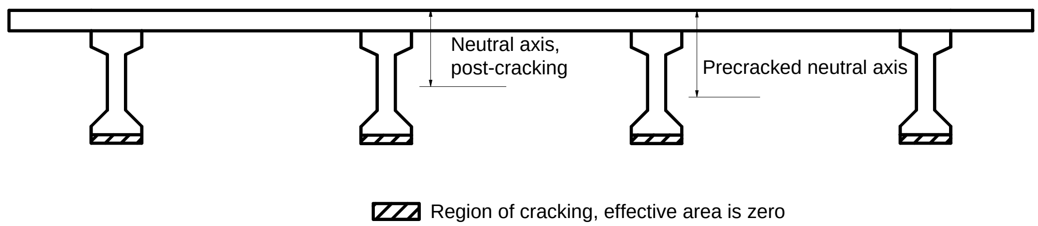

Figure 5.3 Neutral Axis Movement Due to Cracking of Girders

Additionally, concrete parapets or “rails” were assumed to contribute to the overall bending stiffness of the exterior composite section. If the actual contribution of the parapets is less than assumed, the net effect is a decrease in the effective moment of inertia and a shallower neutral axis depth. Figure 5.4 shows a schematic representation of the effect of decreased contribution from the parapets on the neutral axis depth.

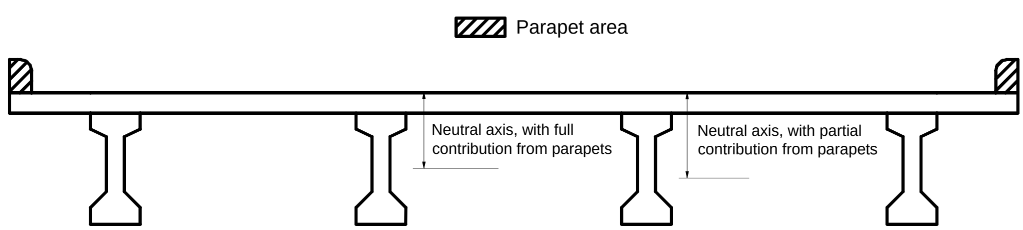

Figure 5.4 Neutral Axis Movement Due to Contribution of the Parapets

5.1.4 Comparison of Inferred Neutral Axis Depths With Adjusted Values

The section properties used to calculated adjusted neutral axis depths are presented in Chapter 2. These adjusted section properties were based on available material test data for each bridge. It is important to note that the adjusted section properties are based on an approximation of present-day concrete strengths (i.e. lower-bound strengths) and more accurate values could only be obtained through destructive testing of material samples taken from the bridges in this study.

Table 5.4 shows the adjusted neutral axis depths along with the inferred values shown previously. As before, the percent difference is calculated by subtracting the inferred value from the calculated value, then dividing by the inferred value. The percentages in the “Change” column reflect changes in the accuracy of the adjusted versus design values relative to the inferred values.

Table 5.4 Comparison of Inferred and Calculated Neutral Axis Depths Using Adjusted Section Properties

Beam Description	Calculated Neutral Axis Depth (inches)	Inferred Neutral Axis Depth (inches)	% Difference	Change
Chandler Creek				
Beam 1,4	12.9	12.9	0.0%	-7.0%
Beam 2,3	12.4	12.9	-3.9%	-7.0%
Beam 5,8	17.1	15.9	7.5%	-4.4%
Beam 6,7	16.5	15.9	3.8%	-3.8%
Lake LBJ				
Beam 1,4	16.3	12.8	27.3%	6.3%
Beam 2,3	14.6	14.0	4.3%	-17.1%
Lampasas River				
Beam 1,4,5,8	17.6	15.2	15.8%	-5.9%
Beam 2,3,6,7	17.2	15.2	13.2%	-8.6%
Willis Creek				
Beam 1,4	16.3	16.5	-1.2%	-3.6%
Beam 2,3	17.8	16.5	7.9%	-3.6%
Wimberley				
Beam 1,5,6,10	12.3	12.1	1.7%	-5.8%
Beam 2-4, 7-9	13.7	14.0	-2.1%	-4.3%
Slaughter Creek				
Beam 1	18.5	30.0	-38.3%	-4.7%
Beam 2	22.0	17.6	25.0%	-3.4%
Beam 3	22.0	22.7	-3.1%	-2.6%
Beam 4	22.0	21.0	4.8%	-2.9%
Beam 5	18.5	22.8	-18.9%	-6.1%
Nolanville				
Beam 1	22.5	21.8	3.2%	-9.6%
Beam 2	20.5	19.3	6.2%	-11.4%
Beam 3	20.5	19.5	5.1%	-11.3%
Beam 4	20.5	21.6	-5.1%	-10.2%
Beam 5	22.5	20.8	8.2%	-10.1%

The effect of adjusting material properties, particularly concrete strength, is to change the dimensions of the transformed composite section, which inevitably changes the calculated neutral axis depth. For each bridge in this study, the neutral axis depth was recalculated using the adjusted material properties in order to have a more accurate estimation of the neutral axis depth. As shown in Table 5.4, thirteen out of the twenty-two values for calculated neutral axis depth have a reduced difference relative to the inferred values.

5.2 LIVE LOAD MOMENTS

5.2.1 Live Load Moments From Simple Statics

As with all measured data in any experiment or test, there must be a baseline, or collection of established data to which the measured data are compared. For this particular study, an appropriate and relatively simple choice for a baseline to evaluate the inferred moments was the moments calculated using simple statics. In order to make the static calculation of live load moments, certain assumptions were made, some of which were more realistic than others. Of course the overriding assumption was that the complex interactions and behavior during loading of a prestressed concrete girder bridge may be simplified into a simple beam model.

First, each and every beam used to model the bridges in this study was assumed to be simply supported, as shown in Figure 5.5. With the exception of the Slaughter Creek bridge, all bridges in this study were constructed with open joints between spans, so this assumption was reasonable. The Slaughter Creek bridge was constructed with a cast-in-place continuous slab that was intended to provide some level of continuity (Matsis 1999).

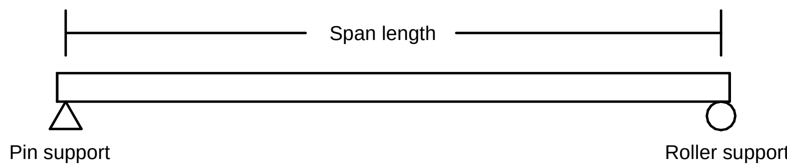

Figure 5.5 Simple Beam Model

Second, the truck loading on the bridges was modeled as a series of moving point loads representing the axle loads. In addition, any dynamic effects due to the movement of the test vehicles were ignored when calculating maximum moments. Because this basic concept is included in the AASHTO LRFD Bridge Design Specifications, it stands to reason that these simplifying assumptions are acceptable (American Association of State Highway and Transportation Officials 2000a). Figure 5.6 shows an example of an arrangement of point loads used in a simple beam analysis.

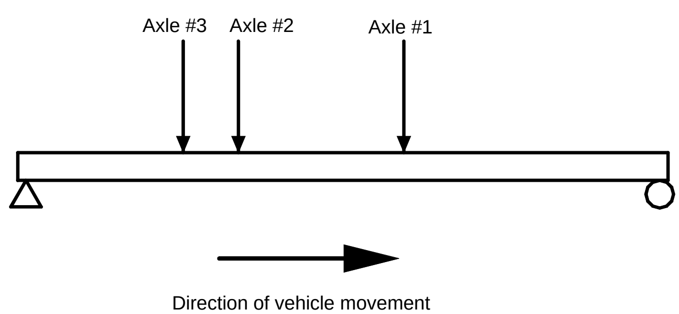

Figure 5.6 Example of Point Loads Used in Simple Beam Analysis

Finally, it was assumed that the effects of skew angle were adequately replicated by adjusting the positions of the concentrated loads according to the degree of skew. Generally, if a bridge is skewed, each girder does not experience maximum moment at the same instant in time as the other girders subjected to a moving live load. This effect is magnified as the skew increases. In order to compensate, the simple beam model was modified, as shown in Figure 5.7. Two simple beams were used instead of one, and then the three axle loads were divided by two and "run" over each simple beam line, with the loads staggered to correspond with the skew angle. This modified model was used only on side-by-side truck loadings.

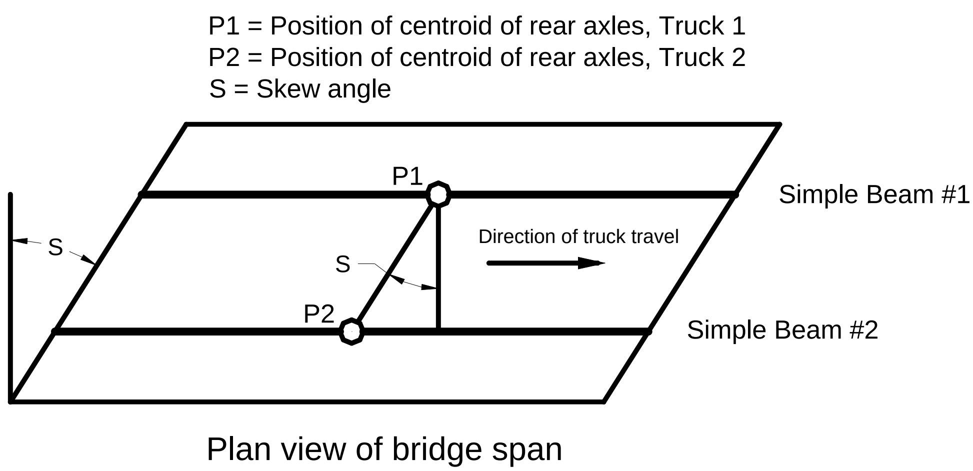

Figure 5.7 Correction for Skew Angle

For each of the loading types on all seven bridges, a simple beam analysis was performed to determine the maximum static moments induced by the simulated vehicle loadings. Only the maximum midspan moments are reported here, with the exception of the Nolanville bridge. The measured axle weights of the test vehicles that were represented by concentrated loads in the simple beam models are listed in Chapter 3.

Tables 5.5 and 5.6 list the maximum static moments calculated from the simple beam analyses. Table 5.5 shows the maximum values for the five bridges tested in Project 1895. Table 5.6 shows the maximum values for the bridges tested in Project 2986.

Table 5.5 Maximum Simple Beam Midspan Moments – Project 1895

Bridge Name	Truck 1 (kip-in)	Truck 2 (kip-in)	Side-by-Side (kip-in)	Back-to-Back (kip-in)
Chandler Creek – 40' Span	3360	3300	6010	3920
Chandler Creek – 60' Span	5790	5700	10800	7850
LBJ Lake	7700	7370	15100	10900
Lampasas River	8600	8390	17000	13100
Willis Creek	7800	7070	15300	10300
Wimberley	4170	3950	7520	4920

Table 5.6 Maximum Simple Beam Moments – Project 2986

Bridge Name	Single Truck (kip-in)				Combination (kip-in)	HETS (kip-in)
	D1	D2	D3	D4		
Slaughter Creek	10700	11200	10500	-	21700	-
Nolanville	-	-	-	9070	-	30900

As shown in Table 5.5, the side-by-side truck configuration yields the largest midspan moment, which makes sense intuitively because this type of configuration can be thought of as a single truck with double the axle weights of one truck. The next largest moments are those produced by the back-to-back placement of the trucks, followed by moments for the single-truck loading.

5.2.2 Live Load Moments Inferred Using Design Section Properties

Once a baseline moment calculation is established, live load moments can be calculated, using design section properties, and be compared to the baseline for verification. In this study, all seven bridges were assigned design section properties based on available design data. Of the seven bridges considered in this study, the as-built drawings were obtained for two bridges, the Willis Creek bridge and the Slaughter Creek bridge. Contract documents were located for all seven bridges, from which girder details were inferred based on span length and known girder type. The specified design concrete strengths were taken from the contract documents. Using these data, design section properties for each bridge were calculated and are summarized in Chapter 2.

For the five bridges tested in Project 1895, the live load moment was calculated from the measured strains using Equation 5.2. In this equation, E_c is the design modulus of elasticity of the girders (ksi), I is the composite moment of inertia based on the transformed section (in^4), ε_{gage} is the measured strain for a given strain gage (με), and d_{gage} is the distance from the strain gage to the design neutral axis depth (in).

$$M = \frac{E_c \cdot I \cdot \varepsilon_{gage}}{d_{gage}} \cdot 10^{-6} \tag{5.2}$$

For the two bridges in the Project 2986 study, the live load moment was calculated using only strains measured from strain gages attached to the bottom of the girders. Equation 5.3 shows the method by which the moments were calculated. In this equation, E_c is the design modulus of elasticity of the girders (ksi), S_b is the design composite section modulus based on the transformed section (in^3), and ε is the measured strain for a given bottom gage (με).

$$M = \left(E_c \cdot S_b \cdot \varepsilon\right) \cdot 10^{-6} \tag{5.3}$$

Tables 5.7 and 5.8 show the average maximum live load moments at midspan calculated using design section properties and measured strains. The values in this table are an average of maximum calculated live load moments for each of the loading types on each bridge. The average of the maximum values is reported rather than the maximum values in order to account for slight fluctuations in the data due to unavoidable noise, which may reflect slightly higher overall maximum moments if not taken into account. Figure 5.8 shows a sample of the maximum total moment data from the side-by-side runs over the 60’ span of the Chandler Creek bridge, with the reported maximum shown as a dashed line.

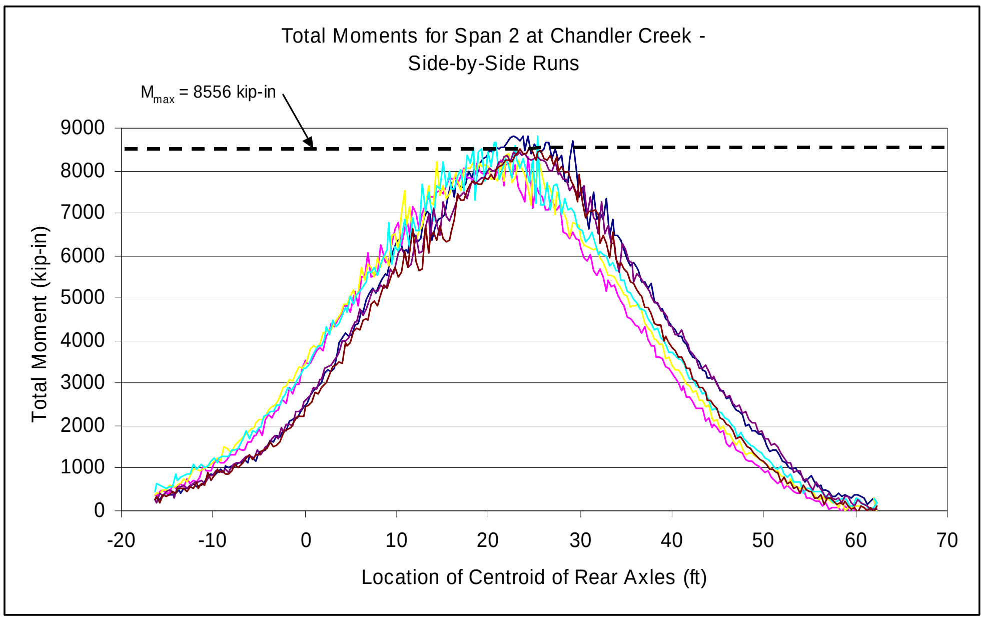

Figure 5.8 Sample Plot of Maximum Midspan Moments

Table 5.7 Maximum Calculated Midspan Moments Using Design Section Properties and Measured Strains – Project 1895

Bridge Name	Single Truck 1 (kip-in)	Single Truck 2 (kip-in)	Side-by-Side (kip-in)	Back-to-Back (kip-in)
Chandler Creek – 40’ Span	2200	2150	4020	3010
Chandler Creek – 60’ Span	4380	4360	8560	7310
Lake LBJ	6030	5830	11300	10600
Lampasas River – Span 1	7200	7120	13900	11600
Lampasas River – Span 2	6880	6730	13400	11400
Willis Creek	5690	5790	10400	8770
Wimberley – Span 1	3090	2860	5660	3630
Wimberley – Span 2	2890	2650	5070	3600

Table 5.8 Maximum Calculated Moments Using Design Section Properties and Measured Strains – Project 2986

Bridge Name	Single Truck (kip-in)				Combination (kip-in)	HETS (kip-in)
	D1	D2	D3	D4		
Slaughter Creek	7550	8090	7420	-	15300	-
Nolanville	-	-	-	5580	-	16200

As shown in Table 5.7, the side-by-side loading yielded the highest moments, as expected, followed by the back-to-back loadings and the single-truck loadings. In Table 5.8, the HETS loading yielded the highest moments, followed by the combination loading and the single-truck loading. This pattern is consistent with the results of the simple beam analyses. From this point in the text, the maximum moments inferred from measured strains and design section properties will be referred to as the “design moments.”

5.2.3 Comparison of Simple Beam Moments With Design Moments

Once the design moments were calculated, they were compared to the simple beam moments. For this study, a moment ratio, MR, was calculated according to Equation 5.4 and was used to evaluate the design moments. Ideally this ratio would be equal to one, but a ratio of 0.90 to 1.10 was deemed reasonable for reliable data.

$$MR = \frac{M_{Design}}{M_{Simple}} \tag{5.4}$$

Tables 5.9 and 5.10 show the comparison of design moments to simple beam moments, including moment ratios, for the bridges tested in Project 1895. Tables 5.11 and 5.12 show the same data for the two bridges tested in Project 2986. Table 5.13 lists the average moment ratios for all seven bridges.

Table 5.9 Comparison of Design Moments to Simple Beam Moments – Project 1895 – Single Truck Loading

Bridge Name	Single Truck 1 (kip-in)		MR	Single Truck 2 (kip-in)		MR
	Design	Simple		Design	Simple	
Chandler Creek – 40’ Span	2200	3360	0.65	2150	3300	0.65
Chandler Creek – 60’ Span	4380	5790	0.76	4360	5700	0.76
Lake LBJ	6030	7700	0.78	5830	7370	0.79
Lampasas River – Span 1	7200	8600	0.84	7120	8390	0.85
Lampasas River – Span 2	6880	8600	0.80	6730	8390	0.80
Willis Creek	5690	7800	0.73	5790	7070	0.82
Wimberley – Span 1	3090	4170	0.74	2860	3950	0.72
Wimberley – Span 2	2890	4170	0.69	2650	3950	0.67

Table 5.10 Comparison of Design Moments to Simple Beam Moments – Project 1895 – Side-by-Side and Back-to-Back Loading

Bridge Name	Side-by-Side (kip-in)		MR	Back-to-Back (kip-in)		MR
	Design	Simple		Design	Simple	
Chandler Creek – 40' Span	4020	6010	0.67	3010	3920	0.77
Chandler Creek – 60' Span	8560	10800	0.79	7310	7850	0.93
Lake LBJ	11300	15100	0.75	10600	10900	0.97
Lampasas River – Span 1	13900	17000	0.82	11600	13100	0.89
Lampasas River – Span 2	13400	17000	0.79	11400	13100	0.87
Willis Creek	10400	15300	0.68	8770	10300	0.85
Wimberley – Span 1	5660	7520	0.75	3630	4920	0.74
Wimberley – Span 2	5070	7520	0.67	3600	4920	0.73

Table 5.11 Comparison of Design Moments to Simple Beam Moments – Slaughter Creek Bridge

Truck D1 (kip-in)		MR	Truck D2 (kip-in)		MR	Truck D3 (kip-in)		MR	Combination (kip-in)		MR
Design	Simple		Design	Simple		Design	Simple		Design	Simple	
7550	10700	0.71	8090	11200	0.72	7420	10500	0.71	15300	21700	0.71

Table 5.12 Comparison of Design Moments to Simple Beam Moments – Nolanville Bridge

Truck D4 (kip-in)		MR	HETS (kip-in)		MR
Design	Simple		Design	Simple	
5580	9070	0.62	16200	30900	0.52

Table 5.13 Average Design Moment Ratios

Bridge Name	MR #1	MR #2	MR #3	MR #4	$M_{average}$
Chandler Creek – 40’ Span	0.65	0.65	0.67	0.77	**0.69**
Chandler Creek – 60’ Span	0.76	0.76	0.79	0.93	**0.81**
Lake LBJ	0.78	0.79	0.75	0.97	**0.82**
Lampasas River – Span 1	0.84	0.85	0.82	0.89	**0.85**
Lampasas River – Span 2	0.80	0.80	0.79	0.87	**0.82**
Willis Creek	0.73	0.82	0.68	0.85	**0.77**
Wimberley – Span 1	0.74	0.72	0.75	0.74	**0.74**
Wimberley – Span 2	0.69	0.67	0.67	0.73	**0.69**
Slaughter Creek	0.71	0.72	0.71	0.71	**0.71**
Nolanville	0.62	0.52	-	-	**0.57**

As shown in previous tables, the moment ratios varied significantly among the bridges. For the five bridges in the Project 1895 study, the moment ratios ranged between 0.65 and 0.97, with an average of 0.77. For the two bridges in the Project 2986 study, the ratios were generally lower, between 0.52 and 0.73. As mentioned previously, the preferred range was between 0.90 and 1.10. Therefore, the moments inferred from measured strains and design section properties did not lie within an acceptable range of accuracy, leading to a revised analysis using adjusted section properties that were more representative of in-situ conditions.

5.2.4 Live Load Moments Calculated Using Adjusted Section Properties

There are two primary sources of disparities between design section properties and in-situ section properties. The first major source of disparity is related to differences in concrete strength. In-situ concrete strengths are generally higher than design strengths for two reasons. First, the concrete supplier will typically deliver concrete that is stronger than the design strength in order to avoid rejection of the concrete and a subsequent financial loss. The amount of strength increase depends on the mix design and level of quality control at the supplier's plant. Second, ultimate concrete strength in structural members is not constant; strength gradually increases with time. In tests of approximately 3600 concrete cylinders under various curing conditions, Wood found that after twenty years the compressive strength of a concrete mix made with Type III portland cement can be as much as twenty to thirty percent higher than the specified 28-day compressive strength (Wood 1991). After several months, however, strength gain can usually be neglected. The adjusted concrete strengths are presented in Chapter 2.

The second source of disparity is due to unavoidable geometric differences between what was designed and what was actually built during the construction process. The differences manifest themselves in many different forms, from incorrect member thickness to variable concrete cover over reinforcing steel, to non-uniform spacing of prestressing strands. While these differences are usually small, they should be taken into account to maximize the accuracy of relevant calculations. Figure 5.9 illustrates the differences between dimensions found on contract drawings and dimensions measured in the field at the Willis Creek bridge. A complete list of actual dimensions is provided in Appendix C. While these differences are present, they are difficult to quantify and therefore were not considered in this study. Only design dimensions were used in calculations of section properties, which may account for a small portion of the difference in the final results.

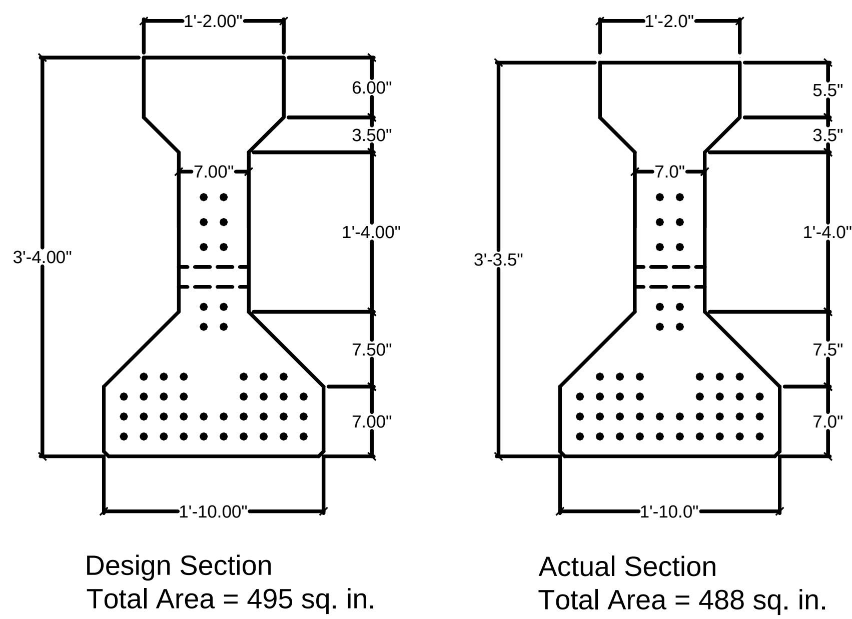

Figure 5.9 Differences in Section Dimensions at Willis Creek– Designed and As-Built

Once the adjusted section properties were established using the assumed concrete strengths, new live load moments were calculated. In order to facilitate this calculation, a moment factor (MF) was calculated based on design and adjusted section properties. The use of this moment factor was based on the moment equation shown in Equation 5.1. The modulus of elasticity, moment of inertia, and calculated neutral axis depth vary with different concrete strengths, but the measured strain remains constant. Therefore, the moment factor was computed as shown in Equation 5.5. In this equation, *E* is the modulus of elasticity of the girders (ksi), *I* is the moment of inertia for the composite

$$MF_{1895} = \frac{\left(\dfrac{E_{adjusted} \cdot I_{adjusted}}{NA_{measured}}\right)}{\left(\dfrac{E_{design} \cdot I_{design}}{NA_{design}}\right)} \tag{5.5}$$

section (in^4), and *NA* is the neutral axis depth (inches). Equation 5.5 applies to the five bridges tested in Project 1895. For the two bridges tested in the Project 2986 study, the moment factor was computed using Equation 5.6. In this equation, *E* is the modulus of elasticity of the girders (ksi), and S_b is the bottom section modulus

$$MF_{2986} = \frac{\left(E_{adjusted} \cdot S_{b\_adjusted}\right)}{\left(E_{design} \cdot S_{b\_design}\right)} \tag{5.6}$$

for the composite section (in^3).

Once the moment factors were computed for each bridge, the design moments were multiplied by this factor to produce the adjusted moments. The maximum adjusted moments were averaged for each bridge and loading type, just as the design moments were. These adjusted maximum moments are shown in the following tables. Table 5.14 shows the moments for the five bridges tested in Project 1895. Table 5.15 shows the moments for the two bridges tested in the Project 2986 study.

Table 5.14 Maximum Calculated Midspan Moments Based On Adjusted Section Properties, Project 1895

Bridge Name	Single Truck 1 (kip-in)	Single Truck 2 (kip-in)	Side-by-Side (kip-in)	Back-to-Back (kip-in)
Chandler Creek – 40' Span	2950	2850	5030	3730
Chandler Creek – 60' Span	5500	5430	10400	8620
Lake LBJ	7420	7320	13300	11900
Lampasas River – Span 1	8120	7900	16000	13000
Lampasas River – Span 2	7260	7220	14000	11800
Willis Creek	8280	8260	15700	12900
Wimberley – Span 1	3970	3660	7020	4720
Wimberley – Span 2	3880	3280	7030	5000

Table 5.15 Maximum Calculated Midspan Moments Based On Adjusted Section Properties – Project 2986

Bridge Name	Single Truck (kip-in)				Combination (kip-in)	HETS (kip-in)
	D1	D2	D3	D4		
Slaughter Creek	10300	11200	10200	-	21100	-
Nolanville	-	-	-	7920	-	23000

As shown in these tables, the same general trend was preserved for moments calculated using adjusted section properties. For the five bridges in the Project 1895 study, moments resulting from the side-by-side loading case were largest, followed by the back-to-back loading and the single-truck loading. For the two bridges in the Project 2986 study, the HETS loading produced the largest moments, followed by the combination loading and the single-truck loading. From this point in the text, the live load moments calculated using adjusted section properties will be referred to as "adjusted moments."

5.2.5 Comparison of Simple Beam Moments to Adjusted Moments

Adjusted moments were compared to simple beam moments in the same manner as the design moments. Once again, moments were compared using the moment ratio (MR), which is simply the adjusted moment divided by the simple beam moment, as shown in Equation 5.7.

$$MR = \frac{M_{\text{Adjusted}}}{M_{\text{Simple}}} \tag{5.7}$$

As shown previously, the moment ratios for design moments ranged from 0.52 to 0.97. One of the goals of using adjusted section properties was to more accurately model the in-situ properties and increase these moment ratios. If the adjusted moment ratios were raised to the desired range of 0.90 to 1.10, the results would indicate that inaccuracy of original moment calculations relative to simple beam moments lies mainly in the estimation of material properties.

Tables 5.16 through 5.19 show the adjusted average maximum moments with the corresponding simple beam moments and corresponding moment ratios. Tables 5.16 and 5.17 show these values for the five bridges tested in Project 1895. Tables 5.18 and 5.19 show these values for the two bridges tested in Project 2986. Table 5.20 shows the average moment ratios for each of the seven bridges.

With the average adjusted moment ratios, a comparison can be made with the average design moment ratios in order to assess the level of improvement achieved by using adjusted section properties. Table 5.21 shows a comparison between the average design moment ratios and the average adjusted moment ratios for all seven bridges. As shown in the table, there is an increase in the moment ratio for all bridges. For the 60' span of the Chandler Creek bridge, the

Lake LBJ bridge, Span 1 of the Lampasas River bridge, and the Slaughter Creek bridge, the moment ratio is between 0.95 and 1.00.

Table 5.16 Comparison of Adjusted Moments to Simple Beam Moments – Project 1895 – Single Truck Loading

Bridge Name	Side-by-Side (kip-in)		Moment Ratio	Back-to-Back (kip-in)		Moment Ratio
	Adjusted	Simple		Adjusted	Simple	
Chandler Creek – 40’ Span	2950	3360	0.88	2850	3300	0.86
Chandler Creek – 60’ Span	5500	5790	0.95	5430	5700	0.95
Lake LBJ	7420	7700	0.96	7320	7370	0.99
Lampasas River – Span 1	8120	8600	0.94	7900	8390	0.94
Lampasas River – Span 2	7260	8600	0.84	7220	8390	0.86
Willis Creek	8280	7800	1.06	8260	7070	1.17
Wimberley – Span 1	3970	4170	0.95	3660	3950	0.93
Wimberley – Span 2	3880	4170	0.93	3280	3950	0.83

Table 5.17 Comparison of Adjusted Moments to Simple Beam Moments – Project 1895 – Side-by-Side and Back-to-Back Loading

Bridge Name	Side-by-Side (kip-in)		Moment Ratio	Back-to-Back (kip-in)		Moment Ratio
	Adjusted	Simple		Adjusted	Simple	
Chandler Creek – 40’ Span	5030	6010	0.84	3730	3920	0.95
Chandler Creek – 60’ Span	10400	10800	0.96	8620	7850	1.10
Lake LBJ	13300	15100	0.88	11900	10900	1.09
Lampasas River – Span 1	16000	17000	0.94	13000	13100	0.99
Lampasas River – Span 2	14000	17000	0.82	11800	13100	0.90
Willis Creek	15700	15300	1.03	12900	10300	1.25
Wimberley – Span 1	7020	7520	0.93	4720	4920	0.96
Wimberley – Span 2	7030	7520	0.94	5000	4920	1.02

Table 5.18 Comparison of Adjusted Moments to Simple Beam Moments – Slaughter Creek Bridge

Truck D1 (kip-in)		MR	Truck D2 (kip-in)		MR	Truck D3 (kip-in)		MR	Combination (kip-in)		MR
Adjusted	Simple		Adjusted	Simple		Adjusted	Simple		Adjusted	Simple	
10300	10700	0.96	11200	11200	1.00	10200	10500	0.97	21100	21700	0.97

Table 5.19 Comparison of Adjusted Moments to Simple Beam Moments – Nolanville Bridge

Truck D4 (kip-in)		MR	HETS (kip-in)		MR
Adjusted	Simple		Adjusted	Simple	
7920	9070	0.87	23000	30900	0.74

Table 5.20 Average Adjusted Moment Ratios

Bridge Name	MR #1	MR #2	MR #3	MR #4	$M_{average}$
Chandler Creek – 40’ Span	0.88	0.86	0.84	0.95	**0.88**
Chandler Creek – 60’ Span	0.95	0.95	0.96	1.10	**0.99**
Lake LBJ	0.96	0.99	0.88	1.09	**0.98**
Lampasas River – Span 1	0.94	0.94	0.94	0.99	**0.95**
Lampasas River – Span 2	0.84	0.86	0.82	0.90	**0.86**
Willis Creek	1.06	1.17	1.03	1.25	**1.13**
Wimberley – Span 1	0.95	0.93	0.93	0.96	**0.94**
Wimberley – Span 2	0.93	0.83	0.94	1.02	**0.93**
Slaughter Creek	0.96	1.00	0.97	0.97	**0.98**
Nolanville	0.87	0.74	-	-	**0.81**

Table 5.21 Comparison of Average Design Moment Ratios to Average Adjusted Moment Ratios

Bridge Name	MR_{Design}	$MR_{Adjusted}$	$MR_{Adjusted} - MR_{Design}$
Chandler Creek – 40' Span	0.69	0.88	0.19
Chandler Creek – 60' Span	0.81	0.99	0.18
Lake LBJ	0.82	0.98	0.16
Lampasas River – Span 1	0.85	0.95	0.10
Lampasas River – Span 2	0.82	0.86	0.04
Willis Creek	0.77	1.13	0.36
Wimberley – Span 1	0.74	0.94	0.20
Wimberley – Span 2	0.69	0.93	0.24
Slaughter Creek	0.71	0.98	0.27
Nolanville	0.57	0.81	0.24

5.3 SUMMARY

5.3.1 Neutral Axis Depths

When observing the change in calculated moments using design and adjusted section properties, it is imperative to consider the effect of the actual neutral axis depth. As shown in Equation 5.2 and inherent in Equation 5.3, the neutral axis depth directly affects the calculated live load moment. For example, if the assumed neutral axis depth is in error by five to ten percent, then the assumed live load moment is incorrectly estimated by five to ten percent. In this study, the neutral axis depths calculated using design section properties were, on average, nine percent different from the neutral axis depths inferred from strain measurements, and the adjusted neutral axis depths were, on average, roughly three percent different.

When these differences in neutral axis depths are considered, the net effect is a significantly different calculated live load moment. Similar to the case of material properties, it is essential to make an accurate prediction of neutral axis depths in order to effectively model live load response.

5.3.2 Simple Beam Moments

In the previous discussions, live load moments calculated from a simple beam analysis were assumed to be the proper measure of accuracy of moments inferred from measured strains. Naturally, the validity of a using simple beam analysis to model the behavior of prestressed concrete girders is debatable. The behavior of these bridges, as with any other bridge, is quite complex and is dependent upon numerous interactions, such as the degree of composite action between the slab and girders, and the level of participation of any intermediate diaphragms. While the simple beam model is used in this study mainly because of its simplicity, perhaps a better tool for measuring the accuracy of calculated moments in individual girders would involve a finite element model. With this type of model, the level of complexity increases significantly, increasing the overall time involved in analysis. In addition, the use of a finite element model requires knowledge of section and material properties, which is a formidable dilemma as already mentioned. The methods used to model a prestressed concrete bridge using a finite element program are also subject to debate. Although the correct method may be debated, it is not difficult to obtain a reasonably accurate finite-element model with relatively minimal effort (Chen and Aswad 1996).

5.3.3 Live Load Moments

As shown previously, calculation of live load moments from measured strains taken from a prestressed concrete girder bridge is a complicated process. It involves the careful selection of material properties and cross-section dimensions in order to model actual behavior. When considering material properties, the fact that these bridges are composed almost entirely of concrete makes the task of accurately ascertaining actual behavior quite difficult. While using design concrete strengths is far too conservative given the nature of the concrete industry and typical construction practice, prediction of in-situ concrete strengths using prescriptive equations may fall short of an accurate assessment of actual conditions. If warranted, the best solution may be to extract concrete core samples from the bridges.

Given the present constraints on load testing of in-service prestressed concrete bridges, the ability to accurately predict their live load behavior is limited. Using the design section properties for the seven bridges considered in this study, the live load moments inferred from the measured strains differed, on average, by roughly twenty to thirty percent relative to simple beam moments. Because using design section properties is very conservative, adjusted section properties were chosen based on available material test data in an attempt to reflect present conditions. This process is discussed further in Chapter 2. By using adjusted section properties for all seven bridges, the live load moments inferred from measured strains differed, on average, by about five to fifteen percent, which is a significant improvement over moments determined using design section properties.

Chapter 6 – Calculation of Live Load Distribution Factors

This chapter addresses the calculation of live load distribution factors for all seven prestressed concrete girder bridges. Live load distribution factors are included in a separate chapter because one of the main goals of this study is to determine if a more accurate calculation of maximum distribution factors leads to a favorable change in the overall bridge load rating. The first section addresses the live load distribution factors calculated based on measured data from Project 1895. The second section contains a revised calculation of live load distribution factors using data from Project 2986, as well as a comparison of revised values with original values. The third section presents a comparison between live load distribution factors inferred from test data and the AASHTO code values.

6.1 LIVE LOAD DISTRIBUTION FACTORS – PROJECT 1895

The calculation of live load distribution factors using measured data obtained during field testing was a relatively easy process. First, live load moments for each beam were calculated from measured strains. These values are presented in Chapter 5. Next, total moments were calculated by summing the moments inferred from measured strain data for each prestressed girder. Finally, live load distribution factors were calculated by dividing individual girder moments by the total moment. Equation 6.1 shows the mathematical relationship for this process. In this equation, the live load distribution factor for a given girder is denoted as DF_i, M_i (kip-in) is the individual girder moment, and the total moment is M_{total} (kip-in).

$$DF_i = \frac{M_i}{M_{total}} \tag{6.1}$$

For every record number in a given test run, this process was completed using data from that record. For the five bridges tested in Project 1895, live load distribution factors were calculated using the adjusted material and section data and inferred neutral axis values. Because there is significant scatter in the data near the ends of the span, as shown in Figure 6.1, only a portion of the data were considered in order to obtain reasonable results. Only live load distribution factors associated with maximum total moment induced by vehicle loading on a single bridge span were considered. Therefore, it is logical to consider only those data associated with loads applied in close proximity to the location that produces maximum total moment. For the bridges tested in Project 1895, only "measured" live load distribution factors from within 15% of the span length from the location of maximum total moment were considered. These values were then averaged to give a mean live load distribution factor for each girder in every run. A schematic of this procedure is shown in Figure 6.2.

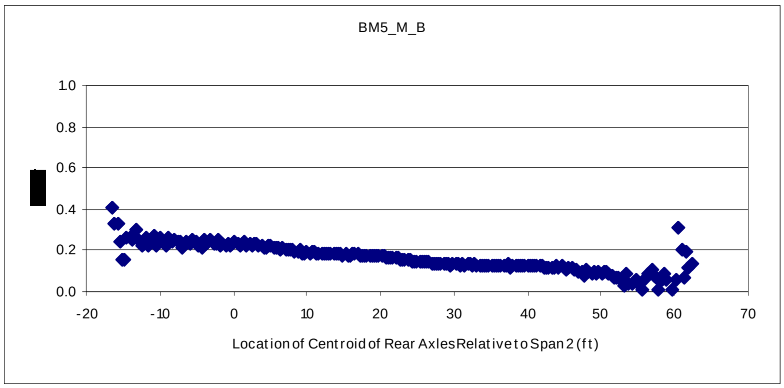

Figure 6.1 Sample Plot of Live Load Distribution Factors

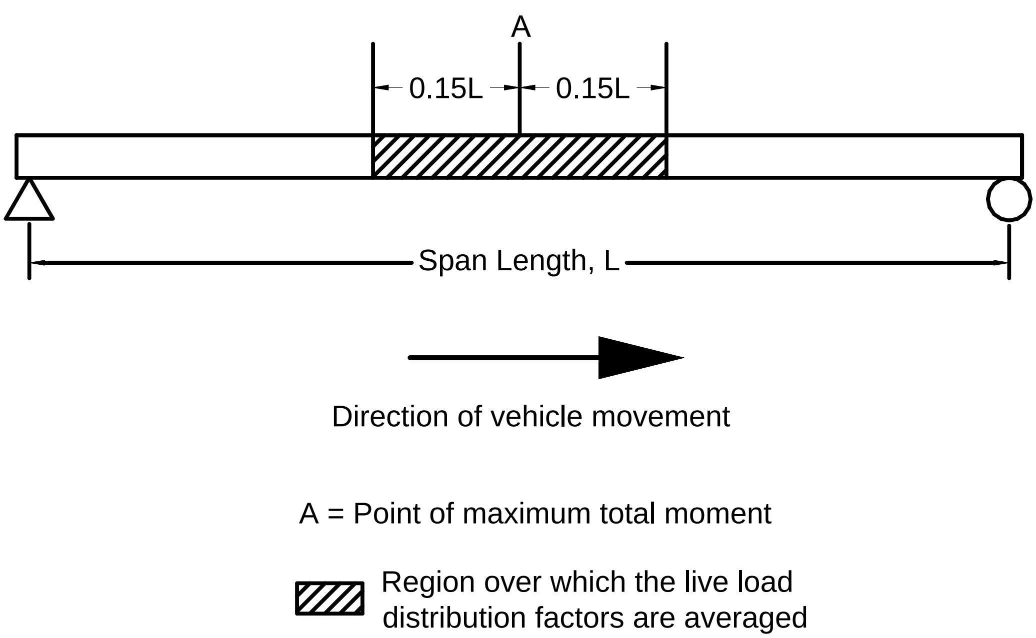

Figure 6.2 Schematic of Live Load Distribution Factor Averaging Technique

Once the average values for live load distribution factors were obtained for every run, the maximum values were identified for each girder. These maximum values reflect the largest portion of total moment distributed to each girder for all the various vehicle loading configurations. As such, they approximate the highest portion of live load moment a given girder will experience during daily use, no matter what the magnitude or configuration of the vehicle loading may be. These values are very useful, therefore, in designing new bridges of similar proportion, and in evaluating performance of existing bridges. Table 6.1 lists the maximum averaged live load distribution factors, abbreviated with the letters "LLDF," for the five bridges tested in Project 1895.

Table 6.1 Maximum Live Load Distribution Factors – Project 1895

Bridge Name	Beam 1 LLDF	Beam 2 LLDF	Beam 3 LLDF	Beam 4 LLDF	Beam 5 LLDF
Chandler Creek – 40' Span	0.53	0.43	0.43	0.55	N/A
Chandler Creek – 60' Span	0.48	0.39	0.37	0.50	N/A
Lake LBJ	0.51	0.35	0.37	0.50	N/A
Lampasas River – Span 1	0.49	0.35	0.36	0.48	N/A
Lampasas River – Span 2	0.50	0.34	0.35	0.49	N/A
Willis Creek	0.49	0.35	0.35	0.52	N/A
Wimberley – Span 1	0.50	0.46	0.44	0.43	0.52
Wimberley – Span 2	0.46	0.38	0.41	0.37	0.42

As shown in Table 6.1, there is a consistent trend in the data that may be explained through basic structural mechanics. For each of the five bridges, the maximum live load distribution factors for the exterior girders are noticeably larger than the distribution factors for the interior girders. This trend is a result of bridge geometry and loading configurations. As a vehicle travels across a bridge, the vertical load is distributed laterally in both directions according to the relative stiffness of the interior and exterior sections. As a given vehicle travels closer to the edge of the bridge deck, the vertical load tends to distribute in both directions, but because there is no girder adjacent to the exterior girder on the outside, the exterior girder must resist all the moment that would have distributed to an adjacent girder. Conversely, as a vehicle travels closer to the middle of the bridge deck, vertical load can distribute laterally in both directions to adjacent girders. Additionally, in some cases, the exterior composite sections are actually stiffer than the interior composite sections, which means that they “attract” a larger portion of the total moment. Figure 6.3 shows a schematic of this behavior. The vertical loads represent wheel loads from a vehicle that is traveling along the bridge.

In the top drawing in Figure 6.3, the wheel loads are relatively close to the edge of the bridge deck. As the dashed lines and arrows indicate, most of the load will be resisted by the two interior girders and the exterior girder on the right.

The wheel load on the left will most likely be supported by all three girders; however, most of the wheel load on the right will be supported by the exterior girder. This particular loading configuration results in a high distribution factor for the exterior girder.

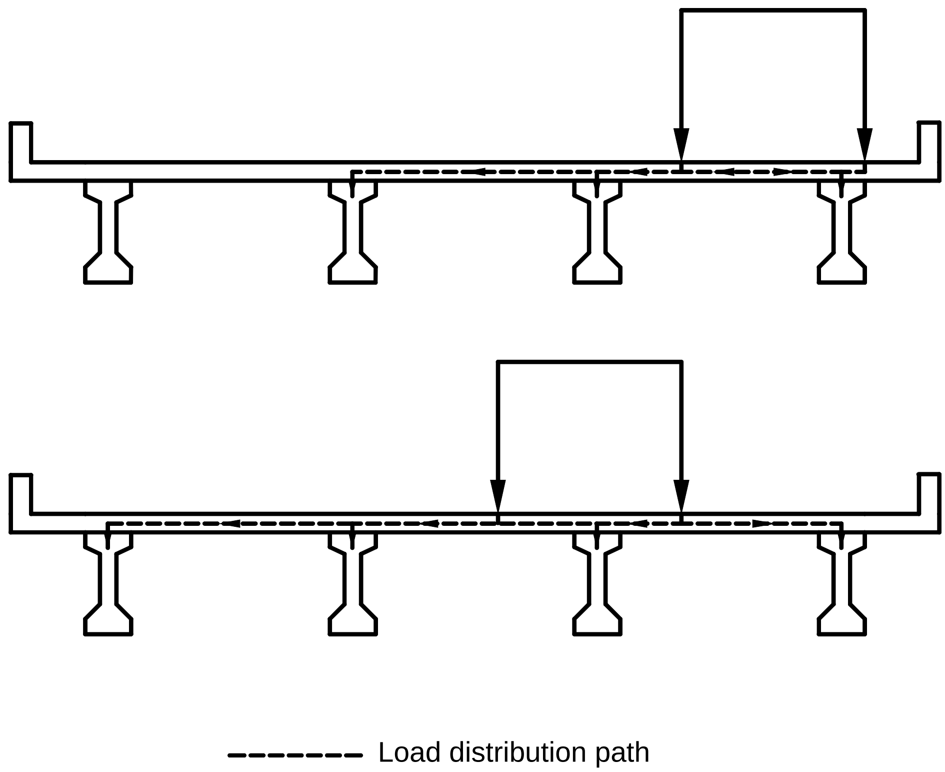

Figure 6.3 Effects of Vehicle Path on Live Load Distribution

In the bottom drawing in Figure 6.3, the wheel loads are closer to the center of the bridge. As a result, all four girders will likely develop significant moments due to the wheel loads, but the two girders on the right will collectively develop more moment than the two girders on the left. This loading configuration will probably result in a lower distribution factor for the exterior girder relative to the first case. These trends were also observed in results of other prestressed concrete bridge studies focusing on live load distribution (Barr, Eberhard, and Stanton 2001).

There is another trend in Table 6.1 that should be evaluated. A common notion in bridge design is that the addition of intermediate diaphragms between adjacent girders improves lateral distribution of vertical load. While this seems to make sense intuitively, some research suggests that the configuration and type of intermediate diaphragms used in a prestressed concrete girder bridge have essentially no effect on live load distribution (Abendroth, Klaiber, and Shafer 1995). Because the test bridges in this study already exist, there was no practical way to move the diaphragms around to test different diaphragm configurations in a single bridge. However, there were three bridges studied in Project 1895 that had similar characteristics but slightly different diaphragm configurations. The 60' span of the Chandler Creek bridge, the Lake LBJ bridge, and the Willis Creek bridge all have span lengths in the range of sixty to sixty-five feet, and the prestressed concrete girders have similar dimensions. Table 6.2 summarizes some of the critical dimensions for each bridge to verify their similarity. Concrete strengths in Table 6.2 are the adjusted values.

Table 6.2 Similar Bridges Tested in Project 1895

Bridge Name	Span Length (ft)	f'$_c$ Girder (psi)	f'$_c$ Slab (psi)	t_{slab} (in)	h_{girder} (in)	$h_{composite}$ (in)
Chandler Creek – 60' Span	58.5	8700	6000	7.25	40	47.25
Lake LBJ	63.5	8000	6000	7.25	40	47.25
Willis Creek	63.5	8600	6000	6.00	40	46.00

As shown in Table 6.1, live load distribution factors for these three bridges are reasonably similar. The maximum distribution factors for the exterior beams are about 0.50, and maximum distribution factors for the interior beams are roughly 0.36. Figure 6.4 shows a graphical representation of the live load distribution across the width of the deck for each of the three bridges. The similarities between the distribution patterns shown in Figure 6.4 appear to reinforce the conclusions of Abendroth, Klaiber, and Shafer, whose research suggests that live load distribution is effectively independent of diaphragm configuration.

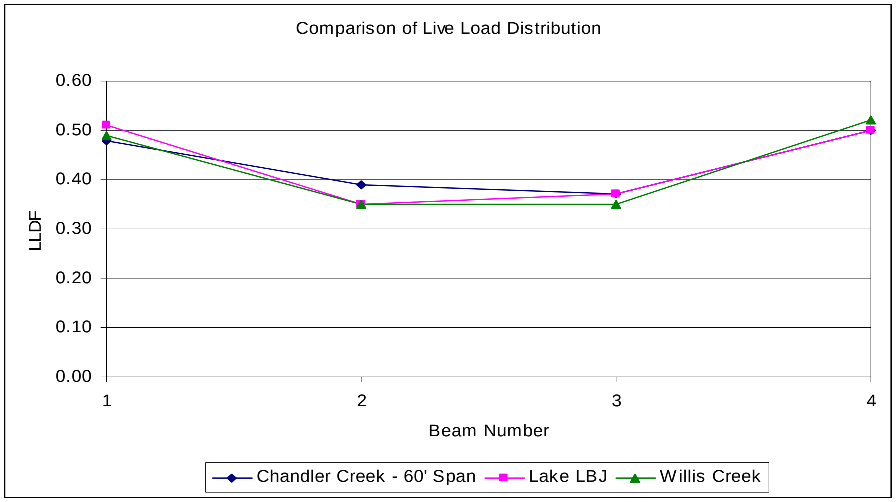

Figure 6.4 Comparison of Live Load Distribution Factors

6.2 LIVE LOAD DISTRIBUTION FACTORS – PROJECT 2986

Calculation of live load distribution factors from the data in Project 2986 involved a slightly different process than described previously, but was based on the same concept. The reason for the differences was that there were no calculations of live load moments based strictly on design section properties. The researcher correctly assumed that actual concrete strengths are higher than design concrete strengths, and accounted for this condition by increasing the modulus of elasticity of the concrete in each girder by approximately 5% above the design values (Matsis 1999). Then, live load moments were calculated based on assumed section properties using the increased concrete moduli. The maximum live load moments for each girder in each run were presented in the project report (Matsis 1999).

In order to make a calculation for live load distribution factors that is comparable to calculations made for the Project 1895 data, maximum live load moments were recalculated based on design section properties as found on the contract drawings and presented in Chapter 2. Then, maximum adjusted live load moments were calculated for each girder in every run based on the moment factor method discussed in Chapter 5. Tables 6.3 and 6.4 show revised maximum moments calculated based on adjusted section properties for the two bridges tested in Project 2986. Table 6.3 shows the maximum moments for runs one through twenty-two on the Slaughter Creek bridge. Table 6.4 shows the maximum moments for runs twenty-three through thirty-three on the Nolanville bridge. Once again, these moments were calculated at the three-quarter span location because unreliable data were recorded at midspan. The tables show that for some runs the exterior girders resisted a negative moment, which indicates a slight uplift on the opposite side of the bridge deck relative to the loading vehicle, as mentioned in Chapter 4.

Using the data in Tables 6.3 and 6.4, the adjusted live load distribution factors were calculated for each run according to Equation 6.1. These values are summarized in Tables 6.5 and 6.6. Table 6.5 shows the adjusted live load distribution factors for the Slaughter Creek bridge and Table 6.6 shows the adjusted live load distribution factors for the Nolanville bridge. Some of the values are negative because they are calculated from negative moments, even though it is illogical to have a negative distribution factor.

As shown in Table 6.5, the maximum distribution factors for the exterior girders of the Slaughter Creek bridge were 0.64 and 0.69, which is the highest of any of the seven bridges considered in this study. This may be the result of two conditions in the Slaughter Creek bridge that do not exist in any of the other bridges. First, the concrete in the exterior girders is much stronger than the interior girders, by as much as twenty percent. Additionally, the 32-inch high concrete parapets make the composite section much stiffer than the interior sections, which tends to “attract” more of the total moment than the interior sections.

Table 6.3 Maximum Adjusted Girder Moments – Slaughter Creek Bridge

Run Number	M_{max} Beam 1 (kip-in)	M_{max} Beam 2 (kip-in)	M_{max} Beam 3 (kip-in)	M_{max} Beam 4 (kip-in)	M_{max} Beam 5 (kip-in)	M_{total} (kip-in)
1	124	358	1090	2380	7980	11930
2	62	289	1030	2330	6910	10621
3	-	-	-	-	-	-
4	742	1540	2740	2550	2190	9762
5	2140	2190	2820	1450	824	9424
6	2160	2110	2710	1250	1090	9320
7	7960	2810	1200	495	103	12298
8	7610	2530	1060	261	206	11667
9	6930	3030	2130	2670	7520	22280
10	6780	3000	2190	2770	7110	21850
11	948	1620	3730	4420	10000	20718
12	1090	1730	3890	4450	9770	20930
13	9480	4400	3780	1720	1260	20640
14	8900	4390	3990	1930	1320	20530
15	41	275	908	2230	7540	10995
16	227	413	908	2230	7870	11648
17	948	1240	2680	1930	2060	8858
18	845	1140	2620	1980	2060	8645
19	2230	2080	2740	1450	1380	9880
20	2270	1950	2730	1420	1300	9670
21	6910	2460	1060	358	-62	10726
22	6870	2520	1070	427	186	11072

Table 6.4 Maximum Adjusted Girder Moments – Nolanville Bridge

Run Number	M_{max} Beam 1 (kip-in)	M_{max} Beam 2 (kip-in)	M_{max} Beam 3 (kip-in)	M_{max} Beam 4 (kip-in)	M_{max} Beam 5 (kip-in)	M_{total} (kip-in)
23	10000	8330	3290	2240	-1240	22620
24	-857	2440	5390	8500	11800	27273
25	2150	4600	7210	4620	3110	21690
26	2350	4850	7380	4300	2830	21710
27	2220	4750	7280	4640	3040	21930
28	-189	695	1560	3090	3400	8556
29	-189	724	1640	3160	3310	8650
30	697	1930	3200	1060	843	7730
31	683	1530	2950	1040	857	7060
32	3530	3070	984	608	-334	7858
33	3580	3040	883	536	-320	7719

Table 6.5 Adjusted Live Load Distribution Factors – Slaughter Creek

Run Number	Beam 1 LLDF	Beam 2 LLDF	Beam 3 LLDF	Beam 4 LLDF	Beam 5 LLDF
1	0.010	0.030	0.091	0.200	0.669
2	0.006	0.027	0.097	0.219	0.651
3	-	-	-	-	-
4	0.076	0.158	0.281	0.261	0.224
5	0.228	0.232	0.299	0.153	0.088
6	0.232	0.226	0.291	0.134	0.117
7	0.625	0.228	0.097	0.040	0.008
8	0.652	0.217	0.091	0.022	0.018
9	0.311	0.136	0.096	0.120	0.338
10	0.310	0.137	0.100	0.127	0.325
11	0.046	0.078	0.180	0.213	0.483
12	0.052	0.083	0.186	0.212	0.467
13	0.459	0.213	0.183	0.083	0.061
14	0.434	0.214	0.194	0.094	0.064
15	0.004	0.025	0.083	0.203	0.686
16	0.019	0.035	0.077	0.196	0.672
17	0.107	0.140	0.303	0.218	0.233
18	0.098	0.132	0.302	0.229	0.238
19	0.226	0.211	0.278	0.146	0.140
20	0.235	0.202	0.282	0.147	0.134
21	0.644	0.230	0.099	0.033	-0.006
22	0.620	0.228	0.097	0.039	0.017
Maximum	**0.644**	**0.230**	**0.303**	**0.261**	**0.686**

Table 6.6 Adjusted Live Load Distribution Factors – Nolanville

Run Number	Beam 1 LLDF	Beam 2 LLDF	Beam 3 LLDF	Beam 4 LLDF	Beam 5 LLDF
23	0.443	0.367	0.145	0.099	-0.055
24	-0.031	0.089	0.198	0.312	0.433
25	0.099	0.212	0.332	0.213	0.143
26	0.108	0.223	0.340	0.198	0.130
27	0.101	0.216	0.332	0.212	0.138
28	-0.022	0.081	0.183	0.361	0.398
29	-0.022	0.084	0.189	0.365	0.383
30	0.090	0.249	0.414	0.137	0.109
31	0.097	0.217	0.418	0.147	0.121
32	0.449	0.391	0.125	0.077	-0.043
33	0.463	0.394	0.114	0.069	-0.041
Maximum	**0.463**	**0.394**	**0.418**	**0.365**	**0.433**

For comparison, the following tables show the live load distribution factors that were reported in the Project 2986 report (Matsis 1999). Table 6.7 shows calculated live load distribution factors for the Slaughter Creek bridge. Table 6.8 shows the live load distribution factors for the Nolanville bridge. Table 6.9 shows the maximum values calculated with the revised approach and the values reported in the Project 2986 report.

Table 6.7 Live Load Distribution Factors from Project 2986 Report – Slaughter Creek

Run Number	Beam 1 LLDF	Beam 2 LLDF	Beam 3 LLDF	Beam 4 LLDF	Beam 5 LLDF
1	0.01	0.04	0.12	0.26	0.58
2	0.00	0.03	0.12	0.28	0.56
3	-	-	-	-	-
4	0.06	0.18	0.31	0.29	0.17
5	0.17	0.26	0.33	0.17	0.07
6	0.18	0.26	0.33	0.15	0.09
7	0.53	0.29	0.12	0.05	0.01
8	0.56	0.28	0.12	0.03	0.02
9	0.26	0.17	0.12	0.15	0.29
10	0.26	0.17	0.13	0.16	0.28
11	0.04	0.10	0.22	0.26	0.39
12	0.04	0.10	0.22	0.26	0.38
13	0.37	0.26	0.22	0.10	0.05
14	0.35	0.26	0.23	0.11	0.05
15	0.00	0.03	0.11	0.26	0.59
16	0.02	0.05	0.10	0.25	0.58
17	0.08	0.16	0.34	0.25	0.18
18	0.07	0.15	0.34	0.26	0.18
19	0.17	0.24	0.32	0.17	0.11
20	0.18	0.23	0.32	0.17	0.10
21	0.54	0.29	0.12	0.04	0.00
22	0.53	0.29	0.12	0.05	0.01
Maximum	**0.56**	**0.29**	**0.34**	**0.29**	**0.58**

Table 6.8 Live Load Distribution Factors from Project 2986 Report – Nolanville

Run Number	Beam 1 LLDF	Beam 2 LLDF	Beam 3 LLDF	Beam 4 LLDF	Beam 5 LLDF
23	0.41	0.33	0.15	0.07	-0.04
24	-0.04	0.08	0.24	0.27	0.37
25	0.13	0.22	0.36	0.18	0.11
26	0.14	0.23	0.36	0.17	0.10
27	0.14	0.21	0.36	0.18	0.11
28	-0.02	0.06	0.24	0.32	0.37
29	-0.02	0.09	0.24	0.31	0.34
30	0.13	0.21	0.40	0.17	0.09
31	0.14	0.20	0.40	0.17	0.09
32	0.40	0.34	0.14	0.07	-0.05
33	0.40	0.34	0.15	0.07	-0.04
Maximum	**0.41**	**0.34**	**0.40**	**0.32**	**0.37**

Table 6.9 Summary of Calculated Live Load Distribution Factors

Bridge Name	Beam 1 $LLDF_{max}$	Beam 2 $LLDF_{max}$	Beam 3 $LLDF_{max}$	Beam 4 $LLDF_{max}$	Beam 5 $LLDF_{max}$
Revised					
Slaughter Creek	0.64	0.23	0.30	0.26	0.69
Nolanville	0.46	0.39	0.42	0.37	0.43
Matsis					
Slaughter Creek	0.56	0.29	0.34	0.29	0.58
Nolanville	0.41	0.34	0.40	0.32	0.37

As shown in Table 6.9, the revised distribution factors are slightly different from the values originally reported in the project report. The revised values tend to be higher, especially for the exterior girders. For both sets of distribution factors, maximum values occur for the exterior girders, which is similar to the pattern found for the five bridges tested in Project 1895.

6.3 COMPARISON OF MEASURED DISTRIBUTION FACTORS TO AASHTO VALUES

As with the measured live load moments, it is imperative to compare the results of the field testing with accepted standard values. In this case, those standard values for live load distribution factors are taken from the 2000 Interim edition of the AASHTO LRFD Bridge Design Specifications. The equations used to calculate live load distribution factors have been updated in this manual, and are significantly more complex than older versions of the specifications, which related distribution factors to girder spacing only (American Association of State Highway and Transportation Officials 1996). Due to the complexity of the updated calculations, they are not presented here, only summarized. The full calculations are presented in Appendix D.

Table 6.10 lists the live load distribution factors for all seven bridge considered in this study, calculated according to current AASHTO design specifications, with only one design lane loaded (American Association of State Highway and Transportation Officials 2000a). The same trend is shown in Table 6.10 that was observed for inferred live load distribution factors summarized in previous tables. Except for the Wimberley bridge, live load distribution factors for interior girders are significantly less than distribution factors for exterior girders. The Wimberley bridge is both skewed and curved in plan, which is probably the cause of differences in results. As shown in the table, the maximum AASHTO distribution factor is 0.76.

Table 6.10 Live Load Distribution Factors Calculated Using AASHTO

Bridge Name	Beam 1 LLDF	Beam 2 LLDF	Beam 3 LLDF	Beam 4 LLDF	Beam 5 LLDF
Chandler Creek – 40’ Span	0.75	0.59	0.59	0.75	N/A
Chandler Creek – 60’ Span	0.75	0.54	0.54	0.75	N/A
Lake LBJ	0.76	0.52	0.52	0.76	N/A
Lampasas River – Span 1	0.73	0.48	0.48	0.73	N/A
Lampasas River – Span 2	0.73	0.48	0.48	0.73	N/A
Willis Creek	0.70	0.49	0.49	0.70	N/A
Wimberley – Span 1	0.52	0.55	0.55	0.55	0.52
Wimberley – Span 2	0.52	0.55	0.55	0.55	0.52
Slaughter Creek	0.63	0.47	0.47	0.47	0.63
Nolanville	0.76	0.51	0.51	0.51	0.76

Table 6.10 shows that the AASHTO distribution factors are significantly larger than inferred distribution factors. In order to assess the magnitude of the difference, the AASHTO values were divided by the measured values. Results of this comparison are shown in Table 6.11. The values range from 0.91 to 2.03, and the average of all values is 1.42. It is reasonable and imperative for code values to be conservative relative to actual conditions because design girder moments are

directly related to the live load distribution factors, and a ratio of 1.42 is conservative.

Table 6.11 Ratio of AASHTO Distribution Factors to Measured Distribution Factors

Bridge Name	Beam 1	Beam 2	Beam 3	Beam 4	Beam 5
Chandler Creek – 40’ Span	1.42	1.36	1.38	1.37	N/A
Chandler Creek – 60’ Span	1.56	1.36	1.45	1.49	N/A
Lake LBJ	1.48	1.50	1.38	1.51	N/A
Lampasas River – Span 1	1.49	1.38	1.33	1.51	N/A
Lampasas River – Span 2	1.46	1.39	1.36	1.48	N/A
Willis Creek	1.44	1.38	1.38	1.35	N/A
Wimberley – Span 1	1.03	1.20	1.26	1.29	1.00
Wimberley – Span 2	1.13	1.47	1.36	1.49	1.24
Slaughter Creek	0.96	2.03	1.56	1.81	0.91
Nolanville	1.65	1.28	1.21	1.38	1.76

An accurate assessment of live load distribution factors for a prestressed concrete girder bridge is vital to the load rating process, as shown in the following chapter. Because the maximum live load distribution factor assigned to each girder determines what portion of the design load it will receive, a conservative, or higher estimate of distribution factors will lead to low bridge load ratings that are unrealistic, and in some cases, uneconomical. A low bridge rating sometimes results in a complete reconfiguration of the trucking routes in a given area, which can lead to increased hauling time and increased cost to the operators and customers who rely on existing truck routes to conduct business.

6.4 SUMMARY

This chapter dealt with the calculation of live load distribution factors using two different methods for the seven bridges considered in this study. First, the distribution factors were calculated from data measured during field testing by dividing maximum moments from each girder into the total maximum moments. Then, live load distribution factors were calculated using the current AASHTO bridge design specifications for comparison to inferred values.

Inferred distribution factors for bridges tested in Project 1895 displayed similar trends between each bridge. The maximum distribution factors were determined for the exterior girders, and the average was approximately 0.50. Maximum distribution factors for interior girders were typically less than the distribution factors for exterior girders by up to twenty percent. For the two bridges tested in Project 2986, the maximum distribution factors were determined for exterior girders. For the Slaughter Creek bridge, the distribution factors for the exterior girders were 0.64 and 0.69 - nearly twice the values for the interior girders. This was attributed to higher concrete strength in the exterior girders and participation of the concrete parapets. For the Nolanville bridge, measured distribution factors were similar to those for the five bridges tested in Project 1895.

The live load distribution factors calculated using the current AASHTO bridge design specifications follow the same pattern found for the inferred values. Values for exterior girders are larger than values for interior girders; some by as much as thirty percent. However, the AASHTO values are generally larger and more conservative than inferred values. When the AASHTO values were divided by inferred values for each girder in each bridge, the resulting ratios ranged from 0.91 to 2.03, and the average ratio was 1.42.

There were two motivations for doing live load distribution factor calculations based on measured data. First, they provided a general picture of how live load response of bridges is affected by different parameters, such as diaphragm size and configuration, slab thickness, and vehicle position. Second, they allowed for a more accurate calculation of load rating. The load ratings for each bridge are presented in the next chapter.

Chapter 7 – Calculation of Load Rating

This chapter addresses the calculation of the AASHTO load rating for each of the seven prestressed concrete girder bridges considered in this study according to current procedure. The first section summarizes the load rating procedure and calculations that were used in this study. The second section presents load ratings obtained using design section properties and AASHTO live load distribution factors. The third section provides load rating values calculated using adjusted section properties and maximum measured live load distribution factors determined in this study, as well as a comparison to the design load rating values.

7.1 SUMMARY OF AASHTO LOAD RATING PROCEDURE

The current measure of serviceability of bridges in the United States is the AASHTO load rating. On a conceptual level, the load rating is simply a rating factor multiplied by the weight of the design vehicle used for live loading. The rating factor is calculated as the ratio of the net moment capacity divided by the live load moment induced by the design vehicle. The net moment capacity is the total moment capacity minus the moment induced by dead loads. This concept is represented in Equation 7.1 and Equation 7.2, which are found in the 2000 Interim

AASHTO Manual for Condition Evaluation of Bridges (American Association of State Highway and Transportation Officials 2000b).

$$RF = \frac{C - A_1 \cdot D}{A_2 \cdot L \cdot (I + 1)} \tag{7.1}$$

RF = rating factor
C = moment capacity of a composite section
A_1 = dead load factor
D = dead load moment on a composite section
A_2 = live load factor
L = live load moment induced by design vehicle
I = dynamic impact factor

$$RT = (RF) \cdot W \tag{7.2}$$

RT = load rating in tons
W = specified weight (tons) of design vehicle

The load rating, or RT in Equation 7.2, is the final number that is kept on record for all public bridges. This load rating may be divided into two categories. The inventory rating reflects the vehicle weight that a bridge can safely handle on a day-to-day basis for an indefinite period. The operating rating is a measure of the maximum permissible live load that should be allowed on a given bridge. If vehicles heavier than this operating rating are allowed to cross regularly, there can be a significant shortening of the usable life of a bridge (American Association of State Highway and Transportation Officials 2000b).

A bridge is said to "fail" the load rating if the rating factor, RF, is less than one, making the load rating lower than the specified weight of the design vehicle. A bridge that "fails" the load rating has to be further evaluated to determine if it must be taken out of service, modified in any way, or simply left as is. A bridge "passes" the load rating as long as the rating factor is equal to or greater than one, which indicates that the bridge can safely handle the design vehicle load. AASHTO allows two different methods to carry out the calculations for load rating. Both the allowable stress method and load factor method are acceptable, but the load factor method was used in this study.

In the case of prestressed concrete girder bridges, AASHTO prescribes five different rating factors for the inventory rating, and two rating factors for the operating rating. The rating factors are listed in Table 7.1 by category. Table 7.2 lists the variables shown in Table 7.1 and their definitions (American Association of State Highway and Transportation Officials 2000b). The minimum of the rating factors in each category is then multiplied by the specified design vehicle weight, yielding the final load rating. For this study and for current AASHTO load ratings, the design vehicle is designated as the HS-20 truck, and the specified design vehicle weight is twenty tons, which is the sum of the first two axle weights divided by two, because AASHTO load ratings are based on one wheel line per design lane.

Table 7.1 AASHTO Load Rating Factors

Description	Abbreviation	Equation
Inventory Rating Factors		
Concrete Tension	CT	$RF = \dfrac{6\sqrt{f_c} - \left(F_d + F_p + F_s\right)}{F_1}$
Concrete Compression$_1$	CC_1	$RF = \dfrac{0.6f_c - \left(F_d + F_p + F_s\right)}{F_1}$
Concrete Compression$_2$	CC_2	$RF = \dfrac{0.4f_c - 0.5\left(F_d + F_p + F_s\right)}{F_1}$
Prestressing Steel Tension	$PST_{Inventory}$	$RF = \dfrac{0.8f_y - \left(F_d + F_p + F_s\right)}{F_1}$
Flexural Strength	$FS_{Inventory}$	$RF = \dfrac{\phi R_n - (1.3D + S)}{2.17L(I + 1)}$
Operating Rating Factors		
Flexural Strength	$FS_{Operating}$	$RF = \dfrac{\phi R_n - (1.3D + S)}{1.3L(I + 1)}$
Prestressing Steel Tension	$PST_{Operating}$	$RF = \dfrac{0.9f_y - \left(F_d + F_p + F_s\right)}{F_1}$

Table 7.2 AASHTO Load Rating Factor Variable Definitions

Variable Symbol	Definition
D	Unfactored dead load moment
f_c	Concrete compressive strength
F_d	Unfactored dead load stress
F_l	Unfactored live load stress including impact
F_p	Unfactored stress due to prestress force after all losses
F_s	Unfactored stress due to secondary prestress forces (not used in this study)*
f_y	Prestressing steel yield stress
I	Dynamic impact factor
L	Unfactored live load moment
S	Unfactored prestress secondary moment (not used in this study)*
ϕR_n	Nominal moment capacity of the composite section
*The variables involving secondary prestressing effects are not used in this study because all seven bridges are simply supported.	

The detailed load rating calculations are not presented in this chapter, only summarized. For the full calculations as well as an estimation of concrete stresses, refer to Appendix E.

A major factor in AASHTO load rating is the live load moment induced by the design vehicle, in this case the HS-20 truck. In addition to the moment created by the truck, AASHTO prescribes a uniform load of 0.640 klf (kips per linear foot) to be applied to each design lane. In order to simplify the entire load rating process and provide some level of uniformity, AASHTO provides a table of HS-20 moments, including the uniform lane load, in Appendix A3 of the Manual for Condition Evaluation of Bridges (American Association of State Highway and Transportation Officials 2000b). Table 7.3 shows the live load moments for each of the seven bridges in this study, inferred from Appendix A3.

Table 7.3 HS-20 Moments for AASHTO Load Rating

Bridge Name	Span Length (ft)	Live Load Moment (kip-in)
Chandler Creek – 40' Span	38.5	5090
Chandler Creek – 60' Span	58.5	9370
Lake LBJ	63.5	10500
Lampasas River	73.8	12600
Willis Creek	63.5	10500
Wimberley	38.4	5060
Slaughter Creek	98.8	18000
Nolanville	101	18500

7.2 AASHTO LOAD RATINGS BASED ON DESIGN PROPERTIES

Now that the process for AASHTO load rating has been established, load rating factors and load ratings may be calculated for all seven bridges using design section properties. This includes using design concrete compressive strengths, design section properties calculated from the design concrete compressive strengths, and live load distribution factors calculated using current AASHTO provisions. Tables 7.4 and 7.5 show the individual rating factors that were calculated for all seven bridges. Table 7.4 shows the rating factors calculated for the interior composite sections for each bridge. Table 7.5 shows the rating factors calculated for the exterior composite sections for each bridge.

Table 7.4 AASHTO Rating Factors Calculated Using Design Properties – Interior Composite Sections

Bridge Name	CT	CC_1	CC_2	$PST_{Inventory}$	$FS_{Inventory}$	$FS_{Operating}$	$PST_{Operating}$
Chandler Creek – 40’ Span	1.18	5.65	4.01	6.17	1.08	1.81	10.10
Chandler Creek – 60’ Span	0.97	3.20	2.51	5.89	1.20	2.00	9.61
Lake LBJ	0.96	2.56	2.13	6.03	1.20	2.01	9.58
Lampasas River	0.60	1.48	1.39	4.64	1.03	1.71	7.72
Willis Creek	0.69	1.77	1.59	6.64	1.04	1.74	11.01
Wimberley	1.83	4.91	3.50	9.34	1.74	2.90	14.23
Slaughter Creek	1.37	2.97	2.58	4.77	1.54	2.57	10.11
Nolanville	1.79	4.11	3.30	7.25	2.14	3.58	12.26

Table 7.5 AASHTO Rating Factors Calculated Using Design Properties – Exterior Composite Sections

Bridge Name	CT	CC_1	CC_2	$PST_{Inventory}$	$FS_{Inventory}$	$FS_{Operating}$	$PST_{Operating}$
Chandler Creek – 40' Span	1.25	5.56	3.91	6.39	1.13	1.88	10.40
Chandler Creek – 60' Span	1.00	3.04	2.34	5.79	1.18	1.97	9.36
Lake LBJ	0.93	2.88	2.46	6.27	1.08	1.81	9.94
Lampasas River	0.58	1.37	1.25	4.26	0.94	1.57	7.05
Willis Creek	0.63	1.91	1.78	6.59	0.94	1.57	10.94
Wimberley	2.45	7.61	5.44	12.45	2.00	3.34	18.92
Slaughter Creek	2.64	7.39	6.47	16.53	3.25	5.43	28.31
Nolanville	2.00	3.94	3.07	8.89	2.10	3.50	14.94

As shown in Tables 7.4 and 7.5, the rating factor for concrete tension is typically the smallest inventory value for each bridge, which seems reasonable. Because concrete is weak in tension, it makes sense that the strength of a structure made of concrete, loaded in flexure, will be governed by the tensile strength of the concrete. For some of the bridges, the inventory flexural strength rating factor is the smallest inventory value, which indicates that the design live load moment is large compared to the net flexural capacity of the composite section. For both the inventory and operating rating factors, prestressing steel tension factors are typically very large relative to other values, which suggests that yielding of the prestressing steel is rarely a controlling factor since other failure modes will have occurred first. As mentioned previously, bridges with a minimum rating factor less than one are said to "fail" the HS-20 load rating criterion.

Tables 7.6 and 7.7 show the load ratings for all seven bridges considered in this study. Table 7.6 shows the load ratings calculated for the interior composite sections of each bridge. Table 7.7 shows the load ratings calculated for the exterior composite sections of each bridge. As mentioned before, the load rating values are simply the load rating factors multiplied by twenty tons, which is the specified design weight for an HS-20 truck.

Table 7.6 AASHTO Load Ratings, in Tons, Calculated Using Design Section Properties – Interior Composite Sections

Bridge Name	CT	CC_1	CC_2	$PST_{Inventory}$	$FS_{Inventory}$	$FS_{Operating}$	$PST_{Operating}$
Chandler Creek – 40’ Span	23.6	113	80.1	123	21.7	36.2	202
Chandler Creek – 60’ Span	19.4	64.0	50.2	118	24.0	40.1	192.
Lake LBJ	19.2	51.3	42.6	121	24.0	40.1	192
Lampasas River	11.9	29.7	27.9	92.7	20.5	34.2	154
Willis Creek	13.9	35.5	31.7	133	20.8	34.8	220
Wimberley	36.6	98.2	70.1	187	34.7	57.9	285
Slaughter Creek	27.3	59.4	51.6	95.4	30.8	51.3	202
Nolanville	35.8	82.2	65.9	145	42.8	71.5	245

Table 7.7 AASHTO Load Ratings, in Tons, Calculated Using Design Section Properties – Exterior Composite Sections

Bridge Name	CT	CC_1	CC_2	$PST_{Inventory}$	$FS_{Inventory}$	$FS_{Operating}$	$PST_{Operating}$
Chandler Creek – 40’ Span	25.0	111	78.2	128	22.5	37.6	208
Chandler Creek – 60’ Span	19.9	60.8	46.8	116	23.6	39.3	187
Lake LBJ	18.5	57.7	49.2	125	21.7	36.2	199
Lampasas River	11.5	27.4	25.1	85.2	18.8	31.4	141
Willis Creek	12.7	38.2	35.5	132	18.8	31.4	219
Wimberley	49.0	152	109	249	40.0	66.7	379
Slaughter Creek	52.8	148	130	331	65.1	109	566
Nolanville	40.0	78.7	61.4	178	42.0	70.1	299

Because only one load rating value is assigned to a given bridge, the minimum values must be taken from Tables 7.6 and 7.7. These minimum values are shown in Table 7.8. As shown, four bridges would "fail" the load rating criterion for the inventory rating. The 60' span of the Chandler Creek bridge, the Lake LBJ bridge, the Lampasas River bridge, and the Willis Creek bridge all have inventory ratings less than twenty, which means they cannot safely carry the current AASHTO design vehicle, the HS-20 truck. However, these ratings have been derived using design section properties and AASHTO live load distribution factors, which, as shown in the next section, produces a very conservative approach to load rating.

Table 7.8 AASHTO Load Ratings, in Tons, Using Design Section Properties

Bridge Name	Inventory Rating	Operating Rating
Chandler Creek – 40' Span	21.7	36.2
Chandler Creek – 60' Span	19.4	39.3
Lake LBJ	18.5	36.2
Lampasas River	11.5	31.4
Willis Creek	12.7	31.4
Wimberley	34.7	57.9
Slaughter Creek	27.3	51.3
Nolanville	35.8	70.1

7.3 AASHTO LOAD RATINGS BASED ON ADJUSTED PROPERTIES

7.3.1 Adjusted Load Ratings

As shown in the previous section, several of the bridges “fail” the AASHTO load rating criterion when considering design section properties and AASHTO live load distribution factors. However, as shown in Chapters 5 and 6, using design section properties for these bridges results in a significant underestimation of their actual strength and performance. Therefore, it stands to reason that in order to assess the true load rating for each of these bridges, adjusted section properties and measured live load distribution factors should be used in the calculations, as permitted in the AASHTO Manual for Condition Evaluation of Bridges. Adjusted material and section properties used in these revised calculations are presented in Chapter 2. Measured live load distribution factors are found in Chapter 6. Once again, the full load rating calculations are not presented in this chapter. The calculations and other relevant details are found in Appendix E.

Tables 7.9 and 7.10 show the revised load rating factors for each bridge, calculated using adjusted section properties and measured live load distribution factors. Table 7.9 shows revised load rating factors calculated for the interior composite sections of each bridge. Table 7.10 shows revised load rating factors calculated for the exterior composite sections of each bridge.

Table 7.9 AASHTO Rating Factors Calculated Using Adjusted Section Properties – Interior Composite Sections

Bridge Name	CT	CC_1	CC_2	$PST_{Inventory}$	$FS_{Inventory}$	$FS_{Operating}$	$PST_{Operating}$
Chandler Creek – 40' Span	2.32	18.1	12.6	13.4	1.96	3.27	22.0
Chandler Creek – 60' Span	2.08	14.1	10.1	14.3	2.30	3.83	23.2
Lake LBJ	2.01	10.2	7.5	14.0	2.37	3.96	22.3
Lampasas River	1.30	7.64	5.89	10.8	1.96	3.27	17.9
Willis Creek	1.55	9.41	7.06	15.9	2.04	3.40	26.5
Wimberley	3.10	15.3	10.6	18.2	2.79	4.66	28.0
Slaughter Creek	3.35	16.8	12.5	10.5	3.56	5.95	22.3
Nolanville	3.38	15.6	11.5	12.8	3.81	6.37	21.7

Table 7.10 AASHTO Rating Factors Calculated Using Adjusted Section Properties – Exterior Composite Sections

Bridge Name	CT	CC_1	CC_2	$PST_{Inventory}$	$FS_{Inventory}$	$FS_{Operating}$	$PST_{Operating}$
Chandler Creek – 40' Span	1.89	13.6	9.37	10.7	1.57	2.62	17.4
Chandler Creek – 60' Span	1.71	10.5	7.46	11.3	1.82	3.04	18.2
Lake LBJ	1.53	9.39	7.02	11.4	1.68	2.81	18.1
Lampasas River	0.99	5.44	4.15	7.92	1.44	2.40	13.0
Willis Creek	1.05	7.84	5.94	11.5	1.34	2.24	19.2
Wimberley	3.14	18.2	12.6	18.4	2.45	4.09	28.2
Slaughter Creek	2.65	17.3	13.1	15.1	3.14	5.24	25.8
Nolanville	3.33	12.6	9.23	13.9	3.34	5.57	23.4

As shown in Tables 7.9 and 7.10, by completing a revised calculation of load ratings using more realistic input values, every bridge except the Lampasas River bridge has rating factors greater than one. In turn, every bridge except the Lampasas River bridge will have load ratings greater than twenty. Not only are the values for concrete compressive strength higher, which leads to a stronger section, live load distribution factors have been reduced significantly from the AASHTO values, sometimes by as much as fifty percent, as shown in Chapter 6.

Tables 7.11 and 7.12 list the load rating values for each bridge, calculated from the load rating factors shown in Tables 7.9 and 7.10. Table 7.11 shows the load rating values for the interior composite sections of each bridge. Table 7.12 shows the load rating values for the exterior composite sections of each bridge.

Tables 7.11 and 7.12 contain the same trends found in Tables 7.6 and 7.7. Typically, the concrete tension load rating is the smallest value of the inventory ratings, and the flexural strength rating is usually the smaller of the two values used to determine operating rating. Once again, the minimum of the inventory and operating values must be identified for each bridge, which becomes its assigned load rating. Table 7.13 lists the final load ratings for all seven bridges based on adjusted section properties and measured live load distribution factors.

Table 7.11 AASHTO Load Ratings, in Tons, Calculated Using Adjusted Section Properties – Interior Composite Sections

Bridge Name	CT	CC_1	CC_2	$PST_{Inventory}$	$FS_{Inventory}$	$FS_{Operating}$	$PST_{Operating}$
Chandler Creek – 40' Span	46.4	363	251	268	39.2	65.5	439
Chandler Creek – 60' Span	41.6	281	202	285	45.9	76.6	464
Lake LBJ	40.2	203	151	280	47.5	79.3	445
Lampasas River	25.9	153	118	216	39.2	65.4	358
Willis Creek	30.9	188	141	318	40.7	68.0	529
Wimberley	62.1	307	212	364	55.8	93.1	560
Slaughter Creek	67.0	335	251	211	71.3	119	446
Nolanville	67.7	311	231	257	76.3	127	434

Table 7.12 AASHTO Load Ratings, in Tons, Calculated Using Adjusted Section Properties – Exterior Composite Sections

Bridge Name	CT	CC_1	CC_2	$PST_{Inventory}$	$FS_{Inventory}$	$FS_{Operating}$	$PST_{Operating}$
Chandler Creek – 40’ Span	37.8	272	187	213	31.4	52.5	348
Chandler Creek – 60’ Span	34.2	209	149	225	36.5	60.8	364
Lake LBJ	30.6	188	141	228	33.7	56.2	362
Lampasas River	19.8	109	83.1	158	28.7	48.0	261
Willis Creek	20.9	157	119	230	26.9	44.8	383
Wimberley	62.8	364	252	367	49.0	81.7	563
Slaughter Creek	53.0	345	262	302	62.8	105	516
Nolanville	66.5	253	185	278	66.8	111	468

Table 7.13 AASHTO Load Ratings, in Tons, Using Adjusted Section Properties

Bridge Name	Inventory Rating	Operating Rating
Chandler Creek – 40’ Span	31.4	52.5
Chandler Creek – 60’ Span	34.2	60.8
Lake LBJ	30.6	56.2
Lampasas River	19.8	48.0
Willis Creek	20.9	44.8
Wimberley	49.0	81.7
Slaughter Creek	53.0	105
Nolanville	66.5	111

7.3.2 Comparison of Adjusted Load Ratings to Design Load Ratings

Now that the adjusted load ratings have been calculated, they can be compared to original "design" values in order to assess the magnitude of the differences. Table 7.14 shows the comparison between adjusted load ratings and design load ratings, using a comparison ratio that is calculated by dividing the adjusted load rating by the design load rating. In addition, "status" columns are included in the table to indicate whether each bridge passes or fails the inventory load rating criterion.

Table 7.14 Comparison of Adjusted Load Ratings to Design Load Ratings

Bridge Name	Inventory Comparison Ratio	Operating Comparison Ratio	Design Inventory Status	Adjusted Inventory Status
Chandler Creek – 40' Span	1.45	1.45	Pass	Pass
Chandler Creek – 60' Span	1.76	1.55	Fail	Pass
Lake LBJ	1.65	1.55	Fail	Pass
Lampasas River	1.72	1.53	Fail	Fail
Willis Creek	1.65	1.43	Fail	Pass
Wimberley	1.41	1.41	Pass	Pass
Slaughter Creek	1.94	2.04	Pass	Pass
Nolanville	1.86	1.59	Pass	Pass
Average Ratio	**1.68**	**1.57**		

As shown in Table 7.14, there is a significant improvement in load ratings when adjusted properties and measured live load distribution factors are used in the calculations. In addition, three of the four bridges that fail the inventory load rating criterion using design section properties pass the same criterion when calculations are made using adjusted section properties and measured live load distribution factors.

7.3.3 Sensitivity Analysis

Due to the complexity of the load rating process and the number of variables, it is difficult to determine which parameter has the greatest effect on the final load rating. As a result, a sensitivity analysis was performed in order to identify the most influential variable. For this analysis, the Lampasas River bridge was selected, because it failed the load rating criterion when both design and adjusted properties were used. Several variables were selected for examination based on their uncertainty and likelihood of changing. Each of the variables was then modified by ten percent, the load rating was recomputed, and the final change in overall load rating was recorded. Table 7.15 shows the results of the sensitivity analysis. For convenience, the variables are defined in Table 7.16. The original inventory load rating was 11.5 tons, and the original operating load rating was 31.4 tons, as shown in Table 7.8.

Table 7.15 Results of Sensitivity Analysis of Load Ratings

Variable	Units	Original Value	New Value	New Inventory Rating (tons)	% Change	New Operating Rating (tons)	% Change
$b_{eff\text{-}interior}$	in	85.0	93.5	10.5	-8.8%	31.4	0.1%
$b_{eff\text{-}exterior}$	in	80.0	88.0	10.3	-10.6%	31.0	-1.1%
$DF_{interior}$	-	0.480	0.432	11.5	-0.1%	31.4	0.1%
$DF_{exterior}$	-	0.727	0.654	11.9	3.3%	34.2	9.1%
$f'_{c\text{-}girder}$	psi	5100	5600	11.9	3.3%	31.5	0.5%
$f'_{c\text{-}slab}$	psi	3000	3300	11.5	-0.1%	31.5	0.5%
f_{pe}	ksi	128	141	14.9	29.4%	31.4	0.1%
H	%	65	71.5	11.7	1.6%	31.4	0.1%
h_f	in	6.5	7.15	10.3	-10.6%	31.4	0.1%
$I_{comp\text{-}interior}$	in^4	257000	282000	11.5	-0.1%	31.4	0.1%
$I_{comp\text{-}exterior}$	in^4	251000	276000	11.9	3.5%	31.4	0.1%
$w_{diaphragm}$	k/ft	0.043	0.047	11.4	-1.0%	31.3	-0.2%
$w_{miscellaneous}$	k/ft	0.035	0.039	11.5	-0.1%	31.3	-0.2%
$w_{overlay}$	k/ft	0.044	0.048	11.5	-0.1%	31.3	-0.2%
$y_{t\ comp\text{-}interior}$	in	18.1	19.9	11.5	-0.1%	31.4	0.1%
$y_{t\ comp\text{-}exterior}$	in	18.5	20.3	11.9	3.5%	31.4	0.0%

Table 7.16 Variable Definitions

Variable	Definition
$b_{eff\text{-}interior}$	Effective slab width for the interior composite section
$b_{eff\text{-}exterior}$	Effective slab width for the exterior composite section
$DF_{interior}$	Maximum live load distribution factor for the interior composite section
$DF_{exterior}$	Maximum live load distribution factor for the exterior composite section
$f'_{c\text{-}girder}$	Compressive strength of concrete in the girders
$f'_{c\text{-}slab}$	Compressive strength of concrete in the slab
f_{pe}	Effective prestress
H	Average daily humidity (used in calculation of effective prestress)
h_f	Thickness of the slab
$I_{comp\text{-}interior}$	Moment of inertia of the interior composite section
$I_{comp\text{-}exterior}$	Moment of inertia of the exterior composite section
$w_{diaphragm}$	Assumed dead load due to diaphragms
$w_{miscellaneous}$	Miscellaneous dead load
$w_{overlay}$	Assumed dead load due to asphalt overlay
$y_{t\ comp\text{-}interior}$	Neutral axis of the interior composite section
$y_{t\ comp\text{-}exterior}$	Neutral axis of the exterior composite section

As shown in Table 7.15, most of the chosen variables have less than a five percent effect on the inventory load rating, and less than one percent effect on the operating rating. The effective prestress has the largest effect on the inventory load rating, which makes sense because the concrete tension rating factor usually controls the load rating, and a higher effective prestress will allow for a greater level of tensile stress to be applied. Unfortunately, the only way to measure the effective prestress with reasonable accuracy is through destructive testing.

7.4 SUMMARY

This chapter deals with the AASHTO load rating of the seven prestressed concrete girder bridges examined in this study. First, the general load rating process based on the 2000 Interim AASHTO LRFD Bridge Design Specifications was explained. Next, the load rating for all seven bridges was calculated based on design section properties and live load distribution factors calculated from the AASHTO code. Then, the load rating was calculated based on adjusted section properties and measured live load distribution factors, which yields a load rating that more closely reflects actual strength and performance of each bridge. Finally, design load ratings were compared to adjusted load ratings in order to measure the degree of improvement.

Based on the design load ratings, four of the bridges do not pass the current AASHTO load rating criterion. The 60' span of the Chandler Creek bridge has a design inventory rating of 19.4, the Lake LBJ bridge has an inventory rating of 18.5, the Lampasas River bridge has an inventory rating of 11.5, and the Willis Creek bridge has an inventory rating of 12.7. Each of the other bridges has a design inventory rating above twenty.

After incorporating adjusted section properties and measured live load distribution factors, the adjusted load ratings were calculated as shown in Appendix E. Based on the adjusted load ratings, only one of the bridges does not pass the AASHTO load rating criterion. The Lampasas River bridge has an adjusted inventory rating of 19.8, which comes from the concrete tension limit set forth in AASHTO. The 60' span of the Chandler Creek bridge has an adjusted inventory rating of 34.2, the Lake LBJ bridge has an adjusted rating of 30.6, and the Willis Creek bridge has an adjusted rating of 20.9.

Upon comparison of the design and adjusted load ratings, a satisfactory result emerged. To make this comparison, a ratio of the adjusted load rating divided by the design rating was used. The values for the inventory comparison ratio ranged from 1.41 to 1.94, with an average of 1.68. The values for the operating comparison ratio ranged from 1.41 to 2.08, with an average of 1.57. Therefore, on average, load ratings for all seven bridges increased by over fifty percent by using adjusted section properties and measured live load distribution factors. While the process of obtaining accurate adjusted section properties, actual concrete strengths, and measuring actual live load distribution factors is quite involved and somewhat time consuming, the results more than justify the extra work.

Chapter 8 – Conclusions

This chapter contains the conclusions drawn from the work on TxDOT Project 1895. The first section is a general review of the AASHTO load rating procedure and a discussion of the importance of bridge load testing when trying to calculate rating factors. The second section contains a summary of findings from Chapters 5 through 7 of this report. The third and final section contains a discussion of lessons learned related to load testing and load rating.

8.1 REVIEW OF AASHTO LOAD RATING

The American Association of State Highway and Transportation Officials (AASHTO) prescribes load rating criteria for public bridges to maintain the strength and serviceability of those bridges. These load rating criteria are designed to predict safe loads that may be permitted on a bridge. They are based on the loading from a standard design vehicle, which has increased in weight in recent decades due to the increasing weight of the average truck that travels on public roads. As a result, many prestressed concrete girder bridges in Texas that were built prior to the 1980's fail to meet the load rating criteria set forth by

AASHTO. As such, these bridges must be inspected annually in order to ensure they are safe for public and commercial travel.

Bridges that fail the AASHTO load rating criteria are a source of concern for two reasons. First, the normal inspection interval for bridges in the state of Texas is two years, rather than one year. Because these bridge inspections are both costly and time-consuming, TxDOT prefers to conduct them every two years. Therefore, it is of interest to TxDOT to be certain that the strength and serviceability of those bridges that fail the AASHTO load rating criteria are not being underestimated during analysis. Second, bridges that fail the load rating criteria must be restricted with load postings or closed. Both outcomes have the potential to result in economic loss for the surrounding areas and the state in general. Consequently, TxDOT will always prefer not to close any bridge or explicitly restrict the allowable weights of vehicles that may travel across public bridges to avoid adverse economic impacts.

One method of providing a more accurate assessment of the strength and performance of inadequate bridges is to carry out diagnostic load testing. During such testing, the live load response to known vehicle loads is measured with the goal of understanding the bridge behavior under normal traffic loads. Measurements taken during load testing range from concrete strains to girder displacements at midspan. In the end, data gathered during load testing is used to calculate a revised load rating that more accurately reflects the true condition of inadequate bridges.

8.2 SUMMARY OF FINDINGS FROM BRIDGE LOAD TESTS

In this study, a total of seven bridges were load tested over a period of four years. Five of the bridges fail the AASHTO load rating criteria, as calculated by TxDOT, and were studied as part of TxDOT Project 1895. These five bridges were the Chandler Creek bridge, the Lake LBJ bridge, the Lampasas River bridge, the Willis Creek bridge, and the Wimberley bridge. The other two bridges were built several decades later, and both satisfy the AASHTO load rating criteria, but were studied as part of another project sponsored by TxDOT, designated Project 2986. These two bridges are the Slaughter Creek bridge and the Nolanville bridge.

During load testing, concrete strains were measured on all bridges on both the prestressed concrete girders and concrete curbs or parapets. From those measured strains and known or assumed girder properties, neutral axis depths, live load moments, lateral live load distribution factors, and revised load ratings were inferred. The following sections summarize findings from calculations made based on strains measured during load testing.

8.2.1 Neutral Axis Depths

One parameter that indicates actual live load behavior of a prestressed concrete girder bridge is the neutral axis depth. This value may be calculated based on known, assumed, or extrapolated section properties, and be compared with a value inferred from strains measured during load tests in order to compare actual live load behavior versus predicted behavior of the girders.

In general, neutral axis depths inferred from measured strains were less than values predicted by calculations based on section properties. When design section properties were used, the difference between the inferred neutral axis depth and calculated neutral axis depth varied between -33.7% and 28.4%, with the average difference being about 9%. When neutral axis depths were calculated based on adjusted section properties, the difference varied between -38.3% and 27.3%, with the average difference reduced to roughly 3%.

There are two possible explanations for the shallower neutral axis depths inferred from measured strains. First, if significant cracking of the concrete below the prestressing steel has occurred due to occasional overloads, then the neutral axis will shift toward the bridge deck. Second, when calculating neutral axis depths based on bridge section properties, it is assumed that concrete curbs or parapets contribute to the bending stiffness of exterior sections. If this contribution is actually less than predicted during calculations, then the bending stiffness of the entire bridge cross section is reduced, and the neutral axis depth will shift upward.

8.2.2 Live Load Moments

The next value that was inferred from measured strains was the live load moment in the girders. Similar to neutral axis depths, live load moments were inferred using two different sets of section properties. The first set used in this study was the design section properties taken from the contract drawings. The second set of section properties used in this study was the adjusted section properties, calculated based on concrete strengths from material test data.

In order to evaluate the inferred moments, girder moments calculated using statics, or theoretical maximum moments, were used for comparison. To make this comparison, a ratio of inferred moment to static moment was employed. When live load moments were inferred based on design section properties, moment ratios varied between 0.52 and 0.97, with average moment ratios for each bridge varying between 0.57 and 0.85. The overall average moment ratio for all bridges was approximately 0.75. When live load moments were inferred based on adjusted section properties, moment ratios varied between 0.74 and 1.25, with the average moment ratios for each bridge varying between 0.81 and 1.13. The overall average moment ratio for all bridges increased to approximately 0.95. As was the case for neutral axis depths, using adjusted section properties to calculate inferred live load moments resulted in an overall increase in accuracy.

8.2.3 Live Load Distribution Factors

The next parameter that was investigated in this study was live load distribution factors. These factors indicate the distribution of vertical loads to each girder of a bridge, in addition to the maximum portion of live load that is supported by each girder. Distribution factors were only calculated from inferred moments based on adjusted section properties in order to obtain values that most accurately reflect actual conditions.

To calculate the distribution factors, live load moments for each girder were divided by the total moment on the bridge. When distribution factors were calculated using the adjusted moments, maximum values varied between 0.23 and 0.69, with the exterior girders generally resisting more live load moment than interior girders. The values calculated with the AASHTO method varied between 0.47 and 0.76. In order to evaluate the calculated distribution factors, they were compared to values calculated according to the AASHTO procedures by using a ratio of the AASHTO factors to the calculated factors. The value of this ratio varied between 0.91 and 2.03, with the average ratio for all bridges being 1.42.

Therefore, on average the AASHTO distribution factors overestimated the maximum live load distribution factor by approximately forty-two percent.

One of the goals of this study was to assess the effect of different diaphragm configurations and locations on live load distribution. A comparison was made between three similar bridges in Project 1895. When comparing live load distribution factors from the Chandler Creek bridge (60’ span), Lake LBJ bridge (65’ span), and Willis Creek bridge (65’ span), the difference in maximum values was minimal. These results appear to support the conclusions of other researchers that suggest that live load distribution factors are not sensitive to diaphragm locations.

8.2.4 AASHTO Load Ratings

The final calculations in this study were made to determine the load ratings for each bridge. Load ratings were calculated with the most current AASHTO procedure, using both design section properties and adjusted section properties, and then the ratings were compared to evaluate the effects of using adjusted properties rather than design properties.

First, the AASHTO load ratings were calculated for each bridge based on design section properties. Based on these load ratings, the 60’ span of the Chandler Creek bridge, the Lake LBJ bridge, the Lampasas River bridge, and the

Willis Creek bridge all failed the load rating criterion with inventory load ratings less than twenty. When load ratings were calculated again based on adjusted section properties, the 60’ span of the Chandler Creek bridge, the Lake LBJ bridge, and the Willis Creek bridge passed the load rating criterion. The Lampasas River bridge still failed, but only marginally, with an inventory load rating of 19.8.

In order to compare the two sets of load ratings, adjusted load ratings were divided by the design load ratings. For the inventory rating, this ratio varied between 1.41 and 1.94, with an average ratio for all bridges of 1.68. For the operating rating, this ratio varied between 1.41 and 2.04, with an average ratio for all bridges of 1.57. Therefore, on average the inventory load rating increased by approximately sixty-eight percent and the operating ratings increased by approximately fifty-seven percent for the seven bridges examined in this study. In addition, a sensitivity analysis was performed to determine which of the selected parameters had the greatest influence on final load ratings. The results suggest that effective prestress has the greatest effect on final load ratings.

8.3 LESSONS LEARNED

As mentioned at the beginning of this chapter, making an accurate assessment of the AASHTO load rating for public bridges is critical for several reasons. Therefore, it is important to be as thorough and accurate as possible when calculating load ratings. If a bridge is deemed inadequate when calculating the load rating based on design section properties, that bridge can be load tested in order to gain a more realistic estimation of its actual performance.

While the concept of load testing is relatively simple, the load tests can be time-consuming and tedious. Components of the actual tests must be carefully planned in advance, including the number of instrumented girders, gage locations, use of curb gages, etc. With sufficient planning, load tests can be highly successful.

As shown in the previous section, the increase in load ratings using adjusted section properties and other parameters calculated during load testing is significant. In this study, both the inventory and operating load ratings increased by over fifty percent, and three bridges that had failed the load rating using design section properties were deemed adequate after subsequent adjusted analysis. These results are encouraging, and suggest that time spent on load testing of major public bridges may be time well spent.

Appendix A – Concrete Test Data and Concrete Strengths

Concrete test data and methods for extrapolating those data to reflect current conditions are presented in this appendix. The first section contains a summary of concrete test data that was obtained from the Texas Department of Transportation. The second section contains calculations that were used to extrapolate the upper-bound concrete strengths using the 1990 CEB-FIP approach.

A.1 CONCRETE TEST DATA

The following tables of concrete test data were obtained from the bridge archives at the Texas Department of Transportation. These strengths are referred to as “lower-bound” strengths in Chapter 2, and are the concrete strengths used in all the analyses in the fifth, sixth, and seventh chapters. Table A.1 shows concrete test data from girders in the Chandler Creek bridge. Table A.2 shows concrete test data from the slab of the Chandler Creek bridge. Tables A.3 through A.6 list the concrete test data from girders in the Lake LBJ bridge, Lampasas River bridge, Willis Creek bridge, and Nolanville bridge, respectively.

Table A.1 Concrete Test Data from the Prestressed Girders – Chandler Creek Bridge

Sample Identification	Beam Type	Length (ft)	Release of Tension Strength (psi)	Age at Release of Tension (hours)	Average Design Strength (psi)	Age (days)
B2 (B-13)	B	40	5082	16	6357	7
B3 (B-110	B	40	5135	17	6375	7
B3 (B-14)	B	40	5082	16	6357	7
B5 (B-10)	B	40	5135	17	6375	7
B5 (B-16)	B	40	4752	14.25	6928	7
B2 (B-09)	B	40	5717	37.5	7916	8
B2 (B-15)	B	40	4700	17.5	6678	8
B3 (B-17)	B	40	4700	17.5	6678	8
A-1 (B-01)	B	40	4069	42	7119	14
A-2 (B-02)	B	40	4069	42	7119	14
A-3 (B-01)	B	40	5547	48	8245	14
A-4 (B-03)	B	40	5547	48	8245	14
B3 (B-07)	B	40	5440	19.5	6889	14
B3 (B-08)	B	40	5440	19.5	6889	14
B5 (B-12)	B	40	4700	14.5	7182	14
A-7 (B-04)	B	40	5476	66	7237	17
A-8 (B-03)	B	40	5476	66	7237	17
A-5 (B-02)	B	40	5511	43	7591	18
A-6 (B-04)	B	40	5511	43	7591	18
B1 (C-05)	C	60	5515	48	-	-
B3 (C-07)	C	60	5498	67.5	-	-
B2 (C-06)	C	60	-	-	8569	14
B2 (C-06)	C	60	-	-	8723	14
B2 (C-06)	C	60	-	-	8523	14
B4 (C-08)	C	60	-	-	8185	14
B4 (C-08)	C	60	-	-	9075	14
B4 (C-08)	C	60	-	-	8808	14
Mean Design Concrete Strengths						
7-8 Day	40’ Beams	6708 psi				
14-18 Day	40’ Beams	7395 psi				
14 Day	60’ Beams	8647 psi				

Table A.2 Concrete Test Data from the Slab – Chandler Creek Bridge

Cylinder Number	Age (days)	Failure Stress (psi)
M1	3	3771
M2	3	3796
M3	3	3733
M13	4	3929
M14	4	3880
M15	4	4200
RC-1	7	3395
RC-2	7	3913
RC-3	7	3767
RC7	7	3813
RC8	7	3796
RC9	7	3696
M4	7	4197
M5	7	4816
M6	7	4699
M10	7	4114
M11	7	4064
M12	7	3579
RC-4	28	5100
RC-5	28	5100
RC-6	28	4682
M7	28	5500
M8	28	5613
M9	28	5748
Mean Design Concrete Strengths		
3 Day	3807 psi	
4 Day	4003 psi	
7 Day	3987 psi	
28 Day	5291 psi	

Table A.3 Concrete Test Data from the Prestressed Girders – Lake LBJ Bridge

Identification	Beam Type	Length (ft)	Release of Tension Strength (psi)	Age at Release of Tension (hours)	Average Release of Tension (days)	Average Design Strength (psi)	Age (days)
B 1-5	C	64’-8”	4500	26	2.2	7292	14
A 1-5	C	64’-8”	5200	27	2.3	7945	14
B 1-5	C	-	5400	90	7.5	9102	14
A 1&2	C	-	5400	47	3.9	7273	14
A 3-5	C	-	5200	28	2.3	8816	14
B 1-5	C	-	5200	28	2.3	7827	14
A 1-5	C	-	4840	24	2.0	7765	19
B-1	C	-	5470	70	5.8	7441	15
B-5	C	-	5420	39	3.3	7760	14
B-3	C	-	4945	28	2.3	7677	14
A-1	C	-	5650	46	3.8	8308	14
A-4	C	-	4315	27	2.3	8318	14
B-1	C	-	4100	27	2.3	8420	14
B 1-3	C	-	5375	90	7.5	7651	14
B 4-5	C	-	5400	70	5.8	8553	14
Mean Design Concrete Strength = 8010 psi							

Table A.4 Concrete Test Data from the Prestressed Girders – Lampasas River Bridge

Identification	Beam Type	Length (ft)	Release of Tension Strength (psi)	Age at Release of Tension (hours)	Average Release of Tension (days)	Average Design Strength (psi)	Age (days)
C-1	C	74’-8”	6254	46	3.8	8036	7
C-2	C	74’-8”	-	-	-	8036	7
C-3	C	74’-8”	-	-	-	8036	7
C-4	C	74’-8”	-	-	-	8036	7
B-1	C	74’-8”	4616	22	1.8	8244	7
B-2	C	74’-8”	-	-	-	8244	7
B-3	C	74’-8”	-	-	-	8244	7
B-4	C	74’-8”	-	-	-	8244	7
A-1	C	74’-8”	6254	43	3.6	8272	7
A-2	C	74’-8”	-	-	-	8272	7
A-3	C	74’-8”	-	-	-	8272	7
A-4	C	74’-8”	-	-	-	8272	7
B1	C	74’-8”	6254	47	3.9	8205	7
B2	C	74’-8”	-	-	-	8205	7
B3	C	74’-8”	-	-	-	8205	7
B4	C	74’-8”	-	-	-	8205	7
A1	C	74’-8”	5930	28	2.3	8256	7
A2	C	74’-8”	-	-	-	8256	7
A3	C	74’-8”	-	-	-	8256	7
A4	C	74’-8”	-	-	-	8256	7
B1	C	74’-8”	6254	42	3.5	7969	7
B2	C	74’-8”	-	-	-	7969	7
B3	C	74’-8”	-	-	-	7969	7
B4	C	74’-8”	-	-	-	7969	7
A-1	C	74’-8”	6254	47	3.9	8140	9
A-2	C	74’-8”	-	-	-	8140	9
A-3	C	74’-8”	-	-	-	8140	9
A-4	C	74’-8”	-	-	-	8140	9
C1	C	74’-8”	6254	72	6.0	8272	10
C2	C	74’-8”	-	-	-	8272	10
C3	C	74’-8”	-	-	-	8272	10
C4	C	74’-8”	-	-	-	8272	10

Mean Design Concrete Strengths	
7 Day	8164 psi
All	8174 psi

Table A.5 Concrete Test Data from the Prestressed Girders – Willis Creek Bridge

Identification	Beam Type	Length (ft)	Release of Tension Strength	Age at Release of Tension (hours)	Average Design Strength (psi)	Age (days)
B (1&2)	C	64'-8"	5300	48	7898	21
B (1&2)	C	64'-8"	5400	72	8862	21
-	C	64'-8"	5400	144	9180	21
-	C	64'-8"	5400	120	8239	21
Mean Design Concrete Strength = 8545 psi						

Table A.6 Concrete Test Data from the Prestressed Girders – Nolanville Bridge

I.D. #1	I.D. #2	Beam Type	Length (ft)	Release of Tension Strength (psi)	Age at Release of Tension (hours)	Design Strength (psi)	Age (days)
B-1	AR-1F	IV	101.67	6348	17.5	8719	7
B-2	AR-1F	IV	101.67	6348	17.5	8486	7
B-3	AR-2	IV	101.67	6348	17.5	8245	7
B-4	AR-2	IV	101.67	6348	17.5	-	-
B1	AR-2X	IV	101.67	6348	17.5	8719	7
B2	AR-2	IV	101.67	6348	17.5	8486	7
B3	AR-2	IV	101.67	6348	17.5	8245	7
B4	AR-2	IV	101.67	6348	17.5	-	-
B-1	AR-1X	IV	101.67	5597	17.75	6762	7
B-2	AR-2X	IV	101.67	5597	17.75	6940	7
B-3	AR-2X	IV	101.67	5597	17.75	7011	7
B-4	AR-2Y	IV	101.67	5597	17.75	-	-
B-1	AR-2	IV	101.67	5517	19	6383	7
B-2	AR-1F	IV	101.67	5517	19	6560	7
B-3	AR-2F	IV	101.67	5517	19	6608	7
B-4	AR-2	IV	101.67	5517	19	-	-
B1	AR-2	IV	101.67	5517	19	6383	7
B2	AR-2	IV	101.67	5517	19	6560	7
B3	AR-2	IV	101.67	5517	19	6608	7
B4	AR-2	IV	101.67	5517	19	-	-
B1	AR-2	IV	101.67	5774	19.5	7206	7
B2	AR-2X	IV	101.67	5774	19.5	6702	7
B3	AR-1	IV	101.67	5774	19.5	6578	7
B4	AR-1	IV	101.67	5774	19.5	-	-

Table A.6 (Continued) Concrete Test Data from the Prestressed Girders – Nolanville Bridge

B-1	AR-2	IV	101.67	5774	19.5	7206	7
B-2	AR-2F	IV	101.67	5774	19.5	6702	7
B-3	AR-1	IV	101.67	5774	19.5	6578	7
B-4	AR-1	IV	101.67	5774	19.5	-	-
B-1	AR-2F	IV	101.67	5632	20	7562	7
B-2	AR-1	IV	101.67	5632	20	7289	7
B-3	AR-2	IV	101.67	5632	20	7314	7
B-4	AR-2	IV	101.67	5632	20	-	-
B1	AR-2Y	IV	101.67	5632	20	7562	7
B2	AR-1	IV	101.67	5632	20	7289	7
B3	AR-2	IV	101.67	5632	20	7314	7
B4	AR-2	IV	101.67	5632	20	-	-
B-1	AR-1	IV	101.67	5706	20	6383	7
B-2	AR-1	IV	101.67	5706	20	6224	7
B-3	AR-1	IV	101.67	5706	20	6162	7
B-4	AR-1	IV	101.67	5706	20	-	-
B-1	AR-2	IV	101.67	6145	20.5	7028	7
B-2	AR-2	IV	101.67	6145	20.5	6897	7
-	AR-2	IV	101.67	-	-	6809	7
B1	AR-1X	IV	101.67	5570	25	5957	7
B2	AR-1	IV	101.67	5570	25	6312	7
B3	AR-1	IV	101.67	5570	25	6330	7
B4	AR-1	IV	101.67	5570	25	-	-
B-1	AR-1F	IV	101.67	5570	25	5957	7
B-2	AR-1	IV	101.67	5570	25	6312	7
B-3	AR-1F	IV	101.67	5570	25	6330	7
B-4	AR-1	IV	101.67	5570	25	-	-
Mean Design Concrete Strength = 6993 psi							

Table A.7 shows a summary of the lower-bound concrete strengths that were used in all analyses. These concrete strengths were used to calculate what is referred to as "adjusted section properties." Because there were no test data available for the Wimberley bridge and Slaughter Creek bridge, mean design concrete strength was assumed based on the other concrete test data. First, for each of the bridges, the increase in concrete strength between design values and lower-bound values was calculated. Then, the average of the percentage increase for the other six bridges was applied to design concrete strengths from the Wimberley bridge and the Slaughter Creek bridge to produce a set of assumed lower-bound concrete strengths.

Table A.7 Summary of Assumed Lower-Bound Concrete Strengths

Bridge Name	**Design 28-Day Concrete Strength (psi)**	**Assumed Lower Bound Strength (psi)**	**% Increase**	**Design 28-Day Slab Strength**	**Assumed Lower Bound Slab Strength (psi)**	**% Increase**
Chandler Creek – 40’ Span	5000	7500	50%	3000	6000	100%
Chandler Creek – 60’ Span	5000	8700	74%	3000	6000	100%
Lake LBJ	5000	8000	60%	3000	6000	100%
Lampasas River –	5100	8200	61%	3000	6000	100%
Willis Creek	5000	8600	72%	3000	6000	100%
Nolanville	6200	9000	45%	3600	7200	100%
Average			**60%**			**100%**
Wimberley - Girders	5000	8500	70%			
Wimberley - Slab	3000	6000	100%			
Slaughter Creek – Interior Girders	5000	8300	66%	-	-	-
Slaughter Creek – Exterior Girders	7700	12000	56%	-	-	-
Slaughter Creek – Prestressed Panel	5000	8300	66%	-	-	-
Slaughter Creek - Slab	3600	7200	100%	-	-	-

A.2 CALCULATING UPPER-BOUND CONCRETE STRENGTHS USING THE 1990 CEB-FIP APPROACH

In order to bound the assumed concrete strengths between two limits, the upper-bound concrete strengths were calculated using a CEB-FIP approach and the 28-day concrete strengths shown in Table A.8. The approach involves the use of two different beta factors that are multiplied by the 28-day strengths and the 28-day moduli of elasticity to obtain the projected concrete properties at any time. Equation A.1 shows the beta factor that is applied to the 28-day concrete strength, and Equation A.2 shows the beta factor that is applied to the 28-day modulus of elasticity.

$$\beta_{cc}(t) = e^{s \cdot \left[1 - \sqrt{\left(\frac{28}{\frac{t}{t_1}}\right)}\right]} \qquad \text{(A.1)}$$

$$\beta_E(t) = \sqrt{\beta_{cc}(t)} \qquad \text{(A.2)}$$

In Equation A.1, s is the cement type coefficient, and is equal to 0.20 for rapid-hardening high-strength cements, 0.25 for normal and rapid-hardening cements, and 0.38 for slowly-hardening cements. The time in days at which the assumed concrete strengths are calculated is designated as t, and t_1 is equal to one day.

Tables A.8 and A.9 show a summary of the inputs used to calculate the upper bound concrete strengths. Table A.8 shows the lower-bound concrete strengths that were multiplied by a strength factor to get the 28-day strengths (Wood 1991).

Table A.8 Adjustment of Concrete Test Data to Twenty-Eight Day Strengths

Bridge Name	Mean Design Concrete Strength (psi)	Strength Factor	28-Day Strength (psi)
Chandler Creek – 40' Span	6708	0.78	8600
Chandler Creek – 60' Span	8647	0.90	9600
Lake LBJ	8010	0.90	8900
Lampasas River	8164	0.78	10500
Willis Creek	8545	0.97	8800
Nolanville	6993	0.78	9000

Table A.9 Summary of Upper-Bound Concrete Strength Calculations

Bridge Name	Assumed 28-Day Concrete Strength (psi)	Modulus of Elasticity at 28 Days (ksi)	s	t (days)	Upper-Bound Concrete Strength (psi)	Upper-Bound Modulus of Elasticity (ksi)
Chandler Creek – 40' Span	8600	5340	0.20	12500	10400	5880
Chandler Creek – 60' Span	9600	5645	0.20	12500	11600	6210
Chandler Creek – Slab	5300	4195	0.25	12500	6700	4730
Lake LBJ	8900	5435	0.20	13500	10800	5980
Lampasas River	10500	5900	0.20	11300	12700	6500
Willis Creek	8800	5405	0.20	14000	10600	5950
Wimberley	8500	5310	0.20	12800	10300	5850
Slaughter Creek – Interior Girders	8300	5250	0.20	2600	9900	5740
Slaughter Creek – Exterior Girders	12000	6310	0.20	2600	15000	6900
Slaughter Creek – Prestressed Panels	8300	5250	0.20	2600	9900	5740
Nolanville	9000	5465	0.20	7700	10900	6000

Appendix B – Strain Gage Locations

This appendix contains a detailed description of strain gage locations for all seven bridges examined in this study. The first section covers the five bridges tested in Project 1895, including detailed measurements of strain gage locations. The second section covers the two bridges tested in Project 2986.

B.1 STRAIN GAGE LOCATIONS – PROJECT 1895

As shown in Chapter 3, strain gages were placed at various locations on each bridge studied in Project 1895. The dimensions shown in Figure 3.4 were used as a general guide for the researchers when the strain gages were installed. While the utmost care was taken to place gages exactly in their intended position, some gages were not installed directly over their marked location due to small voids in the surface of the girders, excessively rough girder surfaces, and human error.

Table B.1 shows the target gage locations for each bridge studied in Project 1895. Figures B.1 through B.8 show diagrams of each bridge cross section with target strain gage locations included as well as the strain gage labels used in reference to the data acquisition system. Figures B.9 through B.13 show photographs of curb gages on each of the bridges tested in Project 1895. Table

B.2 shows actual gage locations as measured in the field before load testing. The values with asterisks indicate measured gage locations that were different from target gage locations. All beam locations were measured from the bottom of the beam, or the beam soffit, for convenience in the analysis.

Table B.1 Target Strain Gage Locations – Project 1895

Bridge Name	**Chandler Creek 40' Span**	**Chandler Creek 60' Span**	**Lake LBJ**	**Lampasas River Span 1**	**Lampasas River Span 2**	**Willis Creek**	**Wimberley Span 1**	**Wimberley Span 2**
Beam 1								
B	0	0	0	0	0	0	0	0
W	15	18	16.5	16.5	16.5	16.5	13.75	13.75
T	32	38	38	38	38	38	N/A	N/A
C	41.25	47.25	57.75	47.25	47.25	57	49.25	49.25
Beam 2								
B	0	0	0	0	0	0	0	0
W	15	18	16.5	16.5	16.5	16.5	13.75	13.75
T	32	38	38	38	38	38	32	32
Beam 3								
B	0	0	0	0	0	0	0	0
W	15	18	16.5	16.5	16.5	16.5	13.75	13.75
T	32	38	38	38	38	38	32	32
Beam 4								
B	0	0	0	0	0	0	0	0
W	15	18	16.5	16.5	16.5	16.5	13.75	13.75
T	32	38	38	38	38	38	32	32
C	41.25	47.25	57.75	47.25	47.25	57	N/A	N/A
Beam 5								
B	0	0	0	0	0	0	0	0
W	N/A	N/A	N/A	N/A	N/A	N/A	13.75	49.25
T	N/A	N/A	N/A	N/A	N/A	N/A	N/A	N/A
C	N/A	N/A	N/A	N/A	N/A	N/A	13.75	49.25
B = Bottom, W = Web, T = Top, C = Curb; All dimensions in inches.								

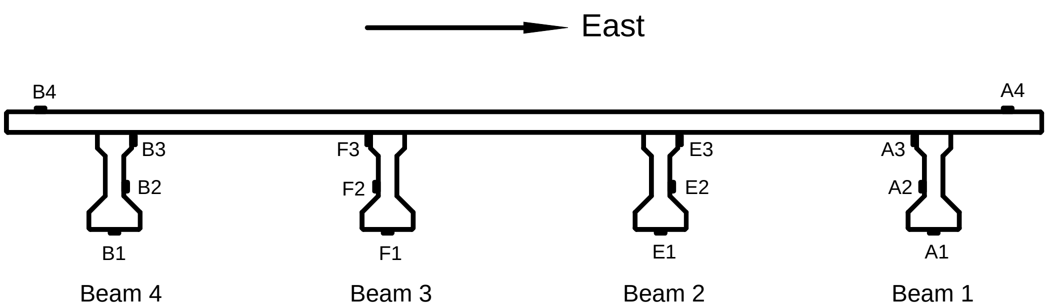

Figure B.1 Strain Gage Locations – Chandler Creek Bridge – 40' Span

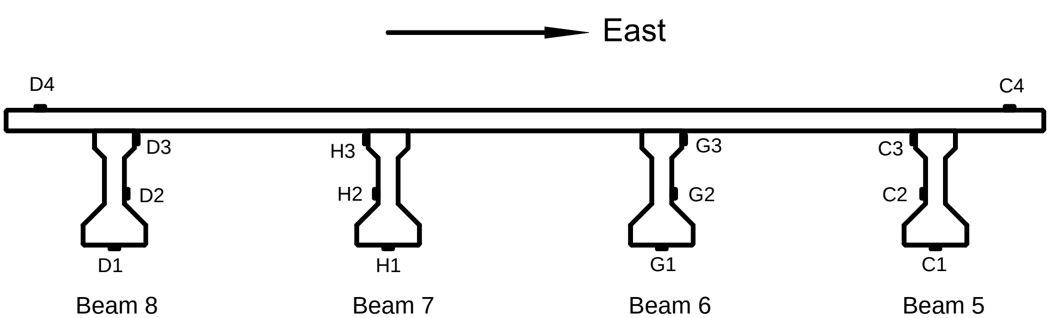

Figure B.2 Strain Gage Locations – Chandler Creek Bridge – 60' Span

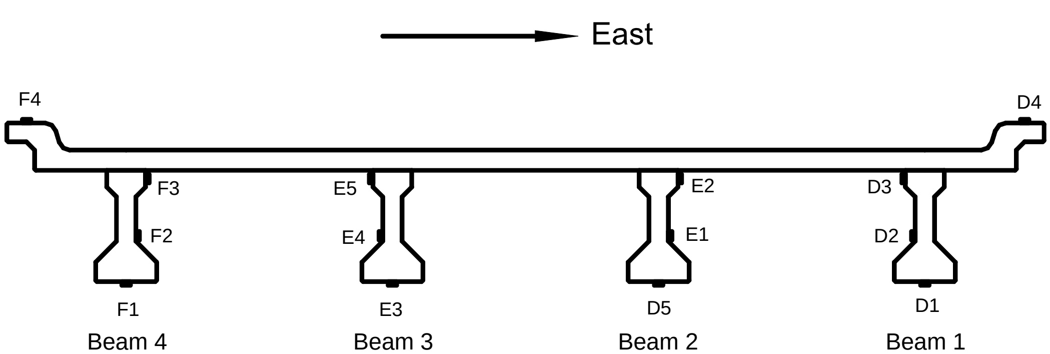

Figure B.3 Strain Gage Locations – Lake LBJ Bridge

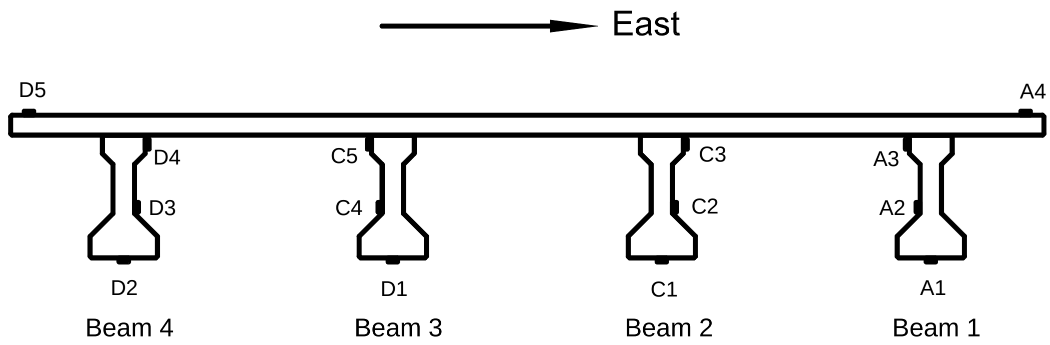

Figure B.4 Strain Gage Locations – Lampasas River Bridge – Span 1

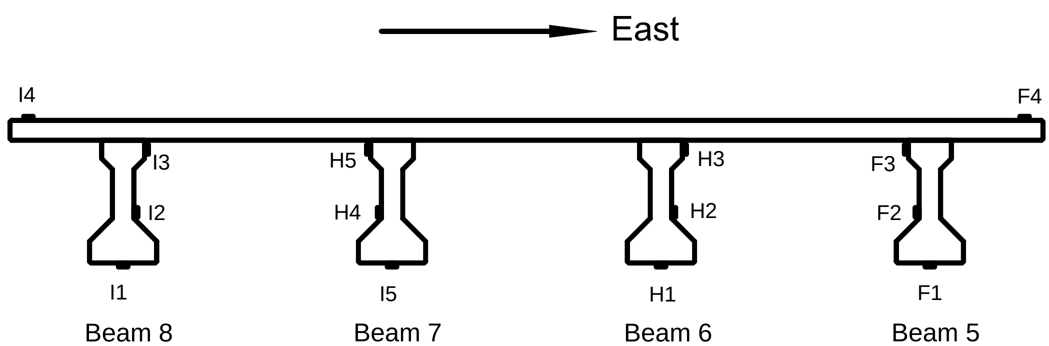

Figure B.5 Strain Gage Locations – Lampasas River Bridge – Span 2

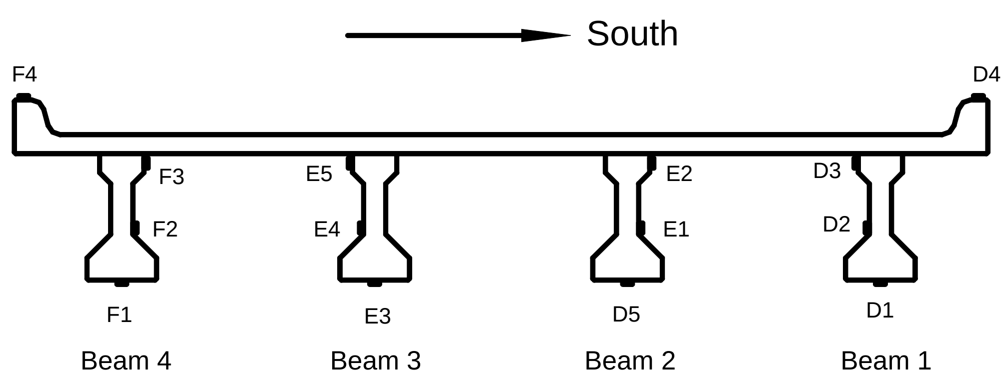

Figure B.6 Strain Gage Locations – Willis Creek Bridge

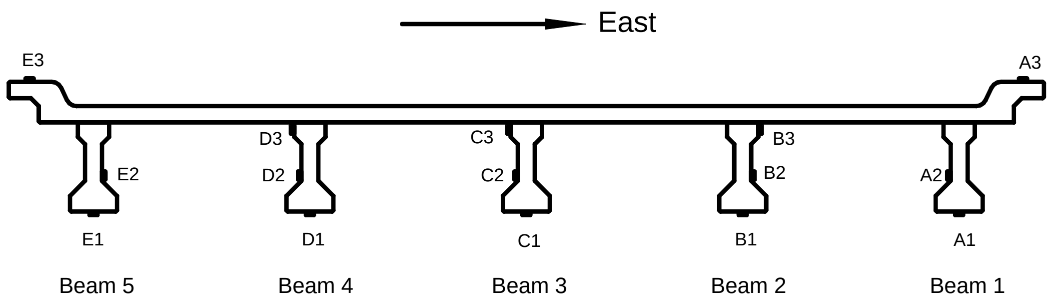

Figure B.7 Strain Gage Locations – Wimberley Bridge – Span 1

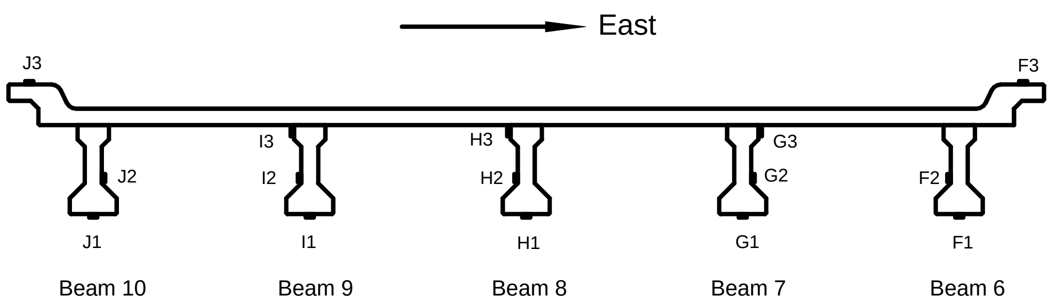

Figure B.8 Strain Gage Locations – Wimberley Bridge – Span 2

Figure B.9 Curb Gages – Chandler Creek Bridge

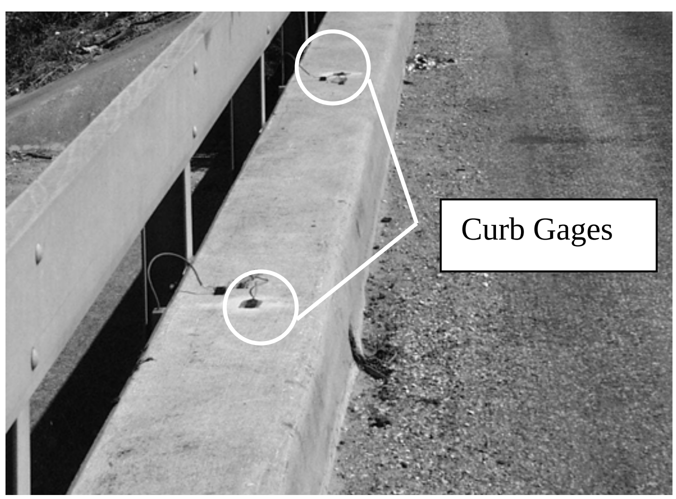

Figure B.10 Curb Gages – Lake LBJ Bridge

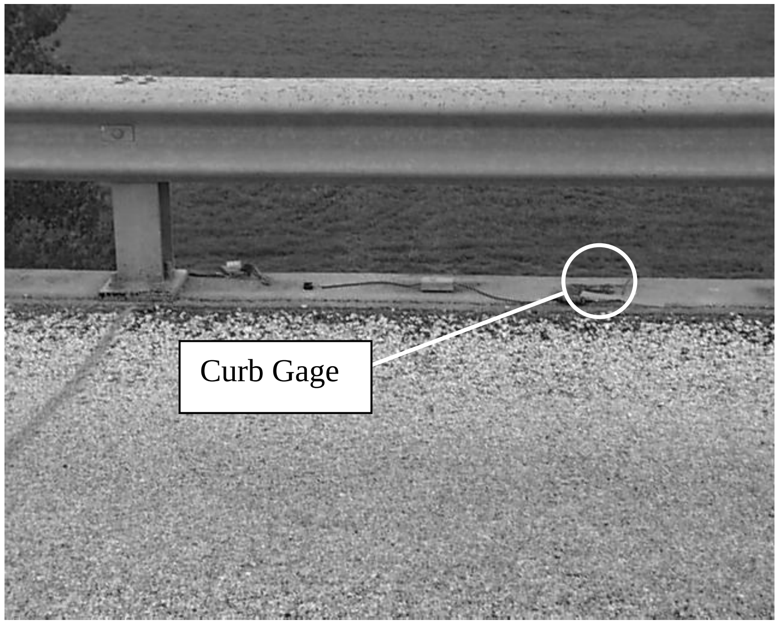

Figure B.11 Curb Gages – Lampasas River Bridge

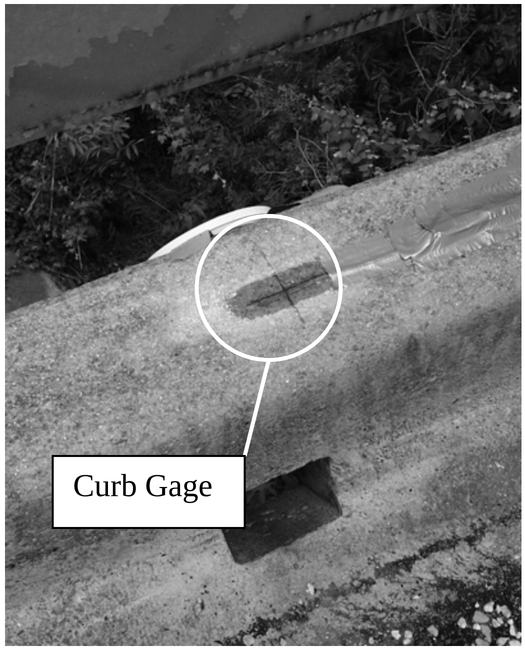

Figure B.12 Curb Gages – Willis Creek Bridge

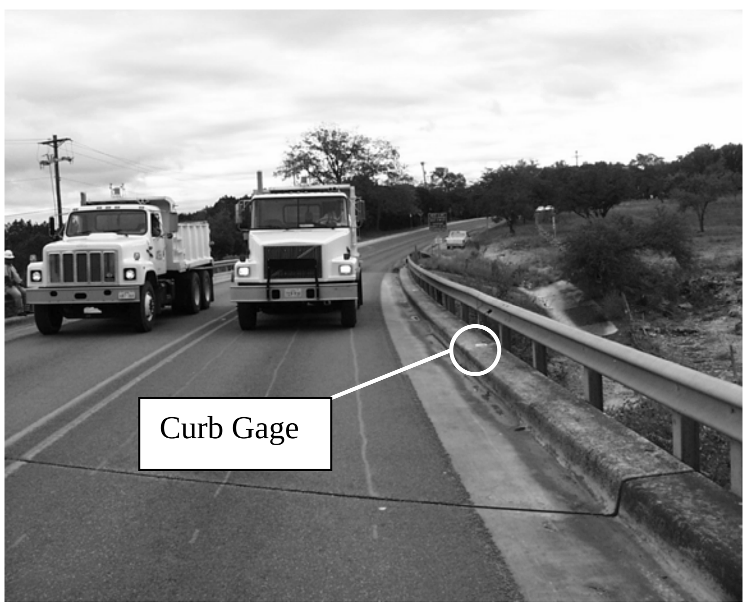

Figure B.13 Curb Gages – Wimberley Bridge

Table B.2 Measured Strain Gage Locations – Project 1895

Bridge Name	Chandler Creek 40' Span	Chandler Creek 60' Span	Lake LBJ	Lampasas River Span 1	Lampasas River Span 2	Willis Creek	Wimberley Span 1	Wimberley Span 2
Beam 1								
B	0	0	0	0	0	0	0	0
W	15	18	16 1/2	16 1/2	16 1/2	16 1/2	13 3/4	14*
T	32	38	38	38	38	38	N/A	N/A
C	41 1/4	47 1/4	57 3/4	47 1/4	49 1/4	57	49 1/4	49 1/4
Beam 2								
B	0	0	0	0	0	0	0	0
W	15	18	16 1/2	16 1/2	16 ¼*	16 1/2	13 3/4	13 3/4
T	32	38	38	37 ¼*	38	38	32	32
Beam 3								
B	0	0	0	0	0	0	0	0
W	15	18	16 1/2	16 1/2	16 1/2	16 1/2	13 3/4	13 3/4
T	32	38	38	37*	38	38	31 7/8*	32 1/8*
Beam 4								
B	0	0	0	0	0	0	0	0
W	15	18	17*	16 1/2	16 1/2	16 1/2	13 3/4	13 3/4
T	32	38	38 1/8*	37 ½*	38	38	31 7/8*	32
C	41 1/4	47 1/4	57 3/4	47 1/4	49 1/4	57	N/A	N/A
Beam 5								
B	N/A	N/A	N/A	N/A	N/A	N/A	0	0
W	N/A	N/A	N/A	N/A	N/A	N/A	13 3/4	13 3/4
T	N/A	N/A	N/A	N/A	N/A	N/A	N/A	N/A
C	N/A	N/A	N/A	N/A	N/A	N/A	49 1/4	49 1/4
B = Bottom, W = Web, T = Top, C = Curb; All dimensions in inches.								

B.2 STRAIN GAGE LOCATIONS – PROJECT 2986

This section contains diagrams of the approximate strain gage locations and their labels for the two bridges tested in Project 2986. There were no field measurements made of strain gage location. Therefore, it was assumed that strain gages were located at the positions shown in Chapter 3. The middle (web) gages were placed twenty inches above the beam soffit, and top gages were placed three inches below the bottom of the bridge deck. Figure B.14 shows the strain gage locations for the Slaughter Creek bridge. Figure B.15 shows the strain gage locations for the Nolanville bridge.

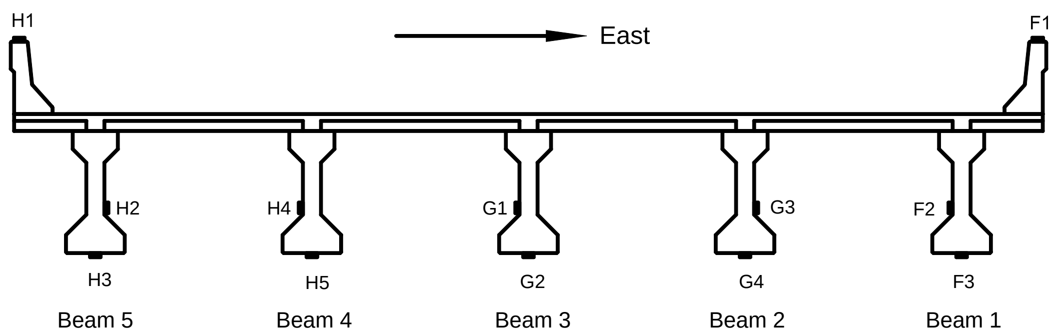

Figure B.14 Strain Gage Locations – Slaughter Creek Bridge

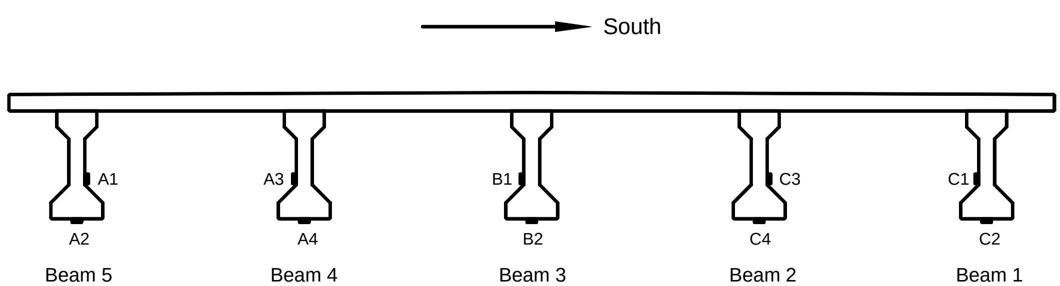

Figure B.15 Strain Gage Locations – Nolanville Bridge

Appendix C – Field Measurements

This appendix contains girder dimensions as measured in the field before load testing. These measurements were taken in order to compare nominal design dimensions with as-built dimensions of the bridges. Because there were no field measurements taken during Project 2986, there are no values presented in this appendix.

Figure C.1 shows general dimensions of each girder as measured in the field and reported on contract drawings. Table C.1 shows values for each of the

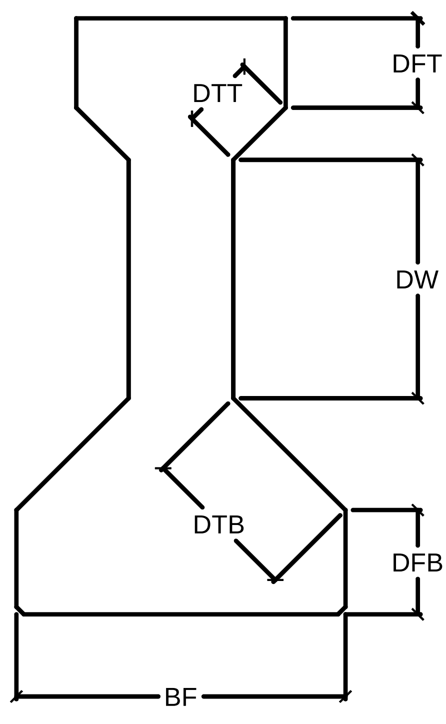

Figure C.1 General Girder Dimensions

general girder dimensions, as measured in the field. All measurements are in inches, taken to the nearest eighth of an inch with a standard tape measure. For reference, Table C.2 shows the same dimensions, as specified on contract drawings. In the "DFT" column for the Willis Creek bridge, there are two values presented. When the bridge was built, the contractor's method for crowning the roadway was to place slab forms at different depths across the cross section. At the exterior girders, the "DFT" was five inches, and for the interior girders, the "DFT" was five and a half inches.

Table C.1 Measured Girder Dimensions

Bridge Name	DFT	DTT	DW	DTB	DFB	BF
Chandler Creek – 40' Span	5	4	14	8	6	18
Chandler Creek – 60' Span	5 1/4	5	16	10 1/2	7 1/4	22
Lake LBJ	6 1/2	5	16	10 1/2	7 1/4	22
Lampasas River	7 1/2	5	16	10 1/2	7 1/4	22
Willis Creek	5-5 1/2	5	16	10 1/2	7	22
Wimberley	5 1/2	4	14	8	6 1/4	19

Table C.2 Design Girder Dimensions

Bridge Name	DFT	DTT	DW	DTB	DFB	BF
Chandler Creek – 40' Span	5.50	2.00	14.00	5.75	6.00	18.00
Chandler Creek – 60' Span	6.00	2.50	16.00	5.25	7.00	22.00
Lake LBJ	6.00	2.50	16.00	5.25	7.00	22.00
Lampasas River	6.00	2.50	16.00	5.25	7.00	22.00
Willis Creek	6.00	2.50	16.00	5.25	7.00	22.00
Wimberley	5.50	2.00	14.00	5.75	6.00	18.00

Appendix D – Calculation of AASHTO Live Load Distribution Factors

This appendix contains a detailed explanation of the method used for calculating the AASHTO live load distribution factors, as presented in Chapter 6. The first section contains the equations used in calculating live load distribution factors found in the 2000 Interim AASHTO LRFD Bridge Design Specifications (American Association of State Highway and Transportation Officials 2000a). The second section contains actual values from each bridge that were input into the equations found in the first section to calculate live load distribution factors.

D.1 AASHTO METHOD FOR CALCULATING LIVE LOAD DISTRIBUTION FACTORS

In previous editions of the AASHTO bridge design guidelines, the calculation of live load distribution factors was simple. Distribution factors for the interior girders were related only to girder spacing, and the distribution factors for exterior girders were calculated using the lever rule. However, in the current AASHTO specifications, the process is more involved and based more on structural mechanics theories. However, similar to previous methods, the calculations are separated according to the position of each beam, either interior or exterior.

For the interior girders of a prestressed concrete bridge with only one design lane loaded and at least four girders in the cross section, live load distribution factors are calculated according to Equation D.1. In this equation, *S* is the girder spacing in feet, *L* is the span length in feet, K_g is the longitudinal stiffness parameter, as shown in Equation D.2, and t_s is the slab thickness in inches. The range of applicability for each of these variables is shown in Table D.1.

$$LLDF = 0.06 + \left(\frac{S}{14}\right)^{0.4} \cdot \left(\frac{S}{L}\right)^{0.3} \cdot \left(\frac{K_g}{12.0 \cdot L \cdot t_s^{\,3}}\right)^{0.1} \tag{D.1}$$

$$K_g = n \cdot \left(I + A \cdot e_g^{\,2}\right) \tag{D.2}$$

Table D.1 Range of Applicability for the Variables in Equation D.1

Variable Name	Lower Bound	Upper Bound
Girder spacing, S	3.5 ft	16.0 ft
Span length, L	20 ft	240 ft
Slab thickness, t_s	4.5 in	12.0 in

In Equation D.2, *n* is the ratio of the modulus of elasticity of the slab concrete to the modulus of elasticity of the girder concrete, *I* is the moment of inertia of the non-composite girder (in^4), *A* is the area of the non-composite girder (in^2), and e_g is the distance between the centers of gravity for the non-composite girder and slab (in).

For the exterior girders, with only one design lane loaded, the live load distribution factors are calculated using the lever rule. The lever rule is simply a summation of moments about one point that is assumed to be hinged in order to find the reactions at other points of a bridge cross section. Figure D.1 shows a diagram of how the lever rule is applied.

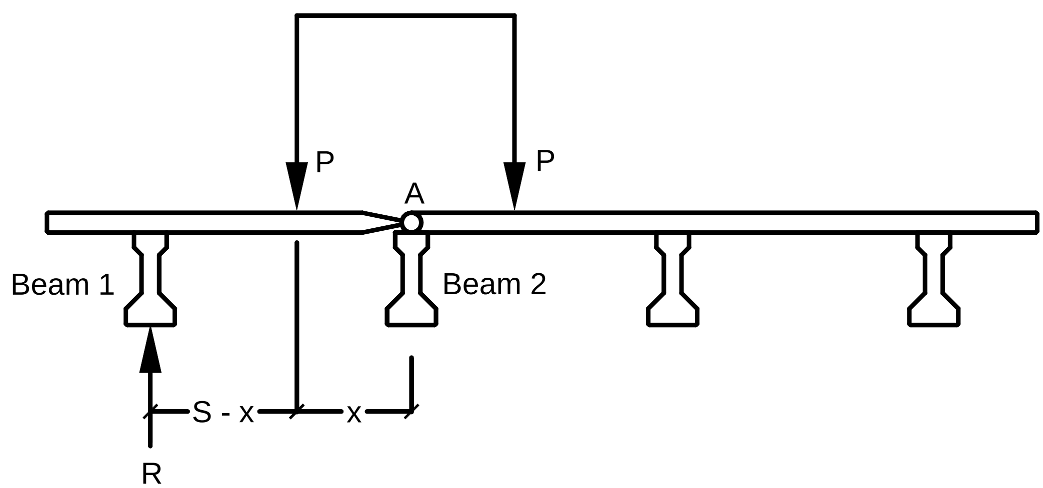

$$\Sigma M_A: \quad P \cdot x = R \cdot S$$

$$R = P \cdot \left(\frac{x}{S} \right)$$

Figure D.1 The Lever Rule

In Figure D.1, the unknown quantity is *R*. By assuming a hinge at *A*, above Beam 2, *R* can be calculated by summing moments about *A*. Then, *R* can be compared to the reaction force on Beam 2 in order to infer a distribution factor.

D.2 INPUT PARAMETERS

The AASHTO live load distribution factors were calculated using adjusted section properties for each bridge. As mentioned previously, the adjusted section properties were derived using the lower-bound concrete strengths. Tables D.2 and D.3 show values that were input into Equations D.2 and D.1, respectively, to calculate live load distribution factors.

Table D.2 Equation D.2 Input Values

Bridge Name	n	I (in^4)	A (in^2)	e_g (in)
Chandler Creek – 40’ Span	1.12	43300	361	22.7
Chandler Creek – 60’ Span	1.20	82800	496	26.6
Lake LBJ	1.16	82800	496	26.6
Lampasas River – Span 1	1.17	82800	496	26.2
Lampasas River – Span 2	1.17	82800	496	26.2
Willis Creek	1.20	82800	496	25.9
Wimberley – Span 1	1.19	43300	361	22.2
Wimberley – Span 2	1.19	43300	361	22.2
Slaughter Creek – Interior Girders	1.07	261000	789	33.5
Slaughter Creek – Exterior Girders	1.29	261000	789	33.5
Nolanville	1.12	261000	789	34.1

Table D.3 Equation D.1 Input Values

Bridge Name	S (ft)	L (ft)	t_s (in)
Chandler Creek – 40’ Span	8.00	38.5	7.25
Chandler Creek – 60’ Span	8.00	58.5	7.25
Lake LBJ	8.00	63.5	6.25
Lampasas River – Span 1	7.33	73.7	6.50
Lampasas River – Span 2	7.33	73.7	6.50
Willis Creek	6.67	63.5	6.00
Wimberley – Span 1	6.92	38.5	6.25
Wimberley – Span 2	6.92	38.5	6.25
Slaughter Creek – Interior Girders	8.00	98.8	7.50
Slaughter Creek – Exterior Girders	8.00	98.8	7.50
Nolanville	9.50	101	8.75

Appendix E – Calculation of AASHTO Load Rating

This appendix contains load rating sheets that were used to calculate both the design and adjusted load ratings presented in Chapter 7. The first section contains a list of all input parameters used in the load rating sheets, along with their definition and a reference where applicable. The second section contains load rating sheets that were used to calculate the design load ratings. The third section contains load rating sheets that were used to calculate the adjusted load ratings.

E.1 INPUT PARAMETER DEFINITIONS

This section contains a complete list of parameters used in the load rating calculations. Their definitions, equations, and references are also presented. They are broken down into sections according to where in the load rating calculation they are used.

E.1.1 Bridge Section Properties

Table E.1 shows bridge section properties that were used to calculate the AASHTO load ratings. As shown in Chapter 7, both the design section properties and adjusted section properties based on lower-bound concrete strengths were used to calculate load ratings.

Table E.1 Bridge Section Properties

Parameter Symbol	Units	Definition	Equation	Reference
A_{curb}	in^2	Cross-sectional area of the curb	-	-
A_{girder}	in^2	Cross-sectional area of the non-composite girder	-	-
A_{ps}	in^2	Total area of prestressing strands	-	-
A_s	in^2	Total area of mild reinforcing steel	-	-
A_{slab}	in^2	Cross-sectional area of the slab associated with the composite section	-	-
b_{eff}	in	Effective slab width	-	-
$b_{eff\text{-}modified}$	in	Effective slab width modified by the modular ratio	-	-
b_w	in	Width of the top flange of the non-composite girder	-	-
DF_1	-	AASHTO live load distribution factor with one design lane loaded	-	-
DF_2	-	AASHTO live load distribution factor with two design lanes loaded	-	-
$d_{overhang}$	in	Overhang distance, from the centerline of the girder	-	-
d_{girder}	in	Depth of the non-composite girder	-	-
$d_{p\text{-}bottom}$	in	Distance from the centroid of the prestressing strands to the girder soffit	-	-
$d_{p\text{-}comp}$	in	Depth from the extreme compression fiber of the composite section to the centroid of the prestressing strands	-	-
E_c	ksi	Modulus of elasticity of the girder concrete	$E_c = \frac{33 \cdot \omega^{1.5} \cdot \sqrt{f_c}}{1000}$	-
$e_{midspan\text{-}girder}$	in	Strand eccentricity at midspan	-	-
E_{ps}	ksi	Modulus of elasticity of the prestressing strands	-	-
E_{slab}	ksi	Modulus of elasticity of the slab concrete	See E_c	-
$f'_{c\text{-}girder}$	ksi	Compressive strength of the girder	-	-
$f'_{c\text{-}slab}$	ksi	Compressive strength of the slab	-	-
f_{pi}	ksi	Initial prestress	-	-

Table E.1 (Continued) Bridge Section Properties

f_{pu}	ksi	Ultimate specified tensile strength of the prestressing strands	-	-
$f_{y\text{-}steel}$	ksi	Yield stress of mild reinforcing steel	-	-
γ_{curb}	pcf	Unit weight of the curb concrete	-	-
γ_{girder}	pcf	Unit weight of the girder concrete	-	-
γ_{slab}	pcf	Unit weight of the slab concrete	-	-
h_f	in	Height of the slab	-	5-35
H	%	Average annual relative humidity at the bridge location	-	5-15
I_{comp}	in^4	Moment of inertia of the composite section	-	-
I_{girder}	in^4	Moment of inertia of the non-composite girder	-	-
L_{beam}	ft	Length of the girder, from end to end	-	-
$L_{bearing}$	in	Distance from end of the girder to the centerline of the bearing pad	-	-
L_{span}	ft	Overall span length	-	-
S_{girder}	ft	Girder spacing	-	-
$w_{diaphragm}$	k/ft	Dead load due to the weight of the diaphragms	-	-
$w_{miscellaneous}$	k/ft	Miscellaneous dead load	-	-
$w_{overlay}$	k/ft	Dead load due to asphalt overlay	-	-
y_{b_comp}	in	Distance from the neutral axis of the composite section to the girder soffit	-	-
y_{b_girder}	in	Distance from the neutral axis of the non-composite girder to the soffit	-	-
y_{t_comp}	in	Distance from the neutral axis of the composite section to the top of the slab	-	-
y_{t_girder}	in	Distance from the neutral axis of the non-composite girder to the top of the slab		

E.1.2 AASHTO Defined Parameters

Table E.2 AASHTO Defined Parameters

Parameter Symbol	Units	Definition	Equation	Reference
A_1	-	AASHTO dead load factor	-	51
A_2 (Inventory)	-	AASHTO live load factor for inventory rating	-	51
A_2 (Operating)	-	AASHTO live load factor for operating rating	-	51
ϕ	-	Strength reduction factor for flexure	-	5-24
f_{py}/f_{pu}	-	Ratio of yield stress to ultimate stress of prestressing strands	-	5-34
I	-	Dynamic load impact factor	-	3-26
k	-	Factor used to calculate f_{ps}	-	5-34
W	tons	Weight of the first two axles of the load rating design vehicle	-	70

E.1.3 Calculated Values

Table E.3 Calculated Values

Parameter Symbol	Units	Definition	Equation	Reference
a	in	Depth of the compression block at ultimate conditions	$a = \beta_1 c$	-
β_1	-	Rectangular stress block factor	$\beta_1 = 0.85-0.05(f'_c-4.0)$	5-34
c	in	Depth of the neutral axis at ultimate conditions	-	-
$c_{rectangular}$	in	Calculated neutral axis based on rectangular section behavior	$c_{rectangular} = \frac{A_{ps} \cdot f_{pu}}{0.85 f_c \cdot \beta_1 \cdot b + k \cdot A_{ps} \cdot \left(\frac{f_{pu}}{d_p}\right)}$	5-34

Table E.3 (Continued) Calculated Values

$c_{T\text{-section}}$	in	Calculated neutral axis based on T-section behavior	$c_{T\_section} = \dfrac{A_{ps} \cdot f_{pu} - 0.85 \cdot \beta_1 \cdot f_c \cdot (b - b_w) \cdot h_f}{0.85 \cdot f_c \cdot \beta_1 \cdot b_w + k \cdot A_{ps} \cdot \left(\dfrac{f_{pu}}{d_p}\right)}$	5-34
D_{comp}	k-ft	Dead load moment on the composite section	$D_{comp} = M_{DL\text{-miscellaneous}} + M_{DL\text{-overlay}}$	-
$D_{noncomp}$	k-ft	Dead load moment on the non-composite girder	$D_{noncomp} = MD_{L\text{-girder}} + M_{DL\text{-slab}} + M_{DL\text{-curb}} + M_{DL\text{-diaphragm}}$	-
Δf_{pES}	ksi	Prestress loss due to elastic shortening of the girders	$\Delta f_{pES} = \dfrac{E_p}{E_{ci}} \cdot f_{cgp}$	5-85
Δf_{pSH}	ksi	Prestress loss due to concrete shrinkage	$\Delta f_{pSH} = (17.0 - 0.150 H)$	5-88
Δf_{pCR}	ksi	Prestress loss due to concrete creep	$\Delta f_{pCR} = 12.0 \cdot f_{cgp} - 7.0 \cdot \Delta f_{cdp}$	5-88
Δf_{pSR}	ksi	Prestress loss due to steel relaxation	$\Delta f_{pSR} = 20.0 - 0.4 \cdot \Delta f_{pES} - 0.2 \cdot (\Delta f_{pSH} + \Delta f_{pCR})$	5-89
Δf_{pTotal}	ksi	Total prestress loss	-	-
$e_{midspan\text{-}comp}$	in	Midspan strand eccentricity of the composite section	-	-
f_{py}	ksi	Yield stress of the prestressing strands	$f_{py} = f_{pu} \cdot \left(\dfrac{f_{py}}{f_{pu}}\right)$	-
f_{cgp}	ksi	Assumed initial stress at the centroid of the prestressing strands	$f_{cgp} = \dfrac{P_i}{A_{girder}} + \dfrac{P_i \cdot (e_{midspan\_girder})^2}{I_{girder}}$	-
$F_{d\text{-}b}$	ksi	Total unfactored dead load tensile stress on the composite section, taken at the girder soffit	$F_{d\_b} = F_{d\_b\_noncomp} + F_{d\_b\_comp}$	-
$F_{d\text{-}b\text{-}comp}$	ksi	Unfactored dead load tensile stress on the composite section, taken at the girder soffit	$F_{d\_b\_comp} = \dfrac{D_{comp} \cdot y_{b\_comp}}{I_{comp}}$	-
$F_{d\text{-}t\text{-}comp}$	ksi	Unfactored dead load compressive stress on the composite section, taken at the top of the girder	$F_{d\_t\_comp} = \dfrac{D_{comp} \cdot y_{t\_comp}}{I_{comp}}$	-

Table E.3 (Continued) Calculated Values

$F_{d\text{-}p\text{-}comp}$	ksi	Unfactored tensile stress on the prestressing strands due to dead load on the composite section	$F_{d\_p\_comp} = \dfrac{D_{comp} \cdot e_{midspan\_comp}}{I_{comp}}$	-
$F_{d\text{-}b\text{-}noncomp}$	ksi	Unfactored dead load tensile stress on the non-composite girder, taken at the girder soffit	$F_{d\_b\_noncomp} = \dfrac{D_{noncomp} \cdot y_{b\_girder}}{I_{girder}}$	-
$F_{d\text{-}t\text{-}noncomp}$	ksi	Unfactored dead load tensile stress on the non-composite girder, taken at the top of the girder	$F_{d\_t\_noncomp} = \dfrac{D_{noncomp} \cdot y_{t\_girder}}{I_{girder}}$	-
$F_{d\text{-}p\text{-}noncomp}$	ksi	Unfactored dead load tensile stress on the prestressing strands due to dead load on the non-composite section	$F_{d\_p\_noncomp} = \dfrac{D_{noncomp} \cdot e_{midspan\_girder}}{I_{girder}}$	-
$F_{d\text{-}p}$	ksi	Total unfactored dead load tensile stress on the prestressing strands	$F_{d\_p} = F_{d\_p\_noncomp} + F_{d\_p\_comp}$	-
$F_{d\text{-}t}$	ksi	Total unfactored dead load compressive stress, taken at the top of the girder	$F_{d\_t} = F_{d\_t\_noncomp} + F_{d\_t\_comp}$	-
F_{L_b}	ksi	Unfactored live load tensile stress due to HS20 loading, taken at the girder soffit	$F_{L\_b} = \dfrac{L \cdot y_{b\_comp}}{I_{comp}}$	69
F_{L_p}	ksi	Unfactored live load tensile stress in the prestressing steel due to HS20 loading	$F_{L\_p} = \dfrac{L \cdot e_{midspan\_comp}}{I_{comp}}$	-
F_{L_t}	ksi	Unfactored live load compressive stress due to HS20 loading, taken at the top of the girder	$F_{L\_t} = \dfrac{L \cdot y_{t\_comp}}{I_{comp}}$	-

Table E.3 (Continued) Calculated Values

ϕM_n	k-ft	Factored moment capacity of the composite section	$\phi M_n = A_{ps} \cdot f_{ps} \cdot \left(d_p - \frac{a}{2}\right) + 0.85 \cdot f_c \cdot (b - b_w) \cdot \beta_1 \cdot h_f \cdot \left(\frac{a}{2} - \frac{h_f}{2}\right)$	5-37
F_{p_b}	ksi	Unfactored tensile stress due to prestressing, taken at the girder soffit	$F_{p\_b} = \frac{P_{eff}}{A_{girder}} + \frac{P_{eff} A_{ps} \cdot y_{b\_girder}}{I_{girder}}$	-
F_{p_t}	ksi	Unfactored compressive stress due to prestressing, taken at the top of the girder	$F_{p\_t} = \frac{P_{eff}}{A_{girder}} + \frac{P_{eff} A_{ps} \cdot y_{t\_girder}}{I_{girder}}$	-
f_{pe}	ksi	Effective prestress after all losses	$f_{pe} = f_{pi} - \Delta f_{pTotal}$	-
$f_{p\text{-}transfer}$	ksi	Assumed stress in the prestressing strands at transfer	-	-
f_{ps}	ksi	Average prestress at ultimate conditions	$f_{ps} = f_{pu} \cdot \left[1 - k \cdot \left(\frac{c}{d_p}\right)\right]$	5-34
L	k-ft	Unfactored live load moment due to HS20 loading	-	70
L(1+I)	k-ft	HS20 moment with impact	-	-
$M_{DL\text{-}curb}$	k-ft	Unfactored dead load moment on the girder due to curb weight	$M_{DL\_curb} = \frac{w_{curb} \cdot L_{span}^2}{8}$	-
$M_{DL\text{-}girder}$	k-ft	Unfactored dead load moment on the girder due to its self weight	$M_{DL\_girder} = \frac{w_{girder} \cdot L_{span}^2}{8}$	-
$M_{DL\text{-}slab}$	k-ft	Unfactored dead load moment due to the slab	$M_{DL\_slab} = \frac{w_{slab} \cdot L_{span}^2}{8}$	-
w_{curb}	k/ft	Dead load due to the curb	-	-
w_{girder}	k/ft	Dead load due to the girder self weight	-	-
w_{slab}	k/ft	Dead load due to slab weight	-	-

*Reference numbers in the form of "X-XX" refer to page numbers in the *2000 Interim AASHTO LRFD Bridge Design Specifications, 2nd Edition.* Reference Numbers in the form of "XX" refer to page numbers in the *2000 Interim AASHTO Manual for Condition Evaluation of Bridges, 2nd Edition.*

E.2 LOAD RATING SHEETS

This section contains the load rating sheets that were used to calculate the design and adjusted load ratings presented in Chapter 7. The sheets were prepared using Microsoft Excel, following guidelines set forth by the American Association of State Highway and Transportation Officials. The first section contains load rating sheets that were used to calculate design load ratings. The second section contains load rating sheets that were used to calculate adjusted load ratings.

E.2.1 Design Load Rating Sheets

This section contains load rating sheets that were used to calculate the design load ratings for all seven bridges considered in this study. Each bridge has three sheets; the first sheet consists of input parameters, the second sheet consists of calculated values, and the third section shows the load rating factors and load ratings.

E.2.1.1 Design Load Rating – Chandler Creek Bridge – 40' Span

User Defined Inputs

Parameter	Units	Interior Girder Values	Exterior Girder Values
A_{ps}	in^2	1.73	1.73
A_s	in^2	0.00	0.00
A_{curb}	in^2	0.00	0.00
A_{girder}	in^2	360.88	360.88
A_{slab}	in^2	674.25	612.63
b_{eff}	in	93.00	84.50
b_w	in	12.00	12.00
d_{girder}	in	34.00	34.00
$d_{overhang}$	in	48.00	38.00
$d_{p\text{-}bottom}$	in	3.01	3.01
$d_{p\text{-}comp}$	in	38.24	38.24
DF_1	-	0.588	0.750
DF_2	-	0.772	0.721
DF_{max}	-	0.772	0.750
E_c	ksi	4287	4287
E_p	ksi	29000	29000
E_{slab}	ksi	3321	3321
$e_{midspan\text{-}girder}$	in	11.90	11.90
$f'_{c\text{-}girder}$	ksi	5.0	5.0
$f'_{c\text{-}slab}$	ksi	3.0	3.0
f_{pi}	ksi	175	175
f_{pu}	ksi	250	250
$f_{y\text{-}steel}$	ksi	60	60
H	%	65	65
h_f	in	7.25	7.25
I_{girder}	in^4	43298	43298
I_{comp}	in^4	163513	158627
L	kip-ft	424.5	424.5
$L_{bearing}$	in	8.50	8.50
L_{span}	ft	38.58	38.58
L_{beam}	ft	40.00	40.00
S_{girder}	ft	8.00	8.00
$w_{diaphragm}$	kip/ft	0.090	0.090
$w_{miscellaneous}$	kip/ft	0.040	0.040
$w_{overlay}$	kip/ft	0.048	0.048
γ_{curb}	lb/ft^3	150	150
γ_{girder}	lb/ft^3	150	150
γ_{slab}	lb/ft^3	150	150
y_{b_girder}	in	14.91	14.91
y_{t_girder}	in	19.09	19.09
y_{b_comp}	in	27.99	27.45
y_{t_comp}	in	13.26	13.80
Strand Type*	-	1	1

*Stress relieved strands are Type 1

*Low relaxation strands are Type 2

AASHTO Specified Values

Parameter	Units	Interior Girder Values	Exterior Girder Values
W	tons	20	20
k	-	0.38	0.38
ϕ	-	1.00	1.00
f_{py}/f_{pu}	-	0.85	0.85
A_1	-	1.3	1.3
A_2 (Inventory)	-	2.17	2.17
A_2 (Operating)	-	1.3	1.3
I	-	1.33	1.33

Stresses and Moments

Parameter	Units	Interior Girder Values	Exterior Girder Values
$e_{midspan-comp}$	in	24.99	24.44
E_p/E_c	-	6.76	6.76
$F_{d-b-comp}$	ksi	0.0336	0.0340
$F_{d-t-comp}$	ksi	-0.016	-0.017
$F_{d-p-comp}$	ksi	0.203	0.205
$F_{d-b-noncomp}$	ksi	0.898	0.849
$F_{d-t-noncomp}$	ksi	-1.150	-1.087
$F_{d-p-noncomp}$	ksi	4.850	4.584
F_{d-b}	ksi	0.932	0.883
F_{d-t}	ksi	-1.166	-1.104
F_{d-p}	ksi	5.053	4.789
F_{L_b}	ksi	0.895	0.879
F_{L_t}	ksi	-0.424	-0.442
F_{L_p}	ksi	5.405	5.297
F_{p_b}	ksi	-1.56	-1.56
F_{p_t}	ksi	0.56	0.56
$6(f'_{c-girder})$^0.5	ksi	0.424	0.424
$7.5(f'_{c-girder})$^0.5	ksi	0.530	0.530
$12(f'_{c-girder})$^0.5	ksi	0.849	0.849
$M_{DL-curb}$	kip-ft	0.00	0.00
$M_{DL-girder}$	kip-ft	70	70
$M_{DL-slab}$	kip-ft	131	119
$P_i{*}e_{midspan-girder}$	kip-in	3342	3342
$P_{eff}{*}e_{midspan-girder}$	kip-in	2706	2701
D_{comp}	kip-ft	16	16
$D_{noncomp}$	kip-ft	217	205
L(1+I)	kip-ft	565	565
w_{curb}	kip/ft	0.000	0.000
w_{girder}	kip/ft	0.376	0.376
w_{slab}	kip/ft	0.702	0.638

Prestress Losses

Parameter	Units	Interior Girder Values	Exterior Girder Values
$f_{p-transfer}$	ksi	162.5	162.5
f_{cgp}	ksi	1.47	1.47
Δf_{pES}	ksi	9.92	9.92
Δf_{pSH}	ksi	7.25	7.25
Δf_{pCR}	ksi	14.57	14.85
Δf_{pSR}	ksi	11.67	11.61
Δf_{pTotal}	ksi	43.41	43.63
f_{pe}	ksi	131.59	131.37
f^*_y	ksi	212.5	212.5

Moment Capacity

Parameter	Units	Interior Girder Values	Exterior Girder Values
β_1	-	0.800	0.800
$0.85f'_c\beta_1$	ksi	3.40	3.40
$b_{eff-modified}$	in	72.04	65.45
$b-b_w$	in	60.04	53.45
$A_{ps}{*}f_{pu}$	kips	432	432
$c_{rectangular}$	in	1.73	1.90
$c_{T-section}$	in	-23.24	-19.64
c	in	1.73	1.90
a	in	1.39	1.52
f_{ps}	ksi	245.69	245.27
ϕM_n	kip-ft	1328	1324

Inventory Rating Factors		
RF	Interior Girder	Exterior Girder
CC_1	5.65	5.56
CC_2	4.01	3.91
CT_6	1.18	1.25
$CT_{7.5}$	1.30	1.37
CT_{12}	1.65	1.73
PST	6.17	6.39
FS	1.08	1.13

Operating Rating Factors		
RF	Interior Girder	Exterior Girder
FS	1.81	1.88
PST	10.10	10.40

Inventory Rating		
RT (tons)	Interior Girder	Exterior Girder
CC_1	113.1	111.2
CC_2	80.1	78.2
CT_6	23.6	25.0
$CT_{7.5}$	25.9	27.4
CT_{12}	33.0	34.7
PST	123.4	127.8
FS	21.7	22.5

Operating Rating		
RT (tons)	Interior Girder	Exterior Girder
FS	36.2	37.6
PST	202.0	208.0

E.2.1.2 Design Load Rating – Chandler Creek Bridge – 60' Span

User Defined Inputs

Parameter	Units	Interior Girder Values	Exterior Girder Values
A_{ps}	in^2	3.24	3.24
A_s	in^2	0.00	0.00
A_{curb}	in^2	0.00	0.00
A_{girder}	in^2	495.50	495.50
A_{slab}	in^2	681.50	616.25
b_{eff}	in	94.00	85.00
b_w	in	14.00	14.00
d_{girder}	in	40.00	40.00
$d_{overhang}$	in	48.00	38.00
$d_{p\text{-}bottom}$	in	4.00	4.00
$d_{p\text{-}comp}$	in	43.25	43.25
DF_1	-	0.535	0.750
DF_2	-	0.729	0.721
DF_{max}	-	0.729	0.750
E_c	ksi	4287	4287
E_p	ksi	29000	29000
E_{slab}	ksi	3321	3321
$e_{midspan\text{-}girder}$	in	13.07	13.07
$f'_{c\text{-}girder}$	ksi	5.0	5.0
$f'_{c\text{-}slab}$	ksi	3.0	3.0
f_{pi}	ksi	175	175
f_{pu}	ksi	250	250
$f_{y\text{-}steel}$	ksi	60	60
H	%	65	65
h_f	in	7.25	7.25
I_{girder}	in^4	82761	82761
I_{comp}	in^4	281470	271646
L	kip-ft	781.2	781.2
$L_{bearing}$	in	8.50	8.50
L_{span}	ft	58.58	58.58
L_{beam}	ft	60.00	60.00
S_{girder}	ft	8.00	8.00
$w_{diaphragm}$	kip/ft	0.090	0.090
$w_{miscellaneous}$	kip/ft	0.040	0.040
$w_{overlay}$	kip/ft	0.048	0.048
γ_{curb}	lb/ft^3	150	150
γ_{girder}	lb/ft^3	150	150
γ_{slab}	lb/ft^3	150	150
y_{b_girder}	in	17.07	17.07
y_{t_girder}	in	22.93	22.93
y_{b_comp}	in	30.18	29.50
y_{t_comp}	in	17.07	17.75
Strand Type*	-	1	1

*Stress relieved strands are Type 1

*Low relaxation strands are Type 2

AASHTO Specified Values

Parameter	Units	Interior Girder Values	Exterior Girder Values
W	tons	20	20
k	-	0.38	0.38
ϕ	-	1.00	1.00
f_{py}/f_{pu}	-	0.85	0.85
A_1	-	1.3	1.3
A_2 (Inventory)	-	2.17	2.17
A_2 (Operating)	-	1.3	1.3
I	-	1.33	1.33

Stresses and Moments			
Parameter	Units	Interior Girder Values	Exterior Girder Values
$e_{midspan-comp}$	in	26.18	25.50
E_p/E_c	-	6.76	6.76
$F_{d-b-comp}$	ksi	0.0486	0.0492
$F_{d-t-comp}$	ksi	-0.027	-0.030
$F_{d-p-comp}$	ksi	0.285	0.288
$F_{d-b-noncomp}$	ksi	1.397	1.325
$F_{d-t-noncomp}$	ksi	-1.877	-1.780
$F_{d-p-noncomp}$	ksi	7.238	6.864
F_{d-b}	ksi	1.446	1.374
F_{d-t}	ksi	-1.905	-1.810
F_{d-p}	ksi	7.523	7.152
F_{L_b}	ksi	0.974	1.015
F_{L_t}	ksi	-0.551	-0.611
F_{L_p}	ksi	5.717	5.937
F_{p_b}	ksi	-1.97	-1.96
F_{p_t}	ksi	0.67	0.67
$6(f'_{c-girder})$^0.5	ksi	0.424	0.424
$7.5(f'_{c-girder})$^0.5	ksi	0.530	0.530
$12(f'_{c-girder})$^0.5	ksi	0.849	0.849
$M_{DL-curb}$	kip-ft	0.00	0.00
$M_{DL-girder}$	kip-ft	221	221
$M_{DL-slab}$	kip-ft	305	275
$P_i*e_{midspan-girder}$	kip-in	6881	6881
$P_{eff}*e_{midspan-girder}$	kip-in	5455	5441
D_{comp}	kip-ft	38	38
$D_{noncomp}$	kip-ft	565	535
L(1+I)	kip-ft	1039	1039
w_{curb}	kip/ft	0.000	0.000
w_{girder}	kip/ft	0.516	0.516
w_{slab}	kip/ft	0.710	0.642

Prestress Losses			
Parameter	Units	Interior Girder Values	Exterior Girder Values
$f_{p-transfer}$	ksi	162.5	162.5
f_{cgp}	ksi	1.73	1.73
Δf_{pES}	ksi	11.70	11.70
Δf_{pSH}	ksi	7.25	7.25
Δf_{pCR}	ksi	16.72	17.10
Δf_{pSR}	ksi	10.53	10.45
Δf_{pTotal}	ksi	46.19	46.50
f_{pe}	ksi	128.81	128.50
f^*_y	ksi	212.5	212.5

Moment Capacity			
Parameter	Units	Interior Girder Values	Exterior Girder Values
β_1	-	0.800	0.800
$0.85f'_c\beta_1$	ksi	3.40	3.40
$b_{eff-modified}$	in	72.81	65.84
$b-b_w$	in	58.81	51.84
$A_{ps}*f_{pu}$	kips	810	810
$c_{rectangular}$	in	3.18	3.51
$c_{T-section}$	in	-11.69	-8.55
c	in	3.18	3.51
a	in	2.54	2.81
f_{ps}	ksi	243.01	242.30
ϕM_n	kip-ft	2754	2738

Inventory Rating Factors		
RF	Interior Girder	Exterior Girder
CC_1	3.20	3.04
CC_2	2.51	2.34
CT_6	0.97	1.00
$CT_{7.5}$	1.08	1.10
CT_{12}	1.41	1.41
PST	5.89	5.79
FS	1.20	1.18

Operating Rating Factors		
RF	Interior Girder	Exterior Girder
FS	2.00	1.97
PST	9.61	9.36

Inventory Rating		
RT (tons)	Interior Girder	Exterior Girder
CC_1	64.0	60.8
CC_2	50.2	46.8
CT_6	19.4	19.9
$CT_{7.5}$	21.6	22.0
CT_{12}	28.1	28.3
PST	117.8	115.7
FS	24.0	23.6

Operating Rating		
RT (tons)	Interior Girder	Exterior Girder
FS	40.1	39.3
PST	192.1	187.3

E.2.1.3 Design Load Rating – Lake LBJ Bridge

User Defined Inputs

Parameter	Units	Interior Girder Values	Exterior Girder Values
A_{ps}	in^2	3.89	3.89
A_s	in^2	0.00	0.00
A_{curb}	in^2	0.00	157.50
A_{girder}	in^2	495.50	495.50
A_{slab}	in^2	681.50	580.00
b_{eff}	in	94.00	80.00
b_w	in	14.00	14.00
d_{girder}	in	40.00	40.00
$d_{overhang}$	in	48.00	33.00
$d_{p\text{-}bottom}$	in	4.67	4.67
$d_{p\text{-}comp}$	in	40.48	40.48
DF_1	-	0.519	0.760
DF_2	-	0.711	0.711
DF_{max}	-	0.711	0.760
E_c	ksi	4287	4287
E_p	ksi	29000	29000
E_{slab}	ksi	3321	3321
$e_{midspan\text{-}girder}$	in	12.40	12.40
$f'_{c\text{-}girder}$	ksi	5.0	5.0
$f'_{c\text{-}slab}$	ksi	3.0	3.0
f_{pi}	ksi	175	175
f_{pu}	ksi	250	250
$f_{y\text{-}steel}$	ksi	60	60
H	%	65	65
h_f	in	7.25	7.25
I_{girder}	in^4	82761	82761
I_{comp}	in^4	285702	334221
L	kip-ft	870.7	870.7
$L_{bearing}$	in	8.50	8.50
L_{span}	ft	63.58	63.58
L_{beam}	ft	65.00	65.00
S_{girder}	ft	8.00	8.00
$w_{diaphragm}$	kip/ft	0.055	0.055
$w_{miscellaneous}$	kip/ft	0.035	0.035
$w_{overlay}$	kip/ft	0.048	0.048
γ_{curb}	lb/ft^3	150	150
γ_{girder}	lb/ft^3	150	150
γ_{slab}	lb/ft^3	150	150
y_{b_girder}	in	17.07	17.07
y_{t_girder}	in	22.93	22.93
y_{b_comp}	in	30.22	31.72
y_{t_comp}	in	17.03	15.53
Strand Type*	-	1	1

*Stress relieved strands are Type 1

*Low relaxation strands are Type 2

AASHTO Specified Values

Parameter	Units	Interior Girder Values	Exterior Girder Values
W	tons	20	20
k	-	0.38	0.38
ϕ	-	1.00	1.00
f_{py}/f_{pu}	-	0.85	0.85
A_1	-	1.3	1.3
A_2 (Inventory)	-	2.17	2.17
A_2 (Operating)	-	1.3	1.3
I	-	1.33	1.33

Stresses and Moments

Parameter	Units	Interior Girder Values	Exterior Girder Values
$e_{midspan-comp}$	in	25.55	27.05
E_p/E_c	-	6.76	6.76
$F_{d-b-comp}$	ksi	0.0532	0.0478
$F_{d-t-comp}$	ksi	-0.030	-0.023
$F_{d-p-comp}$	ksi	0.305	0.276
$F_{d-b-noncomp}$	ksi	1.602	1.675
$F_{d-t-noncomp}$	ksi	-2.152	-2.250
$F_{d-p-noncomp}$	ksi	7.874	8.233
F_{d-b}	ksi	1.656	1.723
F_{d-t}	ksi	-2.182	-2.274
F_{d-p}	ksi	8.179	8.508
F_{L_b}	ksi	1.046	1.003
F_{L_t}	ksi	-0.589	-0.491
F_{L_p}	ksi	5.982	5.786
F_{p_b}	ksi	-2.24	-2.23
F_{p_t}	ksi	0.69	0.69
$6(f'_{c-girder})$^0.5	ksi	0.424	0.424
$7.5(f'_{c-girder})$^0.5	ksi	0.530	0.530
$12(f'_{c-girder})$^0.5	ksi	0.849	0.849
$M_{DL-curb}$	kip-ft	0.00	0.00
$M_{DL-girder}$	kip-ft	261	261
$M_{DL-slab}$	kip-ft	359	305
$P_i*e_{midspan-girder}$	kip-in	7834	7834
$P_{eff}*e_{midspan-girder}$	kip-in	6063	6038
D_{comp}	kip-ft	42	42
$D_{noncomp}$	kip-ft	647	677
L(1+I)	kip-ft	1158	1158
w_{curb}	kip/ft	0.000	0.164
w_{girder}	kip/ft	0.516	0.516
w_{slab}	kip/ft	0.710	0.604

Prestress Losses

Parameter	Units	Interior Girder Values	Exterior Girder Values
$f_{p-transfer}$	ksi	162.5	162.5
f_{cgp}	ksi	1.98	1.98
Δf_{pES}	ksi	13.39	13.39
Δf_{pSH}	ksi	7.25	7.25
Δf_{pCR}	ksi	19.24	19.92
Δf_{pSR}	ksi	9.34	9.21
Δf_{pTotal}	ksi	49.23	49.77
f_{pe}	ksi	125.77	125.23
f^*_y	ksi	212.5	212.5

Moment Capacity

Parameter	Units	Interior Girder Values	Exterior Girder Values
β_1	-	0.800	0.800
$0.85f'_c\beta_1$	ksi	3.40	3.40
$b_{eff-modified}$	in	72.81	61.97
$b-b_w$	in	58.81	47.97
$A_{ps}*f_{pu}$	kips	972	972
$c_{rectangular}$	in	3.79	4.42
$c_{T-section}$	in	-8.42	-3.71
c	in	3.79	4.42
a	in	3.03	3.54
f_{ps}	ksi	241.11	239.62
ϕM_n	kip-ft	3044	3005

Inventory Rating Factors

RF	Interior Girder	Exterior Girder
CC_1	2.56	2.88
CC_2	2.13	2.46
CT_6	0.96	0.93
$CT_{7.5}$	1.06	1.03
CT_{12}	1.37	1.35
PST	6.03	6.27
FS	1.20	1.08

Operating Rating Factors

RF	Interior Girder	Exterior Girder
FS	2.01	1.81
PST	9.58	9.94

Inventory Rating

RT (tons)	Interior Girder	Exterior Girder
CC_1	51.3	57.7
CC_2	42.6	49.2
CT_6	19.2	18.5
$CT_{7.5}$	21.3	20.6
CT_{12}	27.4	27.0
PST	120.5	125.3
FS	24.0	21.7

Operating Rating

RT (tons)	Interior Girder	Exterior Girder
FS	40.1	36.2
PST	191.6	198.8

E.2.1.4 Design Load Rating – Lampasas River Bridge

User Defined Inputs			
Parameter	Units	Interior Girder Values	Exterior Girder Values
A_{ps}	in^2	3.89	3.89
A_s	in^2	0.00	0.00
A_{curb}	in^2	0.00	0.00
A_{girder}	in^2	495.50	495.50
A_{slab}	in^2	552.50	520.00
b_{eff}	in	85.00	80.00
b_w	in	14.00	14.00
d_{girder}	in	40.00	40.00
$d_{overhang}$	in	43.98	37.50
$d_{p\text{-}bottom}$	in	4.65	4.65
$d_{p\text{-}comp}$	in	41.85	41.85
DF_1	-	0.480	0.727
DF_2	-	0.661	0.654
DF_{max}	-	0.661	0.727
E_c	ksi	4329	4329
E_p	ksi	29000	29000
E_{slab}	ksi	3321	3321
$e_{midspan\text{-}girder}$	in	12.42	12.42
$f'_{c\text{-}girder}$	ksi	5.1	5.1
$f'_{c\text{-}slab}$	ksi	3.0	3.0
f_{pi}	ksi	175	175
f_{pu}	ksi	250	250
$f_{y\text{-}steel}$	ksi	60	60
H	%	65	65
h_f	in	6.5	6.5
I_{girder}	in^4	82761	82761
I_{comp}	in^4	256764	251053
L	kip-ft	1052.8	1052.8
$L_{bearing}$	in	7.50	7.50
L_{span}	ft	73.75	73.75
L_{beam}	ft	75.00	75.00
S_{girder}	ft	7.33	7.33
$w_{diaphragm}$	kip/ft	0.043	0.043
$w_{miscellaneous}$	kip/ft	0.035	0.035
$w_{overlay}$	kip/ft	0.044	0.044
γ_{curb}	lb/ft^3	150	150
γ_{girder}	lb/ft^3	150	150
γ_{slab}	lb/ft^3	150	150
y_{b_girder}	in	17.07	17.07
y_{t_girder}	in	22.93	22.93
y_{b_comp}	in	28.43	28.03
y_{t_comp}	in	18.07	18.47
Strand Type*	-	1	1

*Stress relieved strands are Type 1

*Low relaxation strands are Type 2

AASHTO Specified Values			
Parameter	Units	Interior Girder Values	Exterior Girder Values
W	tons	20	20
k	-	0.38	0.38
ϕ	-	1.00	1.00
f_{py}/f_{pu}	-	0.85	0.85
A_1	-	1.3	1.3
A_2 (Inventory)	-	2.17	2.17
A_2 (Operating)	-	1.3	1.3
I	-	1.33	1.33

Stresses and Moments			
Parameter	Units	Interior Girder Values	Exterior Girder Values
$e_{midspan-comp}$	in	23.78	23.38
E_p/E_c	-	6.70	6.70
$F_{d-b-comp}$	ksi	0.0714	0.0720
$F_{d-t-comp}$	ksi	-0.045	-0.047
$F_{d-p-comp}$	ksi	0.400	0.402
$F_{d-b-noncomp}$	ksi	1.909	1.852
$F_{d-t-noncomp}$	ksi	-2.565	-2.488
$F_{d-p-noncomp}$	ksi	9.306	9.028
F_{d-b}	ksi	1.981	1.924
F_{d-t}	ksi	-2.610	-2.536
F_{d-p}	ksi	9.705	9.430
F_{L_b}	ksi	1.230	1.364
F_{L_t}	ksi	-0.782	-0.899
F_{L_p}	ksi	6.889	7.621
F_{p_b}	ksi	-2.29	-2.28
F_{p_t}	ksi	0.71	0.71
$6(f'_{c-girder})$^0.5	ksi	0.428	0.428
$7.5(f'_{c-girder})$^0.5	ksi	0.536	0.536
$12(f'_{c-girder})$^0.5	ksi	0.857	0.857
$M_{DL-curb}$	kip-ft	0.00	0.00
$M_{DL-girder}$	kip-ft	351	351
$M_{DL-slab}$	kip-ft	391	368
$P_i*e_{midspan-girder}$	kip-in	7847	7847
$P_{eff}*e_{midspan-girder}$	kip-in	6198	6187
D_{comp}	kip-ft	54	54
$D_{noncomp}$	kip-ft	771	748
L(1+I)	kip-ft	1400	1400
w_{curb}	kip/ft	0.000	0.000
w_{girder}	kip/ft	0.516	0.516
w_{slab}	kip/ft	0.576	0.542

Prestress Losses			
Parameter	Units	Interior Girder Values	Exterior Girder Values
$f_{p-transfer}$	ksi	162.5	162.5
f_{cgp}	ksi	1.82	1.82
Δf_{pES}	ksi	12.20	12.20
Δf_{pSH}	ksi	7.25	7.25
Δf_{pCR}	ksi	16.92	17.21
Δf_{pSR}	ksi	10.29	10.23
Δf_{pTotal}	ksi	46.65	46.88
f_{pe}	ksi	128.35	128.12
f^*_y	ksi	212.5	212.5

Moment Capacity			
Parameter	Units	Interior Girder Values	Exterior Girder Values
β_1	-	0.795	0.795
$0.85f'_c\beta_1$	ksi	3.45	3.45
$b_{eff-modified}$	in	65.19	61.36
$b-b_w$	in	51.19	47.36
$A_{ps}*f_{pu}$	kips	972	972
$c_{rectangular}$	in	4.16	4.41
$c_{T-section}$	in	-3.06	-1.56
c	in	4.16	4.41
a	in	3.31	3.51
f_{ps}	ksi	240.55	239.98
ϕM_n	kip-ft	3133	3118

Inventory Rating Factors		
RF	Interior Girder	Exterior Girder
CC_1	1.48	1.37
CC_2	1.39	1.25
CT_6	0.60	0.58
$CT_{7.5}$	0.68	0.65
CT_{12}	0.94	0.89
PST	4.64	4.26
FS	1.03	0.94
Operating Rating Factors		
RF	Interior Girder	Exterior Girder
FS	1.71	1.57
PST	7.72	7.05

Inventory Rating		
RT (tons)	Interior Girder	Exterior Girder
CC_1	29.7	27.4
CC_2	27.9	25.1
CT_6	11.9	11.5
$CT_{7.5}$	13.7	13.1
CT_{12}	18.9	17.8
PST	92.7	85.2
FS	20.5	18.8
Operating Rating		
RT (tons)	Interior Girder	Exterior Girder
FS	34.2	31.4
PST	154.4	140.9

E.2.1.5 Design Load Rating – Willis Creek Bridge

User Defined Inputs

Parameter	Units	Interior Girder Values	Exterior Girder Values
A_{ps}	in^2	3.52	3.52
A_s	in^2	0.00	0.00
A_{curb}	in^2	0.00	99.00
A_{girder}	in^2	495.50	495.50
A_{slab}	in^2	474.00	441.00
b_{eff}	in	79.00	73.50
b_w	in	14.00	14.00
d_{girder}	in	40.00	40.00
$d_{overhang}$	in	40.02	34.00
$d_{p\text{-}bottom}$	in	9.05	9.05
$d_{p\text{-}comp}$	in	36.95	36.95
DF_1	-	0.486	0.700
DF_2	-	0.655	0.648
DF_{max}	-	0.655	0.700
E_c	ksi	4287	4287
E_p	ksi	29000	29000
E_{slab}	ksi	3321	3321
$e_{midspan\text{-}girder}$	in	8.02	8.02
$f'_{c\text{-}girder}$	ksi	5.0	5.0
$f'_{c\text{-}slab}$	ksi	3.0	3.0
f_{pi}	ksi	175	175
f_{pu}	ksi	250	250
$f_{y\text{-}steel}$	ksi	60	60
H	%	65	65
h_f	in	6.00	6.00
I_{girder}	in^4	82761	82761
I_{comp}	in^4	234502	270133
L	kip-ft	870.7	870.7
$L_{bearing}$	in	8.50	8.50
L_{span}	ft	63.58	63.58
L_{beam}	ft	65.00	65.00
S_{girder}	ft	6.67	6.67
$w_{diaphragm}$	kip/ft	0.045	0.045
$w_{miscellaneous}$	kip/ft	0.075	0.075
$w_{overlay}$	kip/ft	0.040	0.040
γ_{curb}	lb/ft^3	150	150
γ_{girder}	lb/ft^3	150	150
γ_{slab}	lb/ft^3	150	150
y_{b_girder}	in	17.07	17.07
y_{t_girder}	in	22.93	22.93
y_{b_comp}	in	27.57	29.09
y_{t_comp}	in	18.43	16.91
Strand Type*	-	1	1

*Stress relieved strands are Type 1

*Low relaxation strands are Type 2

AASHTO Specified Values

Parameter	Units	Interior Girder Values	Exterior Girder Values
W	tons	20	20
k	-	0.38	0.38
ϕ	-	1.00	1.00
f_{py}/f_{pu}	-	0.85	0.85
A_1	-	1.3	1.3
A_2 (Inventory)	-	2.17	2.17
A_2 (Operating)	-	1.3	1.3
I	-	1.33	1.33

Stresses and Moments

Parameter	Units	Interior Girder Values	Exterior Girder Values
$e_{midspan\text{-}comp}$	in	18.52	20.04
E_p/E_c	-	6.76	6.76
$F_{d\text{-}b\text{-}comp}$	ksi	0.0820	0.0751
$F_{d\text{-}t\text{-}comp}$	ksi	-0.055	-0.044
$F_{d\text{-}p\text{-}comp}$	ksi	0.373	0.350
$F_{d\text{-}b\text{-}noncomp}$	ksi	1.319	1.405
$F_{d\text{-}t\text{-}noncomp}$	ksi	-1.772	-1.888
$F_{d\text{-}p\text{-}noncomp}$	ksi	4.194	4.467
$F_{d\text{-}b}$	ksi	1.401	1.481
$F_{d\text{-}t}$	ksi	-1.827	-1.932
$F_{d\text{-}p}$	ksi	4.566	4.817
F_{L_b}	ksi	1.070	1.048
F_{L_t}	ksi	-0.715	-0.609
F_{L_p}	ksi	4.863	4.882
F_{p_b}	ksi	-1.72	-1.72
F_{p_t}	ksi	0.10	0.10
$6(f'_{c\text{-}girder})$^0.5	ksi	0.424	0.424
$7.5(f'_{c\text{-}girder})$^0.5	ksi	0.530	0.530
$12(f'_{c\text{-}girder})$^0.5	ksi	0.849	0.849
$M_{DL\text{-}curb}$	kip-ft	0.00	0.00
$M_{DL\text{-}girder}$	kip-ft	261	261
$M_{DL\text{-}slab}$	kip-ft	250	232
$P_i*e_{midspan\text{-}girder}$	kip-in	4587	4587
$P_{eff}*e_{midspan\text{-}girder}$	kip-in	3758	3755
D_{comp}	kip-ft	58	58
$D_{noncomp}$	kip-ft	533	568
L(1+I)	kip-ft	1158	1158
w_{curb}	kip/ft	0.000	0.103
w_{girder}	kip/ft	0.516	0.516
w_{slab}	kip/ft	0.494	0.459

Prestress Losses

Parameter	Units	Interior Girder Values	Exterior Girder Values
$f_{p\text{-}transfer}$	ksi	162.5	162.5
f_{cgp}	ksi	1.30	1.30
Δf_{pES}	ksi	8.76	8.76
Δf_{pSH}	ksi	7.25	7.25
Δf_{pCR}	ksi	13.52	13.66
Δf_{pSR}	ksi	12.34	12.31
Δf_{pTotal}	ksi	41.87	41.99
f_{pe}	ksi	133.13	133.01
f^*_y	ksi	212.5	212.5

Moment Capacity

Parameter	Units	Interior Girder Values	Exterior Girder Values
β_1	-	0.800	0.800
$0.85f'_c\beta_1$	ksi	3.40	3.40
$b_{eff\text{-}modified}$	in	61.19	56.93
$b\text{-}b_w$	in	47.19	42.93
$A_{ps}*f_{pu}$	kips	880	880
$c_{rectangular}$	in	4.05	4.34
$c_{T\text{-}section}$	in	-1.46	0.07
c	in	4.05	4.34
a	in	3.24	3.47
f_{ps}	ksi	239.58	238.83
ϕM_n	kip-ft	2483	2467

Inventory Rating Factors		
RF	**Interior Girder**	**Exterior Girder**
CC_1	1.77	1.91
CC_2	1.59	1.78
CT_6	0.69	0.63
$CT_{7.5}$	0.79	0.73
CT_{12}	1.09	1.04
PST	6.64	6.59
FS	1.04	0.94

Operating Rating Factors		
RF	**Interior Girder**	**Exterior Girder**
FS	1.74	1.57
PST	11.01	10.94

Inventory Rating		
RT (tons)	**Interior Girder**	**Exterior Girder**
CC_1	35.5	38.2
CC_2	31.7	35.5
CT_6	13.9	12.7
$CT_{7.5}$	15.9	14.7
CT_{12}	21.8	20.8
PST	132.9	131.8
FS	20.8	18.8

Operating Rating		
RT (tons)	**Interior Girder**	**Exterior Girder**
FS	34.8	31.4
PST	220.3	218.8

E.2.1.6 Design Load Rating – Wimberley Bridge

User Defined Inputs

Parameter	Units	Interior Girder Values	Exterior Girder Values
A_{ps}	in^2	2.72	2.72
A_s	in^2	0.00	0.00
A_{curb}	in^2	0.00	137.00
A_{girder}	in^2	360.88	360.88
A_{slab}	in^2	506.25	384.38
b_{eff}	in	81.00	61.50
b_w	in	12.00	12.00
d_{girder}	in	34.00	34.00
$d_{overhang}$	in	41.52	21.00
$d_{p\text{-}bottom}$	in	6.77	6.77
$d_{p\text{-}comp}$	in	33.48	33.48
DF_1	-	0.555	0.518
DF_2	-	0.719	0.606
DF_{max}	-	0.719	0.606
E_c	ksi	4287	4287
E_{ps}	ksi	29000	29000
E_{slab}	ksi	3321	3321
$e_{midspan\text{-}girder}$	in	8.14	8.14
$f'_{c\text{-}girder}$	ksi	5.0	5.0
$f'_{c\text{-}slab}$	ksi	3.0	3.0
f_{pi}	ksi	175	175
f_{pu}	ksi	250	250
$f_{y\text{-}steel}$	ksi	60	60
H	%	65	65
h_f	in	6.25	6.25
I_{girder}	in^4	43298	43298
I_{comp}	in^4	144674	172617
L	kip-ft	421.7	421.7
$L_{bearing}$	in	9.50	9.50
L_{span}	ft	38.42	38.42
L_{beam}	ft	40.00	40.00
S_{girder}	ft	6.92	6.92
$w_{diaphragm}$	kip/ft	0.041	0.041
$w_{miscellaneous}$	kip/ft	0.035	0.035
$w_{overlay}$	kip/ft	0.045	0.045
γ_{curb}	lb/ft^3	150	150
γ_{girder}	lb/ft^3	150	150
γ_{slab}	lb/ft^3	150	150
y_{b_girder}	in	14.91	14.91
y_{t_girder}	in	19.09	19.09
y_{b_comp}	in	25.98	27.29
y_{t_comp}	in	14.27	12.96
Strand Type*	-	1	1

*Stress relieved strands are Type 1

*Low relaxation strands are Type 2

AASHTO Specified Values

Parameter	Units	Interior Girder Values	Exterior Girder Values
W	tons	20	20
k	-	0.38	0.38
ϕ	-	1.00	1.00
f_{py}/f_{pu}	-	0.85	0.85
A_1	-	1.3	1.3
A_2 (Inventory)	-	2.17	2.17
A_2 (Operating)	-	1.3	1.3
I	-	1.33	1.33

Stresses and Moments

Parameter	Units	Interior Girder Values	Exterior Girder Values
$e_{midspan-comp}$	in	19.22	20.53
E_{ps}/E_c	-	6.76	6.76
$F_{d-b-comp}$	ksi	0.0318	0.0280
$F_{d-t-comp}$	ksi	-0.017	-0.013
$F_{d-p-comp}$	ksi	0.159	0.142
$F_{d-b-noncomp}$	ksi	0.720	0.732
$F_{d-t-noncomp}$	ksi	-0.922	-0.937
$F_{d-p-noncomp}$	ksi	2.659	2.703
F_{d-b}	ksi	0.752	0.760
F_{d-t}	ksi	-0.939	-0.950
F_{d-p}	ksi	2.818	2.845
F_{L_b}	ksi	0.869	0.645
F_{L_t}	ksi	-0.477	-0.306
F_{L_p}	ksi	4.347	3.282
F_{p_b}	ksi	-1.92	-1.91
F_{p_t}	ksi	0.28	0.28
$6(f'_{c-girder})$^0.5	ksi	0.424	0.424
$7.5(f'_{c-girder})$^0.5	ksi	0.530	0.530
$12(f'_{c-girder})$^0.5	ksi	0.849	0.849
$M_{DL-curb}$	kip-ft	0.00	0.00
$M_{DL-girder}$	kip-ft	69	69
$M_{DL-slab}$	kip-ft	97	74
$P_i*e_{midspan-girder}$	kip-in	3598	3598
$P_{eff}*e_{midspan-girder}$	kip-in	2803	2796
D_{comp}	kip-ft	15	15
$D_{noncomp}$	kip-ft	174	177
L(1+I)	kip-ft	561	561
w_{curb}	kip/ft	0.000	0.143
w_{girder}	kip/ft	0.376	0.376
w_{slab}	kip/ft	0.527	0.400

Prestress Losses

Parameter	Units	Interior Girder Values	Exterior Girder Values
$f_{p-transfer}$	ksi	162.5	162.5
f_{cgp}	ksi	1.74	1.74
Δf_{pES}	ksi	11.80	11.80
Δf_{pSH}	ksi	7.25	7.25
Δf_{pCR}	ksi	19.40	19.77
Δf_{pSR}	ksi	9.95	9.87
Δf_{pTotal}	ksi	48.40	48.70
f_{pe}	ksi	126.60	126.30
f^*_y	ksi	212.5	212.5

Moment Capacity

Parameter	Units	Interior Girder Values	Exterior Girder Values
β_1	-	0.800	0.800
$0.85f'_c\beta_1$	ksi	3.40	3.40
$b_{eff-modified}$	in	62.74	47.64
$b-b_w$	in	50.74	35.64
$A_{ps}*f_{pu}$	kips	680	680
$c_{rectangular}$	in	3.08	4.01
$c_{T-section}$	in	-8.21	-1.59
c	in	3.08	4.01
a	in	2.46	3.21
f_{ps}	ksi	241.27	238.63
ϕM_n	kip-ft	1764	1724

Inventory Rating Factors		
RF	Interior Girder	Exterior Girder
CC_1	4.91	7.61
CC_2	3.50	5.44
CT_6	1.83	2.45
$CT_{7.5}$	1.95	2.61
CT_{12}	2.32	3.11
PST	9.34	12.45
FS	1.74	2.00
Operating Rating Factors		
RF	Interior Girder	Exterior Girder
FS	2.90	3.34
PST	14.23	18.92

Inventory Rating		
RT (tons)	Interior Girder	Exterior Girder
CC_1	98.2	152.2
CC_2	70.1	108.8
CT_6	36.6	49.0
$CT_{7.5}$	39.1	52.3
CT_{12}	46.4	62.1
PST	186.7	249.0
FS	34.7	40.0
Operating Rating		
RT (tons)	Interior Girder	Exterior Girder
FS	57.9	66.7
PST	284.5	378.5

E.2.1.7 Design Load Rating – Slaughter Creek Bridge

User Defined Inputs

Parameter	Units	Interior Girder Values	Exterior Girder Values
A_{ps}	in^2	5.508	8.874
A_s	in^2	0.00	0.00
A_{curb}	in^2	0.00	330.00
A_{girder}	in^2	789.00	789.00
A_{slab}	in^2	720.00	510.00
b_{eff}	in	96.00	68.00
b_w	in	20.00	20.00
d_{girder}	in	54.00	54.00
$d_{overhang}$	in	48.00	26.00
$d_{p\text{-}bottom}$	in	4.00	4.00
$d_{p\text{-}comp}$	in	57.50	57.50
DF_1	-	0.472	0.625
DF_2	-	0.672	0.592
DF_{max}	-	0.672	0.625
E_c	ksi	4595	5467
E_p	ksi	28500	28500
E_{slab}	ksi	3908	3908
$e_{midspan\text{-}girder}$	in	20.75	10.41
$f'_{c\text{-}girder}$	ksi	5.0	7.7
$f'_{c\text{-}slab}$	ksi	3.6	3.6
f_{pi}	ksi	202.5	202.5
f_{pu}	ksi	270	270
$f_{y\text{-}steel}$	ksi	60	60
H	%	70	70
h_f	in	7.5	7.5
I_{girder}	in^4	260740	260740
I_{comp}	in^4	713605	912013
L	kip-ft	1502.4	1502.4
$L_{bearing}$	in	9.00	9.00
L_{span}	ft	98.80	98.80
L_{beam}	ft	100.00	100.00
S_{girder}	ft	8.00	8.00
$w_{diaphragm}$	kip/ft	0.045	0.045
$w_{miscellaneous}$	kip/ft	0.075	0.075
$w_{overlay}$	kip/ft	0.040	0.040
γ_{curb}	lb/ft^3	150	150
γ_{girder}	lb/ft^3	150	150
γ_{slab}	lb/ft^3	150	150
y_{b_girder}	in	24.75	24.75
y_{t_girder}	in	29.25	29.25
y_{b_comp}	in	39.42	42.08
y_{t_comp}	in	22.08	19.42
Strand Type*	-	2	2

*Stress relieved strands are Type 1

*Low relaxation strands are Type 2

AASHTO Specified Values

Parameter	Units	Interior Girder Values	Exterior Girder Values
W	tons	20	20
k	-	0.28	0.28
ϕ	-	1.00	1.00
f_{py}/f_{pu}	-	0.90	0.90
A_1	-	1.3	1.3
A_2 (Inventory)	-	2.17	2.17
A_2 (Operating)	-	1.3	1.3
I	-	1.22	1.22

Stresses and Moments			
Parameter	Units	Interior Girder Values	Exterior Girder Values
$e_{midspan-comp}$	in	35.42	27.74
E_p/E_c	-	6.20	5.21
F_{d-b}	ksi	2.185	2.060
F_{d-t}	ksi	-2.582	-2.434
F_{d-p}	ksi	11.360	4.516
$F_{d-girder\_b}$	ksi	1.142	1.142
$F_{d-girder\_t}$	ksi	-1.350	-1.350
$F_{d-girder\_p}$	ksi	5.940	2.505
F_{d-comp_b}	ksi	1.042	0.917
F_{d-comp_t}	ksi	-1.232	-1.084
F_{d-comp_p}	ksi	5.420	2.011
F_{L_b}	ksi	0.817	0.601
F_{L_t}	ksi	-0.458	-0.277
F_{L_p}	ksi	4.554	2.064
F_{p_b}	ksi	-2.88	-3.12
F_{p_t}	ksi	0.94	-0.14
$6(f'_{c-girder})$^0.5	ksi	0.424	0.526
$7.5(f'_{c-girder})$^0.5	ksi	0.530	0.658
$12(f'_{c-girder})$^0.5	ksi	0.849	1.053
$M_{DL-curb}$	kip-ft	0.00	0.00
$M_{DL-girder}$	kip-ft	1002.84	1002.84
$M_{DL-slab}$	kip-ft	915.14	805.32
$P_i*e_{midspan-girder}$	kip-in	21601	17460
$P_{eff}*e_{midspan-girder}$	kip-in	18437	14389
D	kip-ft	1994	1955
L(1+I)	kip-ft	1833	1833
w_{curb}	kip/ft	0.000	0.344
w_{girder}	kip/ft	0.822	0.822
w_{slab}	kip/ft	0.750	0.660

Prestress Losses			
Parameter	Units	Interior Girder Values	Exterior Girder Values
$f_{p-transfer}$	ksi	189	189
f_{cgp}	ksi	2.08	2.34
Δf_{pES}	ksi	12.91	12.21
Δf_{pSH}	ksi	6.50	6.50
Δf_{pCR}	ksi	18.85	25.41
Δf_{pSR}	ksi	2.93	2.62
Δf_{pTotal}	ksi	41.19	46.74
f_{pe}	ksi	161.31	155.76
f^*_y	ksi	243	243

Moment Capacity			
Parameter	Units	Interior Girder Values	Exterior Girder Values
β_1	-	0.87	0.87
$0.85f'_c\beta_1$	ksi	3.70	5.69
$b_{eff-modified}$	in	81.65	48.61
$b-b_w$	in	61.65	28.61
$A_{ps}*f_{pu}$	kips	1487	2396
$c_{rectangular}$	in	4.81	8.31
$c_{T-section}$	in	-2.74	9.35
c	in	4.81	9.35
a	in	4.19	8.14
f_{ps}	ksi	263.67	257.70
ϕM_n	kip-ft	6706	10198

Inventory Rating Factors		
RF	Interior Girder	Exterior Girder
CC_1	2.97	7.39
CC_2	2.58	6.47
CT_6	1.37	2.64
$CT_{7.5}$	1.50	2.86
CT_{12}	1.88	3.52
PST	4.77	16.53
FS_{other}	1.54	3.25
Operating Rating Factors		
RF	Interior Girder	Exterior Girder
FS_{other}	2.57	5.43
PST	10.11	28.31

Inventory Rating		
RT (tons)	Interior Girder	Exterior Girder
CC_1	59.4	147.8
CC_2	51.6	129.5
CT_6	27.3	52.8
$CT_{7.5}$	29.9	57.2
CT_{12}	37.7	70.3
PST	95.4	330.7
FS_{other}	30.8	65.1
Operating Rating		
RT (tons)	Interior Girder	Exterior Girder
FS_{other}	51.3	108.6
PST	202.2	566.2

E.2.1.8 Design Load Rating – Nolanville Bridge

User Defined Inputs			
Parameter	Units	Interior Girder Values	Exterior Girder Values
A_{ps}	in^2	7.344	7.344
A_s	in^2	0.00	0.00
A_{curb}	in^2	0.00	0.00
A_{girder}	in^2	789.00	789.00
A_{slab}	in^2	936.25	612.50
b_{eff}	in	107.00	70.00
b_w	in	20.00	20.00
d_{girder}	in	54.00	54.00
$d_{overhang}$	in	57.00	24.00
$d_{p\text{-}bottom}$	in	5.08	5.08
$d_{p\text{-}comp}$	in	57.67	57.67
DF_1	-	0.505	0.763
DF_2	-	0.733	0.705
DF_{max}	-	0.733	0.763
E_c	ksi	4595	5467
E_p	ksi	28500	28500
E_{slab}	ksi	3908	3908
$e_{midspan\text{-}girder}$	in	19.67	19.67
$f'_{c\text{-}girder}$	ksi	6.2	6.2
$f'_{c\text{-}slab}$	ksi	3.6	3.6
f_{pi}	ksi	202.5	202.5
f_{pu}	ksi	270	270
$f_{y\text{-}steel}$	ksi	60	60
H	%	70	70
h_f	in	8.75	8.75
I_{girder}	in^4	260740	260740
I_{comp}	in^4	742516	686667
L	kip-ft	1538.4	1538.4
$L_{bearing}$	in	9.00	9.00
L_{span}	ft	100.80	100.80
L_{beam}	ft	102.00	102.00
S_{girder}	ft	9.50	9.50
$w_{diaphragm}$	kip/ft	0.045	0.045
$w_{miscellaneous}$	kip/ft	0.075	0.075
$w_{overlay}$	kip/ft	0.040	0.040
γ_{curb}	lb/ft^3	150	150
γ_{girder}	lb/ft^3	150	150
γ_{slab}	lb/ft^3	150	150
y_{b_girder}	in	24.75	24.75
y_{t_girder}	in	29.25	29.25
y_{b_comp}	in	40.29	38.39
y_{t_comp}	in	22.46	24.36
Strand Type*	-	2	2

*Stress relieved strands are Type 1

*Low relaxation strands are Type 2

AASHTO Specified Values			
Parameter	Units	Interior Girder Values	Exterior Girder Values
W	tons	20	20
k	-	0.28	0.28
ϕ	-	1.00	1.00
f_{py}/f_{pu}	-	0.90	0.90
A_1	-	1.3	1.3
A_2 (Inventory)	-	2.17	2.17
A_2 (Operating)	-	1.3	1.3
I	-	1.22	1.22

Stresses and Moments

Parameter	Units	Interior Girder Values	Exterior Girder Values
$e_{midspan-comp}$	in	35.21	33.31
E_p/E_c	-	6.20	5.21
F_{d-b}	ksi	2.274	2.144
F_{d-t}	ksi	-2.688	-2.534
F_{d-p}	ksi	11.210	8.882
$F_{d-girder\_b}$	ksi	1.189	1.189
$F_{d-girder\_t}$	ksi	-1.405	-1.405
$F_{d-girder\_p}$	ksi	5.861	4.926
F_{d-comp_b}	ksi	1.085	0.955
F_{d-comp_t}	ksi	-1.282	-1.128
F_{d-comp_p}	ksi	5.348	3.956
F_{L_b}	ksi	0.896	0.888
F_{L_t}	ksi	-0.499	-0.564
F_{L_p}	ksi	4.856	4.018
F_{p_b}	ksi	-3.41	-3.45
F_{p_t}	ksi	1.02	1.03
$6(f'_{c-girder})$^0.5	ksi	0.472	0.472
$7.5(f'_{c-girder})$^0.5	ksi	0.591	0.591
$12(f'_{c-girder})$^0.5	ksi	0.945	0.945
$M_{DL-curb}$	kip-ft	0.00	0.00
$M_{DL-girder}$	kip-ft	1043.85	1043.85
$M_{DL-slab}$	kip-ft	952.56	838.25
$P_i{*}e_{midspan-girder}$	kip-in	27302	27302
$P_{eff}{*}e_{midspan-girder}$	kip-in	21374	21637
D	kip-ft	1994	1955
L(1+I)	kip-ft	1877	1877
w_{curb}	kip/ft	0.000	0.000
w_{girder}	kip/ft	0.822	0.822
w_{slab}	kip/ft	0.750	0.660

Prestress Losses

Parameter	Units	Interior Girder Values	Exterior Girder Values
$f_{p-transfer}$	ksi	189	189
f_{cgp}	ksi	2.87	2.87
Δf_{pES}	ksi	17.83	14.98
Δf_{pSH}	ksi	6.50	6.50
Δf_{pCR}	ksi	28.45	29.17
Δf_{pSR}	ksi	1.76	2.06
Δf_{pTotal}	ksi	54.54	52.72
f_{pe}	ksi	147.96	149.78
f^*_y	ksi	243	243

Moment Capacity

Parameter	Units	Interior Girder Values	Exterior Girder Values
β_1	-	0.87	0.87
$0.85f'_c\beta_1$	ksi	4.58	4.58
$b_{eff-modified}$	in	91.00	50.04
$b-b_w$	in	71.00	30.04
$A_{ps}{*}f_{pu}$	kips	1983	1983
$c_{rectangular}$	in	4.65	8.29
$c_{T-section}$	in	-8.54	7.68
c	in	4.65	8.29
a	in	4.04	7.22
f_{ps}	ksi	263.91	259.13
ϕM_n	kip-ft	8988	8573

Inventory Rating Factors		
RF	Interior Girder	Exterior Girder
CC_1	4.11	3.94
CC_2	3.30	3.07
CT_6	1.79	2.00
$CT_{7.5}$	1.92	2.13
CT_{12}	2.32	2.53
PST	7.25	8.89
FS_{other}	2.14	2.10

Operating Rating Factors		
RF	Interior Girder	Exterior Girder
FS_{other}	3.58	3.50
PST	12.26	14.94

Inventory Rating		
RT (tons)	Interior Girder	Exterior Girder
CC_1	82.2	78.7
CC_2	65.9	61.4
CT_6	35.8	40.0
$CT_{7.5}$	38.5	42.7
CT_{12}	46.4	50.6
PST	145.1	177.9
FS_{other}	42.8	42.0

Operating Rating		
RT (tons)	Interior Girder	Exterior Girder
FS_{other}	71.5	70.1
PST	245.2	298.8

E.2.2 Adjusted Load Rating Sheets

This section contains load rating sheets that were used to calculate the adjusted load ratings presented in Chapter 7. Through the use of adjusted concrete strengths and measured live load distribution factors, the adjusted load ratings were calculated and were typically much higher than the design load ratings. See Chapter 7 for a comparison of design load ratings to adjusted load ratings.

E.2.2.1 Adjusted Load Rating – Chandler Creek Bridge – 40' Span

User Defined Inputs

Parameter	Units	Interior Girder Values	Exterior Girder Values
A_{ps}	in^2	1.73	1.73
A_s	in^2	0.00	0.00
A_{curb}	in^2	0.00	0.00
A_{girder}	in^2	360.88	360.88
A_{slab}	in^2	674.25	612.63
b_{eff}	in	93.00	84.50
b_w	in	12.00	12.00
d_{girder}	in	34.00	34.00
$d_{overhang}$	in	48.00	38.00
$d_{p\text{-}bottom}$	in	3.01	3.01
$d_{p\text{-}comp}$	in	38.24	38.24
$DF_{measured}$	-	0.43	0.55
E_c	ksi	5250	5250
E_p	ksi	29000	29000
E_{slab}	ksi	4696	4696
$e_{midspan\text{-}girder}$	in	11.90	11.90
$f'_{c\text{-}girder}$	ksi	7.5	7.5
$f'_{c\text{-}slab}$	ksi	6.0	6.0
f_{pi}	ksi	175	175
f_{pu}	ksi	250	250
$f_{y\text{-}steel}$	ksi	60	60
H	%	65	65
h_f	in	7.25	7.25
I_{girder}	in^4	43298	43298
I_{comp}	in^4	169237	164498
L	kip-ft	424.5	424.5
$L_{bearing}$	in	8.50	8.50
L_{span}	ft	38.58	38.58
L_{beam}	ft	40.00	40.00
S_{girder}	ft	8.00	8.00
$w_{diaphragm}$	kip/ft	0.090	0.090
$w_{miscellaneous}$	kip/ft	0.040	0.040
$w_{overlay}$	kip/ft	0.048	0.048
γ_{curb}	lb/ft^3	150	150
γ_{girder}	lb/ft^3	150	150
γ_{slab}	lb/ft^3	150	150
y_{b_girder}	in	14.91	14.91
y_{t_girder}	in	19.09	19.09
y_{b_comp}	in	28.85	28.32
y_{t_comp}	in	12.40	12.93
Strand Type*	-	1	1

*Stress relieved strands are Type 1

*Low relaxation strands are Type 2

AASHTO Specified Values

Parameter	Units	Interior Girder Values	Exterior Girder Values
W	tons	20	20
k	-	0.38	0.38
ϕ	-	1.00	1.00
f_{py}/f_{pu}	-	0.85	0.85
A_1	-	1.3	1.3
A_2 (Inventory)	-	2.17	2.17
A_2 (Operating)	-	1.3	1.3
I	-	1.33	1.33

Stresses and Moments

Parameter	Units	Interior Girder Values	Exterior Girder Values
$e_{midspan\text{-}comp}$	in	25.84	25.32
E_p/E_c	-	5.52	5.52
$F_{d\text{-}b\text{-}comp}$	ksi	0.0335	0.0338
$F_{d\text{-}t\text{-}comp}$	ksi	-0.014	-0.015
$F_{d\text{-}p\text{-}comp}$	ksi	0.166	0.167
$F_{d\text{-}b\text{-}noncomp}$	ksi	0.898	0.849
$F_{d\text{-}t\text{-}noncomp}$	ksi	-1.150	-1.087
$F_{d\text{-}p\text{-}noncomp}$	ksi	3.960	3.743
$F_{d\text{-}b}$	ksi	0.932	0.883
$F_{d\text{-}t}$	ksi	-1.165	-1.103
$F_{d\text{-}p}$	ksi	4.126	3.910
F_{L_b}	ksi	0.501	0.639
F_{L_t}	ksi	-0.215	-0.292
F_{L_p}	ksi	2.479	3.155
F_{p_b}	ksi	-1.57	-1.57
F_{p_t}	ksi	0.57	0.57
$6(f'_{c\text{-}girder})$^0.5	ksi	0.520	0.520
$7.5(f'_{c\text{-}girder})$^0.5	ksi	0.650	0.650
$12(f'_{c\text{-}girder})$^0.5	ksi	1.039	1.039
$M_{DL\text{-}curb}$	kip-ft	0.00	0.00
$M_{DL\text{-}girder}$	kip-ft	70	70
$M_{DL\text{-}slab}$	kip-ft	131	119
$P_i{*}e_{midspan\text{-}girder}$	kip-in	3342	3342
$P_{eff}{*}e_{midspan\text{-}girder}$	kip-in	2728	2724
D_{comp}	kip-ft	16	16
$D_{noncomp}$	kip-ft	217	205
L(1+I)	kip-ft	565	565
w_{curb}	kip/ft	0.000	0.000
w_{girder}	kip/ft	0.376	0.376
w_{slab}	kip/ft	0.702	0.638

Prestress Losses

Parameter	Units	Interior Girder Values	Exterior Girder Values
$f_{p\text{-}transfer}$	ksi	162.5	162.5
f_{cgp}	ksi	1.47	1.47
Δf_{pES}	ksi	8.10	8.10
Δf_{pSH}	ksi	7.25	7.25
Δf_{pCR}	ksi	14.57	14.85
Δf_{pSR}	ksi	12.40	12.34
Δf_{pTotal}	ksi	42.32	42.54
f_{pe}	ksi	132.68	132.46
f^*_y	ksi	212.5	212.5

Moment Capacity

Parameter	Units	Interior Girder Values	Exterior Girder Values
β_1	-	0.675	0.675
$0.85f'_c\beta_1$	ksi	4.30	4.30
$b_{eff\text{-}modified}$	in	83.18	75.58
$b\text{-}b_w$	in	71.18	63.58
$A_{ps}{*}f_{pu}$	kips	432	432
$c_{rectangular}$	in	1.19	1.31
$c_{T\text{-}section}$	in	-31.98	-27.74
c	in	1.19	1.31
a	in	0.81	0.88
f_{ps}	ksi	247.04	246.74
ϕM_n	kip-ft	1346	1343

Inventory Rating Factors		
RF	Interior Girder	Exterior Girder
CC_1	18.13	13.59
CC_2	12.55	9.37
CT_6	2.32	1.89
$CT_{7.5}$	2.58	2.10
CT_{12}	3.36	2.70
PST	13.39	10.66
FS	1.96	1.57

Operating Rating Factors		
RF	Interior Girder	Exterior Girder
FS	3.27	2.62
PST	21.96	17.39

Inventory Rating		
RT (tons)	Interior Girder	Exterior Girder
CC_1	362.6	271.9
CC_2	251.0	187.4
CT_6	46.4	37.8
$CT_{7.5}$	51.6	41.9
CT_{12}	67.2	54.1
PST	267.8	213.1
FS	39.2	31.4

Operating Rating		
RT (tons)	Interior Girder	Exterior Girder
FS	65.5	52.5
PST	439.3	347.8

E.2.2.2 Adjusted Load Rating – Chandler Creek Bridge – 60' Span

User Defined Inputs

Parameter	Units	Interior Girder Values	Exterior Girder Values
A_{ps}	in^2	3.24	3.24
A_s	in^2	0.00	0.00
A_{curb}	in^2	0.00	0.00
A_{girder}	in^2	495.50	495.50
A_{slab}	in^2	681.50	616.25
b_{eff}	in	94.00	85.00
b_w	in	14.00	14.00
d_{girder}	in	40.00	40.00
$d_{overhang}$	in	48.00	38.00
$d_{p\text{-}bottom}$	in	4.00	4.00
$d_{p\text{-}comp}$	in	43.25	43.25
$DF_{measured}$	-	0.393	0.50
E_c	ksi	5655	5655
E_p	ksi	29000	29000
E_{slab}	ksi	4696	4696
$e_{midspan\text{-}girder}$	in	13.07	13.07
$f'_{c\text{-}girder}$	ksi	8.7	8.7
$f'_{c\text{-}slab}$	ksi	6.0	6.0
f_{pi}	ksi	175	175
f_{pu}	ksi	250	250
$f_{y\text{-}steel}$	ksi	60	60
H	%	65	65
h_f	in	7.25	7.25
I_{girder}	in^4	82761	82761
I_{comp}	in^4	284297	274657
L	kip-ft	781.2	781.2
$L_{bearing}$	in	8.50	8.50
L_{span}	ft	58.58	58.58
L_{beam}	ft	60.00	60.00
S_{girder}	ft	8.00	8.00
$w_{diaphragm}$	kip/ft	0.090	0.090
$w_{miscellaneous}$	kip/ft	0.040	0.040
$w_{overlay}$	kip/ft	0.048	0.048
γ_{curb}	lb/ft^3	150	150
γ_{girder}	lb/ft^3	150	150
γ_{slab}	lb/ft^3	150	150
y_{b_girder}	in	17.07	17.07
y_{t_girder}	in	22.93	22.93
y_{b_comp}	in	30.79	30.11
y_{t_comp}	in	16.46	17.14
Strand Type*	-	1	1

*Stress relieved strands are Type 1

*Low relaxation strands are Type 2

AASHTO Specified Values

Parameter	Units	Interior Girder Values	Exterior Girder Values
W	tons	20	20
k	-	0.38	0.38
ϕ	-	1.00	1.00
f_{py}/f_{pu}	-	0.85	0.85
A_1	-	1.3	1.3
A_2 (Inventory)	-	2.17	2.17
A_2 (Operating)	-	1.3	1.3
I	-	1.33	1.33

Stresses and Moments

Parameter	Units	Interior Girder Values	Exterior Girder Values
$e_{midspan\text{-}comp}$	in	26.79	26.11
E_p/E_c	-	5.13	5.13
$F_{d\text{-}b\text{-}comp}$	ksi	0.0491	0.0497
$F_{d\text{-}t\text{-}comp}$	ksi	-0.026	-0.028
$F_{d\text{-}p\text{-}comp}$	ksi	0.219	0.221
$F_{d\text{-}b\text{-}noncomp}$	ksi	1.397	1.325
$F_{d\text{-}t\text{-}noncomp}$	ksi	-1.877	-1.780
$F_{d\text{-}p\text{-}noncomp}$	ksi	5.487	5.204
$F_{d\text{-}b}$	ksi	1.446	1.375
$F_{d\text{-}t}$	ksi	-1.903	-1.808
$F_{d\text{-}p}$	ksi	5.706	5.425
F_{L_b}	ksi	0.531	0.687
F_{L_t}	ksi	-0.284	-0.391
F_{L_p}	ksi	2.371	3.053
F_{p_b}	ksi	-1.99	-1.99
F_{p_t}	ksi	0.68	0.68
$6(f'_{c\text{-}girder})$^0.5	ksi	0.560	0.560
$7.5(f'_{c\text{-}girder})$^0.5	ksi	0.700	0.700
$12(f'_{c\text{-}girder})$^0.5	ksi	1.119	1.119
$M_{DL\text{-}curb}$	kip-ft	0.00	0.00
$M_{DL\text{-}girder}$	kip-ft	221	221
$M_{DL\text{-}slab}$	kip-ft	305	275
$P_i{*}e_{midspan\text{-}girder}$	kip-in	6881	6881
$P_{eff}{*}e_{midspan\text{-}girder}$	kip-in	5526	5513
D_{comp}	kip-ft	38	38
$D_{noncomp}$	kip-ft	565	535
L(1+I)	kip-ft	1039	1039
w_{curb}	kip/ft	0.000	0.000
w_{girder}	kip/ft	0.516	0.516
w_{slab}	kip/ft	0.710	0.642

Prestress Losses

Parameter	Units	Interior Girder Values	Exterior Girder Values
$f_{p\text{-}transfer}$	ksi	162.5	162.5
f_{cgp}	ksi	1.73	1.73
Δf_{pES}	ksi	8.87	8.87
Δf_{pSH}	ksi	7.25	7.25
Δf_{pCR}	ksi	16.72	17.10
Δf_{pSR}	ksi	11.66	11.58
Δf_{pTotal}	ksi	44.50	44.80
f_{pe}	ksi	130.50	130.20
f^*_y	ksi	212.5	212.5

Moment Capacity

Parameter	Units	Interior Girder Values	Exterior Girder Values
β_1	-	0.650	0.650
$0.85f'_c\beta_1$	ksi	4.81	4.81
$b_{eff\text{-}modified}$	in	78.06	70.59
$b\text{-}b_w$	in	64.06	56.59
$A_{ps}{*}f_{pu}$	kips	810	810
$c_{rectangular}$	in	2.12	2.34
$c_{T\text{-}section}$	in	-19.12	-15.62
c	in	2.12	2.34
a	in	1.38	1.52
f_{ps}	ksi	245.35	244.86
ϕM_n	kip-ft	2819	2809

Inventory Rating Factors		
RF	Interior Girder	Exterior Girder
CC_1	14.06	10.46
CC_2	10.09	7.46
CT_6	2.08	1.71
$CT_{7.5}$	2.35	1.91
CT_{12}	3.14	2.52
PST	14.25	11.26
FS	2.30	1.82

Operating Rating Factors		
RF	Interior Girder	Exterior Girder
FS	3.83	3.04
PST	23.22	18.22

Inventory Rating		
RT (tons)	Interior Girder	Exterior Girder
CC_1	281.2	209.2
CC_2	201.9	149.1
CT_6	41.6	34.2
$CT_{7.5}$	46.9	38.3
CT_{12}	62.7	50.5
PST	285.0	225.2
FS	45.9	36.5

Operating Rating		
RT (tons)	Interior Girder	Exterior Girder
FS	76.6	60.8
PST	464.3	364.4

E.2.2.3 Adjusted Load Rating – Lake LBJ Bridge

User Defined Inputs			
Parameter	Units	Interior Girder Values	Exterior Girder Values
A_{ps}	in^2	3.89	3.89
A_s	in^2	0.00	0.00
A_{curb}	in^2	0.00	157.50
A_{girder}	in^2	495.50	495.50
A_{slab}	in^2	681.50	580.00
b_{eff}	in	94.00	80.00
b_w	in	14.00	14.00
d_{girder}	in	40.00	40.00
$d_{overhang}$	in	48.00	33.00
$d_{p\text{-}bottom}$	in	4.67	4.67
$d_{p\text{-}comp}$	in	40.48	40.48
$DF_{measured}$	-	0.37	0.51
E_c	ksi	5422	5422
E_p	ksi	29000	29000
E_{slab}	ksi	4696	4696
$e_{midspan\text{-}girder}$	in	12.40	12.40
$f'_{c\text{-}girder}$	ksi	8.0	8.0
$f'_{c\text{-}slab}$	ksi	6.0	6.0
f_{pi}	ksi	175	175
f_{pu}	ksi	250	250
$f_{y\text{-}steel}$	ksi	60	60
H	%	65	65
h_f	in	7.25	7.25
I_{girder}	in^4	82761	82761
I_{comp}	in^4	274358	323220
L	kip-ft	870.7	870.7
$L_{bearing}$	in	8.50	8.50
L_{span}	ft	63.58	63.58
L_{beam}	ft	65.00	65.00
S_{girder}	ft	8.00	8.00
$w_{diaphragm}$	kip/ft	0.055	0.055
$w_{miscellaneous}$	kip/ft	0.035	0.035
$w_{overlay}$	kip/ft	0.048	0.048
γ_{curb}	lb/ft^3	150	150
γ_{girder}	lb/ft^3	150	150
γ_{slab}	lb/ft^3	150	150
y_{b_girder}	in	17.07	17.07
y_{t_girder}	in	22.93	22.93
y_{b_comp}	in	30.05	31.67
y_{t_comp}	in	17.20	15.58
Strand Type*	-	1	1

*Stress relieved strands are Type 1
*Low relaxation strands are Type 2

AASHTO Specified Values			
Parameter	Units	Interior Girder Values	Exterior Girder Values
W	tons	20	20
k	-	0.38	0.38
ϕ	-	1.00	1.00
f_{py}/f_{pu}	-	0.85	0.85
A_1	-	1.3	1.3
A_2 (Inventory)	-	2.17	2.17
A_2 (Operating)	-	1.3	1.3
I	-	1.33	1.33

Stresses and Moments

Parameter	Units	Interior Girder Values	Exterior Girder Values
$e_{midspan\text{-}comp}$	in	25.38	27.00
E_p/E_c	-	5.35	5.35
$F_{d\text{-}b\text{-}comp}$	ksi	0.0551	0.0493
$F_{d\text{-}t\text{-}comp}$	ksi	-0.032	-0.024
$F_{d\text{-}p\text{-}comp}$	ksi	0.249	0.225
$F_{d\text{-}b\text{-}noncomp}$	ksi	1.602	1.675
$F_{d\text{-}t\text{-}noncomp}$	ksi	-2.152	-2.250
$F_{d\text{-}p\text{-}noncomp}$	ksi	6.225	6.508
$F_{d\text{-}b}$	ksi	1.657	1.725
$F_{d\text{-}t}$	ksi	-2.184	-2.275
$F_{d\text{-}p}$	ksi	6.474	6.733
F_{L_b}	ksi	0.570	0.698
F_{L_t}	ksi	-0.326	-0.343
F_{L_p}	ksi	2.574	3.184
F_{p_b}	ksi	-2.27	-2.26
F_{p_t}	ksi	0.70	0.70
$6(f'_{c\text{-}girder})$^0.5	ksi	0.537	0.537
$7.5(f'_{c\text{-}girder})$^0.5	ksi	0.671	0.671
$12(f'_{c\text{-}girder})$^0.5	ksi	1.073	1.073
$M_{DL\text{-}curb}$	kip-ft	0.00	0.00
$M_{DL\text{-}girder}$	kip-ft	261	261
$M_{DL\text{-}slab}$	kip-ft	359	305
$P_i*e_{midspan\text{-}girder}$	kip-in	7834	7834
$P_{eff}*e_{midspan\text{-}girder}$	kip-in	6145	6119
D_{comp}	kip-ft	42	42
$D_{noncomp}$	kip-ft	647	677
L(1+I)	kip-ft	1158	1158
w_{curb}	kip/ft	0.000	0.164
w_{girder}	kip/ft	0.516	0.516
w_{slab}	kip/ft	0.710	0.604

Prestress Losses

Parameter	Units	Interior Girder Values	Exterior Girder Values
$f_{p\text{-}transfer}$	ksi	162.5	162.5
f_{cgp}	ksi	1.98	1.98
Δf_{pES}	ksi	10.59	10.59
Δf_{pSH}	ksi	7.25	7.25
Δf_{pCR}	ksi	19.24	19.92
Δf_{pSR}	ksi	10.47	10.33
Δf_{pTotal}	ksi	47.55	48.09
f_{pe}	ksi	127.45	126.91
f^*_y	ksi	212.5	212.5

Moment Capacity

Parameter	Units	Interior Girder Values	Exterior Girder Values
β_1	-	0.650	0.650
$0.85f'_c\beta_1$	ksi	4.42	4.42
$b_{eff\text{-}modified}$	in	81.41	69.28
$b\text{-}b_w$	in	67.41	55.28
$A_{ps}*f_{pu}$	kips	972	972
$c_{rectangular}$	in	2.63	3.08
$c_{T\text{-}section}$	in	-16.73	-11.26
c	in	2.63	3.08
a	in	1.71	2.00
f_{ps}	ksi	243.82	242.77
ϕM_n	kip-ft	3130	3105

Inventory Rating Factors		
RF	**Interior Girder**	**Exterior Girder**
CC_1	10.17	9.39
CC_2	7.54	7.02
CT_6	2.01	1.53
$CT_{7.5}$	2.25	1.72
CT_{12}	2.95	2.30
PST	14.01	11.42
FS	2.37	1.68
Operating Rating Factors		
RF	**Interior Girder**	**Exterior Girder**
FS	3.96	2.81
PST	22.27	18.09

Inventory Rating		
RT (tons)	**Interior Girder**	**Exterior Girder**
CC_1	203.4	187.8
CC_2	150.7	140.5
CT_6	40.2	30.6
$CT_{7.5}$	44.9	34.5
CT_{12}	59.1	46.0
PST	280.3	228.3
FS	47.5	33.7
Operating Rating		
RT (tons)	**Interior Girder**	**Exterior Girder**
FS	79.3	56.2
PST	445.4	361.8

E.2.2.4 Adjusted Load Rating – Lampasas River Bridge

User Defined Inputs

Parameter	Units	Interior Girder Values	Exterior Girder Values
A_{ps}	in^2	3.89	3.89
A_s	in^2	0.00	0.00
A_{curb}	in^2	0.00	0.00
A_{girder}	in^2	495.50	495.50
A_{slab}	in^2	552.50	520.00
b_{eff}	in	85.00	80.00
b_w	in	14.00	14.00
d_{girder}	in	40.00	40.00
$d_{overhang}$	in	43.98	37.50
$d_{p\text{-}bottom}$	in	4.65	4.65
$d_{p\text{-}comp}$	in	41.85	41.85
$DF_{measured}$	-	0.36	0.50
E_c	ksi	5490	5490
E_p	ksi	29000	29000
E_{slab}	ksi	4696	4696
$e_{midspan\text{-}girder}$	in	12.42	12.42
$f'_{c\text{-}girder}$	ksi	8.2	8.2
$f'_{c\text{-}slab}$	ksi	6.0	6.0
f_{pi}	ksi	175	175
f_{pu}	ksi	250	250
$f_{y\text{-}steel}$	ksi	60	60
H	%	65	65
h_f	in	6.5	6.5
I_{girder}	in^4	82761	82761
I_{comp}	in^4	263642	257978
L	kip-ft	1052.8	1052.8
$L_{bearing}$	in	7.50	7.50
L_{span}	ft	73.75	73.75
L_{beam}	ft	75.00	75.00
S_{girder}	ft	7.33	7.33
$w_{diaphragm}$	kip/ft	0.043	0.043
$w_{miscellaneous}$	kip/ft	0.035	0.035
$w_{overlay}$	kip/ft	0.044	0.044
γ_{curb}	lb/ft^3	150	150
γ_{girder}	lb/ft^3	150	150
γ_{slab}	lb/ft^3	150	150
y_{b_girder}	in	17.07	17.07
y_{t_girder}	in	22.93	22.93
y_{b_comp}	in	29.30	28.90
y_{t_comp}	in	17.20	17.60
Strand Type*	-	1	1

*Stress relieved strands are Type 1

*Low relaxation strands are Type 2

AASHTO Specified Values

Parameter	Units	Interior Girder Values	Exterior Girder Values
W	tons	20	20
k	-	0.38	0.38
ϕ	-	1.00	1.00
f_{py}/f_{pu}	-	0.85	0.85
A_1	-	1.3	1.3
A_2 (Inventory)	-	2.17	2.17
A_2 (Operating)	-	1.3	1.3
I	-	1.33	1.33

Stresses and Moments

Parameter	Units	Interior Girder Values	Exterior Girder Values
$e_{midspan\text{-}comp}$	in	24.65	24.25
E_p/E_c	-	5.28	5.28
$F_{d\text{-}b\text{-}comp}$	ksi	0.0716	0.0722
$F_{d\text{-}t\text{-}comp}$	ksi	-0.042	-0.044
$F_{d\text{-}p\text{-}comp}$	ksi	0.318	0.320
$F_{d\text{-}b\text{-}noncomp}$	ksi	1.909	1.852
$F_{d\text{-}t\text{-}noncomp}$	ksi	-2.565	-2.488
$F_{d\text{-}p\text{-}noncomp}$	ksi	7.339	7.120
$F_{d\text{-}b}$	ksi	1.981	1.925
$F_{d\text{-}t}$	ksi	-2.607	-2.532
$F_{d\text{-}p}$	ksi	7.657	7.440
F_{L_b}	ksi	0.676	0.938
F_{L_t}	ksi	-0.397	-0.571
F_{L_p}	ksi	3.004	4.156
F_{p_b}	ksi	-2.31	-2.31
F_{p_t}	ksi	0.72	0.72
$6(f'_{c\text{-}girder})$^0.5	ksi	0.543	0.543
$7.5(f'_{c\text{-}girder})$^0.5	ksi	0.679	0.679
$12(f'_{c\text{-}girder})$^0.5	ksi	1.087	1.087
$M_{DL\text{-}curb}$	kip-ft	0.00	0.00
$M_{DL\text{-}girder}$	kip-ft	351	351
$M_{DL\text{-}slab}$	kip-ft	391	368
P_i*$e_{midspan\text{-}girder}$	kip-in	7847	7847
P_{eff}*$e_{midspan\text{-}girder}$	kip-in	6273	6261
D_{comp}	kip-ft	54	54
$D_{noncomp}$	kip-ft	771	748
L(1+I)	kip-ft	1400	1400
w_{curb}	kip/ft	0.000	0.000
w_{girder}	kip/ft	0.516	0.516
w_{slab}	kip/ft	0.576	0.542

Prestress Losses

Parameter	Units	Interior Girder Values	Exterior Girder Values
$f_{p\text{-}transfer}$	ksi	162.5	162.5
f_{cgp}	ksi	1.82	1.82
Δf_{pES}	ksi	9.62	9.62
Δf_{pSH}	ksi	7.25	7.25
Δf_{pCR}	ksi	16.92	17.21
Δf_{pSR}	ksi	11.32	11.26
Δf_{pTotal}	ksi	45.10	45.34
f_{pe}	ksi	129.90	129.66
f^*_y	ksi	212.5	212.5

Moment Capacity

Parameter	Units	Interior Girder Values	Exterior Girder Values
β_1	-	0.650	0.650
$0.85f'_c\beta_1$	ksi	4.53	4.53
$b_{eff\text{-}modified}$	in	72.71	68.43
$b\text{-}b_w$	in	58.71	54.43
A_{ps}*f_{pu}	kips	972	972
$c_{rectangular}$	in	2.87	3.05
$c_{T\text{-}section}$	in	-10.48	-8.73
c	in	2.87	3.05
a	in	1.87	1.98
f_{ps}	ksi	243.48	243.08
ϕM_n	kip-ft	3228	3218

Inventory Rating Factors		
RF	Interior Girder	Exterior Girder
CC_1	7.64	5.44
CC_2	5.89	4.15
CT_6	1.30	0.99
$CT_{7.5}$	1.50	1.13
CT_{12}	2.10	1.57
PST	10.80	7.92
FS	1.96	1.44

Operating Rating Factors		
RF	Interior Girder	Exterior Girder
FS	3.27	2.40
PST	17.88	13.03

Inventory Rating		
RT (tons)	Interior Girder	Exterior Girder
CC_1	152.8	108.7
CC_2	117.7	83.1
CT_6	25.9	19.8
$CT_{7.5}$	29.9	22.7
CT_{12}	42.0	31.4
PST	216.0	158.3
FS	39.2	28.7

Operating Rating		
RT (tons)	Interior Girder	Exterior Girder
FS	65.4	48.0
PST	357.5	260.6

E.2.2.5 Adjusted Load Rating – Willis Creek Bridge

User Defined Inputs

Parameter	Units	Interior Girder Values	Exterior Girder Values
A_{ps}	in^2	3.52	3.52
A_s	in^2	0.00	0.00
A_{curb}	in^2	0.00	99.00
A_{girder}	in^2	495.50	495.50
A_{slab}	in^2	474.00	441.00
b_{eff}	in	79.00	73.50
b_w	in	14.00	14.00
d_{girder}	in	40.00	40.00
$d_{overhang}$	in	40.02	34.00
$d_{p\text{-}bottom}$	in	9.05	9.05
$d_{p\text{-}comp}$	in	36.95	36.95
$DF_{measured}$	-	0.35	0.52
E_c	ksi	5622	5622
E_p	ksi	29000	29000
E_{slab}	ksi	4696	4696
$e_{midspan\text{-}girder}$	in	8.02	8.02
$f'_{c\text{-}girder}$	ksi	8.6	8.6
$f'_{c\text{-}slab}$	ksi	6.0	6.0
f_{pi}	ksi	175	175
f_{pu}	ksi	250	250
$f_{y\text{-}steel}$	ksi	60	60
H	%	65	65
h_f	in	6.00	6.00
I_{girder}	in^4	82761	82761
I_{comp}	in^4	239059	275624
L	kip-ft	870.7	870.7
$L_{bearing}$	in	8.50	8.50
L_{span}	ft	63.58	63.58
L_{beam}	ft	65.00	65.00
S_{girder}	ft	6.67	6.67
$w_{diaphragm}$	kip/ft	0.045	0.045
$w_{miscellaneous}$	kip/ft	0.075	0.075
$w_{overlay}$	kip/ft	0.040	0.040
γ_{curb}	lb/ft^3	150	150
γ_{girder}	lb/ft^3	150	150
γ_{slab}	lb/ft^3	150	150
y_{b_girder}	in	17.07	17.07
y_{t_girder}	in	22.93	22.93
y_{b_comp}	in	28.18	29.73
y_{t_comp}	in	17.82	16.27
Strand Type*	-	1	1

*Stress relieved strands are Type 1

*Low relaxation strands are Type 2

AASHTO Specified Values

Parameter	Units	Interior Girder Values	Exterior Girder Values
W	tons	20	20
k	-	0.38	0.38
ϕ	-	1.00	1.00
f_{py}/f_{pu}	-	0.85	0.85
A_1	-	1.3	1.3
A_2 (Inventory)	-	2.17	2.17
A_2 (Operating)	-	1.3	1.3
I	-	1.33	1.33

Stresses and Moments

Parameter	Units	Interior Girder Values	Exterior Girder Values
$e_{midspan-comp}$	in	19.13	20.68
E_p/E_c	-	5.16	5.16
$F_{d-b-comp}$	ksi	0.0822	0.0752
$F_{d-t-comp}$	ksi	-0.052	-0.041
$F_{d-p-comp}$	ksi	0.288	0.270
$F_{d-b-noncomp}$	ksi	1.319	1.405
$F_{d-t-noncomp}$	ksi	-1.772	-1.888
$F_{d-p-noncomp}$	ksi	3.198	3.406
F_{d-b}	ksi	1.402	1.481
F_{d-t}	ksi	-1.824	-1.929
F_{d-p}	ksi	3.485	3.676
F_{L_b}	ksi	0.577	0.776
F_{L_t}	ksi	-0.365	-0.425
F_{L_p}	ksi	2.019	2.784
F_{p_b}	ksi	-1.74	-1.74
F_{p_t}	ksi	0.10	0.10
$6(f'_{c-girder})$^0.5	ksi	0.556	0.556
$7.5(f'_{c-girder})$^0.5	ksi	0.696	0.696
$12(f'_{c-girder})$^0.5	ksi	1.113	1.113
$M_{DL-curb}$	kip-ft	0.00	0.00
$M_{DL-girder}$	kip-ft	261	261
$M_{DL-slab}$	kip-ft	250	232
$P_i*e_{midspan-girder}$	kip-in	4587	4587
$P_{eff}*e_{midspan-girder}$	kip-in	3794	3790
D_{comp}	kip-ft	58	58
$D_{noncomp}$	kip-ft	533	568
L(1+I)	kip-ft	1158	1158
w_{curb}	kip/ft	0.000	0.103
w_{girder}	kip/ft	0.516	0.516
w_{slab}	kip/ft	0.494	0.459

Prestress Losses

Parameter	Units	Interior Girder Values	Exterior Girder Values
$f_{p-transfer}$	ksi	162.5	162.5
f_{cgp}	ksi	1.30	1.30
Δf_{pES}	ksi	6.68	6.68
Δf_{pSH}	ksi	7.25	7.25
Δf_{pCR}	ksi	13.52	13.66
Δf_{pSR}	ksi	13.17	13.15
Δf_{pTotal}	ksi	40.62	40.74
f_{pe}	ksi	134.38	134.26
f^*_y	ksi	212.5	212.5

Moment Capacity

Parameter	Units	Interior Girder Values	Exterior Girder Values
β_1	-	0.650	0.650
$0.85f'_c\beta_1$	ksi	4.75	4.75
$b_{eff-modified}$	in	65.99	61.39
$b-b_w$	in	51.99	47.39
$A_{ps}*f_{pu}$	kips	880	880
$c_{rectangular}$	in	2.73	2.93
$c_{T-section}$	in	-7.97	-6.23
c	in	2.73	2.93
a	in	1.77	1.90
f_{ps}	ksi	242.99	242.48
ϕM_n	kip-ft	2570	2561

Inventory Rating Factors		
RF	**Interior Girder**	**Exterior Girder**
CC_1	9.41	7.84
CC_2	7.06	5.94
CT_6	1.55	1.05
$CT_{7.5}$	1.79	1.22
CT_{12}	2.51	1.76
PST	15.92	11.51
FS	2.04	1.34

Operating Rating Factors		
RF	**Interior Girder**	**Exterior Girder**
FS	3.40	2.24
PST	26.45	19.15

Inventory Rating		
RT (tons)	**Interior Girder**	**Exterior Girder**
CC_1	188.2	156.8
CC_2	141.3	118.9
CT_6	30.9	20.9
$CT_{7.5}$	35.8	24.5
CT_{12}	50.2	35.3
PST	318.4	230.3
FS	40.7	26.9

Operating Rating		
RT (tons)	**Interior Girder**	**Exterior Girder**
FS	68.0	44.8
PST	528.9	382.9

E.2.2.6 Adjusted Load Rating – Wimberley Bridge

User Defined Inputs

Parameter	Units	Interior Girder Values	Exterior Girder Values
A_{ps}	in^2	2.72	2.72
A_s	in^2	0.00	0.00
A_{curb}	in^2	0.00	137.00
A_{girder}	in^2	360.88	360.88
A_{slab}	in^2	506.25	384.38
b_{eff}	in	81.00	61.50
b_w	in	12.00	12.00
d_{girder}	in	34.00	34.00
$d_{overhang}$	in	41.52	21.00
$d_{p\text{-}bottom}$	in	6.77	6.77
$d_{p\text{-}comp}$	in	33.48	33.48
DF_{max}	-	0.46	0.52
E_c	ksi	5589	5589
E_{ps}	ksi	29000	29000
E_{slab}	ksi	4696	4696
$e_{midspan\text{-}girder}$	in	8.14	8.14
$f'_{c\text{-}girder}$	ksi	8.5	8.5
$f'_{c\text{-}slab}$	ksi	6.0	6.0
f_{pi}	ksi	175	175
f_{pu}	ksi	250	250
$f_{y\text{-}steel}$	ksi	60	60
H	%	65	65
h_f	in	6.25	6.25
I_{girder}	in^4	43298	43298
I_{comp}	in^4	146977	175973
L	kip-ft	421.7	421.7
$L_{bearing}$	in	9.50	9.50
L_{span}	ft	38.42	38.42
L_{beam}	ft	40.00	40.00
S_{girder}	ft	6.92	6.92
$w_{diaphragm}$	kip/ft	0.041	0.041
$w_{miscellaneous}$	kip/ft	0.035	0.035
$w_{overlay}$	kip/ft	0.045	0.045
γ_{curb}	lb/ft^3	150	150
γ_{girder}	lb/ft^3	150	150
γ_{slab}	lb/ft^3	150	150
y_{b_girder}	in	14.91	14.91
y_{t_girder}	in	19.09	19.09
y_{b_comp}	in	26.55	27.91
y_{t_comp}	in	13.70	12.34
Strand Type*	-	1	1

*Stress relieved strands are Type 1

*Low relaxation strands are Type 2

AASHTO Specified Values

Parameter	Units	Interior Girder Values	Exterior Girder Values
W	tons	20	20
k	-	0.38	0.38
ϕ	-	1.00	1.00
f_{py}/f_{pu}	-	0.85	0.85
A_1	-	1.3	1.3
A_2 (Inventory)	-	2.17	2.17
A_2 (Operating)	-	1.3	1.3
I	-	1.33	1.33

Stresses and Moments

Parameter	Units	Interior Girder Values	Exterior Girder Values
$e_{midspan-comp}$	in	19.79	21.15
E_{ps}/E_c	-	5.19	5.19
$F_{d-b-comp}$	ksi	0.0320	0.0281
$F_{d-t-comp}$	ksi	-0.017	-0.012
$F_{d-p-comp}$	ksi	0.124	0.110
$F_{d-b-noncomp}$	ksi	0.720	0.732
$F_{d-t-noncomp}$	ksi	-0.922	-0.937
$F_{d-p-noncomp}$	ksi	2.039	2.073
F_{d-b}	ksi	0.752	0.760
F_{d-t}	ksi	-0.938	-0.950
F_{d-p}	ksi	2.163	2.183
F_{L_b}	ksi	0.562	0.552
F_{L_t}	ksi	-0.290	-0.244
F_{L_p}	ksi	2.174	2.170
F_{p_b}	ksi	-1.94	-1.94
F_{p_t}	ksi	0.29	0.28
$6(f'_{c-girder})$^0.5	ksi	0.553	0.553
$7.5(f'_{c-girder})$^0.5	ksi	0.691	0.691
$12(f'_{c-girder})$^0.5	ksi	1.106	1.106
$M_{DL-curb}$	kip-ft	0.00	0.00
$M_{DL-girder}$	kip-ft	69	69
$M_{DL-slab}$	kip-ft	97	74
$P_i{*}e_{midspan-girder}$	kip-in	3598	3598
$P_{eff}{*}e_{midspan-girder}$	kip-in	2840	2833
D_{comp}	kip-ft	15	15
$D_{noncomp}$	kip-ft	174	177
L(1+I)	kip-ft	561	561
w_{curb}	kip/ft	0.000	0.143
w_{girder}	kip/ft	0.376	0.376
w_{slab}	kip/ft	0.527	0.400

Prestress Losses

Parameter	Units	Interior Girder Values	Exterior Girder Values
$f_{p-transfer}$	ksi	162.5	162.5
f_{cgp}	ksi	1.74	1.74
Δf_{pES}	ksi	9.05	9.05
Δf_{pSH}	ksi	7.25	7.25
Δf_{pCR}	ksi	19.40	19.77
Δf_{pSR}	ksi	11.05	10.97
Δf_{pTotal}	ksi	46.75	47.05
f_{pe}	ksi	128.25	127.95
f^*_y	ksi	212.5	212.5

Moment Capacity

Parameter	Units	Interior Girder Values	Exterior Girder Values
β_1	-	0.650	0.650
$0.85f'_c\beta_1$	ksi	4.70	4.70
$b_{eff-modified}$	in	68.05	51.67
$b-b_w$	in	56.05	39.67
$A_{ps}{*}f_{pu}$	kips	680	680
$c_{rectangular}$	in	2.08	2.72
$c_{T-section}$	in	-15.07	-7.56
c	in	2.08	2.72
a	in	1.35	1.77
f_{ps}	ksi	244.11	242.29
ϕM_n	kip-ft	1815	1790

Inventory Rating Factors		
RF	**Interior Girder**	**Exterior Girder**
CC_1	15.33	18.18
CC_2	10.60	12.57
CT_6	3.10	3.14
$CT_{7.5}$	3.35	3.39
CT_{12}	4.09	4.14
PST	18.21	18.37
FS	2.79	2.45

Operating Rating Factors		
RF	**Interior Girder**	**Exterior Girder**
FS	4.66	4.09
PST	27.99	28.16

Inventory Rating		
RT (tons)	**Interior Girder**	**Exterior Girder**
CC_1	306.7	363.6
CC_2	211.9	251.5
CT_6	62.1	62.8
$CT_{7.5}$	67.0	67.8
CT_{12}	81.8	82.8
PST	364.2	367.4
FS	55.8	49.0

Operating Rating		
RT (tons)	**Interior Girder**	**Exterior Girder**
FS	93.1	81.7
PST	559.7	563.3

E.2.2.7 Adjusted Load Rating – Slaughter Creek Bridge

User Defined Inputs

Parameter	Units	Interior Girder Values	Exterior Girder Values
A_{ps}	in^2	5.508	8.874
A_s	in^2	0.00	0.00
A_{curb}	in^2	0.00	330.00
A_{girder}	in^2	789.00	789.00
A_{slab}	in^2	720.00	510.00
b_{eff}	in	96.00	68.00
b_w	in	20.00	20.00
d_{girder}	in	54.00	54.00
$d_{overhang}$	in	48.00	26.00
$d_{p\text{-}bottom}$	in	4.00	4.00
$d_{p\text{-}comp}$	in	57.50	57.50
DF_1	-	-	-
DF_2	-	0.300	0.650
DF_{max}	-	0.300	0.650
E_c	ksi	4595	5467
E_p	ksi	28500	28500
E_{slab}	ksi	3908	3908
$e_{midspan\text{-}girder}$	in	20.75	10.41
$f'_{c\text{-}girder}$	ksi	8.3	12.0
$f'_{c\text{-}slab}$	ksi	7.2	7.2
f_{pi}	ksi	202.5	202.5
f_{pu}	ksi	270	270
$f_{y\text{-}steel}$	ksi	60	60
H	%	70	70
h_f	in	7.5	7.5
I_{girder}	in^4	260740	260740
I_{comp}	in^4	713020	959767
L	kip-ft	1502.4	1502.4
$L_{bearing}$	in	9.00	9.00
L_{span}	ft	98.80	98.80
L_{beam}	ft	100.00	100.00
S_{girder}	ft	8.00	8.00
$w_{diaphragm}$	kip/ft	0.045	0.045
$w_{miscellaneous}$	kip/ft	0.075	0.075
$w_{overlay}$	kip/ft	0.040	0.040
γ_{curb}	lb/ft^3	150	150
γ_{girder}	lb/ft^3	150	150
γ_{slab}	lb/ft^3	150	150
y_{b_girder}	in	24.75	24.75
y_{t_girder}	in	29.25	29.25
y_{b_comp}	in	39.96	43.49
y_{t_comp}	in	21.54	18.01
Strand Type*	-	2	2

*Stress relieved strands are Type 1

*Low relaxation strands are Type 2

AASHTO Specified Values

Parameter	Units	Interior Girder Values	Exterior Girder Values
W	tons	20	20
k	-	0.28	0.28
ϕ	-	1.00	1.00
f_{py}/f_{pu}	-	0.90	0.90
A_1	-	1.3	1.3
A_2 (Inventory)	-	2.17	2.17
A_2 (Operating)	-	1.3	1.3
I	-	1.22	1.22

Stresses and Moments

Parameter	Units	Interior Girder Values	Exterior Girder Values
$e_{midspan\text{-}comp}$	in	35.96	29.15
E_p/E_c	-	6.20	5.21
$F_{d\text{-}b}$	ksi	2.185	2.060
$F_{d\text{-}t}$	ksi	-2.582	-2.434
$F_{d\text{-}p}$	ksi	11.360	4.516
$F_{d\text{-}girder\_b}$	ksi	1.142	1.142
$F_{d\text{-}girder\_t}$	ksi	-1.350	-1.350
$F_{d\text{-}girder\_p}$	ksi	5.940	2.505
$F_{d\text{-}comp\_b}$	ksi	1.042	0.917
$F_{d\text{-}comp\_t}$	ksi	-1.232	-1.084
$F_{d\text{-}comp\_p}$	ksi	5.420	2.011
F_{L_b}	ksi	0.370	0.648
F_{L_t}	ksi	-0.199	-0.268
F_{L_p}	ksi	2.064	2.264
F_{p_b}	ksi	-2.88	-3.12
F_{p_t}	ksi	0.94	-0.14
$6(f'_{c\text{-}girder})$^0.5	ksi	0.547	0.657
$7.5(f'_{c\text{-}girder})$^0.5	ksi	0.683	0.822
$12(f'_{c\text{-}girder})$^0.5	ksi	1.093	1.315
$M_{DL\text{-}curb}$	kip-ft	0.00	0.00
$M_{DL\text{-}girder}$	kip-ft	1002.84	1002.84
$M_{DL\text{-}slab}$	kip-ft	915.14	805.32
P_i*$e_{midspan\text{-}girder}$	kip-in	21601	17460
P_{eff}*$e_{midspan\text{-}girder}$	kip-in	18437	14389
D	kip-ft	1994	1955
L(1+I)	kip-ft	1833	1833
w_{curb}	kip/ft	0.000	0.344
w_{girder}	kip/ft	0.822	0.822
w_{slab}	kip/ft	0.750	0.660

Prestress Losses

Parameter	Units	Interior Girder Values	Exterior Girder Values
$f_{p\text{-}transfer}$	ksi	189	189
f_{cgp}	ksi	2.08	2.34
Δf_{pES}	ksi	12.91	12.21
Δf_{pSH}	ksi	6.50	6.50
Δf_{pCR}	ksi	18.85	25.41
Δf_{pSR}	ksi	2.93	2.62
Δf_{pTotal}	ksi	41.19	46.74
f_{pe}	ksi	161.31	155.76
f^*_y	ksi	243	243

Moment Capacity

Parameter	Units	Interior Girder Values	Exterior Girder Values
β_1	-	0.69	0.69
$0.85f'_c\beta_1$	ksi	4.87	7.04
$b_{eff\text{-}modified}$	in	81.65	48.61
$b\text{-}b_w$	in	61.65	28.61
A_{ps}*f_{pu}	kips	1487	2396
$c_{rectangular}$	in	3.67	6.77
$c_{T\text{-}section}$	in	-7.30	5.81
c	in	3.67	6.77
a	in	2.54	4.67
f_{ps}	ksi	265.17	261.10
ϕM_n	kip-ft	6844	10651

Inventory Rating Factors		
RF	**Interior Girder**	**Exterior Girder**
CC_1	16.76	17.25
CC_2	12.54	13.10
CT_6	3.35	2.65
$CT_{7.5}$	3.72	2.90
CT_{12}	4.83	3.66
PST	10.53	15.07
FS_{other}	3.56	3.14
Operating Rating Factors		
RF	**Interior Girder**	**Exterior Girder**
FS_{other}	5.95	5.24
PST	22.30	25.81

Inventory Rating		
RT (tons)	**Interior Girder**	**Exterior Girder**
CC_1	335.1	345.0
CC_2	250.8	262.0
CT_6	67.0	53.0
$CT_{7.5}$	74.4	58.0
CT_{12}	96.5	73.2
PST	210.5	301.5
FS_{other}	71.3	62.7
Operating Rating		
RT (tons)	**Interior Girder**	**Exterior Girder**
FS_{other}	119.0	104.7
PST	446.0	516.2

E.2.2.8 Adjusted Load Rating – Nolanville Bridge

User Defined Inputs

Parameter	Units	Interior Girder Values	Exterior Girder Values
A_{ps}	in^2	7.344	7.344
A_s	in^2	0.00	0.00
A_{curb}	in^2	0.00	0.00
A_{girder}	in^2	789.00	789.00
A_{slab}	in^2	936.25	612.50
b_{eff}	in	107.00	70.00
b_w	in	20.00	20.00
d_{girder}	in	54.00	54.00
$d_{overhang}$	in	57.00	24.00
$d_{p\text{-}bottom}$	in	5.08	5.08
$d_{p\text{-}comp}$	in	57.67	57.67
DF_1	-	-	-
DF_2	-	0.420	0.460
DF_{max}	-	0.420	0.460
E_c	ksi	4595	5467
E_p	ksi	28500	28500
E_{slab}	ksi	3908	3908
$e_{midspan\text{-}girder}$	in	19.67	19.67
$f'_{c\text{-}girder}$	ksi	9.0	9.0
$f'_{c\text{-}slab}$	ksi	7.2	7.2
f_{pi}	ksi	202.5	202.5
f_{pu}	ksi	270	270
$f_{y\text{-}steel}$	ksi	60	60
H	%	70	70
h_f	in	8.75	8.75
I_{girder}	in^4	260740	260740
I_{comp}	in^4	799172	745436
L	kip-ft	1538.4	1538.4
$L_{bearing}$	in	9.00	9.00
L_{span}	ft	100.80	100.80
L_{beam}	ft	102.00	102.00
S_{girder}	ft	9.50	9.50
$w_{diaphragm}$	kip/ft	0.045	0.045
$w_{miscellaneous}$	kip/ft	0.075	0.075
$w_{overlay}$	kip/ft	0.040	0.040
γ_{curb}	lb/ft^3	150	150
γ_{girder}	lb/ft^3	150	150
γ_{slab}	lb/ft^3	150	150
y_{b_girder}	in	24.75	24.75
y_{t_girder}	in	29.25	29.25
y_{b_comp}	in	42.47	40.53
y_{t_comp}	in	20.28	22.22
Strand Type*	-	2	2

*Stress relieved strands are Type 1

*Low relaxation strands are Type 2

AASHTO Specified Values

Parameter	Units	Interior Girder Values	Exterior Girder Values
W	tons	20	20
k	-	0.28	0.28
ϕ	-	1.00	1.00
f_{py}/f_{pu}	-	0.90	0.90
A_1	-	1.3	1.3
A_2 (Inventory)	-	2.17	2.17
A_2 (Operating)	-	1.3	1.3
I	-	1.22	1.22

Stresses and Moments

Parameter	Units	Interior Girder Values	Exterior Girder Values
$e_{midspan-comp}$	in	37.39	35.45
E_p/E_c	-	6.20	5.21
F_{d-b}	ksi	2.274	2.144
F_{d-t}	ksi	-2.688	-2.534
F_{d-p}	ksi	11.210	8.882
$F_{d-girder\_b}$	ksi	1.189	1.189
$F_{d-girder\_t}$	ksi	-1.405	-1.405
$F_{d-girder\_p}$	ksi	5.861	4.926
F_{d-comp_b}	ksi	1.085	0.955
F_{d-comp_t}	ksi	-1.282	-1.128
F_{d-comp_p}	ksi	5.348	3.956
F_{L_b}	ksi	0.503	0.563
F_{L_t}	ksi	-0.240	-0.309
F_{L_p}	ksi	2.745	2.568
F_{p_b}	ksi	-3.41	-3.45
F_{p_t}	ksi	1.02	1.03
$6(f'_{c-girder})$^0.5	ksi	0.569	0.569
$7.5(f'_{c-girder})$^0.5	ksi	0.712	0.712
$12(f'_{c-girder})$^0.5	ksi	1.138	1.138
$M_{DL-curb}$	kip-ft	0.00	0.00
$M_{DL-girder}$	kip-ft	1043.85	1043.85
$M_{DL-slab}$	kip-ft	952.56	838.25
$P_i*e_{midspan-girder}$	kip-in	27302	27302
$P_{eff}*e_{midspan-girder}$	kip-in	21374	21637
D	kip-ft	1994	1955
L(1+I)	kip-ft	1877	1877
w_{curb}	kip/ft	0.000	0.000
w_{girder}	kip/ft	0.822	0.822
w_{slab}	kip/ft	0.750	0.660

Prestress Losses

Parameter	Units	Interior Girder Values	Exterior Girder Values
$f_{p-transfer}$	ksi	189	189
f_{cgp}	ksi	2.87	2.87
Δf_{pES}	ksi	17.83	14.98
Δf_{pSH}	ksi	6.50	6.50
Δf_{pCR}	ksi	28.45	29.17
Δf_{pSR}	ksi	1.76	2.06
Δf_{pTotal}	ksi	54.54	52.72
f_{pe}	ksi	147.96	149.78
f^*_y	ksi	243	243

Moment Capacity

Parameter	Units	Interior Girder Values	Exterior Girder Values
β_1	-	0.69	0.69
$0.85f'_c\beta_1$	ksi	5.28	5.28
$b_{eff-modified}$	in	91.00	50.04
$b-b_w$	in	71.00	30.04
$A_{ps}*f_{pu}$	kips	1983	1983
$c_{rectangular}$	in	4.05	7.24
$c_{T-section}$	in	-11.25	5.17
c	in	4.05	7.24
a	in	2.79	5.00
f_{ps}	ksi	264.69	260.50
ϕM_n	kip-ft	9116	8796

Inventory Rating Factors		
RF	**Interior Girder**	**Exterior Girder**
CC_1	15.55	12.63
CC_2	11.53	9.23
CT_6	3.38	3.33
$CT_{7.5}$	3.67	3.58
CT_{12}	4.52	4.34
PST	12.83	13.91
FS_{other}	3.81	3.34
Operating Rating Factors		
RF	**Interior Girder**	**Exterior Girder**
FS_{other}	6.37	5.57
PST	21.69	23.37

Inventory Rating		
RT (tons)	**Interior Girder**	**Exterior Girder**
CC_1	311.0	252.5
CC_2	230.5	184.6
CT_6	67.7	66.5
$CT_{7.5}$	73.3	71.6
CT_{12}	90.3	86.7
PST	256.7	278.3
FS_{other}	76.3	66.8
Operating Rating		
RT (tons)	**Interior Girder**	**Exterior Girder**
FS_{other}	127.3	111.5
PST	433.7	467.5

Works Cited

1. Abendroth, R.E.; Klaiber, F.W. and Shafer, M.W. "Diaphragm Effectiveness in Prestressed-Concrete Girder Bridges." *Journal of Structural Engineering*, September 1995, pp. 1362-1369.

2. American Association of State Highway and Transportation Officials. *Standard Specifications for Highway Bridges, 16th Edition*. Washington, D.C., 1996.

3. American Association of State Highway and Transportation Officials (2000a). *2000 Interim AASHTO LRFD Bridge Design Specifications, Second Edition*. Washington, D.C., 2000.

4. American Association of State Highway and Transportation Officials (2000b). *2000 Interim Manual for Condition Evaluation of Bridges, Second Edition*. Washington, D.C., 2000.

5. Barr, P.J.; Eberhard, M.O., and Stanton, J.F. "Live-Load Distribution Factors in Prestressed Concrete Girder Bridges." *Journal of Bridge Engineering*, September/October 2001, pp. 298-306.

6. Chen, Yohchia, and Aswad, Alex. "Stretching Span Capability of Prestressed Concrete Bridges Under AASHTO LRFD." *Journal of Bridge Engineering*, August 1996, pp. 112-120.

7. Comite Euro-International Du Beton. "CEB-FIP Model Code 1990." July 1991.

8. Hurst, M.K. *Prestressed Concrete Design, Second Edition*. Routledge, New York, New York, 1998.

9. Matsis, Photis. "Diagnostic Load Tests of Two Prestressed Concrete Girder Bridges." M.S.E. Thesis, The University of Texas at Austin, August 1999.

10. Texas Department of Transportation. "Bridge Inventory, Inspection, and Appraisal Program (BRINSAP) Database." May 2002.

11. Wood, S.L. "Evaluation of Long-Term Properties of Concrete." *ACI Materials Journal*, November-December 1991, pp. 630-643.